DISSERTATION

GEOSPATIAL ANALYSIS OF SPECIFIC DEGRADATION IN SOUTH KOREA

Submitted by

Woochul Kang

Department of Civil and Environmental Engineering

In partial fulfillment of requirements

For the Degree of Doctor of Philosophy

Colorado State University

Fort Collins, Colorado

Summer 2019

Doctoral Committee:

Advisor: Pierre Y. Julien

Neil S. Grigg
Ryan Morrison
Stephanie Kampf

ABSTRACT

GEOSPATIAL ANALYSIS OF SPECIFIC DEGRADATION IN SOUTH KOREA

South Korea experienced many local and concentrated sediment problems such as landslides, upland erosion, rills and valleys, aggradation/degradation, and flood plain sediment deposition. These problems vary in space and time, therefore a reliable and consistent approach to model sediment processes is desirable. In contrast to sediment yield at the basin scale, Specific Degradation (SD) is defined as the ratio of the sediment yield divided by the watershed area. Field measurements of discharge and sediment concentration are analyzed at 70 stations in South Korea. Half of the sampled river basins (35 stations) represent streams in mountain regions and the other half represent rivers. The Modified Einstein Procedure (MEP) was used to determine the total sediment load at all stations. The Flow Duration – Sediment Rating Curve (FD-SRC) method was used to determine the sediment yield and specific degradation for all gauging stations. The annual sediment yield of 70 rivers and streams in South Korea ranged from 10 to 1,000 tons/km^2▪yr. The application of three existing models from the literature showed Root Mean Square Errors (RMSE) in excess of 1,400 tons/km^2▪yr and gave negative values of the Nash-Sutcliffe Efficiency coefficient (NSE) for existing models, which indicates that the observed mean is a better predictor than the model.

The main characteristics of each watershed were analyzed using GIS tools such as ArcGIS version 10.3.1. The data used for the analysis included: (1) daily precipitation data at 60 stations from the Korea Meteorological Administration (KMA); (2) a detailed soil map from the National Institute of Agriculture Sciences; (3) a 5m by 5m resolution Digital Elevation Model

(DEM); and (4) land cover raster data at a 10 m resolution from the Ministry of Environment (ME). Seven regression models based on these watershed characteristics are proposed to estimate the mean annual sediment yield and specific degradation. In decreasing order of importance, the meaningful parameters are: (1) drainage area; (2) mean annual precipitation; (3) percentage of urbanized area; (4) percentage of sand of the surface soil (upper 50cm); (5) percentage of wetland and water; and (6) morphometric parameters such as watershed average slope and two parameters of the hypsometric curve. The RMSE for the newly developed models decreased to 90 tons/km^2▪yr and the NSE increased from -50 to 0.5, which shows good agreement between the model and the measured sediment yield on these watersheds. The calculated specific degradation and mean annual soil loss of mountain streams were larger than alluvial rivers.

Erosion loss mapping at 5m, 30m and 90m was also developed from the Revised Universal Soil Loss Equation (RUSLE). Satellite images and aerial photos were used to better represent geospatial features affecting erosion and sedimentation. Long-term reservoir sedimentation measurements were available to determine the Sediment Delivery Ratio (SDR). An important finding from this analysis is that the percentage of the area covered with wetland and water is well-correlated with the estimated sediment delivery ratios. It suggests that the transfer of sediment to the rivers is affected by wetlands located near alluvial rivers. The erosion maps at 5m resolution could clearly show unique erosion features (i.e. hill slopes, croplands, and construction sites) and locate areas for sediment deposition (i.e. wetlands and agricultural reservoirs). In comparison, the gross erosion rates at 90 m resolution were highly distorted and could not delineate the areas with high upland erosion rates. Sustainable sediment management with these methodologies could be helpful to solve various erosion and sedimentation problems.

ACKNOWLEDGMENTS

I am very thankful to thank everyone who helped me throughout my time at Colorado State University. My experiences at CSU were great time and it could be motivation and inspiration not only for my future study also for my life.

I would like to thank my advisor Dr. Pierre Julien for the amazing support, great guidance, and encouragement during the Ph. D program at CSU. I also give great thanks to my committee members: Dr. Neil Grigg, Dr. Ryan Morrison, and Dr. Stephanie Kampf who gave me helpful comments and assistance during my study.

My thanks go to rising stars: Dr. Jai Hong Lee, Dr. Hwayoung Kim, Dr. Marcos Palu, Neil Andika, Weimin Li, Kristin LaForge, Susan Cundiff, and Sydney Doidge. Thanks to Dr. Chunyao Yang for working with me on the Korean project. Special thanks to visiting scholars: Dr. Eunkyung Jang, Dr. Joonhak Lee, Dr. Seongjoon Byeon, and Dr. Xudong Chen. Friday seminars with you helped me improve my thinking.

I would also like to extend my appreciation to Korean Friends at CSU: Seongyun Kim, Youngho Seo, Kyungseop Shin, Sunah Kim, Jongseok Cho, Youngjai Jung, Seonggyu Park, Jungho Kim and Heechan Han. Thanks to Dr. Michael Gooseff, Dr. Ryan Bailey, Dr. Jorge Ramirez, K-Water, and CEMML for providing the funding.

I am grateful for the support of all our family in South Korea, especially my parents Changyong Kang and Moonhwa Joo, and my sister Hyeji Kang. I am thankful for their support, encouragement and unconditional love. I love you.

TABLE OF CONTENTS

LIST OF TABLES

LIST OF FIGURES

Chapter 1
Introduction

1.1. Problem Statement

The Korean Peninsula is located between the Yellow Sea and East Sea on Eastern of the Asian Continent. South Korea has distinctive climatic and topographic characteristics with upland steep mountains areas and valleys with wide alluvial plains. In terms of climate characteristics, Korea is classified as a humid continental and humid subtropical. Especially, the East Asia monsoon impacts South Korea, such that precipitation occurs primarily during the summer season from June to September. About two-thirds of the annual precipitation (1000mm~1400mm) happens during summer. This condition complicates water resource management so that various dams and reservoirs have been constructed for water use and management during the past couple of decades. In steep mountain areas, abundant soil loss occurs during typhoons. The generated sedimentation from upstream also resulted in the sediment problem in reservoirs (*Figure 1*).

(a) (b)

Figure 1. (a) Upstream of Imha reservoir, and (b) Imha reservoir after typhoon Maemi (Kim, 2006)

South Korea experiences rapid urbanization and industrial areas demand large scale water resources management projects such as dam construction. Additional sediment problems (e.g.

riverbed degradation) occur the downstreams of dams (*Figure 2*a). The urbanization and increased human activity induce changes in sediment yield and the cost of the maintenance and dredging for removing the deposited sediment often are unexpectedly high (*Figure 2*b). For instance, the annual cost for dredging at the Nakdong River Estuary Barrage (NREB) is approximately $2 million (Ji, 2006). While there are few large scale erosion and sedimentation problems in South Korea, numerous local and concentrated sediment problems such as upland erosion losses have occurred in South Korea.

(a)

(b)

Figure 2. (a) Bridge-scour problem and (b) dredging near Nakdong River Estuary Barrage

It is required that a reliable and consistent method to predict sediment transport and yield which could consider local conditions (Yoon and Woo, 2000). To predict the sediment yield and transport under different condition, priority should be given to understand spatially varied erosion and sedimentation processes at different condition. The erosion and sedimentation processes depend on various factors, such as geographic factors, soil, vegetation, climatology, and anthropogenic factor. Many efforts have been made on the development of physical, empirical and conceptual models with consideration of the above factors to estimate sediment yield and understand their mechanism. However, the models often produced highly variable results because the models were generated with different conditions and purposes.

1.2. Research Objectives

The three specific objectives of this study are:

1. Estimate the annual total sediment load for 70 gauging stations in South Korean Rivers from the Flow Duration and Sediment Rating Curve (FD-SRC) method, and determine the annual sediment yield for reservoirs from sediment deposition measurements. Calculate the specific degradation at the basin scale from the sediment yield and drainage area. Test existing models for predicting specific degradation in South Korean Rivers.
2. Analyze the various watershed characteristics with a Geographic Information System (GIS, ArcGIS version 10.3.1) and develop an empirical model for specific degradation based on watershed characteristics at the basins scale. Test and validate the proposed model with the data from the first objective, and define expected mean values and confidence intervals.
3. Map upland erosion rates with the Revised Universal Soil Loss Equation (RUSLE) and estimate the Sediment Delivery Ratio (SDR) corresponding to the measured sediment load. Analyze the effects of grid size on soil erosion mapping and compare with visual information from aerial photos and satellite images. The erosion maps at different scales will highlight erosion and sedimentation features including roadways, construction sites, wetlands, agricultural reservoirs, etc.

1.3. Approach

To predict sediment yield and understand the process with consideration of local scale, the different conditions of local watershed and their characteristics will be studied. The detailed approaches for this study are:

- Analyze river flows/sediment yield;
- Analyze Specific Degradation (SD) at watershed scale;

- Validate existing statistical models from the estimated Specific Degradation (SD);
- Analyze watershed characteristics at watershed scale with GIS;
- Develop new regression models;
- Create erosion maps with the Revised Universal Soil Loss Equation (RUSLE) at 5m, 30m, and 90m resolution;
- Conduct geospatial analysis with erosion maps, satellite images, and aerial photos;
- Analyze resolution effects on erosion maps.

Chapter 2
Literature Review

2.1. Erosion and Sedimentation Process

The process of soil erosion involves three stages: detachment, transport, and subsequent deposition. In detail, the detached sediment is deposited during transportation, generally, the sediment measurement at the river is conducted at a cross-section of the stream. To understand sediment yield, the overall sediment budget of a catchment and sediment output should be considered together. The terminology related to sediment is organized first. “Gross erosion” represent all erosion in the watershed. At a specific location, the gross erosion material transported downstream is called “sediment yield”. The sediment yield can be calculated from the gross erosion and the “sediment delivery ratio”. The gross erosion is generally estimated by the Universal Soil Loss Equation (USLE), however in only considers sheet and rill erosion. Commonly, the sediment yield is measured at a river gauging station or as accumulation in a reservoir. In a given time (daily or annual interval), the sediment discharge is measured with various methods. In this study, the term "Specific Degradation (SD)” refers to ratio of sediment yield to the watershed area (Julien, 2010).

2.1.1. Erosion Process in Watershed

The detachment of soil materials during rains storms results from rainfall energy and the shearing force from the water flow on the land surface. The intense shear stresses from raindrop splash depend on raindrop size and sheet-flow depth and detach soil particles (Hartley, 1990). When the shear stress from overland flow exceeds the cohesive strength of a soil, it also contributed to sediment detachment. Commonly, the erosion from water is classified into sheet erosion (inter-rill erosion), rill erosion, gully erosion, and instream erosion. Sheet erosion is a

detachment of soil particles by overland flow or raindrop impact as a widespread thin sheet layer. The term “Inter-rill erosion” is often used instead of sheet erosion. Rill erosion is a movement of land surface materials due to a concentration of runoff. Both erosions are often classified as overland flow erosion for the detachment of surface profile only (Merritt and Letcher, 2003). In upland erosion, raindrop impact is less important in soil particle detachment (Bennett, 1974). Gully erosion has large erosion potential than previous two erosions due to sufficient depth and slope. Instream erosion is the direct detachment of sediment from channel banks and stream bed. During flood seasons, channel erosion can be the dominant sediment source in the stream channel (Meyer and Wischmeier, 1969; Haan et al., 1994; Merritt et al., 2003; Julien, 2010).

When the soil particles are detached, they become part of the flow and transported by water. The amount of sediment and distance are related to the sediment transport capacity depending on various factors. These variables could be grouped into two categories: (1) hydraulic parameters which effects on transporting capacity, such as channel geometry, width, depth, shape, slope, roughness, velocity distribution, turbulence, fluid properties, sediment characteristics and uniformity of discharge; and (2) various characteristics impacting on the quality and quantity of material made available for transport by the stream includes watershed topography, geology, rainfall duration and intensity, land use, soil type, particle size, resistance to wear, settling velocity, surface erosion, and sediment supply from tributaries. Various researchers have developed sediment transport formulas since the mid-1900s. The formulas based on transport capacity have commonly developed with 4 approaches: (1) formula based on sediment flux; (2) energy transport concept; (3) continuity equation for rill and inter-rill detachment; and (4) empirical equation and regression analysis (Haan et al., 1994; Julien, 2010).

2.1.2. Total Sediment Load in Streams

Einstein suggested that each sediment moving a cross-section of a stream must have eroded from somewhere in the watershed and it must be transported by water flow to the given cross-section (Chow, 1964). When the soil particles are transported, they could be classified into bedload, suspended load, or wash load. The bed load is a flux of sediments moving by rolling or sliding in the thin layer near bed which ranges from 1mm in the sand bed streams to tens of centimeter in gravel channels. The suspended load refers to sediment staying in suspension by enough turbulence velocity fluctuation. The wash load consists of particles smaller than the channel bed material and it commonly generated from the channel bank and upslope areas. This classification could change with fluid, sediment, and hydraulic conditions (Simons and Sentürk, 1976; Haan et al., 1994; Julien, 2010). The total sediment load in a channel could be classified in three ways (Julien, 2010).

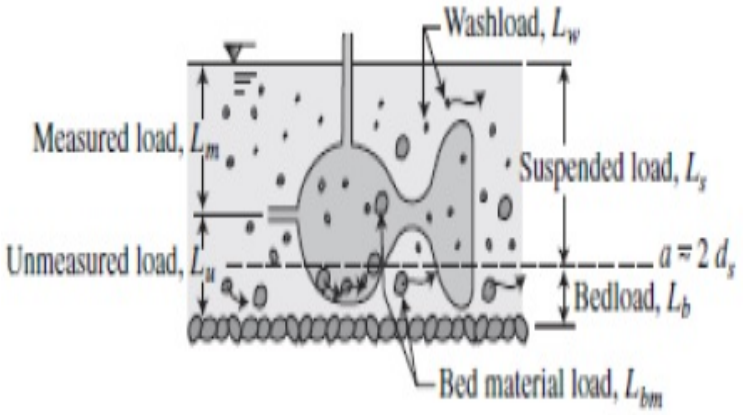

Figure 3. Sketch of ways to determine the total load (Julien, 2010)

(1) By the type of movement: The total sediment load L_T could be classified into the bed load L_b, and the suspended load L_s.

$$L_T = L_b + L_s \qquad \text{Eqn 2-1}$$

(2) By the method of measurement: The total sediment load is composed of the measured load L_m and the unmeasured load L_u. The most samplers can only measure from the water surface to near bed, not to bed surface. Therefore, the unmeasured load consists of the bedload L_b and some fraction of the suspended load.

$$L_T = L_m + L_u \qquad \text{Eqn 2-2}$$

(3) By the source of sediment: The total sediment load L_T can be divided into wash load L_W and the coarse sediment from the bed material load L_{bm}. Commonly, the 10th percentile of the bed material d_{10} is used as dividing size between bed material load and wash load. The reason why it is difficult to determine the total sediment load is that the wash load depends on sediment supply and sediment transport capacity. Also, as mentioned in the last chapter, there are many factors affecting sediment supply and sediment transport capacity (Simons and Sentürk, 1976; Julien, 2010).

$$L_T = L_w + L_{bm} \qquad \text{Eqn 2-3}$$

Einstein (Einstein, 1950) proposed the method to calculate total sediment discharge

$$q_t = q_b + \int_a^h Cv\, dz \qquad \text{Eqn 2-4}$$

where q_t is the total sediment discharge per unit width

q_b is the unit bed sediment discharge

C is the sediment concentration

v is the velocity at a distance above the river bed

a is the thickness of the bed layer

h is the flow depth

In *Figure 4*, this approach used bed load function to estimate the suspended load.

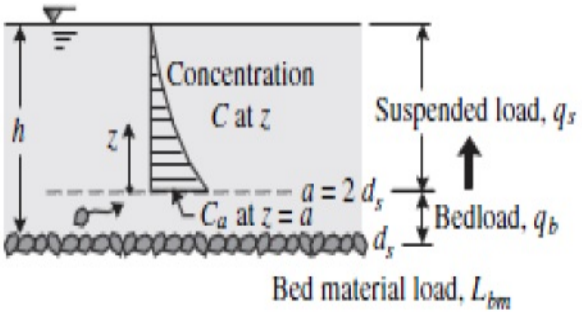

Figure 4. Sketch of the Einstein's method (Julien, 2010)

Keulegan (1938) proposed a logarithm velocity distribution for a hydraulic rough boundary.

$$\frac{v}{u_*} = \frac{1}{\kappa}\ln\left(\frac{z}{z_0}\right) \qquad \text{Eqn 2-5}$$

where v is the velocity at a distance above the river bed

u_* is the shear velocity

κ is the von Karman constant (assumed as 0.4)

z_0 is the vertical elevation at velocity is zero

From experiments, z_0 is the grain roughness height equal to k'_s = 30.

$$v_x = \frac{u_*}{\kappa}\ln\left(\frac{30z}{k'_s}\right) \qquad \text{Eqn 2-6}$$

Rouse suggested a formula for the equilibrium concentration profile (Rouse, 1937). He proposed that the relative concentration C as follows

$$\frac{C}{C_a} = \left(\frac{h-z}{z}\frac{a}{h-a}\right)^{\frac{\omega}{\beta_s \kappa u_*}} \qquad \text{Eqn 2-7}$$

where C_a is the reference concentration at a specified distance "a" from the bed

a is the bed layer thickness

β_s is the ratio of sediment to momentum exchange coefficient

ω is the settling velocity

The grain roughness height can be considered as sediment size d_s from Eqn 2-6. When the concertation is substituted with v_x from Eqn 2-5, the total unit bed sediment discharge from Eqn2-4 become

$$q_t = q_b + \int_a^h C_a \frac{u_*}{\kappa}\left(\frac{h-z}{z}\frac{a}{h-a}\right)^{\frac{\omega}{\beta_s \kappa u_*}} \ln\left(\frac{30z}{d_s}\right) dz \qquad \text{Eqn 2-8}$$

The reference concentration is calculated from the unit bed sediment discharge q_b transported in the bed layer of thickness, and the bed layer of thickness could be obtained from $2d_s$ *(Figure 4)*. The velocity at the top of the bed layer, $v_a = (u_*/\kappa) ln(30a/d_s) = 4.09(u_*/\kappa)$, Einstein used $v_a = 11.6u_*$. By subsisting $z^* = z/h\,, E = 2d_s/h\,, and\ R_0 = \omega/\beta_s \kappa u_*$, Eqn 2-8 is rewritten as dimensionless form.

$$q_t = q_b + \left[1 + I_1 ln\frac{30h}{d_s} + I_2\right] \qquad \text{Eqn 2-9}$$

where

$$I_1 = 0.216\frac{E^{R_0-1}}{(1-E)^{R_0}} \underbrace{\int_E^1 \left[\frac{1-z^*}{z^*}\right]^{R_0} dz^*}_{J_1(R_0)} \qquad \text{Eqn 2-10}$$

$$I_2 = 0.216\frac{E^{R_0-1}}{(1-E)^{R_0}} \underbrace{\int_E^1 \left[\frac{1-z^*}{z^*}\right]^{R_0} lnz^* dz^*}_{J_2(R_0)} \qquad \text{Eqn 2-11}$$

The Einstein's method has been commonly used to estimate the total sediment flux, and it also has been modified and developed by various researchers (Colby and Hembree, 1955; Lara, 1966; Burkham and Dawdy, 1980; Shen and Hung, 1983; Holmquist-Johnson, 2006; Shah-Fairbank, 2009). Colby and Hembree (1955) developed the MEP to estimate the total sediment load in the sand bed of Niobrara River, Nebraska with a depth-integrated suspended sediment sampler and a sample of the bed material through sieve analysis. Therefore, the Rouse number R_o is estimated from the total load determined based on measured suspended sediment and the measured bed

material (Colby and Hembree, 1955). Lara (1966) proposed that Colby's method is subjective to determine R_o, so a least squares regression is used to determine the R_o. Lara suggested that the Rouse number does not always vary with the settling velocity to a power $C_z = 0.7$ from the calculated R_o.

$$R_o = C_1(\omega)^{C_2} \qquad \text{Eqn 2-12}$$

where C_1 and C_2 are the constants from the regression analysis

The Bureau of Reclamations Automated Modified Einstein Procedure (BORAMEP) has been developed by Holmquist-Johnson (2006) from Lara's modification. This computer program does not require judgment from engineers for the Rouse number. It calculated the total sediment load with inputs of at-a-station hydraulic data, suspended sediment concentration, and particle size distribution of suspended and bed material (Shah-Fairbank, 2009; Julien, 2010). Shah-Fairbank (2009) reviewed and found three main errors on BORAMEP. First, it could not determine total load when the bed was armored because BORAMEP needs a minimum of two overlapping bins. Second, it is possible to generate a negative relationship between the Rouse number and settling velocity by BORAMEP. Finally, the program could underestimate the total sediment discharge with estimated R_o. In somecases, the calculated total load was less than the measured load.

2.1.3. Sediment Deposition in Watershed

Sedimentation is the deposition of soil particles in suspension from the fluid. Deposition of transported sediment in overland flows or in a stream can occur anywhere in the stream or even before reaching the stream. When the transport capacity of runoff is not sufficient to sustain transport, sediment is deposited. To quantify the amount of sediment deposition, the sediment delivery ratio S_{DR} has been defined as

$$Y = A_T S_{DR} \qquad \text{Eqn 2-13}$$

where Y is the sediment yield at a given stream

A_T is the gross erosion from the watershed upstream of the measuring point

The annual soil loss A_T is commonly obtained from the gross erosion which is composed of sheet and rill erosion. The sediment delivery ratio tends to increase with increasing basin size as shown in *Figure 5*.

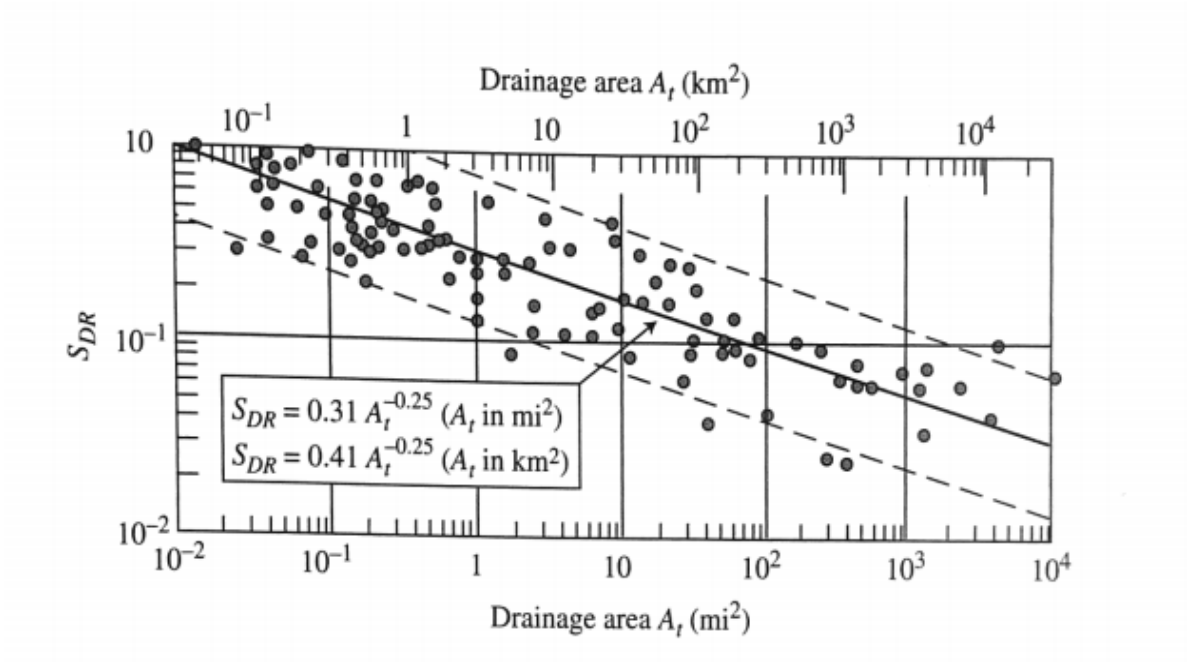

Figure 5. Sediment delivery ratio (modified after Boyce, 1975)

The magnitude of sediment delivery ratio is influenced by many factors such as geomorphological, and environmental factors (Walling, 1983). Many empirical relationships between the sediment delivery ratio and watershed area have been analyzed (*Table 1*).

*Table 1.*Various equations between sediment delivery ratio and watershed area

Author	Equation
Boyce (1975)	$S_{DR} = 0.4724A^{-0.125}$
Vanoni (1975)	$S_{DR} = 0.3750A^{-0.238}$
Renfro (1975)	$S_{DR} = 6.01A^{-0.142}$
Bagarello et al. (1991)	$S_{DR} = 5.371A^{-0.695}$
Julien (2010)	$S_{DR} = 0.41A^{-0.25}$ (A in km^2)

Ferro and Minacapilli (1995) suggested the slope of relationship could be up to -0.7. *Figure 6* illustrated the wide range of delivery ratios from various individual studies. These uncertainties result from the lack of a generally-applicable predictive technique,i.e. the simple relationship between sediment delivery ratio and gross erosion (Walling, 1983).

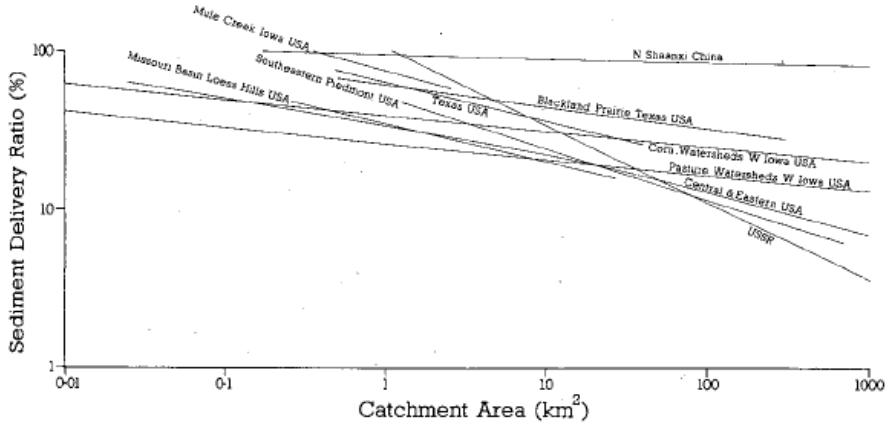

Figure 6. Relationships between sediment delivery ratio and watershed area (Walling, 1983)

Various researchers have analyzed the relationship by considering other watershed characteristics (*Table 2*). The Forest Service developed the method to predict sediment delivery ratio with a single storm event. This graphical method used delivery distance, slope shape, surface roughness, slope gradient, surface runoff texture of the eroded material, and percent ground cover to determine the sediment delivery ratio. The simple relationship of sediment delivery ratio has some limitations. To be specific, it can generate temporal and spatial lumping problems (Dickinson and Wall, 1977). The delivery ratio could vary widely for a given region due to the seasonal distribution of precipitation, and it causes some problems in the temporal attenuation of sediment delivery resulting from storage and remobilization. Also, a single number of sediment delivery ratio could not explain the spatial diversity of land use, soil conditions, and topographic. Since the sediment delivery ratio includes many processes, it is difficult to forecast future changes and to explain the precise influence of various factors.

Walling (1983) suggested that improvement of understanding and representation of the sediment delivery process is important because of these problems.

Table 2. Example of proposed equations between sediment delivery ratio and watershed characteristics (after Walling, 1983)

Author	Region	Equation
Maner (1958)	Kansas, U.S.A.	$\log S_{DR} = 2.962 + 0.869logR - 0.854logL$
Roehl (1962)	Southeastern U.S.A.	$\log S_{DR} = 4.5 - 0.23log10A - 0.510 \times cologR/L - 2.786logBR$
Williams and Berndt (1972)	Brushy Creek, Texas, U.S.A.	$S_{DR} = 0.627 \times SLP^{0.403}$
Renfro (1975)		$\log S_{DR} = 2.94259 + 0.82362logR/L$
Mutchler and Bowie (1976)	Pigeon Roost Creek, Mississippi, U.S.A.	$S_{DR} = 0.488 - 0.006A + 0.01RO$
Williams (1977)	Texas, U.S.A.	$S_{DR} = 1.366 \times 10^{-11} A^{-0.1} R/L^{0.363} CN^{5.444}$
Jinze and Qingmei (1981)	Dali River Basin Shaanxi, China	$S_{DR} = 1.29 + 1.37lnR_c - 0.025lnA$

R=basin relief; L=basin length; A=basin area; R/L=relief/length ratio; BR=bifurcation ratio, SLP=% slope of main stem channel; CN=Soil Conservation Service curve number; RO=annual runoff; R_c=gully density;
Note: Units vary between equations

2.1.4. Reservoir Sedimentation

Another common method to estimate specific degradation is based on reservoir surveys. A reservoir is the main place for sediment deposition in a watershed. When the water in the natural stream enter reservoirs, the stream flow depth increases and the flow velocity decreases. It resulted in a decrease of transport capacity of the stream and settling of sedimentation. The amount of deposited sediment depends on the sediment production from the upstream watershed, the rate of transportation, and the mode of deposition (Julien, 2010). To quantify the amount of sediment trapped in the reservoir, the trap efficiency T_{Ei} has been used with the various method. The most popular method for trap efficiency was developed by Brune (1953). According to the relationship curve between trap efficiency and reservoir capacity-inflow ratio included measurement from 40 ponded reservoirs (*Figure 7*).

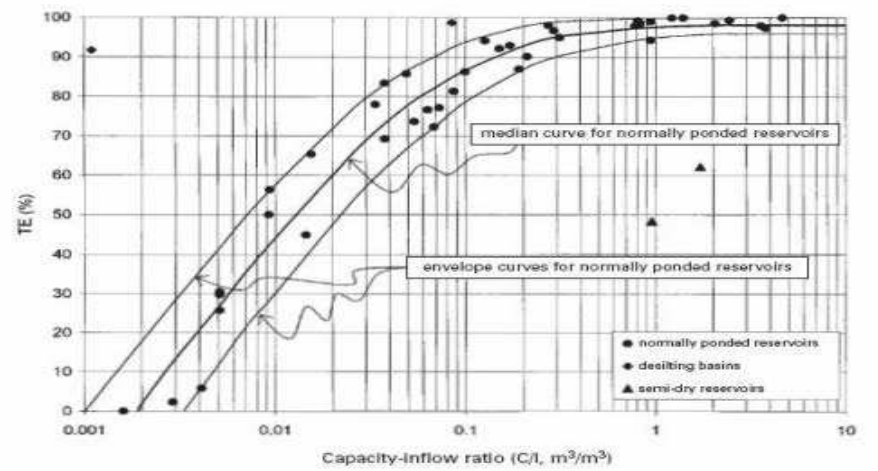

*Figure 7.*Trap efficiency related to a capacity-inflow ratio (Brune, 1953)

Heinemarm (1981) tested the Brune's relationship to small agricultural 20 reservoirs, and his resulted proposed lower T_{Ei}. Churchill (1948) proposed a relationship between suspended sediments in the reservoir and the sediment index of suspended sediment measurement from near reservoirs. The index estimated as retention time divided by the mean flow velocity through the reservoir. Yang (2006) suggested the general guideline to use the Brune's method for large reservoirs and the Churchill method for the small reservoir and settling basin (*Figure 8*).

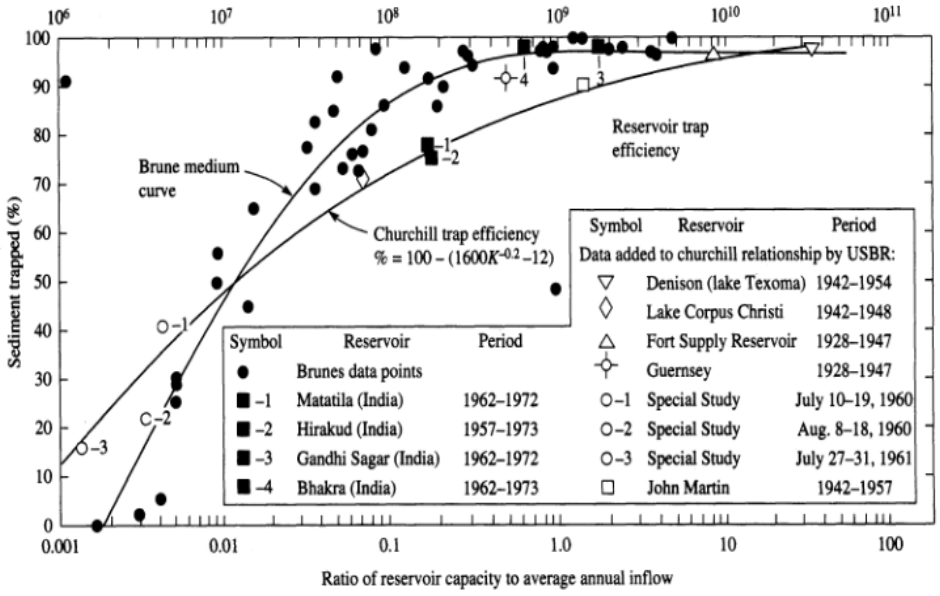

*Figure 8.*Trap efficiency versus reservoir capacity to average inflow (Yang, 2006)

Borland (1971) developed a new method to compute trap efficiency with a fraction of material and settling velocity. Julien (2010) also derived a similar trap efficiency formula with consideration of grain sizes of a given sediment fraction.

$$T_{Ei} = 1 - e^{-\frac{1.055L\omega}{Vh}} \quad \text{Eqn 2-14}$$

$$T_{Ei} = 1 - e^{-\frac{L\omega}{Vh}} \quad \text{Eqn 2-15}$$

where *L* is the total length of the reservoir

ω is the falling velocity

V is the mean velocity f flow

h is the flow depth

Specific degradation is the ratio of sedimentation yield divided by watershed area. Kane and Julien (2007) suggested that specific degradation from the field measurement of US reservoirs resulted as a function of total annual rainfall and drainage area as shown in *Figure 9*.

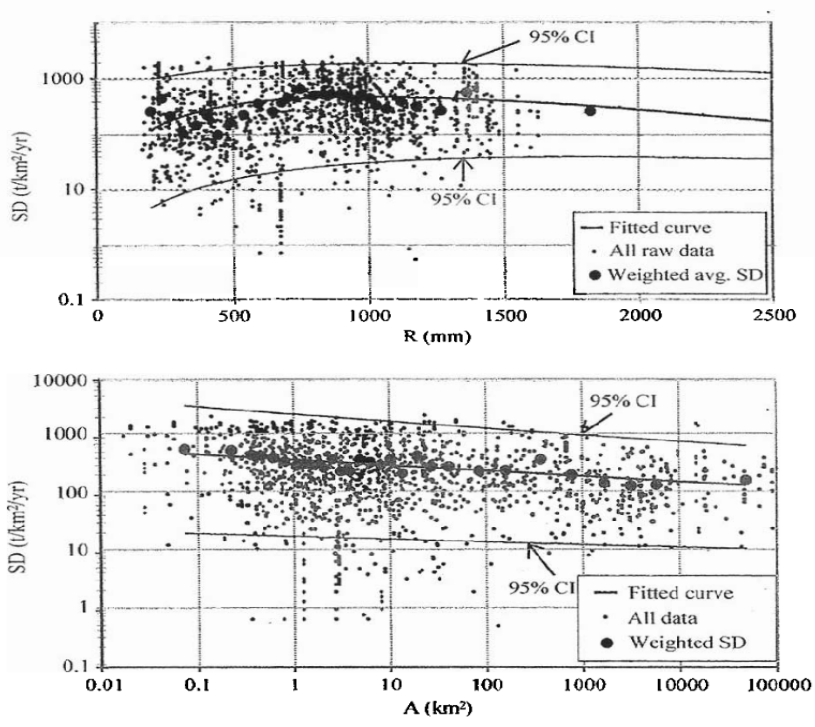

*Figure 9.*Specific Degradation as a function of annual rainfall and area (Kane and Julien, 2007)

When the reservoir sediment deposited data is used as sediment yield, the record length is important since the sediment yield varied from year to year. Additionally, the small watershed of the reservoir could not adequately describe the characteristics of reservoir watershed (Haan et al., 1994).

2.2. Erosion and Sediment Model

Various types of models exist to simulate erosion and sediment delivery. These models have different processes, consideration, and input data. To use the most appropriate model, the user should consider the objective and the characteristics of the catchment. Generally, the models are classified into three main categories: (1) empirical or statistical model; (2) conceptual model; and (3) physical model. The empirical model is commonly based on analysis of observation, and seek to find response between characteristics and observation (Wheater et al., 1993). Conceptual models include a general description of catchment processes as a series of internal storages. Physical models are based on the solution of the physical equation for sediment and streamflow (Merritt et al., 2003). This dissertation is focusing on empirical and statistical models for erosion and sediment yield.

2.2.1. Universal Soil Loss Equation (USLE)

The Universal Soil Loss Equation has been widely used worldwide to estimate annual soil erosion from hill slope and gross erosion for sediment yield. Wischmeier and Smith (1965) used annual data from 10,000 test plots from agricultural areas in the U.S. The test plots were managed with a standard of 22m flow lengths. Wischmeier and Smith (1978) modified the equation from 1965 as

$$A = RKLSCP \qquad \text{Eqn 2-16}$$

where A is the average annual soil loss

R is the rainfall erosivity factor

K is the soil erodibility factor

L is the field length factor

S is the field slope factor

C is the cropping management factor

P is the conservation practice factor

The model has been modified and enhanced during the past 50 years by various researchers. Williams (1975) developed the Modified Universal Soil Loss Equation (MUSLE), and it replaced the rainfall factor by a runoff factor from 778 storm runoff events in 18 watersheds. The Revised Universal Soil Loss Equation (RUSLE) upgraded the USLE by focusing on better parameter estimation (Renard et al., 1997). In summary, the RUSLE revised soil erodibility factor depends on seasonal weather changes, the slope gradient and length, and a new procedure to calculate the cover vegetation factor. Both USLE and RUSLE are possible to estimate the average annual soil loss with a simple equation, but there are a number of limitations for both empirical models. For instance, the models are not event-based, so that mean annual soil losses are considered. Also, the models only consider upland erosion. It means that the gully erosion which can change as sheet and rill erosion and deposition of sedimentation are not considered in the models. In the case of applications of USLE outside the US, the parameters occasionally need adaptation (Lane et al., 1995; Evans and Loch, 1996; Merritt et al., 2003; Julien, 2010).

2.2.2. Geographic Information System and Soil Erosion Modeling

A Geographic Information System (GIS) is a system that visualizes, analyzes, interprets, stores, analyzes and manages all type of spatial and geographical data by a link to coordinates or locations. Characteristics of the data can be stored as attributes, and each variable in the system

supports the application. Therefore, the system is possible for users to understand the relationship, patterns, and trends of data (ESRI, 2011). The system has been widely used for hydrologic and hydraulic modeling since the 1970s with utilized grid cell and raster storage of information. The use of raster representing terrain leads to a large database or digital elevation model (DEM). Analysis of DEM enables the user to define streams networks and boundaries of the watershed. With the analysis of DEM, non-topographic information could include hydrologic attributes, such as catchment areas, flow lengths, land slope, surface roughness, soil type, and land cover, land use, ground cover, groundwater conditions, and their characteristics or below the land surface (Moore et al., 1991; Tarboton et al., 1991; DeVantier and Feldman, 1993). To overcome the spatial lumping problem, the GIS system and grid approach have been used for sediment yield calculation. *Figure 10* illustrates the process of RUSLE with GIS.

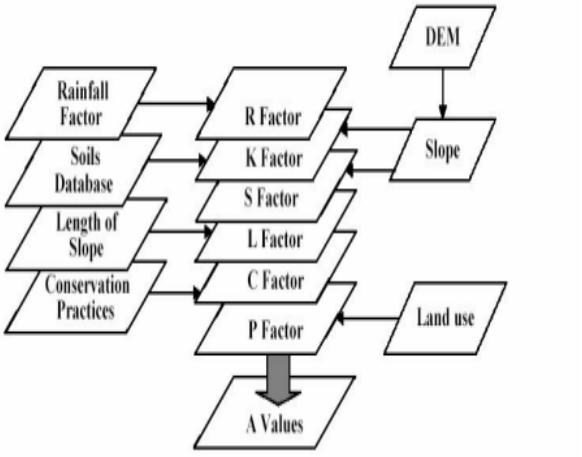

Figure 10. Procedures of RUSLE with GIS (Kim, 2006)

With the numerous advantages of GIS, various researchers have tried to obtain more reasonable results of sediment yield. Kane (2003) said that a negative trend between specific degradation and the slope is not as intuitively expected. But often a steep mountain watersheds are forested, while floodplains are covered by urban and agriculture.

Julien and Frenette (1987) used the correction factor to extend the applicability of the USLE to large watershed. Molnár (1997) compared soil loss erosion to different grid size cell and concluded the large grid cell size underestimates soil loss. Both papers suggested the fine-meshed grid is required to reliable sediment yield. This resolution of DEM problem is directly related to L factor in the USLE/RUSLE so that the calculating method and resolution of DEM are very important to the accuracy of L factor (Thompson et al., 2001). Various methods for L and S factors for GIS has been suggested; Moore and Burch (1986) used the unit stream power method and Cowen (1993) proposed a method based on triangulated irregular networks (TIN). Additionally, Desmet and Govers (1996) provided a contributing area method, and Hickey (2000) suggested the grid cumulating method. Liu and his research team (2011) tested various methods for L factor on various resolutions, and they concluded that for higher resolution DEM, L calculation methods are not very important when applied to low resolution. Kling (1975) calculated gross erosion by USLE and described a sediment movement as a grid in the Canadarago Lake watershed in New York, US. Numerous GIS analyses with the USLE/RUSLE have been carried out by Dr. Julien's research team in Korea (Kim, 2006), Malaysia (Teh, 2011), Afghanistan (Sahaar, 2013), and Congo (Goy, 2015).

2.2.3. Effect of Watershed Characteristics on Erosion and Sediment Yield

Numerous researchers have investigated the relationship between sediment yield and watershed characteristics using a statistical model. Even though statistical models would have limitations such as temporal and spatial lumping problems, they are able to quantify the relative importance of individual parameters. Also, significant parameters could be used for other conceptual and physical models (Vente et al., 2011). The author organized various factors in the classification presented in *Table 3*. The classification is divided into: (1) Morphometry (Linear

aspect, Aerial aspect, and Relief Aspect); (2) Climatology; (3) Pedology; (4) Land use; and (5) Hydraulic factor related to discharge. In *Table 4*, it provides various regression equations for sediment yield from previous researchers with selected various factors in *Table 3*. The variables are finally selected for their purpose and methods for measurement and analysis. The regression models provide a wide range of the coefficient of determination (0.08~0.97). The slope of the same factor in other equation can change from positive to negative, vice versa. For example, the watershed area has a positive correlation with sediment yield; however, the relationship with specific degradation is negative. It would be depending on area variation of samples.

*Table 3.*Considered variables in the empirical model for sediment yield and specific degradation

Classification		Factors
Morphometry	Linear Aspect	Stream order, Total drainage length, Length Ratio
	Aerial Aspect	Watershed area, Drainage density, Catchment form, Drainage basin order,
	Relief Aspect	Relief ratio, Specific runoff, Maximum Elevation, Altitude, Hypsometric Index, Index of ruggedness, Distance between valley outlet and highest point at the divide Difference between highest and lowest point
Climatology		Mean annual precipitation, precipitation erosivity index Maximum mean monthly precipitation, Mean annual precipitation, Mean annual temperature, Annual temperature range, Fournier index, Maximum mean monthly precipitation, Precipitation temperature ratio
Pedology		Lithology Index, Soil erodibility factor, Proneness to erosion parameter, Percentage with erodible lithology, Percentage of sieve analysis results
Land use	Vegetation	Vegetation group index, Percentage of forest cover, Percentage of forest transition, Percentage of bush/shrub cover
	Anthropogenic	Areas with terrace, Percentage of orchard, Percentage of poorly vegetated land, Percentage of agricultural land, Percentage of urbanized area
	Others	Percentage of snow ice cover, Flood plain
Hydraulic factors related to discharge		Torrential Index, Mean annual discharge, Mean maximum river discharge, Mean annual runoff, Exceedance Probability
Other		Index for gully and bank erosion,

Table 4. Published statistical model for the prediction of sediment yield (revised after Maner, 1958)

Author	Regression model	Location	R^2	N	**Data
Langbein and Schumm (1958)	$SD = 10P^{2.3}/1 + 0.0007P^{3.33}$ $SD = 20P^{2.3}/1 + 0.0007P^{3.33}$	US		170 163	River Reservoir
Fournier (1960)	$* SD = 6.14p^2/MAP - 49.78;\ (low\ relief, p^2/MAP \leq 20)$ $SD = 27.12p^2/MAP - 475.4;\ (low\ relief, p^2/MAP > 20)$ $SD = 52.49p^2/MAP - 513.2;\ (high\ relief, MAP > 600$ $SD = 91.78p^2/MAP - 737.62;\ (high\ relief, 200 < MAP < 600)$	Global		78	River data
Roberts (1973)	SD=1.45P-0.78	South Africa	0.78	15	
Flaxman (1974)	$\log(SD + 100) = 6.21 - 2.19 \log\ (PT + 100) + 0.06 \log\ (S + 100)$ $-0.02 \log(CS + 100) + 0.04(AI + 100)$	US			
Jansen and Painter (1974)	$logSD = 4.35 + 1.53logD - 0.3logA + 0.29logRR - 3.42logT\ (A)$ $logSD = 12.13 - 0.34logD + 1.59logH + 3.7logP + 0.94logT - 3.5logV\ (B)$ $logSD = -3.08 + 1.0logD + 0.69logRR + 4.29logT - 5.03logB\ (C)$ $logSD = -5.07 + 0.51logH + 2.22logP - 3.71logV + 1.45logG\ (D)$ $logSD = 6.97 + \ 0.44logD - 1.67logA + 3.86logH - 1.67logRR + 3.43logT\ (E)$ $logSD = -3.06 - 1.13logA + 0.59logH + 1.1logRR + 3.06logP - 3.05logV(F)$ $logSD = -2.03 + 0.1logD - 0.31logA + 0.75logH + 1.10logP + 0.37logT$ $-2.32logV + 0.79logG\ (f)$;from A to F is classified with climate condition (Watershed area > 5000 km^2)	Global	0.94 0.86 0.63 0.64 0.76 0.95 0.58	79	Suspended load
Dendy and Bolton (1976)	$SD = 1280Q^{0.46}(1.43 - 0.26logA); for\ Q < 2\ in/year$ $SD = 1958Q^{-0.055Q}(1.43 - 0.26logA); for\ Q > 2\ in/year$ (with SD in t/mi^2, Q in inches, and A in mi^2)	US	0.75	505	
Demmak (1982)	$SD = 26.62LI + 5.07PI + 9.774Tor - 593.56$	Algeria	0.92	30	River data
Allen (1986)	$SD = 0.39DD + 1.85; with\ DD\ based\ on\ permanet\ and\ ephemeral\ stream$ $SD = 2.81DD + 1.81; with\ DD\ based\ on\ permanenet\ stream$ $SD = 0.75 + 1.81; with\ DD\ based\ on\ aerial\ photos$	US	0.02 0.08 0.83	17	
Ichim (1990)	$\log SY = 4.50 - 0.18logO + 0.75logA + 0.04 \log FF + 0.10 \log DD$ $+0.33 \log RR + 0.54logMAP; Subcarpathians$ $\log SY = 7.99 - 0.81logA - 0.31 \log BR + 0.15 \log DD - 0.15 \log RR$ $+0.09logFor - 1.57logMAP; Flysch\ Mountain$	Romania	0.74 0.92	63 36	River data

Table 4. Continued previous page

Author	Regression model	Location	R^2	N	**Data
Probst and Suchet (1992)	$lnSD = 4.78 + 54 \times 10^{3}K + 4 \times 10^{-3} - 5.6 \times 10^{-5}A$	Maghreb	0.71	36	River
Bazzoffi et al. (1997)	$SD = 497.61 - 1.74A + 129.42E - 12.61S - 0.29MAP + 121.18DD$	Italy	0.82	42	Reservoir
Hovius (1998)	$lnSD = -0.416lnA + 4.26 \times 10^{-4}H_{max} + 0.15T_m + 0.095T_{range} + 0.026R + 3.585$	Global	0.49	86	
Ludwig and Probst (1998)	$SD = 0.02(R \times S_r \times Four)$	Global	0.91	58	River
Verstraeten and Poesen (2001)	$SD = 25A^{-0.4}$ $(with\ area\ in\ ha)$ $SY = 25A^{0.6}$ $(with\ area\ in\ ha)$ $\ln SD = 3.72 - 0.72lnA - 0.84lnHI + 0.11lmSL$ $(with\ area\ in\ ha)$ $\ln SY = 0.21L + 22.2HD - 988HI$ $(with\ area\ in\ ha)$	Belgium	0.64 0.80 0.76 0.92	26	Reservoir
Verstraeten et al. (2003)	$20.6RR + 18D - 14For - 33Foma - 31Orch - 173PV$	Spain	0.80	22	Reservoir
Syvitski et al. (2003)	$Q_s = 2 \times 10^{-5}A^{0.5}HD^{1.5}e^{0.1T_m}$ $(for\ Polar\ region, T_m < 0℃)$ $Q_s = 6.1 \times 10^{-5}A^{0.55}HD^{1.12}e^{0.07T_m}$ $(for\ temperate\ region, latitude > 30^{\circ}N)$ $Q_s = 0.31A^{0.40}HD^{0.66}e^{-0.1T_m}$ $(for\ tropical\ region, 0 - 30^{\circ}N)$ $Q_s = 0.57A^{0.50}HD^{0.37}e^{-0.1T_m}$ $(for\ tropical\ region, 0 - 30^{\circ}S)$ $Q_s = 1.3 \times 10^{-3}A^{0.43}HD^{0.96}(for\ temperate\ region, latitude > 30^{\circ}S)$	Global	0.76 0.63 0.58 0.67 0.54	48 162 62 42 26	
Haregeweyn et al.(2005)	$SY = 690TDL - 0.58SWC$ $SD = 0.86S - 0.269SWC + 10$	Ethiopia	0.96 0.80	11 11	Reservoir
Tamene et al. (2006)	$logSD = 2.33 + 0.007GulB + 0.003EL + 0.002RG - 0.007Bush$	Ethiopia	0.96	11	Reservoir
Restrepo et al. (2006)	$logSD = -0.88 + 0.81logQ - 0.39logQ_{max}$	Colombia	0.58	32	
Kane and Julien (2007)	$SD = 0.02MAP^{1.7}e^{-0.0017MAP}$ $SD = 410A^{-0.009}$ $SD = 402e^{-0.13S}$	US	0.06 0.06 0.12	1463 1463 551	Reservoir
Syvitski and Milliman (2007)	$Q_s = 0.02B \times Q^{0.31}A^{0.5}R \times T_m, for\ T_m \geq 2℃$ $Q_s = 0.04B \times q60.31A^{0.5}R, for\ T_m < 2℃$	Global	0.96	488	

Table 4. Continued previous page

Author	Regression model	Location	R^2	N	**Data
Faran Ali and De Boer (2008)	$SD = 654 + 38.4LC_s + 10.2p - 3787HI + 0.82EL_{ch} - 5711R_{pk}$; whole basin $SD = 319 + 25.4$; whole basin $SD = -522 + 0.172HD$; main Indus River $SD = 5445 + 21.3LC_s + 0.915EL_{ch} - 4916HI$; upper glacierized subbasin $SD = -8867 + 9.72MAP$; lower, monsoon subbasin	Indus River	0.90 0.73 0.90 0.97 0.98	14 12 5 11 3	
Roman et al. (2012)	$Q_s = e^{-20.1}A^{1.06}Ur^{0.32}P_{May}^{2.44}P_{seas}^{0.34}\%NO200^{1.77}B^{0.199}$	Eastern US	0.80	590	Suspended load
Vanmaercke et al. (2013)	$SD = 1.49e^{1.24PGA}MLR^{0.66}e^{-0.05For}R^{0.24}$	Africa	0.40	507	River and Reservoir
Wuttichaikitcharoen and Babel (2014)	$SD = 0.0068DSR^{1.8506}$ $SY = 28.74A^{1.1636}$	Thailand	0.08	30	Suspended load

R^2 correlation coefficient, *N* number of observations, *A* catchment area (km^2), *AI* aggregation index, *Ag %* of agricultural land, *B* factor representing glacial erosion, lithology and reservoir or lake trapping efficiency, *BR* bifurcation ratio, *Bush %* bush/shrub cover, *CS %* soil particles coarser than 1 mm, *D* distance between valley outlet and highest point at the divide (km), *DD* drainage density (km km^{-2}), *DSR*, dry season rain fall, *E* erodible surface area (km^2), *EL %* with erodible lithology, *FF* catchment form factor (−), *Foma %* transition forest Matorral, *For %* forest cover, *Four* fournier Index (mm), *G* proneness to erosion parameter, *GulB* index for gully and bank erosion, *H* altitude, H_{max} maximum elevation (m), *HI* hypsometric integral, *HD* difference between highest and lowest point (m), *K* soil erodibility factor, *L* valley length (km), *LI* Lithology Index, *LR* length ratio, LC_s % snow/ice cover, *P LR/BR, MAP* mean annual precipitation (mm), *MLR* mean local relief, *O* catchment order, *Orch %* orchards, *p* maximum mean monthly precipitation (mm), *PGA* peak ground acceleration with the exceedance probability of 10% in 50years. *PI* precipitation erosivity index, *PT* precipitation temperature ratio (mm/°C), *PV %* poorly vegetated, *Q* mean annual runoff (m^{3}s^{-1}), Q_a mean annual discharge (km^{3}a^{-1}), Q_{max} mean maximum river discharge (m^3 s^{-1}), *Qs* long-term sediment load (kg s−1), *R* specific runoff (mm a^{-1}), *RG* index of ruggedness (km^{-1}), *RR* relief ratio (m km^{-2}), *S* average slope gradient (%), *Sr* average slope gradient (radian), *SL* total stream length (m), *SWC %* of catchment treated with soil and water conservation measures, *SY* absolute sediment yield (t a^{-1}), *T %* area with terraces, *T* and T_m mean annual temperature (°C), T_{range} annual temperature range (°C), *TDL* total drainage length (km), *Tor* torrentiality index, *Ur %* of urban, *V* natural vegetation group index, *W* average catchment width (km). *%NO200* Average value of percent by weight of soil material less than 3 in. in size and passing a No. 200 sieve

*SSY area-specific sediment yield (t km^{-2} a^{-1}) changes as SD (t km^{-2} a^{-1}) in (Maner, 1958)

** Data means how to calculate SD or SSY or where it comes from river or reservoir deposition

Some researchers suggested that the human activities (i.e. land use and reservoir) effects on sediment yield and the overall sediment budget of a catchment and the sediment output should be considered together to understand the impact of land use on sediment yields (Knox, 1977; Walling, 1999; Boix-Fayos et al., 2008).

2.3. Existing Models for Sediment Yield and River Characteristics in South Korea

In this section, the author focuses on the existing models (especially the regression models) for predicting sediment yield in South Korea. The existing models have been used for dam construction and channel stabilization and they are organized in *Table 5*.

Table 5. Regression model for sedimentation in South Korea

Author	Models	R^2	N	Data
You and Min (1975)	$logV_r = 0.179 + 0.108logA - 6.72logP + 2.2logS$		30	Reservoir
*Ryu and Kim (1976)	$V_r = 1.43(C_d/A)^{0.531}$ $V_r = 672.61P^{0.024}$ $V_r = 267.21S^{0.587}$		9 9 9	Reservoir
*Saemaeul (1978)	$V_s = 255.4A^{0.1816}C^{0.5774}$			Reservoir
Yoon (1981)	$V_s = 1{,}334.08A^{0.8}E_t^{6.2668}$	.92		Reservoir
*Ahn and Lee (1984)	$V_s = 1{,}744{,}301.05A^{0.02}E_t^{17.017}S^{0.429}S_f^{0.684}A_g^{-1.157}$ (1) $V_s = 66{,}023.72A^{0.546}E_t^{11.06}S^{0.068}S_f^{0.353}A_g^{0.877}$ (2) $V_s = 1{,}488.675A^{0.934}E_t^{4.985}A_g^{0.122}$ (3)			Reservoir
KICT MOC(1992)	$SD = 972D^{1.039}M^{-0.825};\ for\ 200 < A < 2000$ $SD = 17.6D^{2.572}R^{0.847}M^{-0.938};\ for\ 200 < A < 2000$ $SD = 8668A^{-0.896};\quad for\ A < 200$ $SD = 23{,}564A^{-1.341}{A_f}^{0.403}K^{0.582};\ for\ A < 200$		8	MEP with River
Yoon and Choi MOC (2011)	$V_r = 7.0632 \times 10^{11}D^{1.72}K^{5.45}{C_{usle}}^{-3.65}S^{-7.2}M^{-0.85}$	.95	10	Reservoir

A watershed area (km^2), A_f forest area (km^2), A_g duration of deposition of sediment (yr), *C* initial reservoir capacity, C_{usle} cover management factor, *C/A* initial reservoir capacity/ area, C_d/A designed reservoir capacity/area, *D* drainage density (km/km^2), E_t trap efficiency, *I* annual inflow in reservoir(mm), *K* soil erdobility factor, *M* bed material size (mm), *P* mean annual precipitation, *S* average watershed slope (%), *SD* specific degradation (tons/km^2/yr), S_f watershed shape factor, V_s annual deposited sediment (m^3/yr), V_r specific sediment deposit (m^3/km^2/yr)
* Reference from the report (MOC, 1992)

In South Korea, three methods have been mainly used to estimate the amount of sedimentation. First, the total sediment load is calculated with the Flow Duration-Sediment Rating Curve (FD-SRC) method, and SRC was commonly generated with the Modified Einstein Procedure based on stream measurements of flow discharge and sediment concentration. Second, the specific degradation is estimated with sediment deposition in reservoirs located on similar watersheds. Third, various models have been used to estimate sedimentation. In *Table 5*, Empirical models for South Korea also show a wide variation in slope. For example, the coefficient for annual precipitation varied from -6.72 to 0.024, and the coefficient for the watershed slope varied from -7.2 to 2.2. This can result in large discrepancies in the calculations. Specifically, You and Min and Ryu and Kim tested regression equation on very small reservoirs in the Jinyang and Sapgyo stream. The regression equation based on the specific small region could not represent the sediment yield in other regions. In *Figure 11*, the fluvial system is conceptually classified into 3 zones (Schumm, 1977; Julien, 2002).

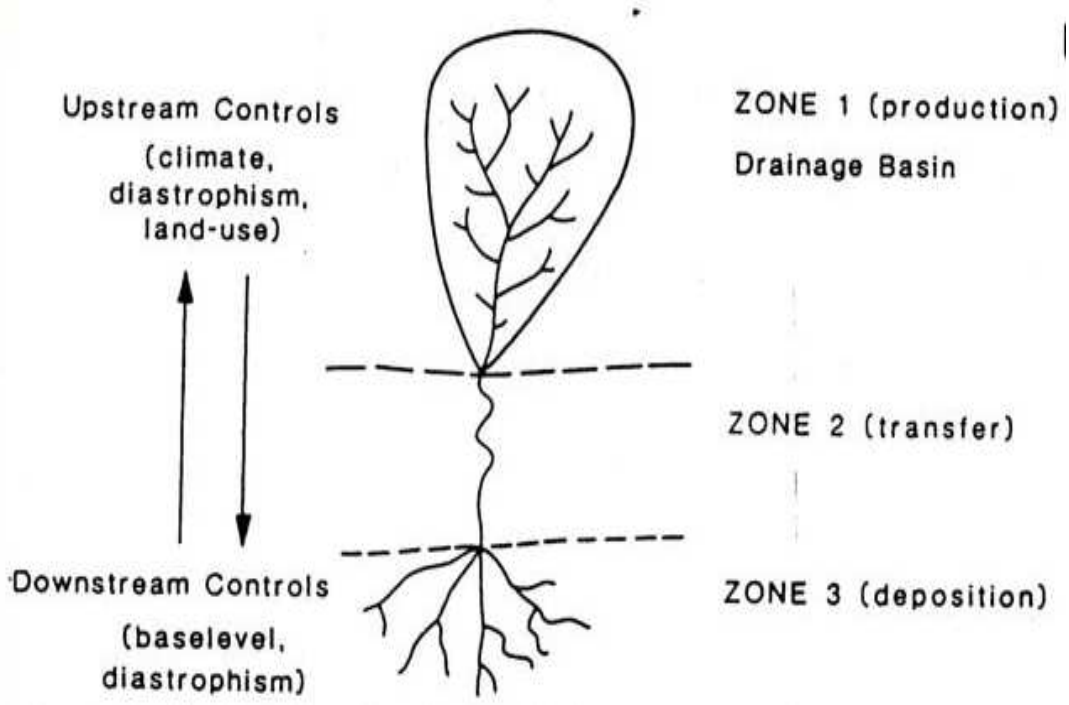

*Figure 11.*The fluvial system (Schumm, 1977)

Zone 1 is the erosional zone in upland areas with sediment production into steep bed streams and rivers. Mountain streams flow rapidly through steep slopes in a V-shape valley. In the case of South Korean rivers, many upstream mountain headwaters flow directly on bedrock streams. Zone 2 is a transport zone of water and sediment with long sand-bed river. The transfer zone (i.e. Zone 2) is common in low elevations, so streams merge and flow down through mild slope. Also, this zone is relatively stable than other zones, but a dynamic response in terms of degradation and aggradation locally occurs. Korean rivers are almost alluvial rivers (Woo et al., 2015). Zone 3 is commonly a mouth of the river, and it has fluvial fan between the sea and river. Also, clay is dominant in this area. This portion of the fluvial system functions as the deposition. This dissertation focuses primarily on the first two zones and channels in zone 1 will be referred to as streams and those in zone 2 will be called rivers.

Chapter 3
Specific Degradation in South Korean Rivers and Reservoirs

This chapter describes methods to estimate the total sediment load and specific degradation of rivers and reservoirs in South Korea. Also, the existing models were validated from the estimated specific degradation.

3.1. Study Sites

As mentioned in the introduction, South Korea has unique characteristics for climatic and topographic characteristics, that is, 65% of precipitation occurs in the summer season and 70% of the area of Korea consists of mountains and steep upland areas. There are 5 main rivers (i.e. Han, Nakdong, Geum, Yeongsan, and Seomjin) and they flow generally from east to west except the Nakdong River (*Figure 12*). In terms of land use, most of the watershed is covered with forest and plains are used mostly (65%) as paddy fields which cover 13% of the total national land surface. This characteristic is favorable to hold water and sediment during floods. Korean researchers (Woo et al., 1991; Yoon and Woo, 2000) have suggested that South Korea has relatively low sediment yield, so suspended sediment is small when compared to western US. However, most sedimentation problems happen during the biggest monsoon events (i.e. typhoon). The sedimentation problems are not at large-scale but often occur at specific locations (Yoon and Woo, 2000). In this chapter, the specific degradation of 70 gauging stations was estimated from sediment measurements, and the existing model was validated from the estimation.

3.2. Data Description

The major reservoirs with multipurpose dams (green triangle) were constructed in the mountain region.

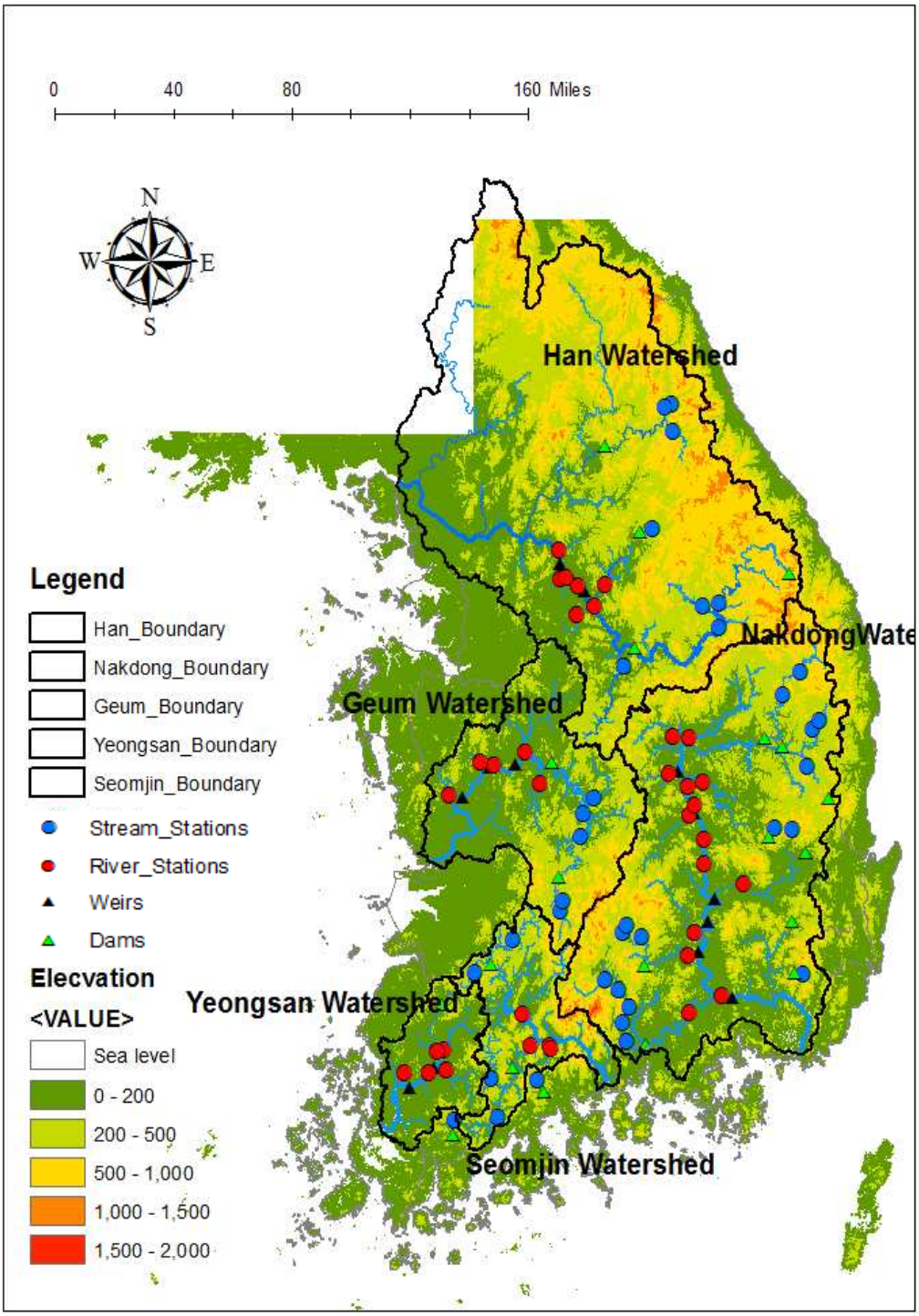

*Figure 12.*South Korea Rivers and site locations

There are 70 gauging stations which are located upstream (35 stations, blue circle) and downstream (35 stations, red circle) of major reservoirs (*Figure 12*). The averaged value for channel characteristics from sediment measurement data is in *Figure 13.* Therefore, the watersheds were classified as “river” and “stream” depending on location downstream and upstream of major reservoirs.

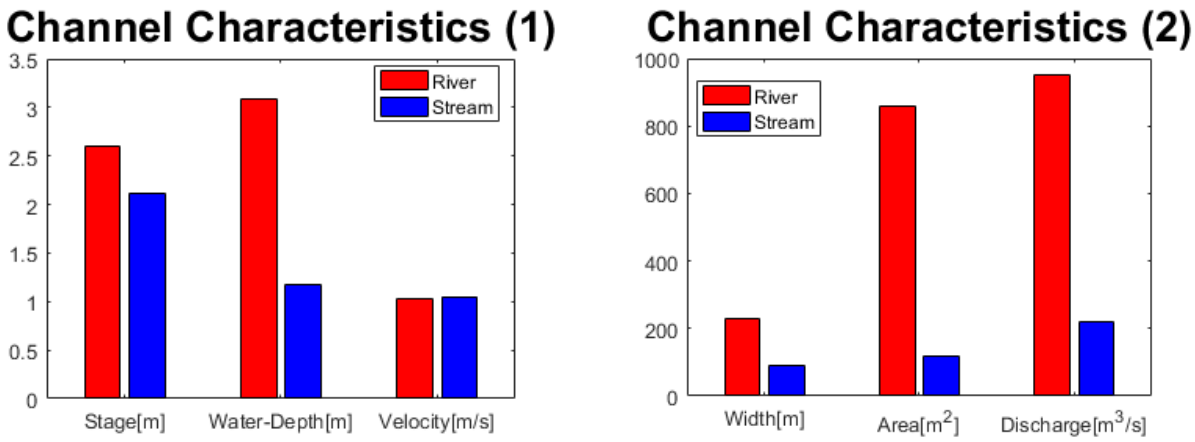

Figure 13. Different channel characteristics between upstream and downstream

3.2.1. River and Stream Data

The 10 years of daily discharge and suspended sediment measurement and estimated total sediment in stream and river are provided by Ministry of Land, Infrastructure and Transport (MOLIT) and Korea Water Resources Corporation (K-Water). Gauging stations in streams and rivers have different assignment organization: The Ministry of Land, Infrastructure, and Transport oversees the river gauging stations, and K-water is in charge of the stream gauging stations. The gauging stations for streams and rivers are in the mountain regions and alluvial plains respectively, they have different channel characteristics. Gauging stations in rivers have a relatively deep and wide channel, so they have bigger discharge and cross-section area. However, their velocities do not show big differences (*Figure 13*). Because of these differences, some measurements were conducted with different tools. Sediment measurements for South

Korean Rivers are classified into grab-sampler, depth –integrating, point-integrating, and surface sampling. The measurement method is commonly selected with consideration flow velocity and water depth. The grab sampler is used for low velocity ($V < 0.6$m/s) and low suspended load. In the case of high flow velocity ($0.6 < V < 3.7$m/s) and low water depth ($H < 4.6$m), depth-integrating (D-series) and point-integrating (P-series) could be selected. Selection between the two methods depends on the size of the stream. If the water depth is higher than 4.6m with high flow velocity, point-integrating was selected for the measurements. Finally, the surface sampler is used for extreme flow velocities ($V > 3.7$ m/s). In rivers, sediment measurements were conducted with a depth-integrating method with D-74 (mostly), point sampling with P-61A, or a surface sampler. On the other hand, sediment in streams was measured with depth-integrating with DH-48 (mostly) and D-74, or surface sampler. This difference in measurement depends on different channel characteristics, and it is hard to install a cable for D-74 sampling in stream gauging stations. In both gauging stations, the bed materials were sampled by US BM-54 material sampler, 60L Van Veen Grab sampler or by grid sampling and analyzed with sieve analysis and suspended material was analyzed with the Bottom Withdrawal tube method. Information on flow and sediment measurement for river and stream gauging stations and sediment measurement were provided by a Korean research team to estimate the mean annual sediment yield (Julien et al., 2017). In terms of flow data, the daily discharges for 35 river gauging stations from 2005 to 2014 are provided. In case of stream gauging stations, the daily discharge was estimated with daily stage data and an equation for a stage-discharge relationship from Korea Annual Hydrological Report from 2006 to 2015 (MLTM, 2008a, 2008b, 2010, 2011, 2012, 2013; MOLIT, 2014, 2015, 2016; MOCT, 2006, 2007). A total 2,693 measurements (1,808 for rivers and 885 for streams) was used to estimate the total sediment discharge. The FD-SRC

method was used to estimate the specific degradation for each gauging station. When a missing daily discharge was over 10% in each year, the selected year was removed to prevent distortion of specific degradation.

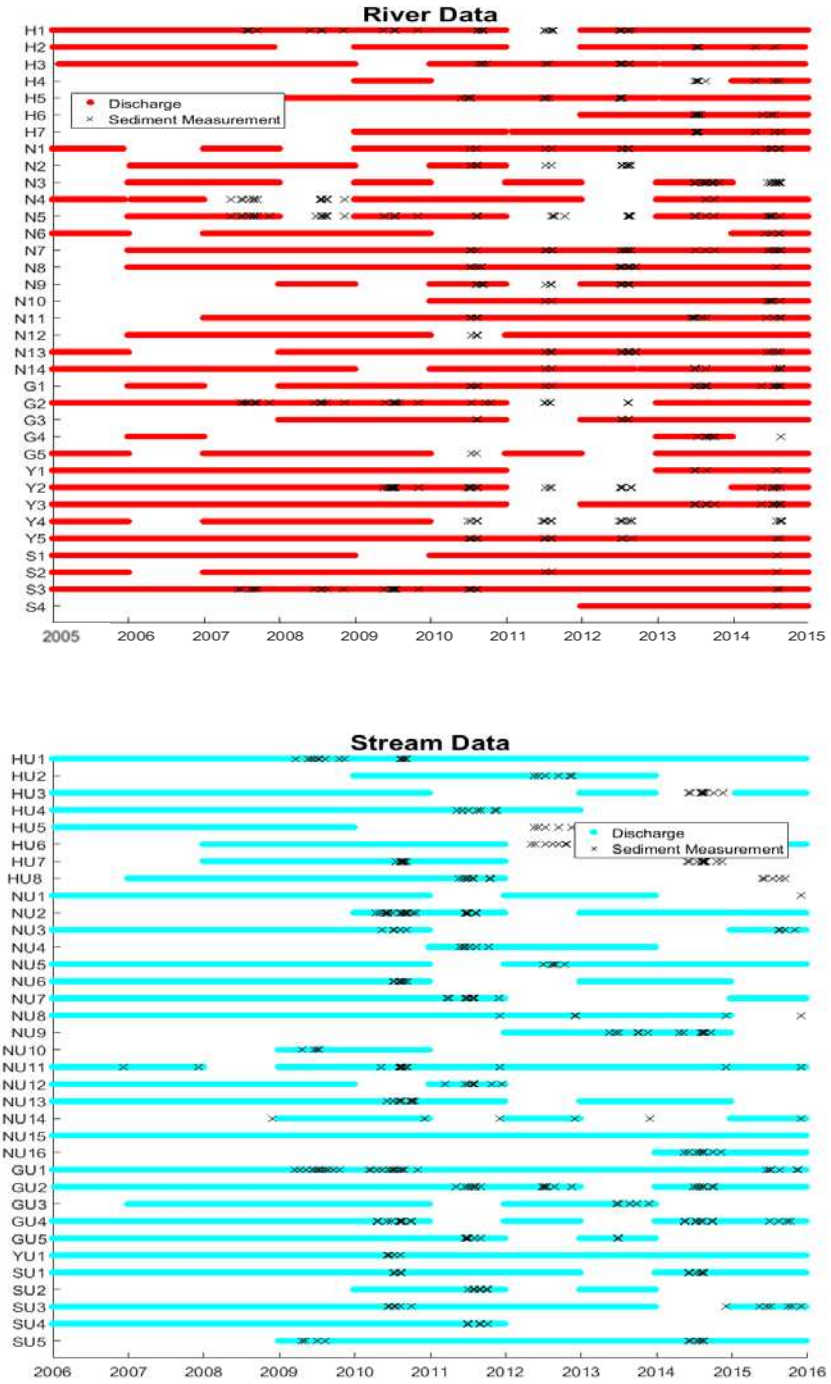

Figure 14.Daily discharge (line) and sediment measurement(x) data for FD-SRC

3.2.2. Total Sediment Discharge and Specific Degradation

First, the flow duration curve was generated with daily discharge measurements. The exceedance probability (P) was calculated with the Weibull plotting position Formula

$$P = m/(1 + N) \qquad \text{Eqn 3-1}$$

where P is the exceedance probability that a given discharge will be exceeded (%)

m is the rank of discharge value from the largest daily discharge

N is the number of events (=daily discharge) for a period

The daily discharge measurements and flow duration curve of Socheon station (NU1) are demonstrated in *Figure 15*.

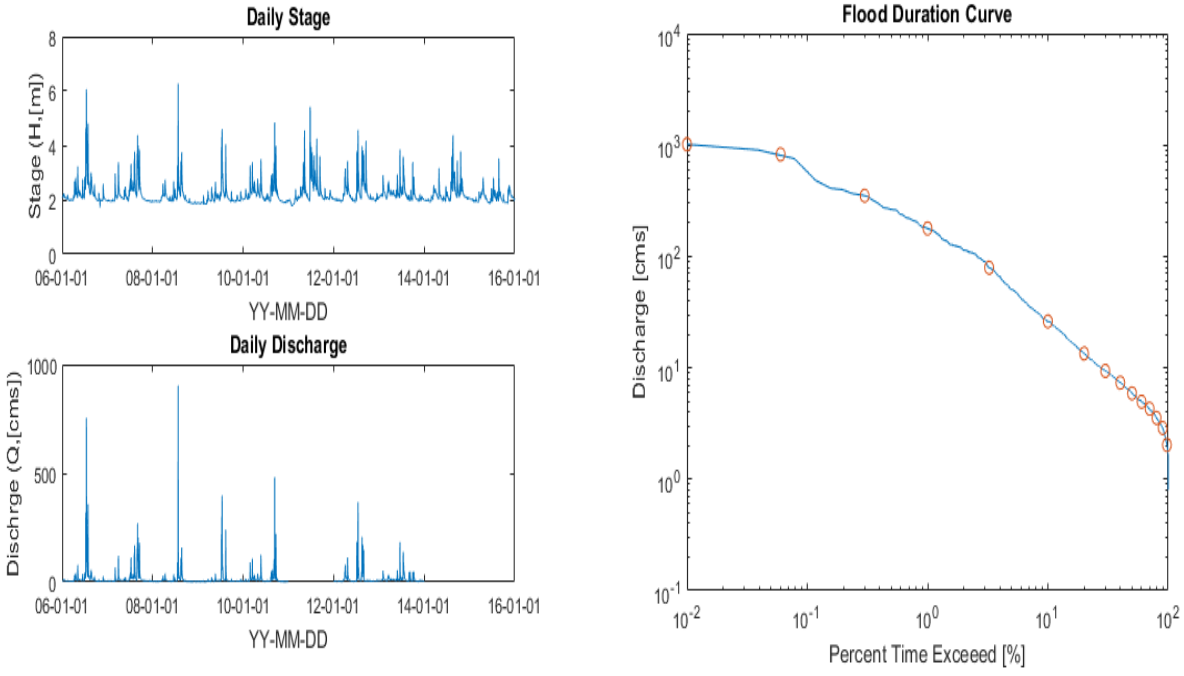

(a) (b)

Figure 15.(a) Daily stage and daily discharge of Socheon station from 2006 to 2015 and (b) flow duration curve of Socheon station (red points are midpoints for FD-SRC method)

MOLIT developed a Sediment Discharge Computation System (SDCS) based on MEP in 2009 to estimate the total sediment load (Lee et al., 2009). The total sediment load results

were estimated with the SDCS. The relationship between the total sediment discharges and the flow discharge in streams and rivers has a different trend (*Figure 16*). Especially, the total sediment load is high at low discharge in stream. With the estimated total sediment load, specific degradation was estimated by the FD-SRC method. The sediment rating curve from MEP for NU1 was $Q_t=6.278Q^{1.344}$. The mean annual sediment load is shown in *Table 6.* The total sediment load for each probability was estimated by integrating the results of FD and SRC. The average daily total sediment discharge is given by the sum of column (6), and it could be converted as annual total sediment load with 365 days.

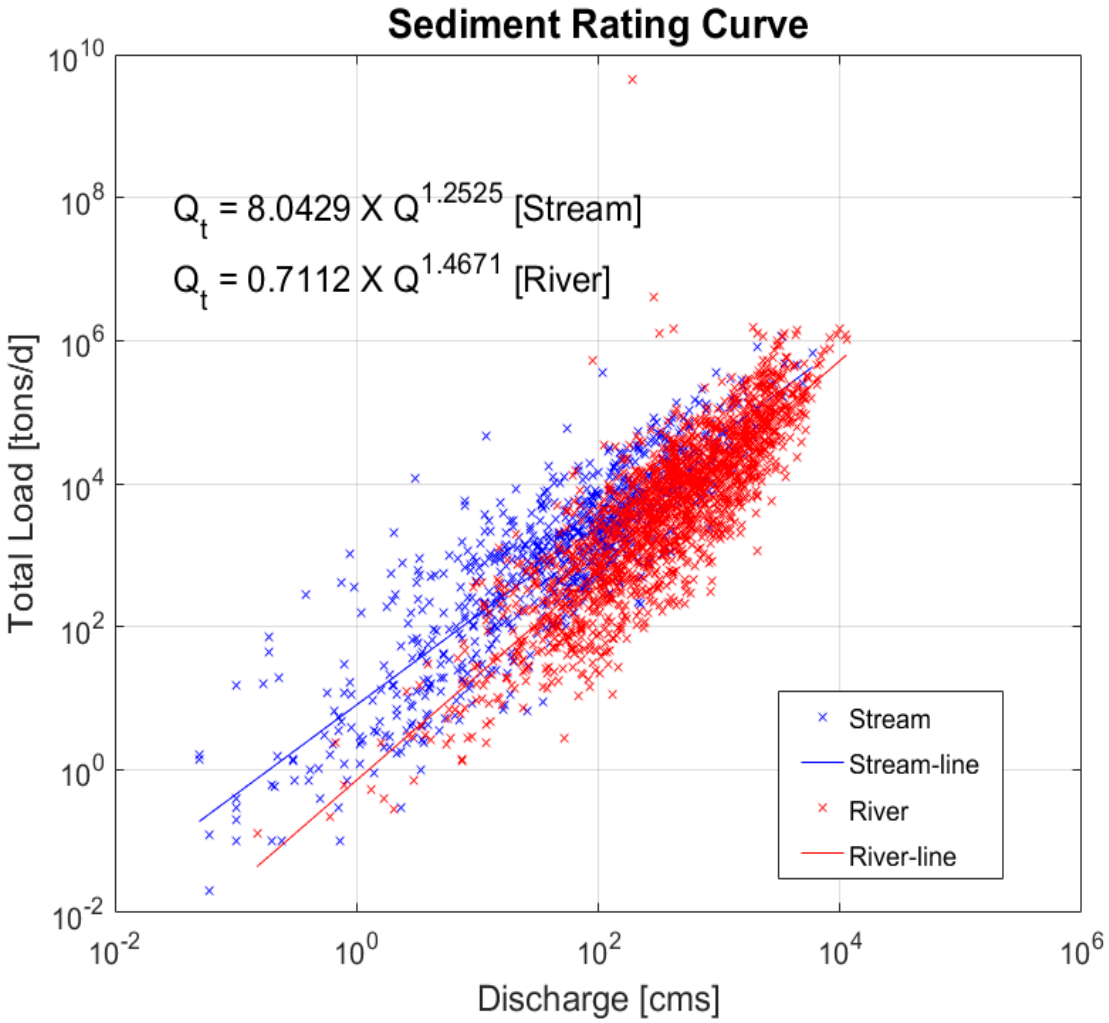

Figure 16. Sediment rating curve of streams and rivers

*Table 6.*Total sediment load at NU1 using the FD-SRC method

Interval	Interval mid	Interval ΔP	Discharge Q [m^3/s]	Sediment Load Q_t [tons/day]	$Q_t \times \Delta P$ [tons/day]
(1)	(2)	(3)	(4)	(5)	(6)
0-0.02	0.01	0.02	1,013.89	68,905	13.78
0.02-0.1	0.06	0.08	823.76	52,122	41.70
0.1-0.5	0.3	0.4	350.89	16,552	66.21
0.5-1.5	1	1	178.16	6,656	66.56
1.5-5	3.25	3.5	79.18	2,238	78.32
5-15	10	10	26.10	503	50.35
15-25	20	10	13.46	207	20.67
25-35	30	10	9.38	127	12.72
35-45	40	10	7.35	91.6	9.16
45-55	50	10	5.90	68.2	6.82
55-65	60	10	4.96	54.0	5.40
65-75	70	10	4.29	44.5	4.45
75-85	80	10	3.55	34.4	3.44
85-95	90	10	2.88	26.0	2.60
95-100	97.5	5	2.03	16.3	0.81
Total		100			383

The final specific degradation (SD) was obtained from an annual total sediment load divided by the watershed area.

$$SD\ [\frac{tons}{Km^2 \cdot yr}] = Daily\ sediment\ load\ [\frac{tons}{day}] \times \frac{365day}{1yr} \times \frac{1}{Area(km^2)} \qquad \text{Eqn 3-2}$$

The SD results for all stations are organized in *Table 7*. The SD results varied from 4 to 1,308 tons/km^2▪yr. Yoon and Woo (2000) suggested that the upper limit of total sediment load in South Korea is 1,000 tons/km^2▪yr, therefore the estimated SD results are reliable.

Table 7. SD result and data information of all gauging stations

Station	Name	Water shed	Area [km^2]	# of Q	#of Sed	Annual Sediment load [tons/ yr]	Specific Degradation [tons/km^2▪yr]
H1	Yeoju		11,047	3,256	97	1,295,000	117
H2	Heungcheon		284	2,832	26	114,000	404
*H3	Munmak		1,346	3,213	48	1,543,000	1,147
H4	Yulgeuk		173	730	29	35,000	203
**H5	Cheongmi		519	3,246	49	1,000	412
H6	Namhanriver		8,823	1,084	30	207,000	24
H7	Heukcheon		307	2,148	37	23,000	75
HU1	Yeongchun	Han	4,782	3,633	33	582,000	124
**HU2	Samok bridge		2,298	1,437	22	2,586,000	1,057
HU3	Yeongwol1		1,615	2,530	27	352,000	213
**HU4	Dalcheon		1,390	2,557	11		
**HU5	Maeil		164	1,428	18	228,000	1,308
**HU6	Bukcheon		304	1,804	21	85,000	278
**HU7	Naerincheon		1,039	1,461	40	111,000	107
**HU8	Wontong		531	1,461	41	173,000	326
N1	Seonsan		979	2,878	67	69,000	71
N2	Dongchon		1,541	1,430	44	67,000	43
N3	Gumi		10,913	1,774	33	229,000	21
N4	Nakdong		9,407	2,517	53	413,000	44
N5	Waegwan		11,101	2,136	147	622,000	56
*N6	Ilseon bridge		9,533	1,826	14	39,000	4
N7	Jindong		20,381	3,275	84	2,087,000	102
N8	Jeongam		2,999	3,287	74	100,000	33
N9	Hyangseok		1,512	1,809	63	127,000	84
N10	Dongmun		175	1,826	29	13,000	75
N11	Jeomchon		615	2,922	48	24,000	39
***N12	Yonggok	Nak	1,318	2,900	15	61,000	46
N13	Jukgo	dong	1,239	2,908	69	46,000	37
N14	Gaejin2		750	3,242	57	39,000	52
NU1	Socheon		697	2,557	13	140,000	201
NU2	Yangsam		1,147	1,789	31	232,000	203
NU3	Yeongyang		314	2,191	34	61,000	193
**NU4	Dongcheon		143	1,096	12	45,000	318
**NU5	Cheongsong		308	3,287	12	7,000	24
NU6	Geochang1		228	2,556	31	39,000	172
NU7	Geochang2		179	2,556	19	18,000	99
**NU8	Jisan		161	3,287	14	176,000	1,093
**NU9	Donggok2		34	1,096	26	2,000	62
**NU10	Gohyeon		15	730	4	6,000	400

Table 7. Continued previous page

Station	Name	Water shed	Area [km^2]	# of Q	#of Sed	Annual Sediment load [tons/yr]	Specific Degradation [tons/km^2▪yr]
**NU11	Daeri	Nak dong	61	3,286	26	87,000	1,434
NU12	Changchon		334	1,826	18	41,000	122
NU13	Sancheong		1132	2,921	31	164,000	145
NU14	Taesu		243	1,461	16	52,000	215
**NU15	Imcheon		467	3,652	14	528,000	1,132
NU16	Oesong		1232	730	16	128,000	104
G1	Hoedeok	Geum	606	2,902	50	72,000	119
G2	Gongju		6275	2,891	105	682,000	109
G3	Hapgang		1850	2,192	30	247,000	134
G4	Useong		258	730	21	16,000	61
*G5	Guryong		208	2,556	7	12,000	60
**GU1	Okcheon		1985	3,652	51	448,000	226
GU2	Cheongseong		491	3,266	53	56,000	115
**GU3	Hotan		1003	2,192	9	18,000	18
GU4	CheonCheon		291	2,922	52	67,000	230
GU5	Donghyang		165	2,556	21	24,000	148
Y1	Hakgyo	Yeon gsan	190	2,921	40	19,000	97
Y2	Naju		2039	2,532	109	233,000	114
Y3	Mareuk		668	3,269	36	111,000	166
Y4	Nampyeong		580	1,422	80	27,000	47
Y5	Seonam		552	3,634	68	22,000	40
**YU1	Bongdeok		44	3,648	8	3,000	77
***S1	Jukgok	Seom jin	1269	3,264	15	41,000	32
***S2	Gokseong		1788	3,274	15	80,000	45
S3	Gurye2		3818	3,640	102	172,000	71
*S4	Yongseo		128	1,096	14	4,000	28
SU1	Gwanchon		359	3,287	44	43,000	120
**SU2	Ssangchi2		133	1,095	14	18,000	135
SU3	Gyeombaek		295	3,277	56	17,000	56
**SU4	Jangjeon2		273	2,191	11	57,000	207
SU5	Songjeon		59	2,556	33	20,000	331

* excluded from regression models with 28 and 47 specific degradations

** excluded from regression model with 47 specific degradations

***only excluded from regression models with 28 specific degradations

3.2.3. Reservoir Data

Several dams and reservoirs have been constructed in South Korea to secure domestic and agricultural water resources from the summer concentrated precipitation pattern. There are 15 multipurpose dams, 12 hydroelectric dams, 54 storage dams, and 17,649 agricultural reservoirs in South Korea (MOLIT, 2013). K-water has conducted a sediment survey for multipurpose and storage dams every 10years from impounded water (*Table* 8 and *Figure* 17). In the sediment survey, the water elevation and ground level measurement was done to estimate the change of reservoir capacity. In the past, the ground level measurement was conducted by the total station method and the single beam echo sounder was used for the water elevation measurement. With the development of the measurement technique, the Aerial Lidar with GPS and multi-beam echo sounder are used for each measurement. Overtime, the measurement resolution also decreased from 200m ~ 100m to 5m. From the measurement results, the Area-capacity curve was created and the relationship between reservoir capacity, area and elevation are analyzed with regression equation. Regression equation should be used for specific depth interval and general form of the regression equation is

$$V = ah^4 + bh^3 + ch^2 + dh + e$$
$$A = ah^4 + bh^3 + ch^2 + dh + e \qquad \text{Eqn 3-3}$$

where V is the reservoir capacity ($m^3/km^2 \cdot yr$)

A is the reservoir surface area (km^2)

a, b, c, d, and e are the regression coefficients.

The reservoir capacity is estimated by the method of average ends of area with the estimated area in specific depth interval. Based on designed flood elevation, the total sediment deposition is estimated by the difference between initial and measured reservoir capacities.

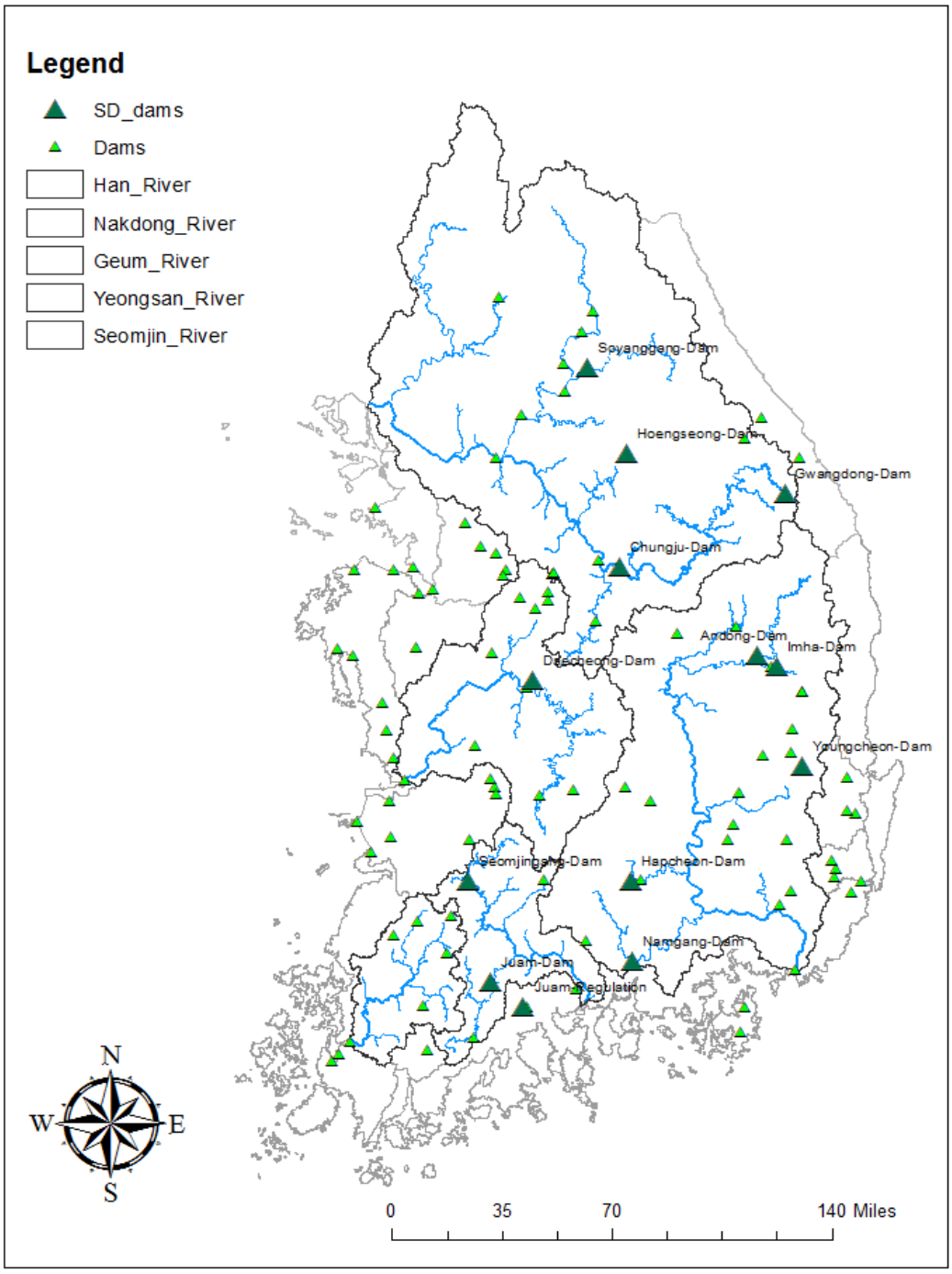

*Figure 17.*Dams for estimating specific degradation of the reservoir (dark green) and other multi-purpose, storage, hydro electronic dams

$$V_r = \frac{V_m - V_i}{A \times t}, \qquad \text{Eqn 3-4}$$

where V_r is the sediment deposit rate ($m^3/km^2 \cdot yr$)

V_m is the measured value of reservoir capacity from imthe poundment of water (m^3)

V_i is the initial capacity of rethe servoir at impoundment of water (m^3)

A is the catchment area (km^2)

t is the time from the impoundment of water to measurement

The validation could be performed by comparing the measured sediment deposit rate and the specific degradation in each watershed. To compare two values, the trap efficiency and dry specific mass are applied.

$$V_r = (SD \times T_{Ei})/\rho_{md} \qquad \text{Eqn 3-5}$$

where T_{Ei} is the trap efficiency (%)

ρ_{md} is the dry specific mass of the sediment deposit ($tons/m^3$)

The reservoir trap efficiencies for multiple purpose dam in South Korea are estimated with Brune Curve (1953) and they are generally larger than 96%. A dry specific mass and trap efficiency were assumed as 1.6 $tons/m^3$ and 99% when field measurements are not available. The processes of validation and estimation of SD are demonstrated below. The results of the sediment deposit rate in Andong reservoir were 109(2008), 361(1996), and 201(1983) $m^3/km^2 \cdot yr$, respectively. From the sediment survey report in 2006, the sediment deposit rate was calculated as

$$V_r = \frac{total\ sediment(m^3)}{Area(km^2) \times time(yr)} = \frac{5{,}514{,}315\ m^3}{1{,}584\ km^2 \times 32(75\sim07)} = 109\,\frac{m^3}{km^2 \cdot yr} \qquad \text{Eqn 3-6}$$

*Table 8.*Reservoir sedimentation data for multipurpose dams (above) and storage dams (below)

Division	Basin	Unit	Han River			Nakdong River					Geum River		Seomjin River			etc.		
	Dam		Soyang River	Chungju	Hoengseong	Andong	Imha	Hapcheon	Nam River	Miryang	Daecheong	Yongdam	Seomjin River	Juam (main)	Juam (control)	Buan	Boryeong	Jangheung
catchment area		km^2	2,703	6,648	209	1,584	1,361	925	2,285	95.4	4,134	930	763	1,010	134.6	59.0	163.6	193.0
impoundment of water			Nov. 10, 1972	Nov. 1, 1984	Dec. 28, 1999	Dec. 4, 1975	Dec. 3, 1991	Jul. 1, 1988	Oct., 1998	Oct. 4, 2000	Jun. 30, 1980	Nov. 9, 2000	Sep., 1928	Mar. 12, 1990	Nov. 9, 1990	Sep. 29, 1995	Oct. 31, 1996	Dec. 17, 2004
sediment rate	design values	m^3/km^2·yr	500	1,000	550	800	300	695	414	380	300	400	500	400	400	650	350	394
	measured values	m^3/km^2·yr	914 (930) (1,039)	853 (1,099)	183	109 (361) (201)	300 (680)	893 (639)	350	380	616 (114)	-	459	469	1,089	650	350	-
total sediment	design values	10^6·m^3	650	596	13.5	248	124	150	27.5	3.8	450	70	82	45	20	5.7	8.2	12
	measured values	10^6·m^3	81.5	130.5	0.5	5.5	5.6	19.0	12.5	-	81.4	-	19.0	5.0	2.1	0.6*	0.8*	-
measurement year			2006 (1994) (1983)	2007 (1996)	2013	2008 (1996) (1983)	2007 (1997)	2012 (2002)	2004	2013	2006 (1991)	2011	1983	2003	2003	2011	2011	-

Table 8. Continued previous page

Division	Basin	Unit	Taebaek		Pohang			Unmun	Ulsan				Geoje		Yeosu	Jeonnam
	Dam		Gwangdong	Dalbang	Yeongcheon	Angye	Gampo	Unmun	Daegok	Sayeon	Daeam	Seonam	Yeoncho	Gucheon	Sueo	Pyeongrim
catchment area		km^2	125.0	29.4	235.0	6.7	3.67	301.3	57.5	67.0	77.0	1.2	11.7	12.7	49.0	19.9
impoundment of water			'88.8	89.9	79.8.26	71.12	05.12.22	93.10.20	04.11	65.12	69.12	64.12	79.12	87.11.21	77.11.1	06.11.14
sediment rate	design values	$m^3/km^2 \cdot yr$	460	746	500	-	500	374	200	800	800	-		200	350	350
	measured values	$m^3/km^2 \cdot yr$	714	493 (712)	1,534	-		301		219	1,184	-	830	1,976	428	
total sediment	design values	$10^6 \cdot m^3$	3.0	1.09	3.1	-	0.18	11.2	0.58	5.0	3.1	-		0.13	1.43	0.348
	measured values	$10^6 \cdot m^3$	0.892	0.16 (0.27)	9.4	-		1.1		1.1	3.2	-	0.72	0.45	0.59	
measurement year			2012 (2002)	2013 2004	2005	-		2005		2005	2005	-	2004	2004	2005	

Because measurement techniques have been continuously developed and the specific degradation of the river is estimated with the recent period, only the recent results are used. This research only focused on sediment deposit results from reservoirs located stream or river previously discussed (K-water, 2002a, 2002b, 2006a, 2006b, 2008a, 2008b, 2014). The location of the selected reservoirs shown in *Figure 17* and estimated SD results are demonstrated in *Table* 9. When the dry mass density was not in the report, the 1.6 tons/ km^2▪yr is used to calculate specific degradation. In the case of Miryang and Buan Dams, they have the same result design value and estimated sediment deposit rate (*Table 8*). Both survey reports concluded that the estimated sediment survey results were not reliable so that they are removed for analysis. Yeongcheon Dam is not used for this analysis because the survey report is not available and the estimated specific degradation is excessively large (SD=2,454 tons/km^2▪yr). The estimated specific degradation for reservoirs varies from 300 to 1,800 tons/km^2▪yr.

*Table 9.*The specific degradation of reservoirs

Watershed	Name	Area [km^2]	Total sediment [$10^6 \times m^3$]	Sediment deposit rate [m^3/km^2▪yr]	Dry mass density [tons/m^3]	Specific degradation [tons/km^2▪yr]
Han	Soyang river	2,703	81.5	914	1.29	1,179
	Chungju	6,648	130.5	853	1.67	1,425
	Hoengseong	209	0.5	183	1.6	293
	Gwangdong	125	0.9	714	1.6	1,142
Nakdong	Andong	1,584	5.5	109	1.6	174
	Imha	1,361	5.6	680	1.6	1,088
	Hapcheon	925	19	893	1.1	982
	Namriver	2,285	12.5	350	1.6	560
	*Miryang	95	3.8	380	1.6	608
	*Yeongcheon	235	9.4	1,534	1.6	2,454
Geum	Daecheong	4,134	81.4	616	1.38	850
Seomjin	Juam(Main)	1,010	5.0	469	2.1	985
	Juam(regulation)	135	2.1	1,089	1.6	1,742
	Seomjinriver	763	19.0	459	1.6	734

*The estimated SD is not used for analysis

3.3. Estimated Specific Degradation of River, Stream, and Reservoir

The common method of representing specific degradation (SD) with the area is shown in *Figure 18*. Different trends of specific degradation between gauging stations are delineated for streams (red) and rivers (blue) and reservoirs (green). The specific degradation of reservoirs and streams are higher than the specific degradation of rivers.

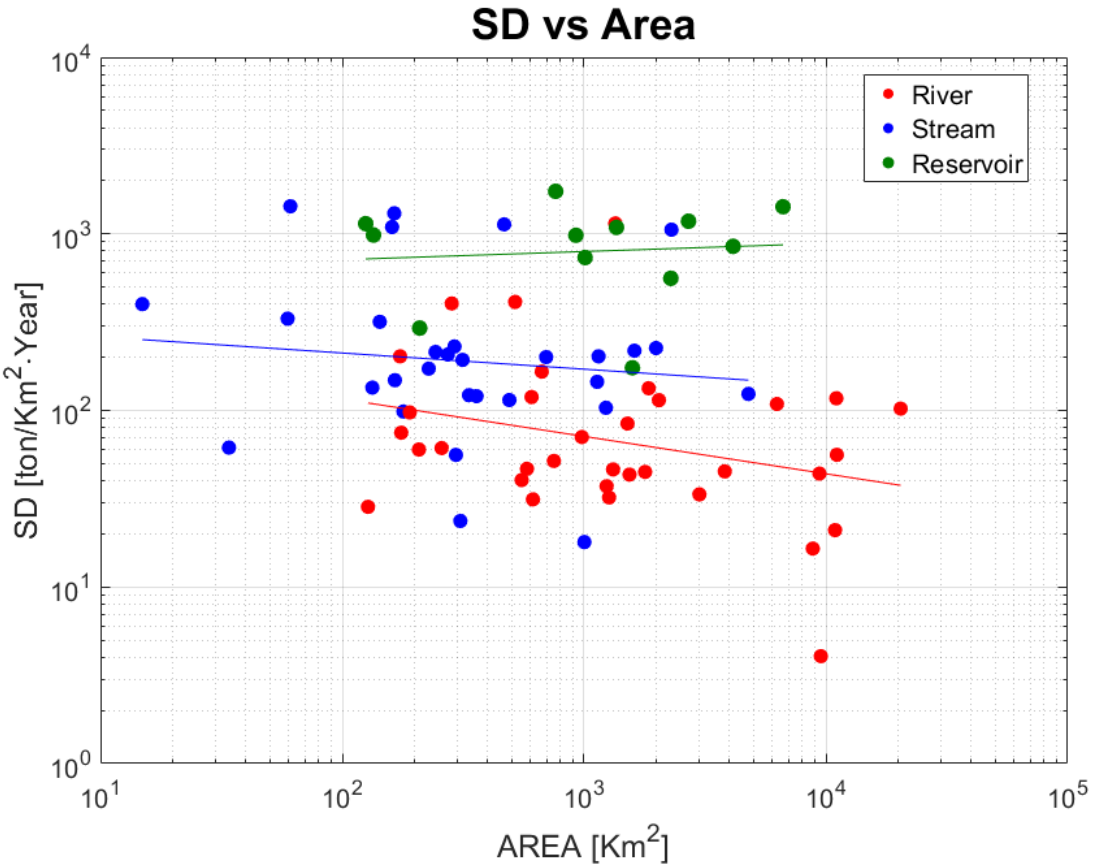

Figure 18. Specific degradation versus area

The specific degradation (SD) of reservoirs is fairly constant with an average value of 930tons/km^2▪yr. Therefore, we separate rivers and streams from reservoirs. The SD results for rivers and streams decrease with the watershed area and SD for streams are slightly higher than SD for rivers. Three existing models (KICT1, KICT 2, and Yoon and Choi in *Table* 5) developed by the Ministry of Construction (MOC) and Yoon and Choi are validated with the estimated specific degradations at 35 river gauging stations (MOC, 1992; MLTM, 2011). Three regression

equations included the bed material size (d_{50}) as a variable and it was classified as d_{50} in before and after a flood event in data, therefore the results were provided with averaged value and have variation from minimum and maximum of bed material size. Because the bed material sizes for streams were not available, SD for streams was not used for validation. In *Figure 19*, the vertical arrow for each result shows the variation of simulated specific degradation from the maximum and minimum bed material size. Other models in *Table* 5 including parameters related to a reservoir (e.g. reservoir capacity, trap efficiency) were not validated in this study. To evaluate the existing model's accuracy, the Root Mean Square Errors (RMSE) and Nash-Sutcliffe Efficiency coefficient (NSE) were used with the below equation

$$RMSE = \sqrt{\frac{1}{n}\sum_{i=1}^{n}(y_i - \hat{y}_i)^2} \qquad \text{Eqn 3-7}$$

The Root Mean Square Error (RMSE) for each model was 275, 655, and 1,409 tons/km^2▪yr, respectively. Additionally, the Nash-Sutcliffe Efficiency coefficient (NSE) was also calculated for each model (Nash and Sutcliffe, 1970).

$$NSE = 1 - \frac{\sum_{t=1}^{T}(Q_m^t - Q_o^t)^2}{\sum_{t=1}^{T}(Q_o^t - \bar{Q}_0)^2} \qquad \text{Eqn 3-8}$$

where Q_o is the observed SD,

Q_m is the modeled SD,

Q_o^t is the observed SD at time t

$\overline{Q}_0$ is the mean of observed SD

The NSE varies from $-\infty$ to 1 and it indicates that the model predictions well matches the observations when it is close to 1.

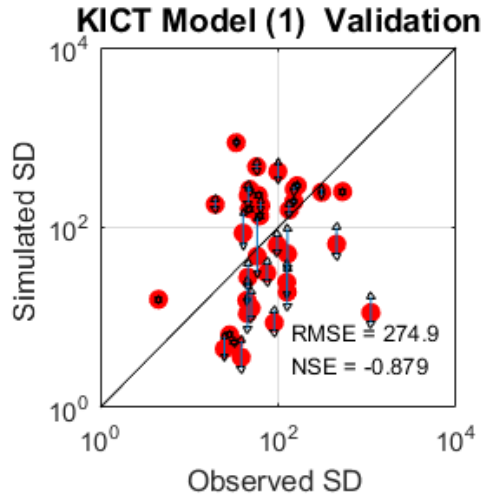

(a)

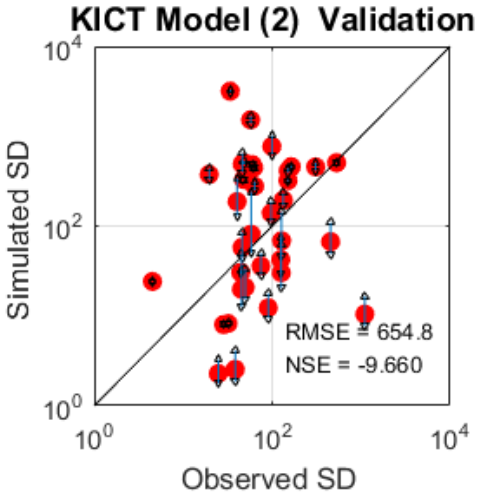

(b)

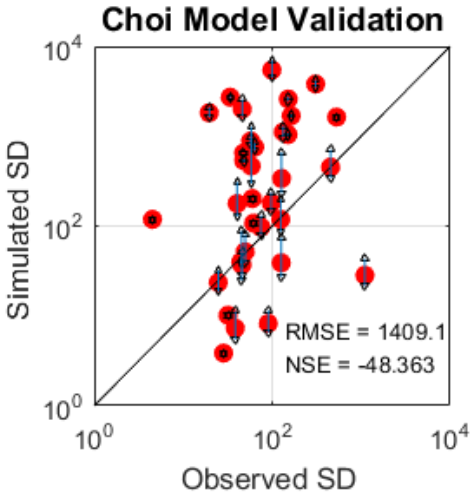

(c)

Figure 19. Validation of existing specific degradation (SD) model (a) KICT model 1, (b) KICT model 2, and (b) Choi's model (units: tons/km^2▪yr)

The NSE for each model was -0.88, -0.97, and -48.4, respectively. Because Yoon and Choi's model was based on the specific degradation of reservoir data, the model has a tendency to overpredict the sediment load of rivers.

In this chapter, the specific degradation for 35 rivers and 35 streams gauging stations was estimated by the FD-SRC method. The flow duration curve was determined with 10-year daily discharge and the sediment rating curve was generated by sediment measurements and the Modified Einstein Procedure (MEP). The specific degradation for 13 reservoirs also was estimated from field measurement. The estimated specific degradation was larger for reservoirs than stream and rivers. The validation of 3 existing models with the SD for 35 rivers had large RMSE values (250 to 1,409 tons/km^2▪yr), and the NSE (-0.88 to -48.3) indicated that the existing models had low predictability.

Chapter 4
Regression Models with Watershed Characteristics

In this chapter, watershed characteristics were analyzed using GIS tools (section 4.1) and regression models for the estimated specific degradation were developed with the watershed characteristics (section 4.2).

4.1. Watershed Characteristics with GIS Analysis

In the last chapter, we found the different specific degradations for streams, rivers, and reservoirs in South Korea. This chapter focuses on explaining the differences in terms of watershed characteristics. The Watershed morphometric analysis has been commonly used since Horton (1945) to understand sediment transport on watershed. This dissertation focused on the watershed morphometric characteristics impacting erosion and sedimentation and they are classified into linear, areal, and relief aspects with 1, 2, and 3 dimensions, respectively. Other parameters (i.e. precipitation, land use, soil type) were also analyzed. All parameters were considered for regression models to predict a specific degradation of ungauged watersheds. The detailed processes for this analysis are found in APPENDIX C and a summary of the procedure and results is presented in this chapter.

4.1.1. Watershed Morphometric Characteristics

Linear watershed characteristics include parameters describing stream network (i.e. stream length, stream order, and etc.). The stream length was analyzed with the Korea Reach File (KRF) version 3 provided by the Ministry of Environments (ME). It was classified into three parts: (1) mainstream length (Main); (2) tributary length (Tri); and (3) total stream length (Total). Strahler's stream ordering system is applied to KRF (SO1). Additional stream network parameters were generated from 5m by 5m resolution DEM to describe the stream order. To the

delineated stream networks from DEM, the Strahler's stream ordering system (SO2) and Shreve's ordering system were also applied (SO3) to delineate streams. The R-square values for total, main, tributary stream length were 0.217, 0.244, and 0.208, respectively (*Figure* 20 a-c). In terms of stream order, the stream orders at gauging stations were exported after applying stream order to the entire watershed.

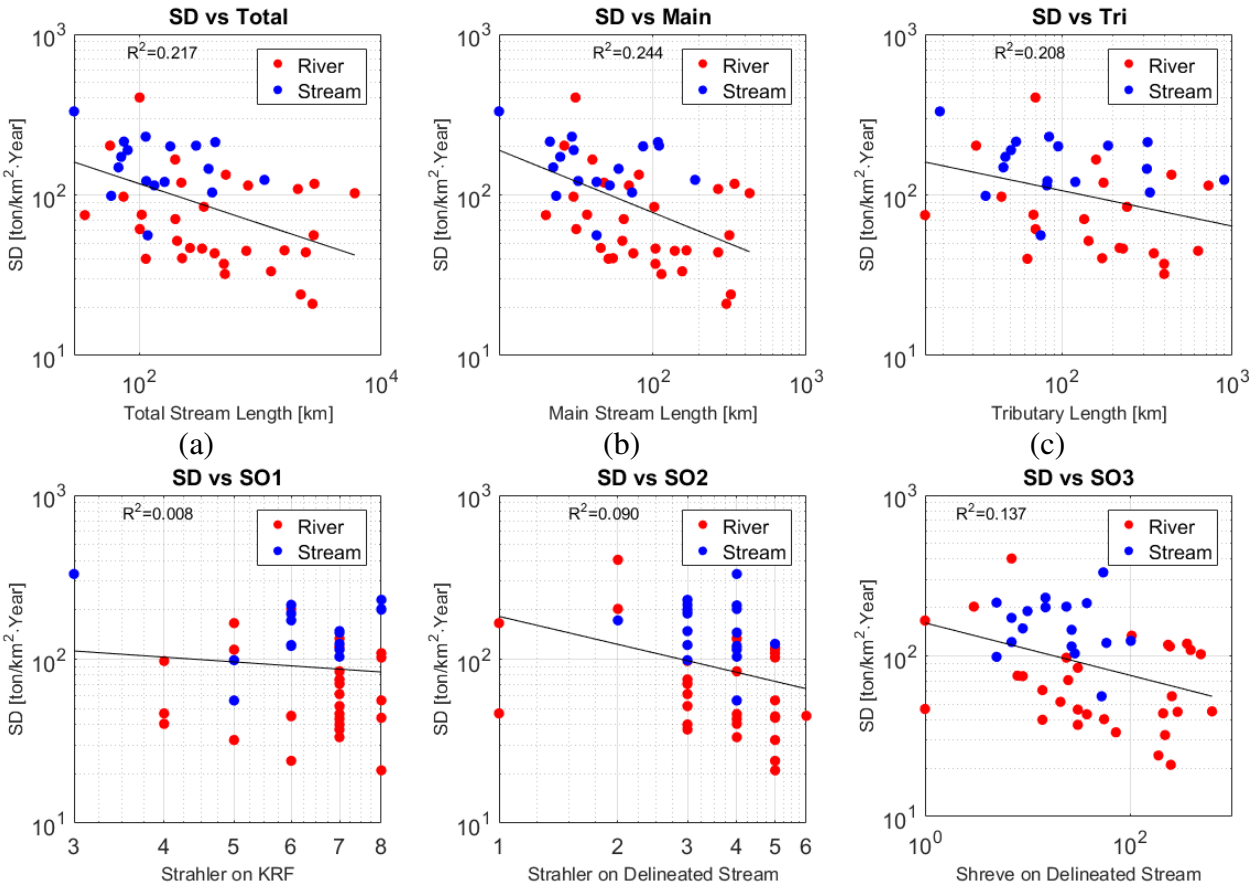

Figure 20. Stream length versus specific degradation (a) Total stream length, (b) Main stream length, and (c) Tributary stream length

In *Figure* 20 d-f, the Shreve stream order (SO3) from the delineated DEM (R^2=0.137) is better correlated than Strahler's stream order (SO1 and SO2). It means that the summation of every tributary's magnitude could well explain the difference between upstream and downstream. Though Shreve's stream order does not have direct physical meaning in terms of erosion and

sedimentation, the result shows that it explains the differences between specific degradations. It separates streams from rivers with alluvial plain characteristics. The areal aspect includes common 2-dimensional characteristics, such as watershed area (A, Area), drainage density (DD), and length factor. The watershed area is directly related to a size of storm events so that it has an inverse relationship with characteristics related to run off and discharge per unit area. The length factor (LF) and shape factor (SF) were considered as watershed shape characteristics, and they were calculated with A/ L_b^2 and L_b^2/A respectively. The length of watershed (L_b) could be estimated with various methods (Horton, 1932). In this paper, two methods were used to estimate the basin length: (1) Mainstream length; and (2) Axial stream length. Among aerial aspects, the shape factor ($R^2 = 0.227$) from mainstream length provides a better correlation than two factors (*Figure* 21). Commonly, high shape factor indicates elongated watershed and peak flow for a longer duration, while the low shape factors typically describe high peak flows during a short duration. Therefore, it is expected that the sinuosity and long travel time in the alluvial mainstream is meaningful to specific degradation. When the specific degradation of the rivers only considered, the shape factor will provide a better correlation. Additionally, two ratios considering reservoir area are applied because sediment deposition occurs in the reservoirs, and they are represented as A* and A**, respectively.

$$A^* = \frac{Reservoir\ catchment\ area\ [Km^2]}{watershed\ area\ [Km^2]} \qquad \text{Eqn 4-1}$$

$$A^{**} = \frac{(Watershed\ area - Reservoir\ catchment\ area)\ [Km^2]}{watershed\ area\ [Km^2]} \qquad \text{Eqn 4-2}$$

For watershed without reservoirs A*= 0 or A**=1. Different with the expectation that both ratios could be a great indicator to explain specific degradation, both parameters provided low correlation (*Figure 22*).

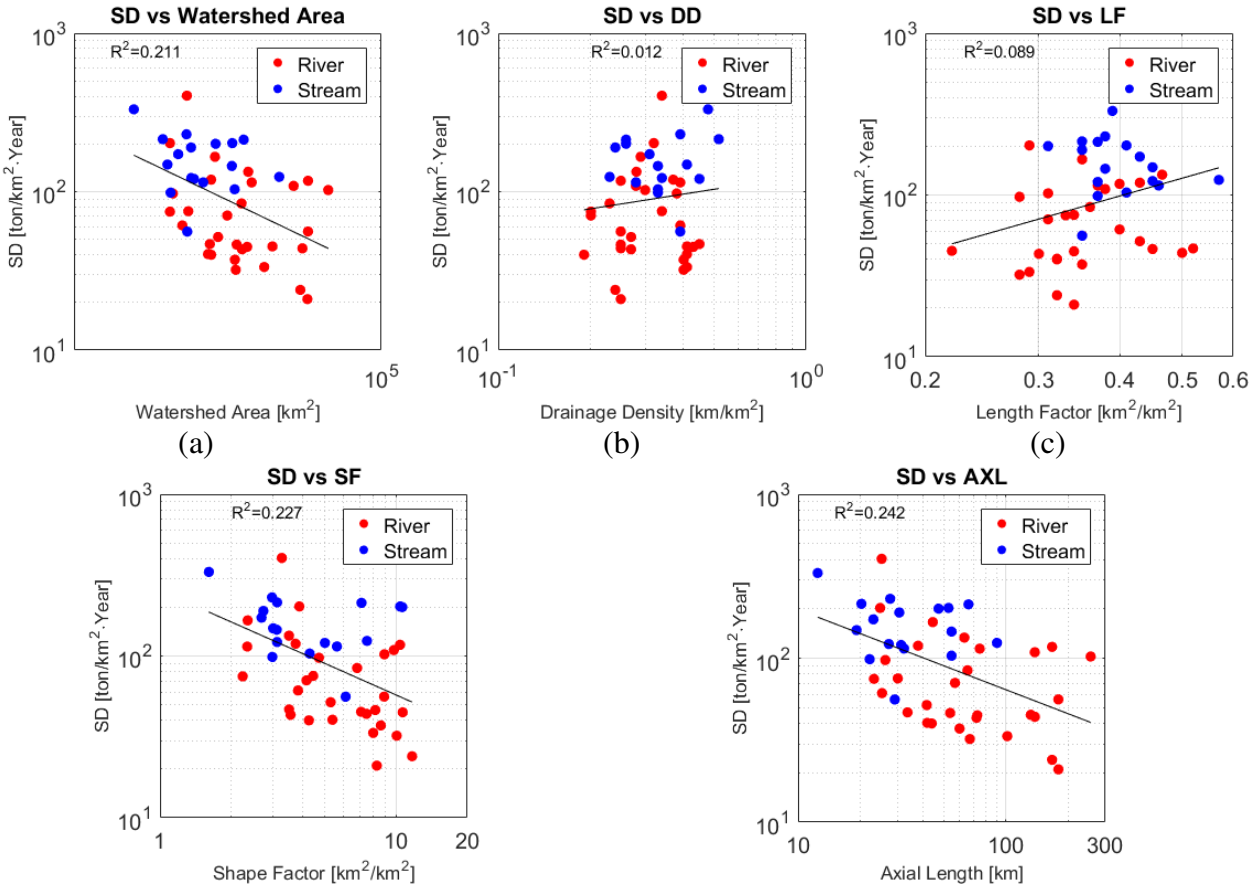

Figure 21. The areal aspects versus specific degradation (a) Watershed area, (b) Drainage density, (c) Length factor, (d) Shape factor, and (e) Axial Length

The hypsometric analysis is the distribution of surface area with respect to elevation. It has been generally used for calculation of hydrologic information because the basin hypsometry is related to flood response and soil erosion and sedimentation process (Langbein, 1947; Strahler, 1952). The 3-dimensional variables introduced to describe relief aspect consider relative elevation differences on a watershed. It is expected that the relief factor is the most important variable to explain the different SD due to different location. Commonly, the mean elevation (ME) and watershed average slope (Sl, Avg_slope) have been used to express the difference between mountain-valley and alluvial plain.

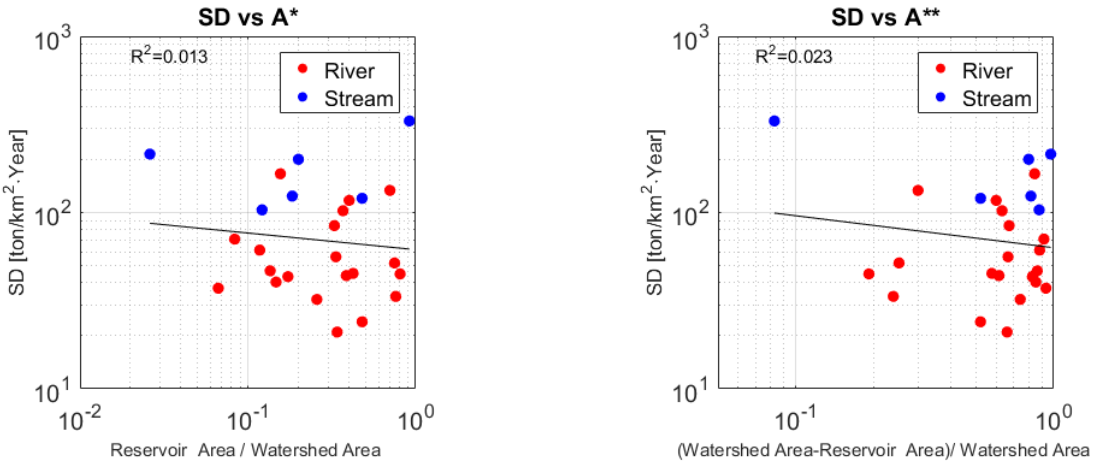

(a) (b)

Figure 22. The ratio considering reservoirs area versus specific degradation (a) A* and (b) A**

The hypsometric curve can figure out the hypsometric analysis, and commonly it expressed with the normalized cumulative area and normalized height from the outlet of the watershed outlet. The hypsometric curve was created for all watersheds and obvious different curves were created between stream and river (*Figure 23*).

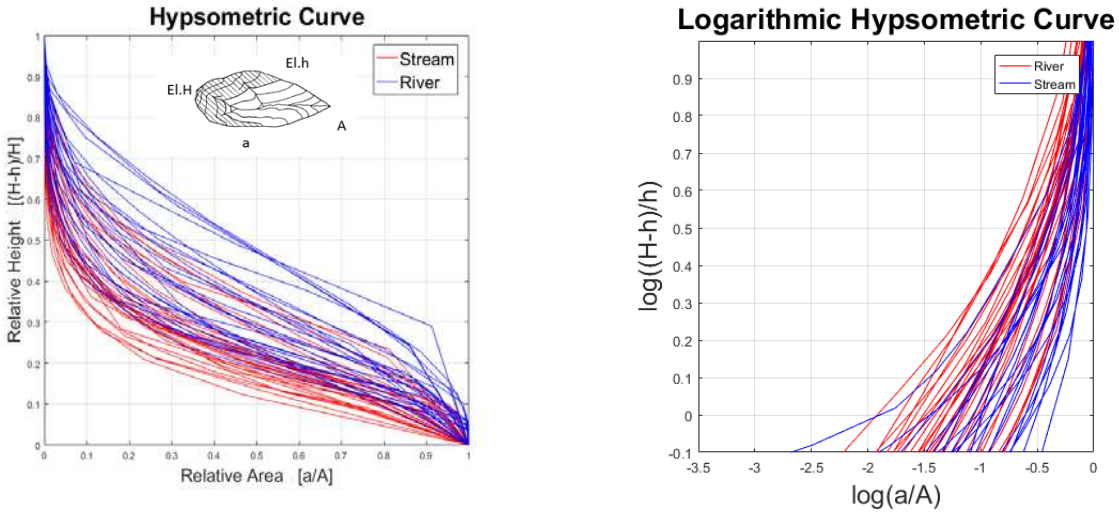

(a) (b)

Figure 23. (a) The hypsometric curve for all watersheds and (b) Logarithmic hypsometric curve

Three values are exported from the hypsometric curve: (1) Relative height at the mid relative area (Hyp1); (2) Elevation at the mid relative area (Hyp2); and (3) Slope between 0.2 and 0.8 of the relative area (Hyp3). The logarithmic hypsometric curve in *Figure 23*b (detail process in

Appendix C) also defined as an additional relief aspect (hypc). Especially, the relative height at mid relative area makes a good separation between specific degradation from stream and river (*Figure 25*). First and second highest SD from the river results from H2 and H3 which have large urbanized area. In *Figure 24* and *Figure 25*, the green dashed line shows the regression line from 46 watersheds.

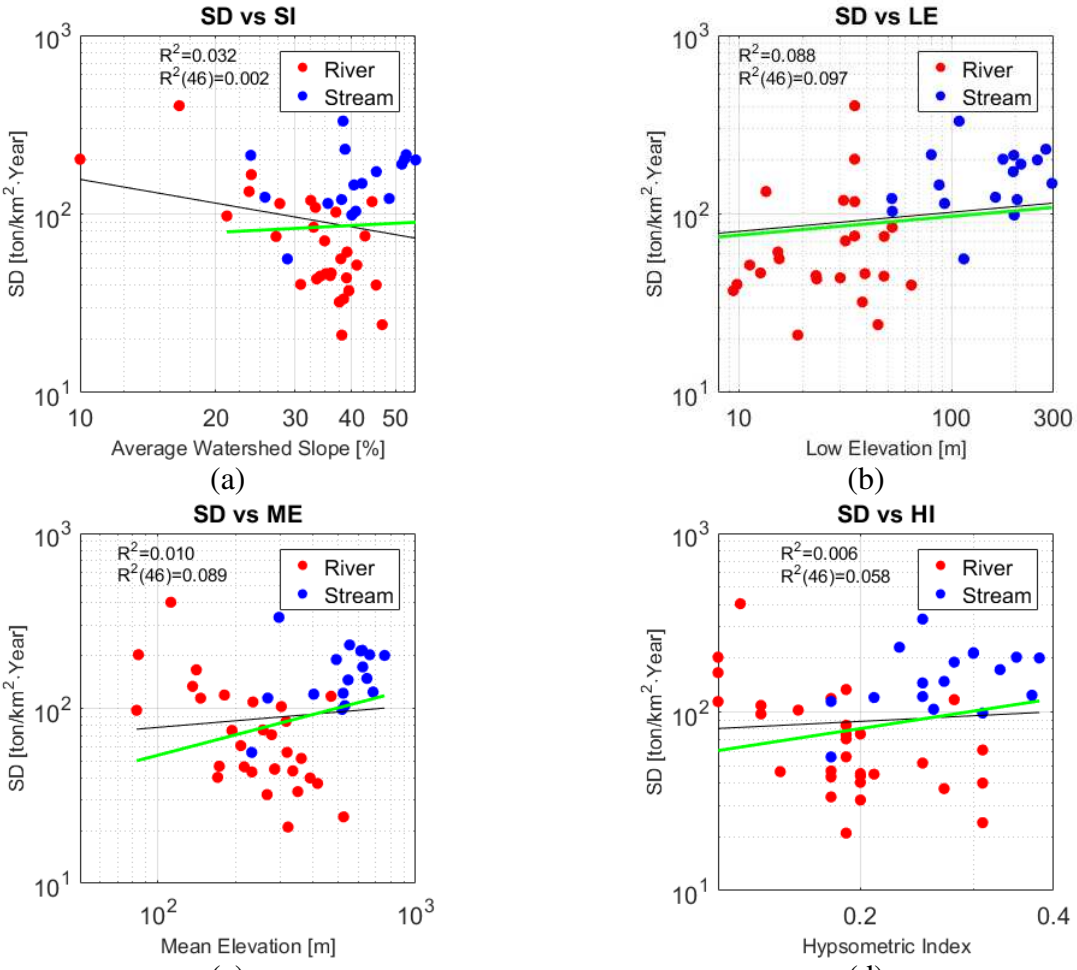

Figure 24. Existing parameters related to relief aspects versus specific degradation (a) Average watershed slope, (b) Low Elevation, (c) Mean Elevation, and (d) Hypsometric Index

In this result, the parameters from the hypsometric curve provide better correlation than existing parameters about the relief aspect. Especially, the elevation at the mid relative area shows relatively good correlation among relief parameters ($R^2 = 0.11$, *Figure 25 b*).

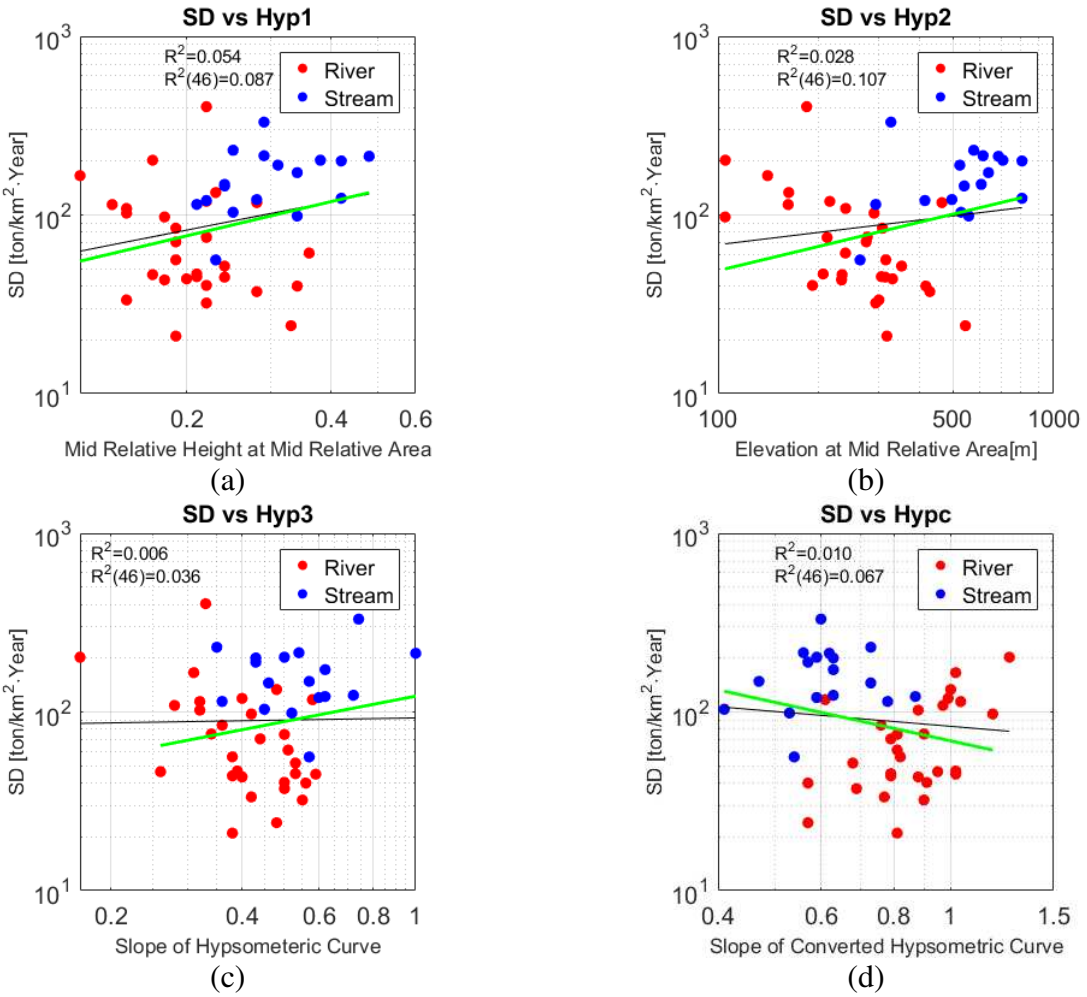

Figure 25. Parameters from hypsometric curve versus specific degradation (a) Relative height at the mid relative area, (b) Elevation at the mid relative area, and (c) Slope between 0.2 and 0.8 of the relative area, and (d) Slope of the logarithmic hypsometric curve

4.1.2. Watershed Characteristics about Precipitation

Precipitation is the main agent of erosion and sedimentation process. It directly impacts on soil detachment with raindrop hit and delivers the sediment to downstream after changing as runoff. The 60 points of daily precipitation data from the Korea Meteorological Administration (KMA) were used for analysis. From the raster result of kriging, two values of mean annual precipitation are exported. One was the point value of mean annual precipitation at gauging station (P, P_point); another was averaged mean annual precipitation value from watershed area (P_area).

The rainfall erosivity (R-factor) for the same 60 points was calculated and original kriging was also applied for estimation of gross erosion. The point value of R-factor at gauging station (R_point); and averaged R-factor from watershed area (R_area) were exported for regression parameters. The simple linear regression results between the specific degradation and 4 parameters from the mean annual precipitation and R-factor from kriging result are in *Figure 26*.

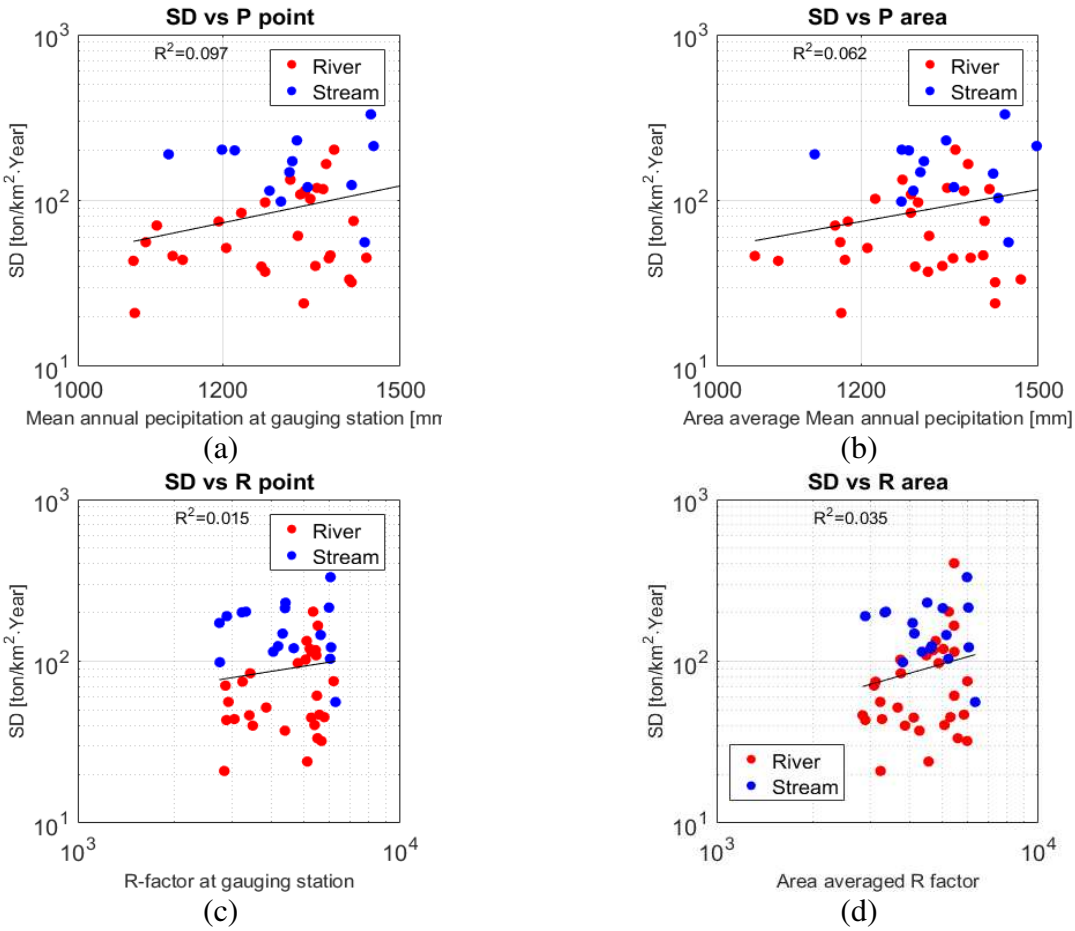

Figure 26. Mean annual precipitation parameters versus specific degradation (a) Point P-value at gauging station, (b) Area averaged P-value, (c) Point R-value at gauging station, and (d) Area averaged R-value

Different from the expectation that area averaged mean annual precipitation ($R^2 = 0.062$) show less correlation than point mean annual precipitation value ($R^2 = 0.0097$). The parameters related to R-factor also provide week correlation than mean annual precipitation. It seems that 60 points values of mean annual precipitation are not enough to explain the mean annual precipitation

pattern of entire Korea. Even though precipitation has been used as a factor in many models, all parameters could not show very good correlation with specific degradation results.

4.1.3. Watershed Characteristics about Soil Type and Land Use

Soil type has influences on soil erosion and sedimentation process. To estimate the percentage of soil type and K factor, the detailed soil map from National Institute of Agriculture Sciences is used. It is classified into: (1) clay ($d_{clay} \leq 0.002$mm); (2) silt ($0.002 < d_{silt} \leq 0.05$mm); (3) sand ($0.05 < d_{sand} \leq 2$mm); and (4) rock ($2\text{mm} < d_{rock}$) at each effective soil depths: (1) 0~10cm; (2) 10~30cm; (3) 30~50cm; (4) 0~30cm; and (5) 0~50cm. As shown in *Figure 27* for a given soil type, they provide weak correlation with the specific degradation than other parameters.

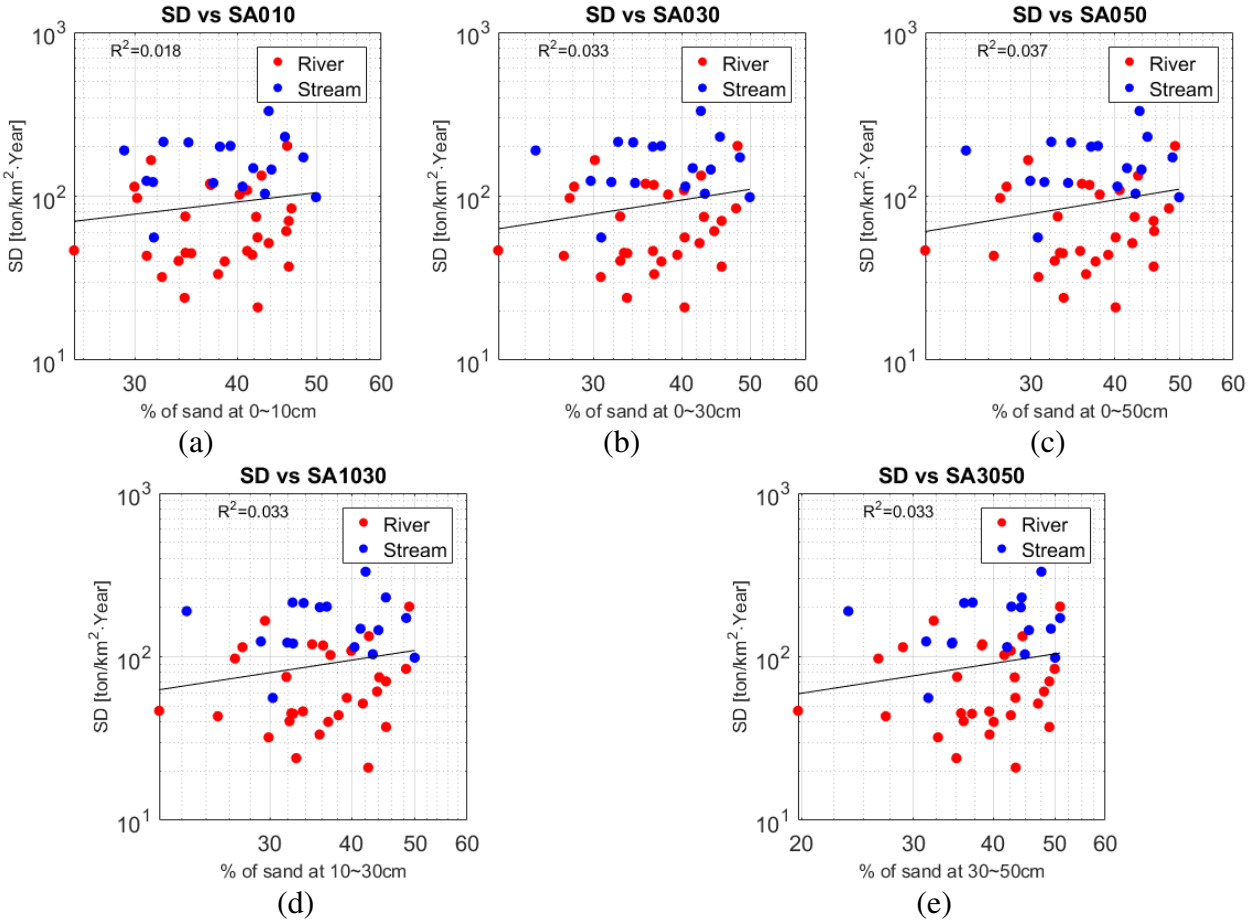

Figure 27. Specific degradation vs percentage of sand at (a) 0~10cm, (b) 0~30cm, (c) 0~50cm, (d) 10~30cm, and (e) 30~50cm

The R-square varies from 0.001 to 0.06. Among them, the percentage of sand at all effective soil depths could not well classify the difference between stream and river, however, they provide a consistent and plausible relationship with specific degradation. Land use also influences soil erosion and sedimentation processes. The land cover raster (10m resolution) from the Ministry of Environment (ME) and detailed soil map (vector) from the National Institute of Agriculture Sciences are used for analysis. In terms of land use, the land cover raster classified 23 types of land cover and they are simplified as 7 types; 1) Urban, 2) Agriculture, 3) forest, 4) wetland, 5) pasture, 6) bare land, and 7) water. The percentage of urbanized area has low R-square value (*Figure 28*, $R^2 = 0.004$).

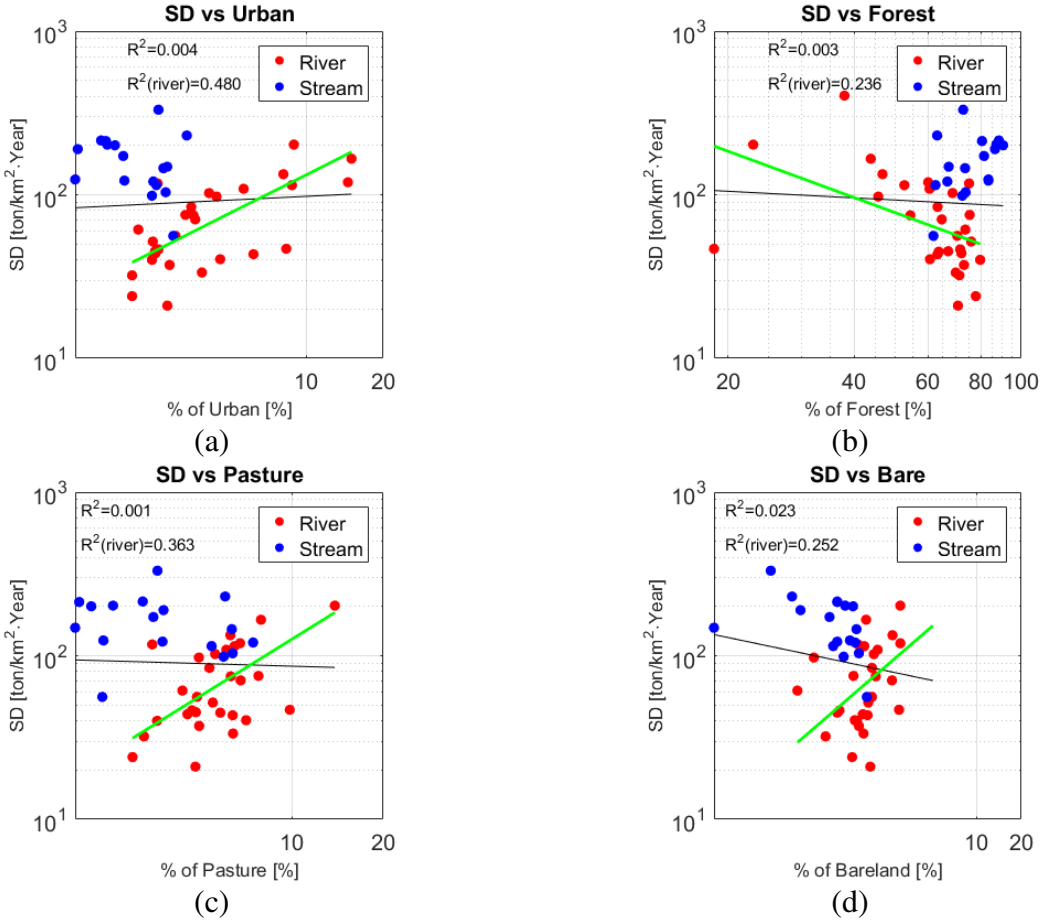

Figure 28. Land use versus specific degradation (a) Urban, (b) Forest, (c) Pasture, and (d) Bare-land

The river watersheds have definitely a positive relationship with specific degradation ($R^2 = 0.048$, *Figure 28*a). The percentage of forest and pasture do not provide distinct relationships (*Figure 28*b and c). In the case of forest areas, the forested area commonly produces less sediment due to their sediment delivery ability only in river watersheds (R^2=0.0238, *Figure 28*b). Commonly, the bare lands produce more sediment. However, the percentage of bare-land has unreasonable relationships with specific degradation (*Figure* 28d). The percentage of urban, forest, and bare land shows unexpected relationship with specific degradation due to the spatial lumping problem from steep mountain regions providing more sediment. The increase of agricultural land typically decreases specific degradation (*Figure 29a*).

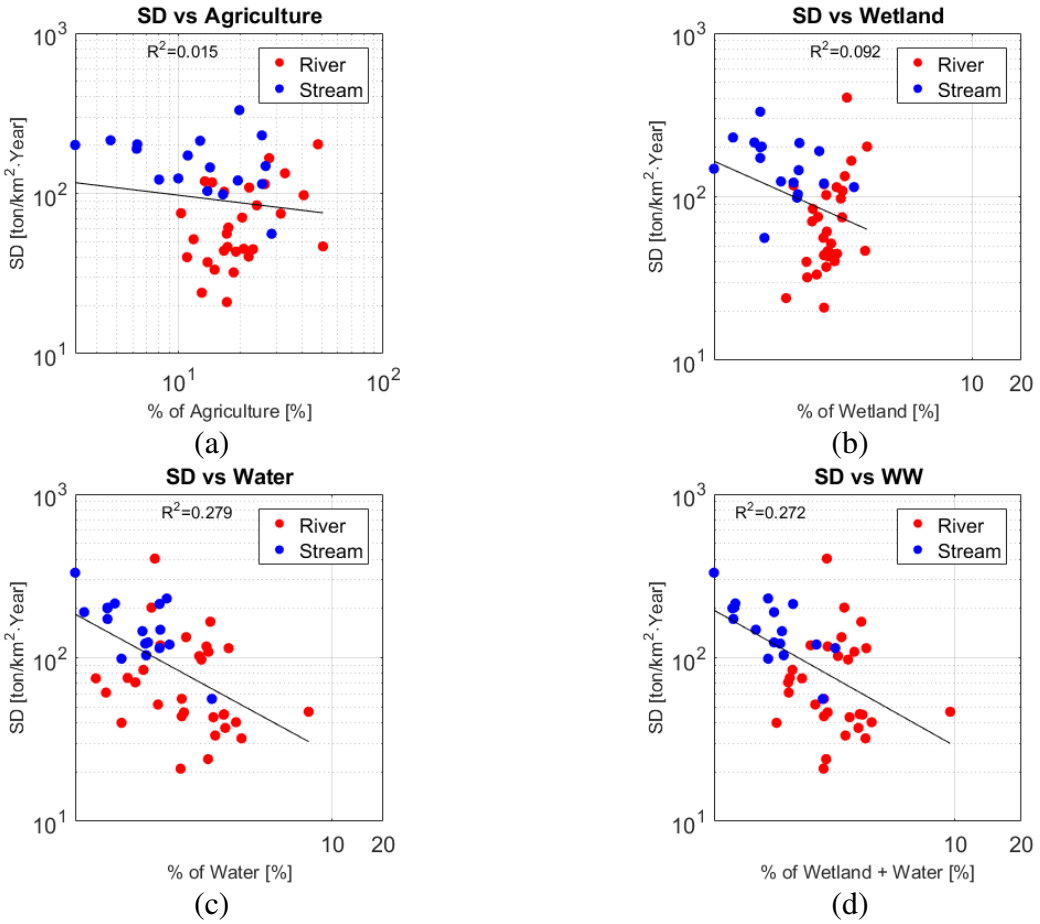

Figure 29. Land use versus specific degradation (a) Agriculture, (b) Wetland, (c) Water, and (d) Wetland + water

This may be explained because agricultural land used for paddy fields which effectively works as small reservoirs during summer season in South Korea. In contrast with the previous variables, the percentage of wetland and water provides better correlation with the specific degradation and their physical relationships are also reasonable (*Figure* 29b, c, and d).The wetland typically traps sediment and the wetland is located in near alluvial river. Therefore, the negative slope between summation of wetland and water and specific degradation is reasonable and they provide great correlation ($R^2 = 0.272$) with specific degradation could be expected (*Figure* 29d).

4.2. Regression Model for Specific Degradation

In total 51 watershed parameters related to sediment are estimated using GIS to explain specific degradation. The regression analysis was done with the "R" version 3.3.2. The general form of multiple linear regression model with normal error terms could be presented as

$$Y_i = \beta_0 + \beta_1 X_{i1} + \beta_2 X_{i2} + \cdots + \beta_{p-1} X_{i,p-1} + \epsilon_i \qquad \text{Eqn 4-3}$$

Where Y_i is the response variable

$X_{i1}, \cdots, X_{i,p-1}$ are the explanatory variables

$\beta_{i1}, \cdots, \beta_{i,p-1}$ are the regression coefficients

ϵ_i is the error term

p-1 is the number of explanatory variables

In this study, the response variable is the specific degradation, and the explanatory variables are the characteristics of the watershed. Commonly, the regression model for specific degradation and sediment yield has been used log-log transformation to linearize regression relation and stabilize error variation. It could be expressed as

$$Y_i = \beta_0 + \beta_1 X_{i1} + \beta_2 X_{i2} + \cdots + \beta_{p-1} X_{i,p-1} + \epsilon_i \qquad \text{Eqn 4-4}$$

Which is equivalent to

$$SD_i = e^{\beta_0} \times {X_{i1}}^{\beta_1} \times {X_{i2}}^{\beta_1} \times \cdots \times {X_{p-1}}^{\beta_{p-1}} \quad \text{Eqn 4-5}$$

Total 51 of explanatory variables from GIS analysis are used for a regression model to explain the specific degradation. The ratios considering reservoir area (A* and A**) are excluded because some watershed in upstream areas do not have reservoir, which results in A* = 0. Furthermore, the confidence and prediction intervals were suggested as follows.

$$X_h = \begin{bmatrix} 1 \\ logA \end{bmatrix}, X_h = \begin{bmatrix} 1 \\ logA \\ \log P \end{bmatrix}, X_h = \begin{bmatrix} 1 \\ logA \\ \log P \\ \log U \end{bmatrix}, \cdots, or\ X_h = \begin{bmatrix} 1 \\ logA \\ \log P \\ \vdots \\ \log Hyp \end{bmatrix} \quad \text{Eqn 4-6}$$

where, X_h is the observation for estimating the mean response.

$$SD_h \pm t\left(1 - \frac{\alpha}{2}; n - p\right) s\{SD_h\} \quad \text{Eqn 4-7}$$

where, α is the level of significant (α = 0.05),

In multiple regressions, the prediction interval is difficult to display. Therefore 5000 randomly samples generated with the value within the range of data for new 95% prediction intervals based on the below equations.

$$s\{SD_h\} = \sqrt{MSE\ X_h^T (X^T X)^{-1} X_h} \quad \text{Eqn 4-8}$$

where, $s\{SD_h\}$ is the estimated standard deviation.

This estimated standard deviation is in training dataset X

$$X = \begin{bmatrix} 1 & \log A_1 & \cdots \\ \vdots & \vdots & \vdots \\ 1 & \log A_{29} & \cdots \end{bmatrix} \quad \text{Eqn 4-9}$$

For the new observation, the 95% of prediction interval is

$$SD_h \pm t\left(1 - \frac{\alpha}{2}; n - p\right) s\{\text{pred}\} \quad \text{Eqn 4-10}$$

The estimated variation of predictions is

$$s^2\{\text{pred}\} = MSE\left(1 + X_{h(new)}^T (X^T X)^{-1} X_{h(new)}\right) \quad \text{Eqn 4-11}$$

The range of prediction interval increases as more variables were used.

Therefore, when applying the models, we should be cautious if a new observation falls outside the scope of the model. In that case, the prediction may not be accurate. Another prediction interval at 95% is suggested. This approximated prediction interval is calculated as

$$\bar{Y} \pm 1.96\sigma, \qquad \sigma = s\left\{\log\left(\frac{SD_m}{SD_c}\right)\right\} \quad \text{Eqn 4-12}$$

where, σ is the standard deviation of the log of measured to calculated specific degradation ratios from calibration dataset,

SD_m is the measured specific degradation from FD-SRC

SD_c is the specific degradation from the regression model.

Figure 30 shows the comparison of measured specific degradation and modeled specific degradation (blue dots). The vertical bars show the 95% confidence interval of the estimate. The green dots show the 95% prediction interval from 5000 random generated results. The prediction interval at 95% interval (blue solid line) for GUI has a similar boundary with the random simulation. Therefore, only the prediction interval at 95% (blue solid line) is considered for application.

4.2.1. Regression Models

The 51 watershed parameters were used as explanatory variables for the regression models. Also, 28 specific degradation data (except H3, N12, N6, G5, S1, S2, and S4) in the river were used for the river regression models (M1 ~ M6) and 47 specific degradation data were used as response variables for a combined river and stream regression model (M7). The specific degradation at gauging stations which do not have enough sediment measurements or daily discharge could be distorted (APPENDIX D). The discarded station from each regression model

was organized in *Table* 7 and they were used for validation (*Table 10*). A total of seven regression models were developed. First, 5 models for rivers (M1~M5) were based on the USLE structure with confidence intervals were developed to estimate the mean annual specific degradation (SD) in tons/km^2▪yr for ungauged watersheds based on watershed characteristics and precipitation data. Two additional models were developed with additional consideration of hypsometric curve and wetland. The model M6 is applicable to rivers only while model M7 applies to both river and streams.

$M1)\ SD = 357.16A^{-0.204}$	RMSE=118	Eqn 4-13
$M2)\ SD = 3.35 \times 10^{-7}A^{-0.16}P^{2.864}$	RMSE=113	Eqn 4-14
$M3)\ SD = 0.0003 \times A^{-0.08}P^{1.65}U^{0.75}$	RMSE=101	Eqn 4-15
$M4)\ SD = 1.75 \times 10^{-7}A^{-0.05}P^{1.89}U^{0.89}Sa^{1.931}$	RMSE=84	Eqn 4-16
$M5)\ SD = 1.77 \times 10^{-5}A^{-0.009}P^{1.91}U^{0.53}Sa^{1.09}Sl^{-0.93}$	RMSE=87.6	Eqn 4-17
$M6)\ SD = 2.45 \times 10^{-7}A^{-0.04}P^{1.94}U^{0.61}W^{-0.64}Sa^{1.51}Hypc^{1.84}$	RMSE=81	Eqn 4-18
$M7)\ SD = 1.75 \times 10^{-5}A^{-0.07}P^{2.23}U^{0.4}WW^{-1.04}Hyp3^{-0.42}$	RMSE=51	Eqn 4-19

First, the models (M1~M5) based on USLE structure were analyzed (*Figure 30* and *31*). The meaningful parameters of the watershed characteristics were the watershed area in square kilometers (A), the mean annual precipitation in millimeters (P), the percentage of urbanized area (U), the percentage of sand in the soil (Sa), the average watershed slope (Sl). The negative trend between specific degradation and watershed average slope is because the steep watersheds are in remote mountains area and covered by forest while the floodplains are where urban and agriculture developed (Kane and Julien, 2007). The watershed area is the fundamental and accessible parameter, and it is also widely used in literature for the prediction of sediment yield. Mean annual precipitation is highly related to RUSLE R-factor (Lee and Heo, 2011), and it is much easier to obtain compared to the R-factor. Percentage of urban is the one has the highest adjusted R-squared when we tested with all the land use parameters with only river data.

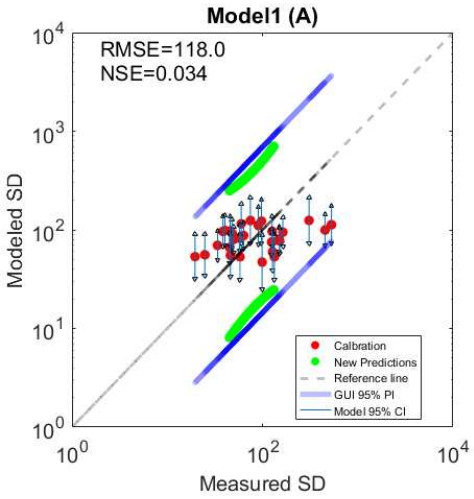

(a)1 var model

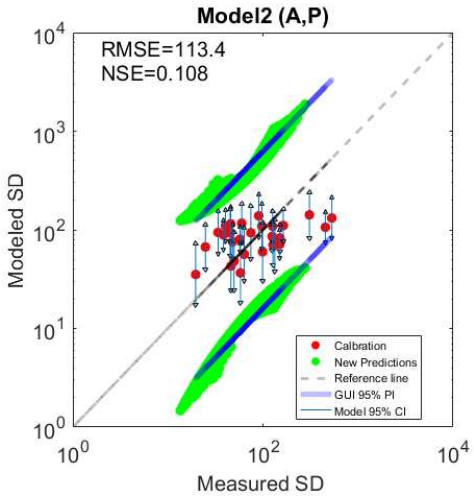

(b) 2 vars model

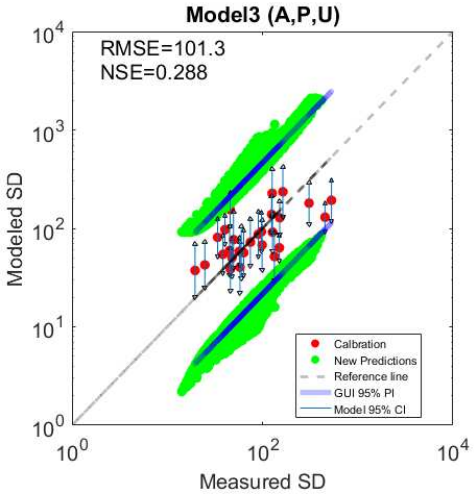

(c) 3 vars model

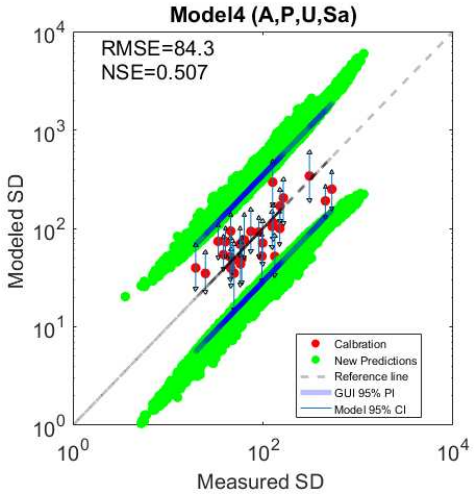

(d) 4 vars model

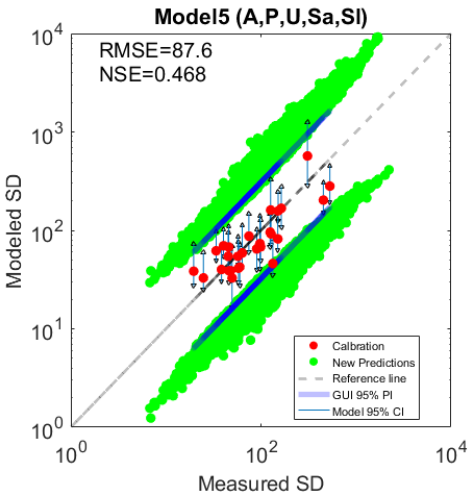

(a) 5 vars model

Figure 30. Confidence and prediction intervals of the five regression models based on USLE (units: tons/km^2▪yr)

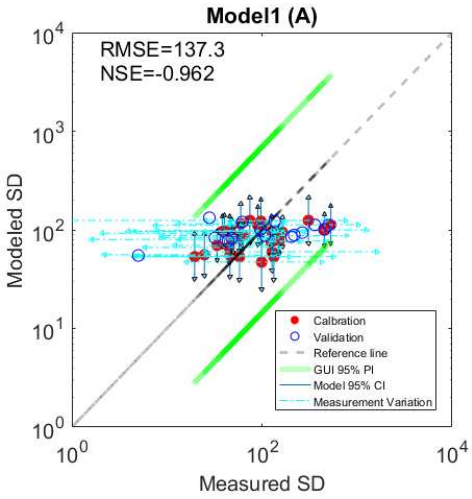

(a) 1 var model

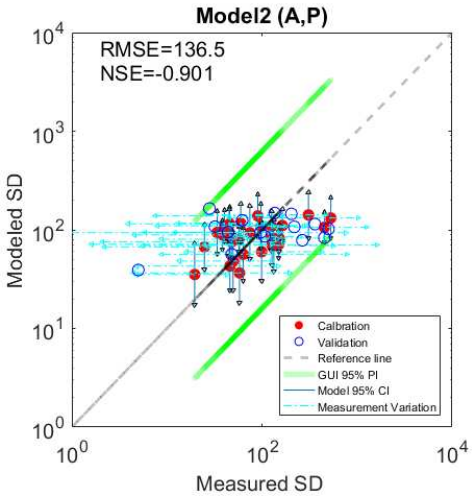

(b) 2 vars model

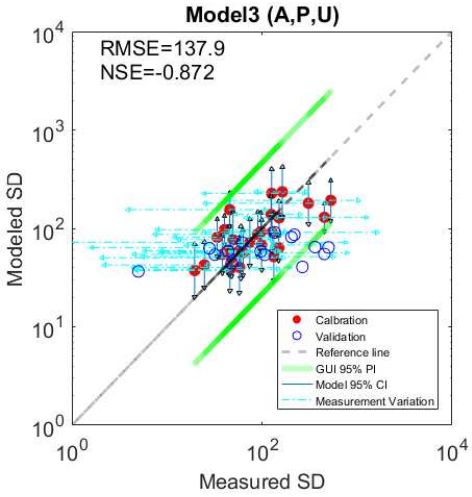

(c) 3 vars model

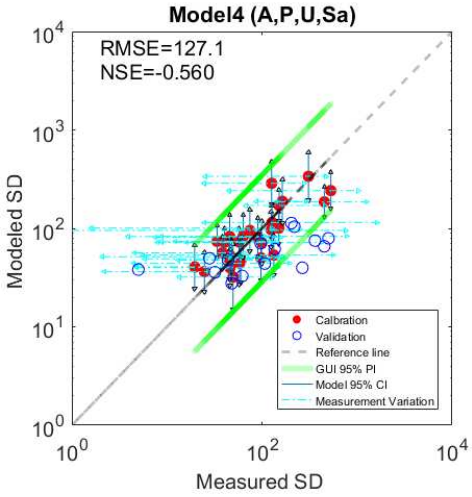

(d) 4 vars model

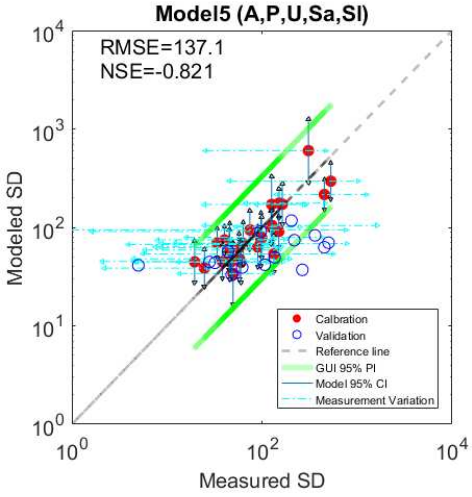

(e) 5 vars model

Figure 31. Validation and GUI 95% prediction intervals of the five regression models based on USLE (units: tons/km^2▪yr)

Each parameter could represent the 6 factors in the USLE. The negative trend between specific degradation and watershed average slope is because the steep watersheds are in remote mountains areas while urbanization and agricultural land develop in lowland areas (Kane and Julien, 2007). Since the proposed models were based on 10 years daily discharge and sediment measurement. The temporal variability in specific degradation was estimated for every year and it was displayed with minimum and maximum yearly SD as a horizontal dashed arrow (*Figure 31)*. They varied from 4 to 8,000 tons/km^2▪yr. The extreme specific degradation results generated from low sediment measurements in a year including large storm everns. It suggested that the estimated SD from short period could be distorted, therefore using 10 year data and removing the SD from low sediment measurement is reasonable.

Table 10. Validation dataset for developed regression models

Name	Class	A [km^2]	P [mm]	W [%]	U [%]	Sa [%]	Sl [%]	Hyp3	Hypc	SD [tons/km^2▪yr]
N12	River	1,318	1,123	1.3	2.7	32	36	0.95	48	48
N6		9,533	1,106	1.3	2.6	44	40	0.80	5	5
G5		208	1,333	1.6	2.9	26	34	1.03	62	62
S1		1,269	1,404	1.0	2.1	33	38	0.90	32	32
S2		1,788	1,370	1.5	2.6	37	35	1.02	44	44
S4		128	1,429	1.0	2.0	39	44	0.69	28	28
Hwajeon Bridge	River	188	1,407	0.2	3.5	33	44	1.68	136	136
Janghyeon Bridge	Stream	923	1,376	0.8	4.0	47	45	1.37	219	219
Seokpo Bridge	Stream	299	1,269	0.6	2.9	51	37	1.52	501	501
Songriwon Bridge	Stream	491	1,215	0.5	2.7	50	36	1.36	453	453
Daeso Bridge	Stream	971	1,279	0.3	2.5	38	44	1.24	107	107
NU1	Stream	697	1,214	0.5	1.9	45	45	0.56	266	266
NU13		1,130	1,548	0.9	2.9	52	33	0.57	204	204
GU4		291	1,318	0.3	2.6	49	30	0.78	361	361
GU2		490	1,271	1.9	2.7	50	26	0.73	97	97

To validate the developed models based on the USLE structure, the specific degradation at 15 additional stations was used (*Table 10*). They were from other reference and excluded results from regression analysis (MOC, 1992). The validation results of the proposed models were shown as empty circles in *Figure 31*.Most of the validation results were within the range of 95% prediction interval. Model M1-M5 reduced the RMSE to approximately 137.1 tons/km^2▪yr which is much lower than the very high values from the methods discussed in Section 3.3 (i.e. RMSE > 275 tons/km^2▪yr). This model M6 was developed for rivers only to include the percentage area covered by wetlands (W), and the slope of the logarithmic hypsometric curve (Hypc). The percentage of wetland provides a negative relationship with the specific degradation. The specific degradation also increases with the slope of the logarithmic hypsometric curve (*Figure 32*).

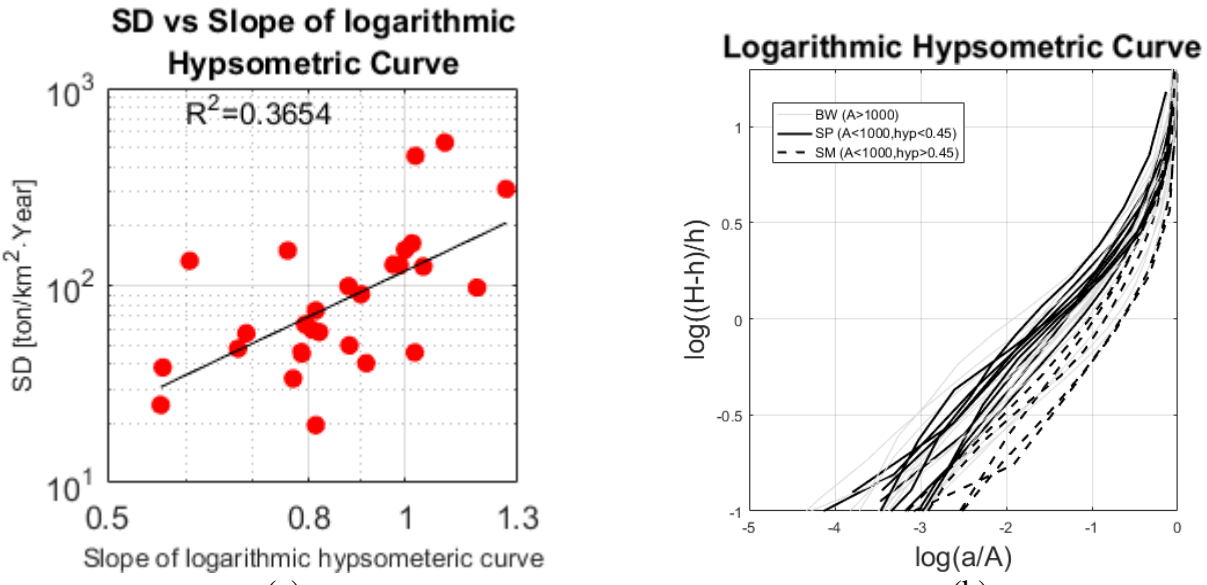

(a) (b)

Figure 32. Relationship between the specific degradation and (b) The slope of logarithmic hypsometric curve, and (c) The logarithmic hypsometric curve for river watersheds

In *Figure 33* shows that RMSE of Model 6 is 80.1 tons/km^2▪yr for calibration and 150.1 tons/km^2▪yr including validation. However, the RMSE is higher than model 5. It means that the model 5 shows better performance for rivers than model 6. Therefore, an additional regression

model (M7) was developed with 48 specific degradation data including both rivers and streams. In model M7, two additional parameters [i.e. the percentage area covered by wetlands and water (WW), and the slope of the hypsometric curve (Hyp3)] are used to explain the specific degradation. Model 7 well predicts the specific degradation for both streams and rivers. The validation is conducted with the reference from MOC (1992), and all points are within the 95% prediction intervals. The RMSE of the prediction decreases to 88.8 tons/km^2▪yr and NSE increases to 0.516 (*Figure 33*b).

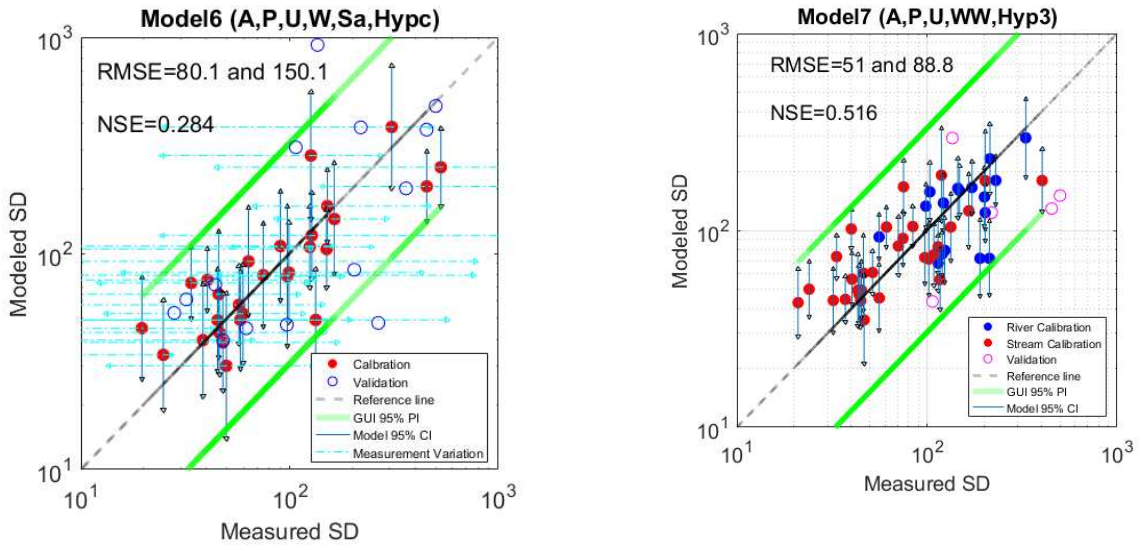

(a) (b)

Figure 33. Validation and 95% prediction intervals of (a) Model M6 and (b) Model M7

In *Figure 34*b, the multicollinearity problem was tested by checking the variance inflation factor (VIF) as below.

$$\mathrm{VIF}_i = \frac{1}{1 - R_i^2} \qquad \text{Eqn 4-20}$$

where, R_i^2 is the coefficient of determination of the regression equation

A rule of thumb is that when multicollinearity is high, VIF is larger than 10 (Kutner et al., 2004). Therefore, all models did not have a multicollinearity problem (*Figure 34*b).However, the model had some statistical limitation. Specifically, the model had relatively low adjusted R-squared

value ($R^2_{adj} = 0.51$) and the variable could not perfectly pass the null-hypothesis (P-values). These statistical problems are attributed to the relatively short sampling program for sediment in South Korea. Improvement in regression models can be expected when additional specific degradation measurements become available and when sediment periods of record exceed at least 20 years.

```
Call:
lm(formula = SD ~ Area + Precip + Urban + WW + Hyp3, data = log(df))

Residuals:
     Min       1Q   Median       3Q      Max
-0.93382 -0.28359 -0.07416  0.29725  1.08422

Coefficients:
            Estimate Std. Error t value Pr(>|t|)
(Intercept) -10.96545    6.02994  -1.818  0.07630 .
Area         -0.07357    0.06043  -1.217  0.23044
Precip        2.22707    0.82244   2.708  0.00983 **
Urban         0.40062    0.19236   2.083  0.04357 *
WW           -1.04141    0.20574  -5.062 9.19e-06 ***
Hyp3         -0.41850    0.31779  -1.317  0.19519
---
Signif. codes:  0 '***' 0.001 '**' 0.01 '*' 0.05 '.' 0.1 ' ' 1

Residual standard error: 0.491 on 41 degrees of freedom
Multiple R-squared:  0.5665,    Adjusted R-squared:  0.5137
F-statistic: 10.72 on 5 and 41 DF,  p-value: 1.238e-06
```

(a)

Model	Var1	Var2	Var3	Var4	Var5	Var6
M1	-	-	-	-	-	-
M2	1.06	1.06	-	-	-	-
M3	1.16	1.13	1.21	-	-	-
M4	1.18	1.13	1.28	1.06	-	-
M5	1.33	1.13	2.17	1.17	2.24	-
M6	1.36	1.14	2.74	3.39	1.06	4.67
M7	1.40	1.18	2.46	1.90	1.85	-

(b)

Figure 34. (a) Statistical summary of Model 7 and (b) Calculated VIF values for the 7 models

4.3. Graphical User Interface of Developed Models for Rivers

In website http://feelingwc.wixsite.com/ungaugedsd, two version (i.e. website and excel spreadsheet) of Graphical User Interface (GUI) for developed models (M1~M5) for river was developed for sediment yield estimation from ungauged watersheds (*Figure 35*). When the user enters the watershed area, the mean specific degradation and sediment yield will be estimated as well as the developed 95% prediction intervals. The prediction interval of specific degradation decreases when the variables for equations increase. It means that the equation which has more variable could provide better specific degradation. By counting the number of variables within the measured range, an index for the applicability of the regression equations is defined and shown in *Table 11*. If only the watershed area is entered, the one-variable model will be used. The GUI shows the number of inputs that are within the range of calibration dataset (1 is within the range and 0 is outside the range), and total number of variables of which values are within range of calibration dataset.

Table 11. Applicability index of GUI for developed models

# of variable within measured range	Predictability
5	Good
4	Moderate
3	Fair
2	Poor
1	Very poor

Additionally, when the percentage of urban is lower than 2%, the index value is "-1" to consider some possible watersheds which have low percentage of urban. This index could provide information when the user put the extreme value of variables for small watershed, city, and drought/flood regions. In the meantime, the 95% prediction intervals for specific degradation and sediment yield will be calculated and displayed next to the mean.

Input variables		
Variables	Unit	Value
Watershed area, A	km^2	800
Precipitation, P	mm	1322
% of urban, U	%	2.66
% Sand at 0~50cm, Sand	%	32
Watershed avg slope, S	%	35

Dataset information			
Var	Mean	Range	
A	3482	173	20380
P	1287	1072	1425
U	5	2	15
Sand	43	22	60
S	34	10	47

Applicability index:	Good
Watershed area, A	1
Precipitation, P	1
% of urban, %U	1
% Sand at 0~50cm, Sand	1
Watershed avg slope, S	1
# of data within range	5

Index
0: No confidence
1: Very poor
2: poor
3: Fair
4: Moderate
5: Good

Results							
Equations	Specific Degradation			Sediment Yield			# of data within range
	Mean	Predicion Intervals		Mean	Predicion Intervals		
	tons/km^2·year			tons/year			
1var eqn	100	18	562	79867	14194	449381	1
2vars eqn	108	21	550	86241	16889	440377	2
3vars eqn	70	16	309	56134	12730	247525	3
4vars eqn	38	12	122	30018	9257	97342	4
5vars eqn	40	13	129	32126	10034	102853	5

- Values for applicability index
Input is in range of dataset: "1"
Input is out range of dataset: "0"
+) Urban of percentage is "-1" when it is lower than 2.09%

- Higher number of data in reliable range could be indicator of better result
- SD result from more variable provides better results than others

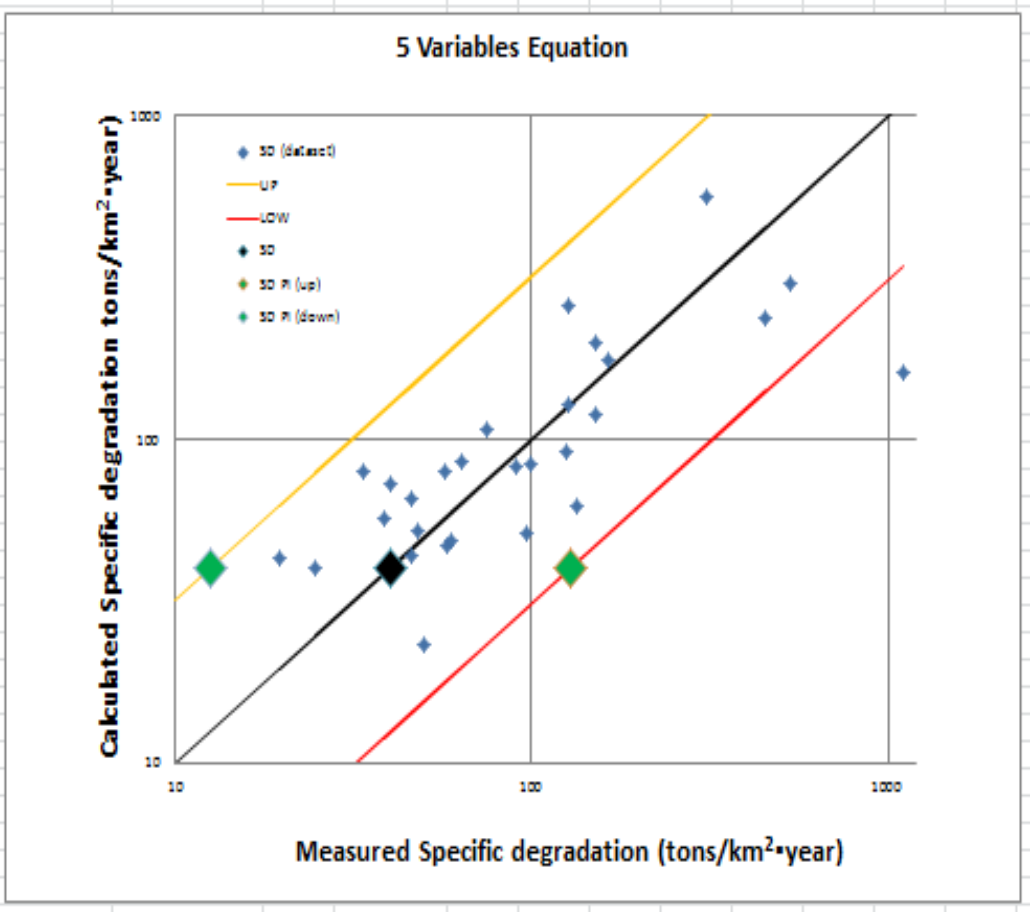

Figure 35. Graphical User Interface (GUI) for the developed model (excel spreadsheet)

The developed Model and GUI were tested by a Korean Research Team to the research project "Multivariate Regression Analysis and Model Development for the Estimation of Sediment Yield and sediment management from Ungauged Watershed in the Republic of Korea". They compared the simulated the specific degradation for 12 watersheds with K-Water hydrologic & hydraulic Distributed Runoff Model (K-DRUM) and SD from sediment measurements. The developed models provided similar SD with measurement than SD from K-DRUM (K-Water, 2017). Especially, M4 showed best performance in predicting specific degradation. They also evaluated the developed applicability index and 95% prediction interval. They also suggest the result from the developed model could be distorted in the small watershed area ($A < 170$ km^2), watershed with low precipitation ($P < 1070$ mm), and small urbanized area ($U < 2\%$). They concluded the developed model and applicability index could be helpful for decision making. In this chapter, 51 parameters related to precipitation and watershed characteristics were estimated. The R-square value between all parameters and the specific degradation is listed in *Table 12*.

Table 12. R-square value between the specific degradation from 48 stations and parameters

Parameter	R-square	Parameter	R-square	Parameter	R-square
Total	0.217	*hyp3	0.006	R3050	0.066
Main	0.244	*hypc	0.01	C030	0.044
Tri	0.208	*P_point	0.097	SI030	0.005
SO1	0.008	P_area	0.062	SA030	0.033
SO2	0.09	R_point	0.015	R030	0.039
SO3	0.137	R_area	0.035	C050	0.047
*Area	0.211	C010	0.06	SI050	0.004
DD	0.012	SI010	0.025	*SA050	0.037
SF	0.227	SA010	0.018	R050	0.044
AXL	0.242	R010	0.001	*Urban	0.004
LF	0.089	C1030	0.038	Agriculture	0.015
*Avg_slope	0.032	SI1030	0.002	Forest	0.003
LE	0.088	SA1030	0.033	pasture	0.001
ME	0.01	R1030	0.041	*wetland	0.092
HI	0.006	C3050	0.011	bare	0.023
hyp1	0.054	SI3050	0.001	water	0.279
hyp2	0.028	SA3050	0.033	*WW	0.272

* Parameters used in the developed models

A total of seven models (6 for rivers, and 1 for streams and rivers) were developed. The 95% prediction intervals were developed based on the specific degradation from models and measurements. The most validation results were within the 95% prediction intervals. The predictability of the developed models showed better accuracy compared to existing statistical models. The Root Mean Square Error of the prediction is less than 100 tons/km^2▪yr, which is a significant improvement upon the existing methods (RMSE > 275 tons/km^2▪yr) detailed in Chapter 3.3.

Chapter 5
Geospatial Analysis of Upland Erosion

In this chapter, the geospatial analysis for upland erosion was conducted with erosion maps using Revised Soil Loss Equation (RUSLE), satellite images, and aerial photos. The resolution effects (i.e. 5m, 30m, and 90m resolution) on the erosion maps also tested.

5.1. Erosion Mapping with RUSLE

Walling (1999) suggested that the overall sediment budget of a catchment and the sediment output should be considered together to understand the impact of land use on sediment yield. In this chapter, the erosion mapping with RUSLE was conducted to estimate the overall sediment budget, and identify at different grid size meaningful erosional features through erosion mapping. The gross erosion for some watersheds was calculated with GIS, and then a geospatial analysis was conducted through a comparison of model calculation with satellite images and aerial photos.

5.1.1. Factors for RUSLE

First, the rainfall erosivity (R-factor) at 60 stations was calculated with Eqn 5-1 and original kriging was applied.

$$R = \sum E \cdot I_{30}\,, E = \sum e \cdot \Delta P, e = 0.29[1 - 0.72\exp(-0.05 \cdot I)] \qquad \text{Eqn 5-1}$$

where R is the rainfall erosivity factor (10^7 J/ha▪mm▪hr)

I_{30} is the maximum 30-minute rainfall intensity (mm/hr)

E is the total storm kinetic energy (10^7 J/ha)

ΔP is the rainfall increasing between duration of rainfall interval (mm)

e is the estimated unit rainfall kinetic energy (MJ/ha▪mm)

I is the rainfall intensity (mm/hr)

The soil erodibility factor (K) was estimated for each great soil group with the Eqn 5-2 (Wischmeier et al., 1971).

$$K = \frac{0.00021 \cdot M^{1.14} \cdot (12 - OM) + 3.25(C_{soilstr} - 2) + 2.5\left(C_{perm} - 3\right)}{100} \quad \text{Eqn 5-2}$$

$$M = (m_{silt} + m_{vfs}) \cdot (100 - m_c) \quad \text{Eqn 5-3}$$

$$\mathrm{OM} = 1.72 \cdot \mathrm{orgC} \quad \text{Eqn 5-4}$$

where K is the soil erodibility factor (ton·acre·hr/hundreds of acre·foot-tonf·inch)

M is the particle-size parameter

OM is the percentage of organic matter (%)

$C_{soilstr}$ is the soil structure code used in soil classification (1~4)

C_{perm} is the profile permeability class (1~6)

m_{silt} is the percentage of silt (%)

m_{vfs} is the percentage of fine sand (%)

m_c is the the percentage of clay (%)

orgC is the percentage of organic carbon content of the layer (%)

The slope length (L) in RUSLE was calculated as (McCool et al., 1987; Renard et al., 1997)

$$L = (X_h/72.6)^m \quad \text{Eqn 5-5}$$

$$m = {}^{\varepsilon}/_{(1+\varepsilon)} \quad \text{Eqn 5-6}$$

$$\varepsilon = {}^{\sin\theta}/_{0.0896 \times [3 \times (\sin\theta)^{0.8} + 0.56]} \quad \text{Eqn 5-7}$$

where X_h is the horizontal slope length (ft)

m is the variable slope length exponent

ε is the variable for the usceptible condition to rill and inter-rill erosion

θ is the slope length

The slope steepness (S) in RUSLE was calculated (McCool et al., 1987; Renard et al., 1997)

$$S = 10.8 \times \sin\theta + 0.03 \quad \sigma \leq 9\%$$
$$S = 16.8 \times \sin\theta - 0.5 \quad \sigma > 9\% \qquad \text{Eqn 5-8}$$

where σ is the slope gradient (%)

Van Remortel, Maichle and Hickey's method (2004) was used to estimate both factors. This method considers the downhill slope angle with a directional component and non-cumulative slope length for high points. This method could avoid the over extensions of slope lengths. The field runoff length (=horizontal slope length, X_h) is very important and to estimate the slope length steepness. The value of slope length steepness is plotted in *Figure 36*. The cropping management factor (C) and conservation practice factor (P) were mainly referenced from Kim and ME's regulation (ME, 2012). The values for each variable in C and P are organized in *Table 13 and 14*. The most cropping management factors follow the regulation from the ME and Kim (2006). In case of generic agricultural land, the averaged value from paddy field and farm was used. Also, the value for the vinyl greenhouse is the lowest value for agricultural land is applied. The conservation practice factor depends on the condition of slope and land use. The percentage of the slope is estimated with DEM, and land use is referenced from the land cover raster. To unify a grid size of all parameters as 5m resolution, the land use and soil classification were downscaled by using the majority function which could determine the new value of the cell based on the most popular values within the corresponding cells.

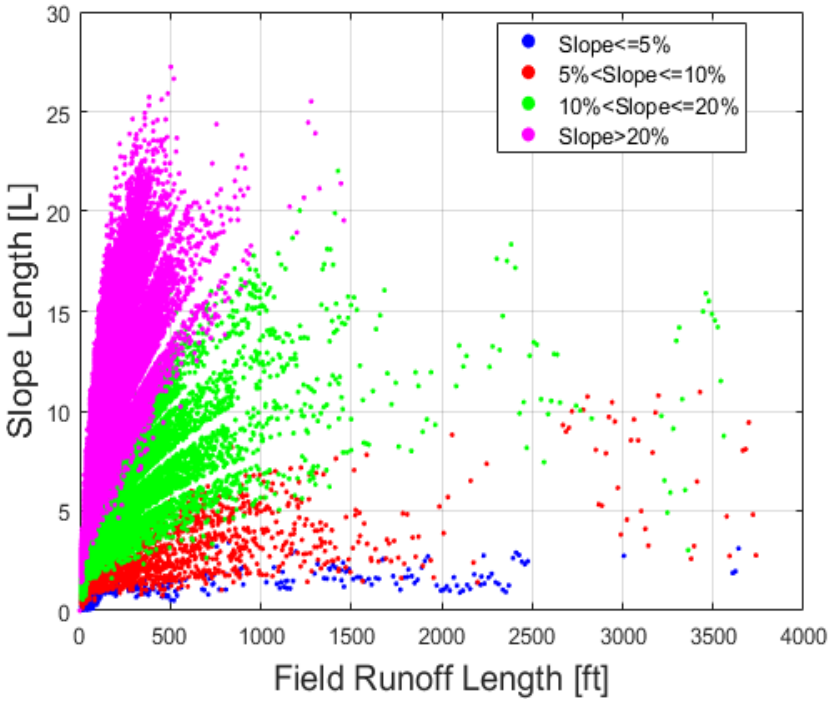

(a)

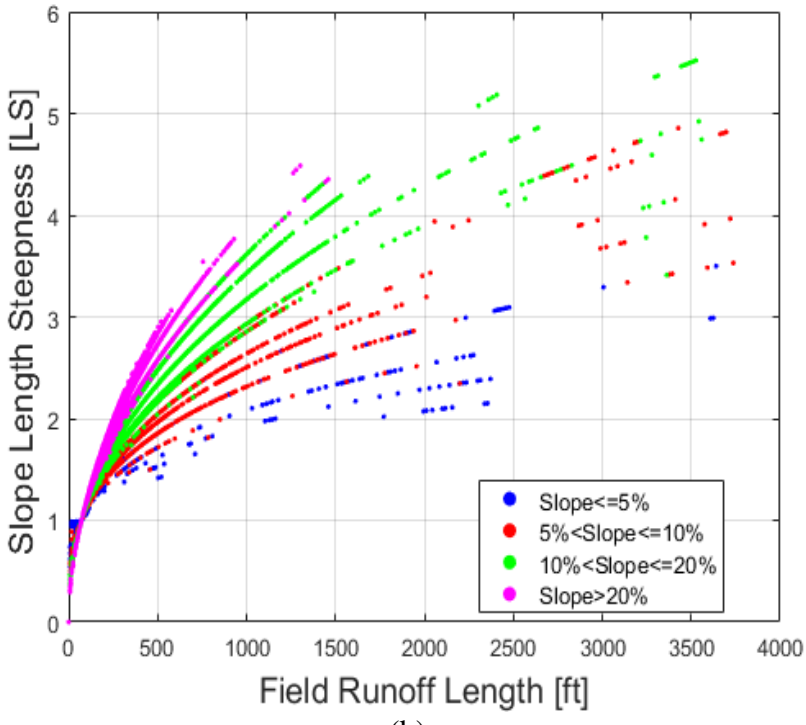

(b)

Figure 36. (a) Slope Length and (b) Slope length steepness factor of RUSLE with horizontal slope length (X_h) from DEM at 5m resolution

Table 13. Cropping management factor (Revised after ME 2012)

Major category	Sub category	C-value	Reference
Urban	Urban residential region Urban industrial region Urban commercial region Urban recreational region Urban for transportation region Urban for institutional region	0.01	(Kim, 2006)
Agriculture	Paddy field	0.1	(ME, 2012)
	Farm	0.3	(ME, 2012)
	Vinyl greenhouse	0.1	Assumption
	Orchard	0.09	(ME, 2012)
	Generic agricultural land	0.2	Assumption
Forest	Deciduous forest Evergreen forest Mixed forest	0.05	(ME, 2012)
Pasture	Natural pasture Golf Other pasture	0.15	(ME, 2012)
Wet land	Inland wetland Coast wetland	0	(Kim, 2006)
Bare land	Mining site Other bare land	1	(ME, 2012)
Water	Inland water Coast wetland	0	(ME, 2012)

Table 14. Practice management factor (ME, 2012)

Land Use	Slope (%)	P-value
Bare land		1
Paddy field	Slope < 2%	0.12
	2~7%	0.1
	7~15%	0.12
	15~30%	0.16
	Slope > 30%	0.18
Farm	Slope < 2%	0.6
	2~7%	0.5
	7~15%	0.6
	15~30%	0.9
	Slope > 30%	1
Pasture		1
Forest		1
Orchard		1

5.1.2. Gross Erosion and Sediment Delivery Ratio from RUSLE

The gross erosions for some watershed are calculated with GIS. As an example, the results for each parameter and gross erosion for Imha watershed are in *Figure 37* (Unit: tons/acre▪yr, 1 tons/acre▪yr= 246.91 tons/km^2▪yr). From the gross erosion result, the sediment delivery ratio was calculated through equation 2-13. The estimated specific degradation from rivers and streams was used for sediment yield at given stream or river, and the estimated specific degradation from sediment deposition in reservoir data was used for sediment delivery ratio for each reservoir catchments. The results of gross erosion and sediment delivery ratio at a 5m resolution are shown in the *Table 15*. Four reservoirs were selected as study area and each watershed includes 2 and 3 upstream gauging stations (*Table* 15).

Table 15. Estimated mean annual soil loss and sediment delivery ratio (SDR)

Name	Data	Mean annual soil loss		Area	Specific Degradation	SDR
		[tons/acre▪yr]	[tons/km^2▪yr]	[km^2]	[tons/km^2▪yr]	
N1	River	9.91	2,450	979	71	0.03
N10	River	9.56	2,360	175	75	0.03
N14	River	15.52	3,840	750	52	0.01
Andong	Reservoir	15.85	3,920	1,584	174	0.04
NU1	Stream	14.05	3,470	697	201	0.06
NU2	Stream	15.57	3,850	1,147	203	0.05
Imha	Reservoir	16.36	4,040	1,361	1,088	0.27
NU3	Stream	16.41	4,060	314	193	0.05
NU4	Stream	18.33	4,530	143	318	0.07
NU5	Stream	14.37	3,550	308	24	0.01
Seomjingang	Reservoir	21.9	5,420	763	734	0.14
SU1	Stream	20.2	4,990	359	120	0.02
SU2	Stream	21.88	5,410	133	135	0.02
Juam	Reservoir	24.8	6,130	1,010	964	0.16
SU3	Stream	11.4	2,820	295	56	0.02
SU4	Stream	22.1	5,460	273	207	0.04

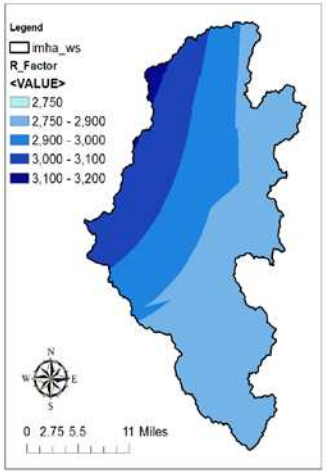

(a) R-Factor

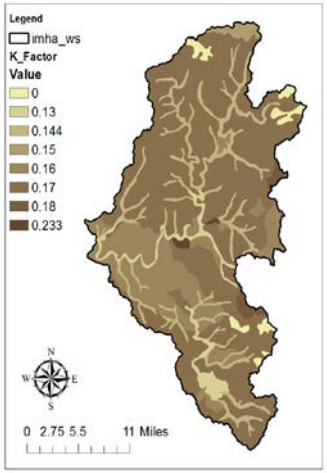

(b) K-Factor

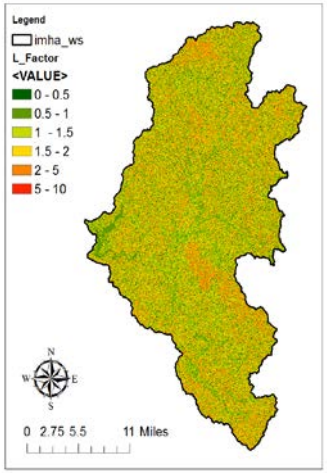

(c) L-Factor

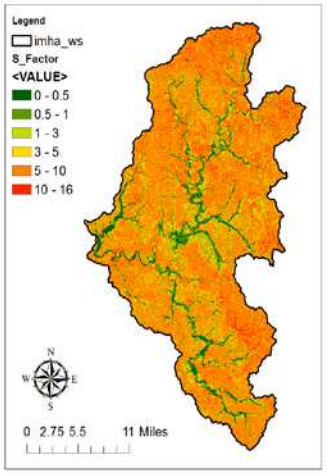

(d) S-Factor

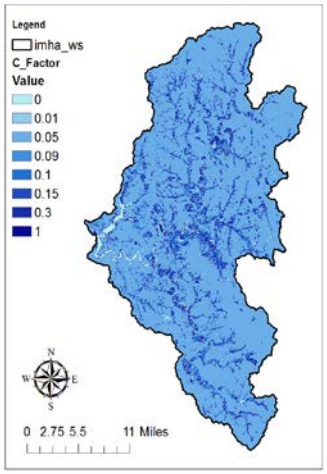

(e) C-Factor

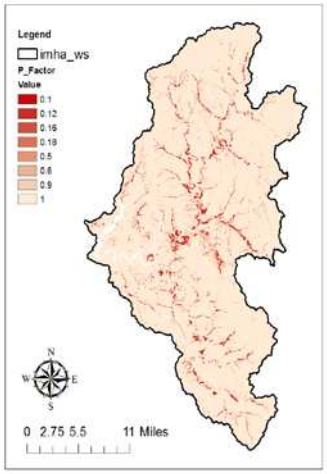

(f) P-Factor

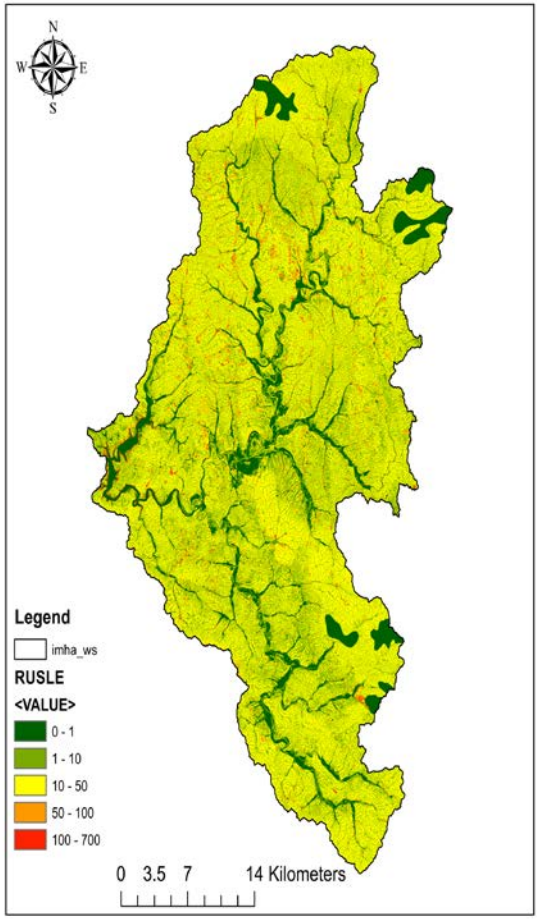

(g)

Figure 37. RUSLE results and parameters for Imha watershed (a) R, (b) K, (c) L, (d) S, (e) C, (f) P, and (g) Gross Erosion

In the result of SDR, Imha and Seomjingang reservoir have relatively high sediment delivery ratio results because the specific degradation resulted from the 1997 and 1983 surveys, respectively (*Figure 38*).

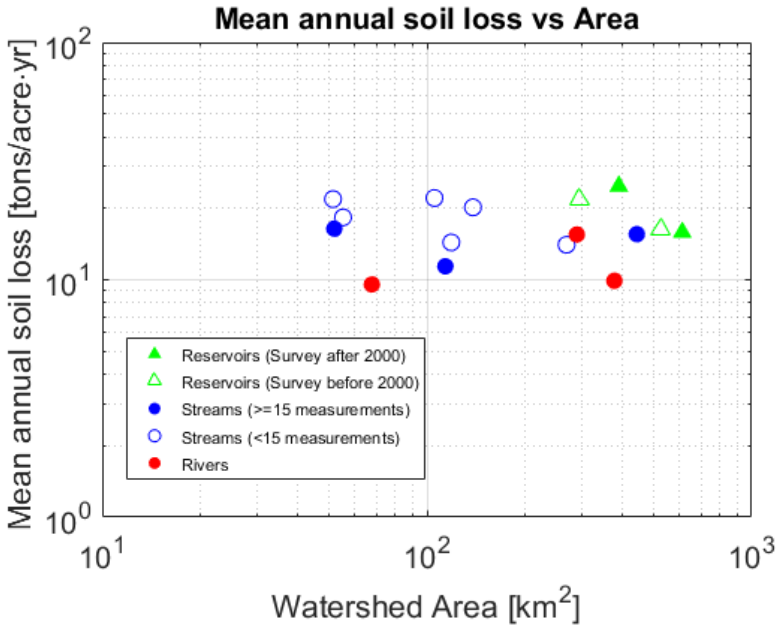

(a)

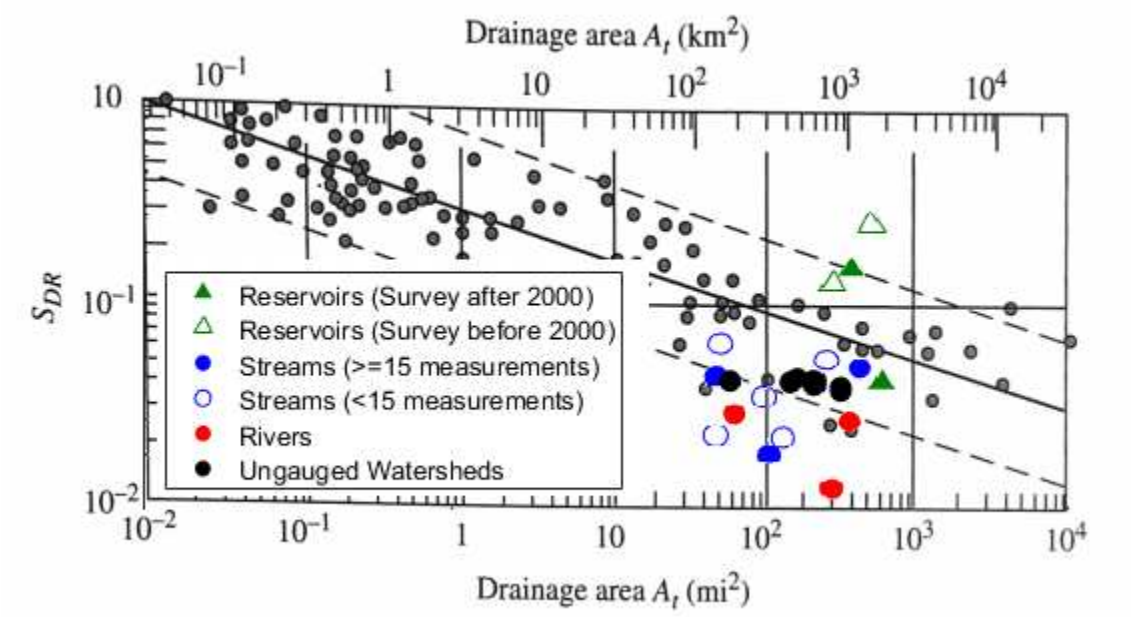

(b)

Figure 38. (a) Gross erosion versus watershed area, and (b) Sediment delivery ratio for the stream (blue), river (red), and reservoir (green), ungauged watersheds (black) (after Boyce 1975)

In *Figure 38*, the empty symbols mean that the sediment measurement was not enough (number of sediment measurements < 15) or the specific degradation was from past survey results (i.e. Imha and Seomjinggang reservoir). The sediment delivery ratio of reservoirs (green triangle) is higher than for rivers (red and blue circle). The annual average soil loss (=gross erosion) does not correlated with watershed area (*Figure 38*a). However, the estimated sediment delivery ratios decrease with the size of watershed area, and most of them were within the range of other references (Julien, 2018). From the results of the sediment delivery ratios for rivers, the relationships with watershed characteristics which were meaningful parameters in the relationship with the specific degradation of river are analyzed. The relationships between the sediment delivery ratio and land use which were used in the regression analysis were very similar to the relationship with specific degradation. The negative relationship between the percentage wetland and water and the specific degradation means that area of wetland and water provides the opportunity for deposition of sedimentation (*Figure 39a*). In terms of the percentage of urbanized area, the sediment delivery ratio increases when the urbanized area increases. However, it is quietly different for streams (*Figure 39b*).

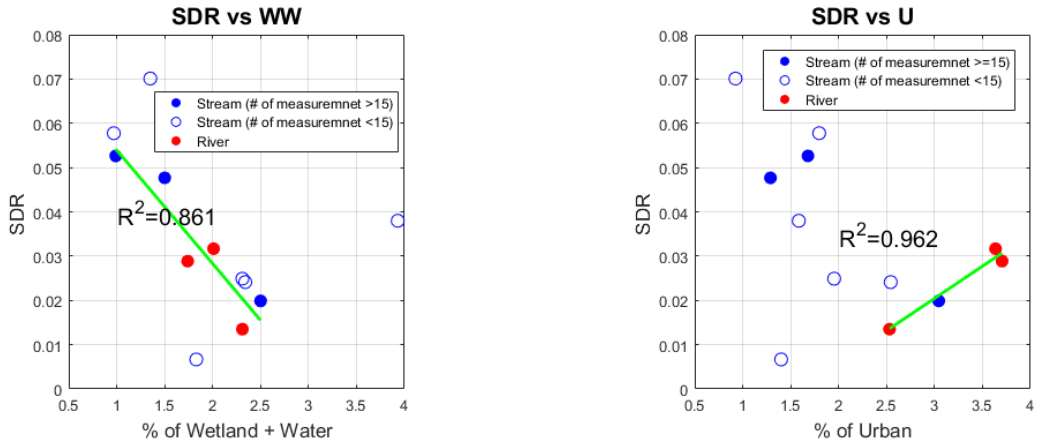

(a) (b)

Figure 39. The relationship between the sediment delivery ratio and (a) The percentage of wetland and water, and (b) The percentage of urbanization

It seems that the less urbanized mountain regions could bring more sediment. In the relationship between the sediment delivery ratio and relief aspects from the hypsometric curve and average watershed slope, three parameters show high sediment delivery ratio in steep streams (*Figure 40*). However, it is difficult to find some distinct relationships due to a small sample. Most of the gross erosion results are estimated for relatively small mountain watersheds and only three watersheds have a steep slope in remote mountain areas.

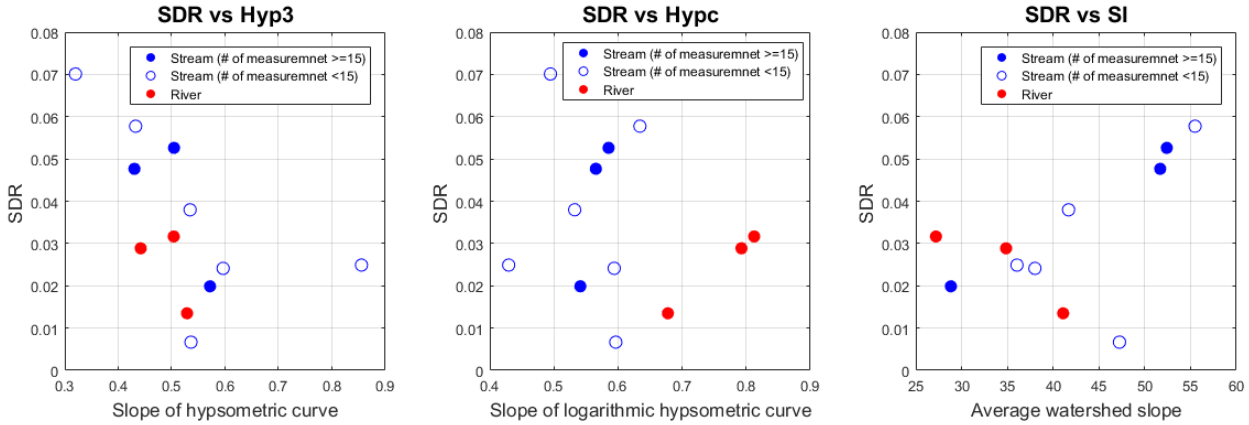

(a) (b) (c)

Figure 40. The relationship between the sediment delivery ratio and (a) The slope of hypsometric curve, (b) The slope of logarithmic hypsometric curve and (c) The average watershed slope

5.1.3. Validation with Ungauged Watershed

The developed regression model in last chapter 4 was validated with ungauged watershed. Three watersheds in N1 and one watershed in NU3 were used for validation and watershed characteristics for the four ungauged watersheds were organized (*Table 16* and *Figure 40)*. The model 7 (M7) was used to estimate the specific degradation of ungauged watersheds (*Table 16*).

Table 16. Watershed characteristics and simulated specific degradation of ungauged watersheds

Name	Class	A [km^2]	P [mm]	W [%]	U [%]	WW [%]	Hyp3	Model SD [tons/km^2▪yr]
WS1	River	854	1115	0.87	3.77	1.23	0.454	111
WS2		580	1135	0.74	3.44	1.03	0.486	131
WS3		405	1150	0.58	1.73	0.87	0.491	145
WS4	Stream	164	1133	0.29	1.84	0.82	0.454	173

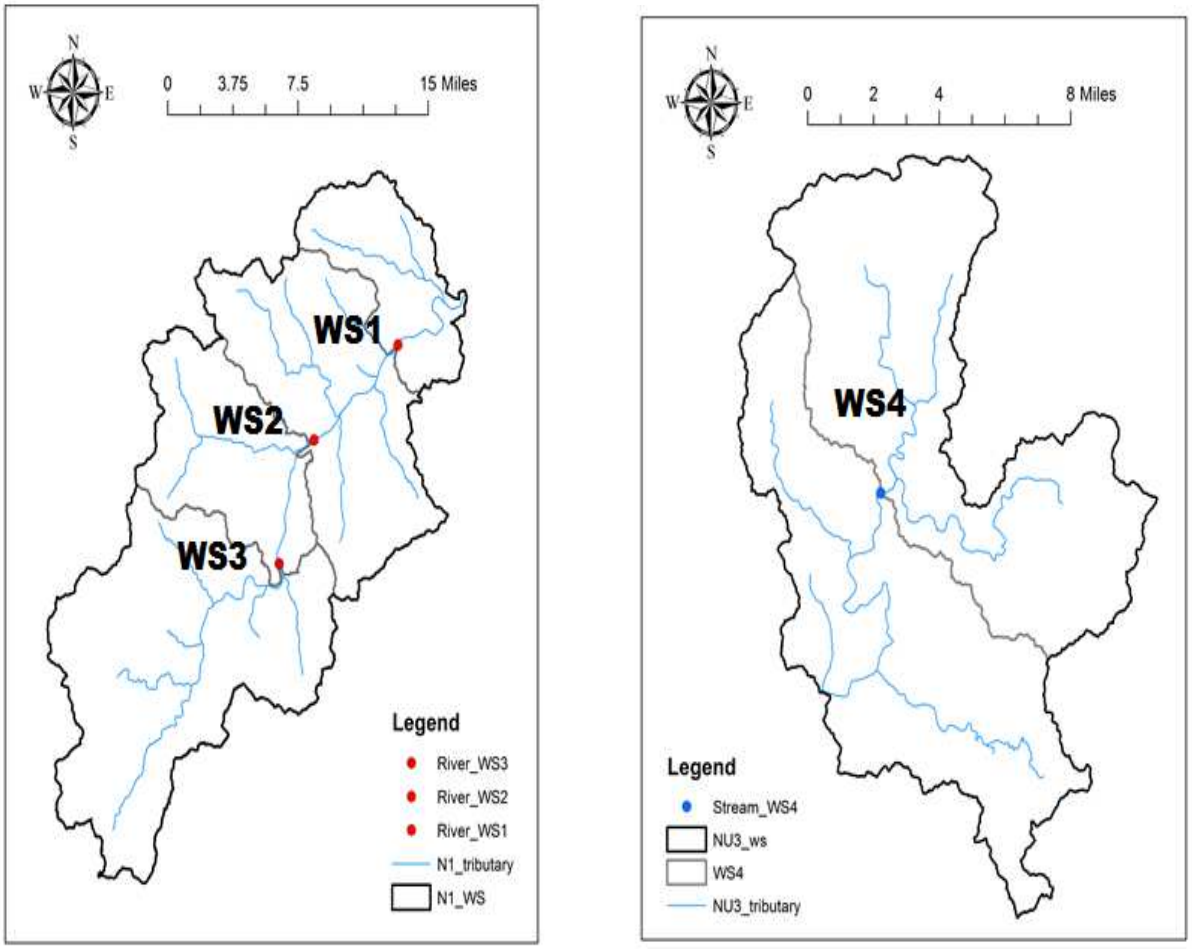

(a) (b)

Figure 41. Ungauged watersheds from (a) River (N1) and (b) Stream

In the simulated result, the ungauged watershed from stream (WS4) has the highest specific degradation (=173 tons/km^2▪yr). The one ungauged watershed from river (WS3) has relatively high specific degradation (=145 tons/km^2▪yr), because it has small watershed area and low percentage of wetland and water. The sediment delivery ratio of ungauged watersheds also calculated from estimated mean annual soil loss at each resolution (*Table 17*). The mean annual soil loss is the lowest in the flat river watershed (WS1) and estimated sediment delivery ratio is higher in steep mountain watersheds (i.e. WS3 and WS4). The calculated sediment delivery ratios are also within the range of other references (Black circles in *Figure 38b*).

Table 17. Sediment delivery ratio of ungauged watersheds

Watershed	Class	Soil loss [tons/km^2▪yr]		Model SD [tons/km^2▪yr]	SDR
WS1	River	5m	2728	111	0.041
		30m	2701		0.042
		90m	2679		0.043
WS2		5m	3024	131	0.043
		30m	2945		0.044
		90m	2849		0.046
WS3		5m	3269	145	0.044
		30m	3197		0.045
		90m	3096		0.047
WS4	Stream	5m	3823	173	0.044
		30m	3795		0.045
		90m	3768		0.047

5.2. Geospatial Analysis of Erosion Maps, Satellite Images, and Aerial Photos

The simple relationship between sediment related value (i.e. SD and SDR) and the watershed characteristics could be distorted from the temporal and spatial lumping problem. Therefore, the RUSLE results are compared with satellite images and aerial photos to evaluate the calculated results at different resolutions. This analysis is rather limited by few measurement and reservoir sedimentation surveys are requried.

5.2.1. Difference between Streams and Rivers

First, the difference between streams and rivers was compared with the satellite image. The satellite images for stream (NU3, *Figure 42*) were shown compared to river (N1, *Figure 43*). In *Figure 42*, gravel-and cobble-bed streams are commonly found in moderately steep mountain valleys (*Figure 42a*) and they are deposited when waters slow down (*Figure 42*c). Most wetlands in South Korea are alluvial features located besides a channel which is frequently inundated. Wetlands generated sediment deposition during floods. The NU3 does not have wetland and flood plain (*Figure 42*b and d). In contrast streams, there are many wetland and

flood plain region near alluvial rivers and the sand is the main material for the flood plains (*Figure 43*b). In both erosion maps, the river includes more wetland and water (purple) when it compares to streams (NU3). Additionally, it is well correlated with the total stream profile. The gross erosion for NU3 (16.4tons/acre▪yr) was also larger than N1 (9.9 tons/acre▪yr). Moreover, the specific degradation of N1 and NU3 are 71 and 193 tons/km^2▪yr, respectively. This result suggests that stream watersheds carry more sediment and alluvial rivers provide more chance for deposition.

5.2.2. Resolution Effects on Erosion Mapping

To analyze resolution effects on erosion map, the erosion map for two watersheds: (1) N1 (river); and (2) NU3 (stream) were generated at 3 resolutions: (1) 5m; (2) 30m; and (3) 90m. The gross erosion for NU3 is 16.4, 15.5, and 14.2 tons/acre▪yr at 5m, 30m, and 90m resolution, respectively. Also, the gross erosion for N1 is 9.9, 9.3, and 8.6 tons/acre▪yr at 5m, 30m, and 90m resolution, respectively (*Figure 44 and 45*). These results are similar to other references (Molnár, 1997; Wu et al., 2005) in that gross erosion slightly decreases when the resolution of DEM decreases. Especially, the RUSLE result from 5m resolution could be helpful for watershed which has sediment related problem. In *Figure 46*, erosion map at 5m well shows the high risk erosion areas such as meandering channel without bank protection (black circles). However, it is hard to find the erosion feature in the erosion map at 90m resolution.

(a)

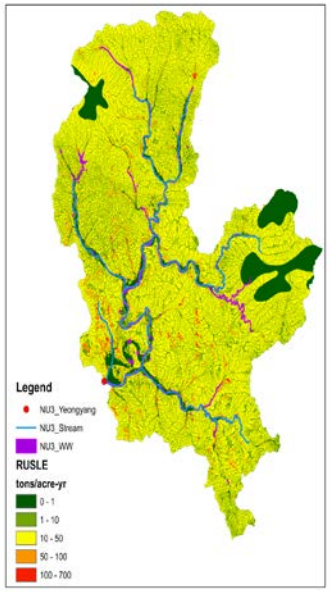

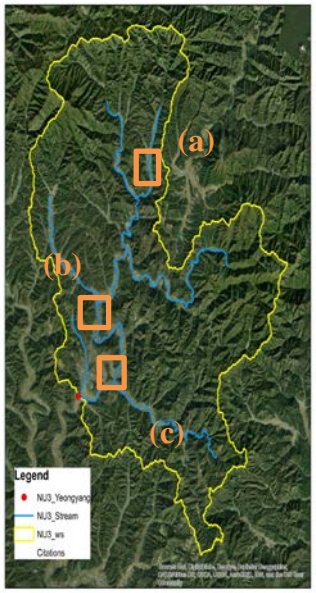

(c)

(b)

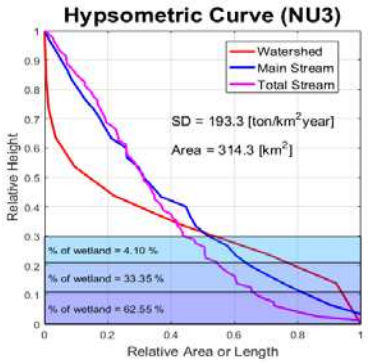

(d)

Figure 42. Erosion map, Satellite and aerial images of stream watershed (NU3, Yeoungyang)

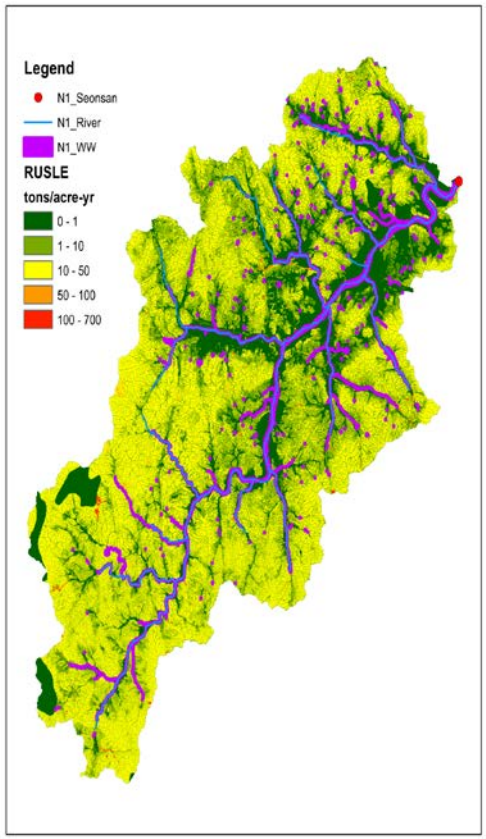

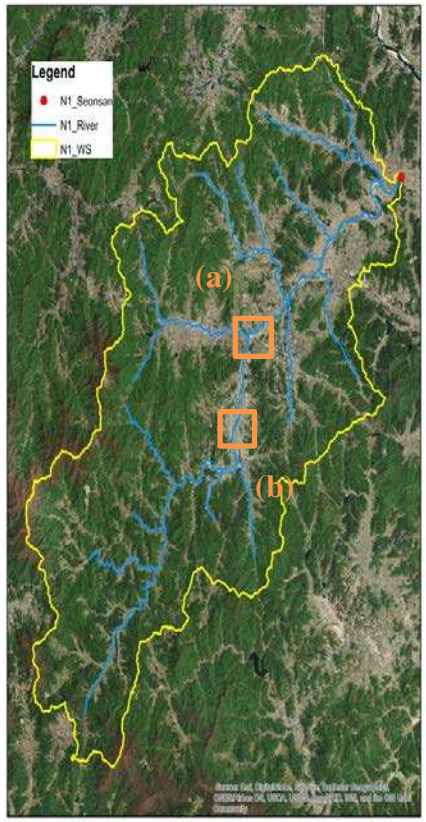

(a)

(b)

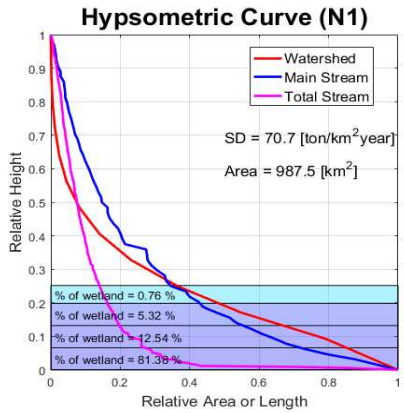

(c)

Figure 43. Erosion map, satellite and aerial images for rivers (N1, Seonsan)

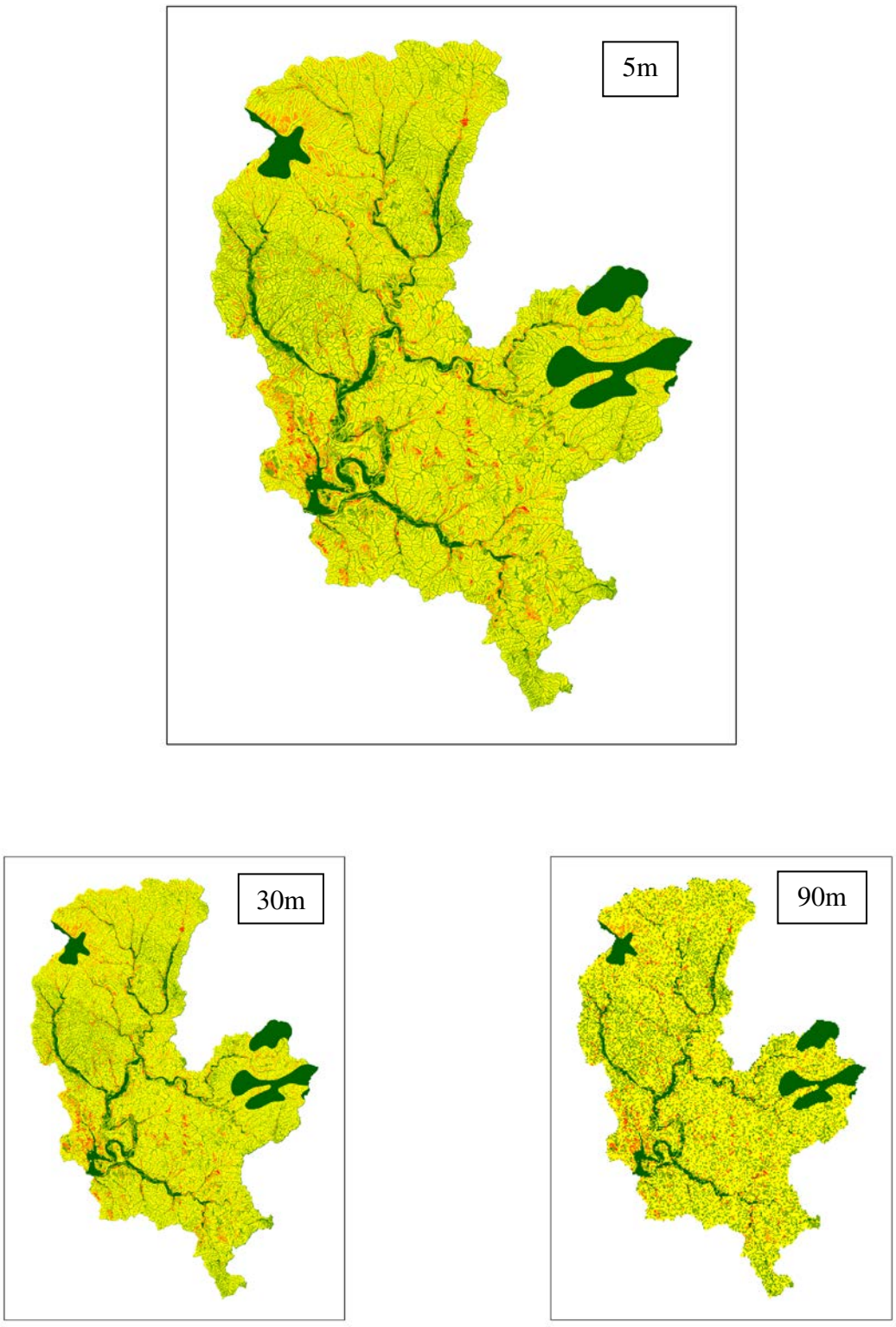

Figure 44. Erosion map of NU3 at each resolution 5m, 30m, and 90m

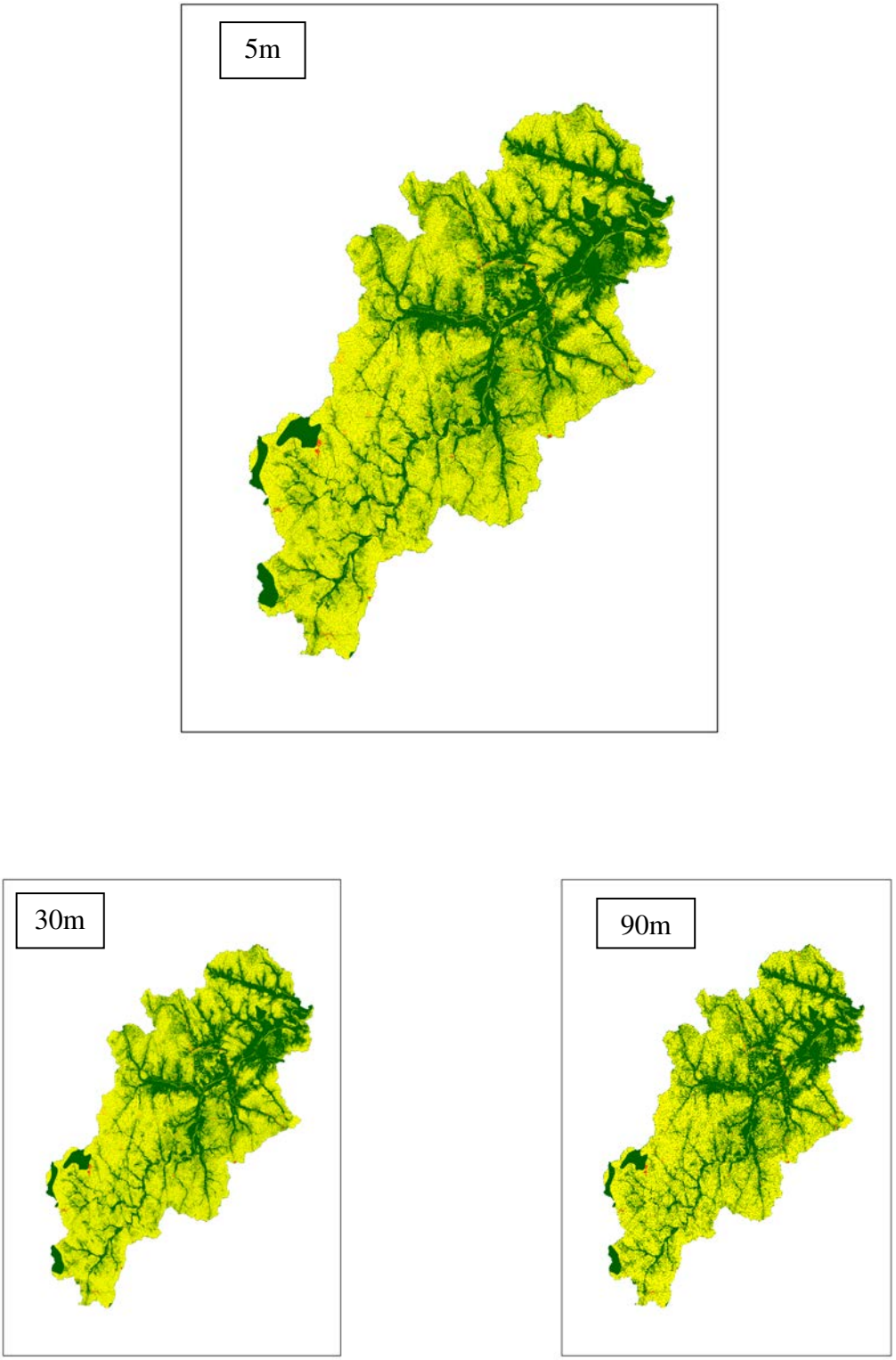

Figure 45. Erosion map of N1 at each resolution 5m, 30m, and 90m

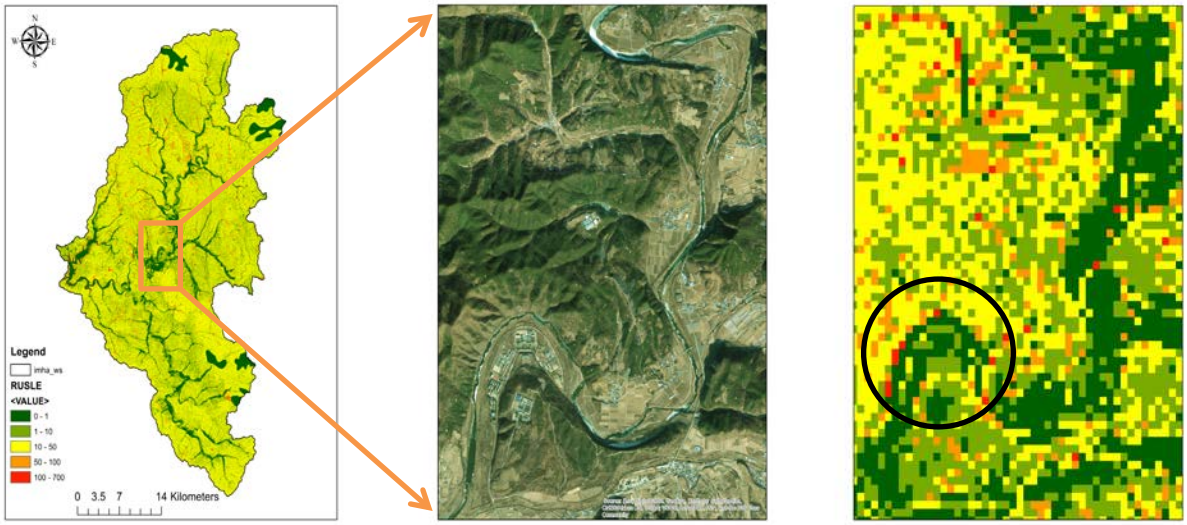

(a) (b) (c)

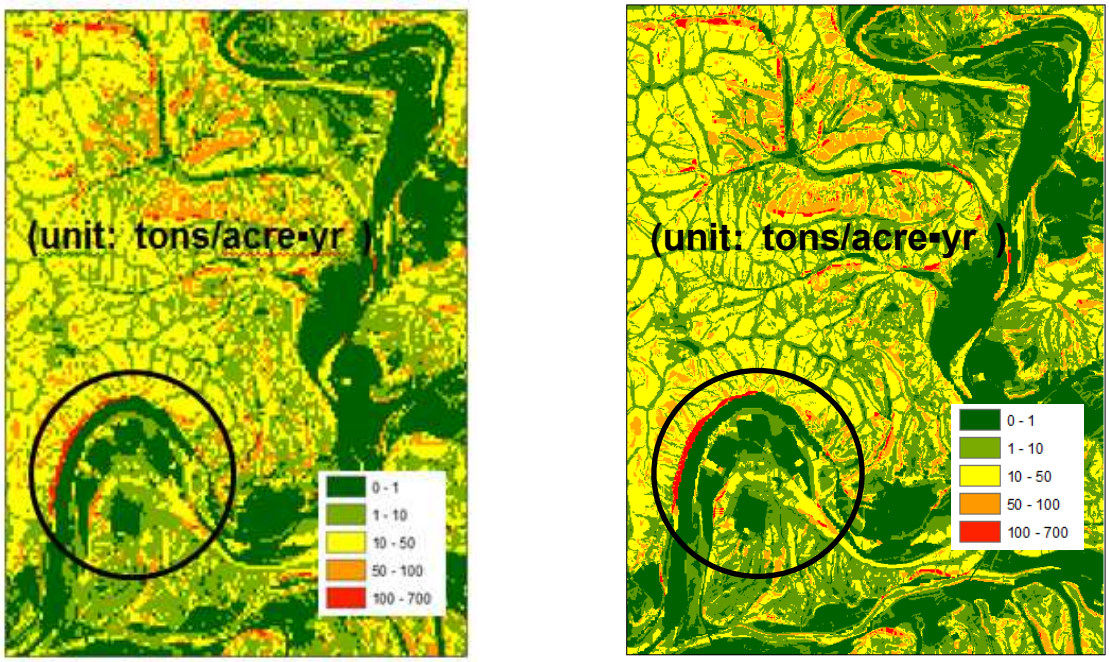

(d) (e)

Figure 46. The satellite image and gross erosion result from (c) 90m (d) 30m, and (e) 5m resolution

5.2.3. Geospatial Analysis for Meaningful Parameters: Upland erosion & Wetland and Water

From the erosion map, aerial photos, and satellite images, the geospatial analysis for meaningful parameters related to land use (e.g. wetland, water, and urbanized area) was conducted. When the erosion map for stream (NU3, *Figure 42*) and river (N1, *Figure 43*) were compared, NU3 included more high erosion risk site. Aerial photo images and erosion maps for a crop field area at NU3 which has high gross erosion are shown in *Figure 47*.

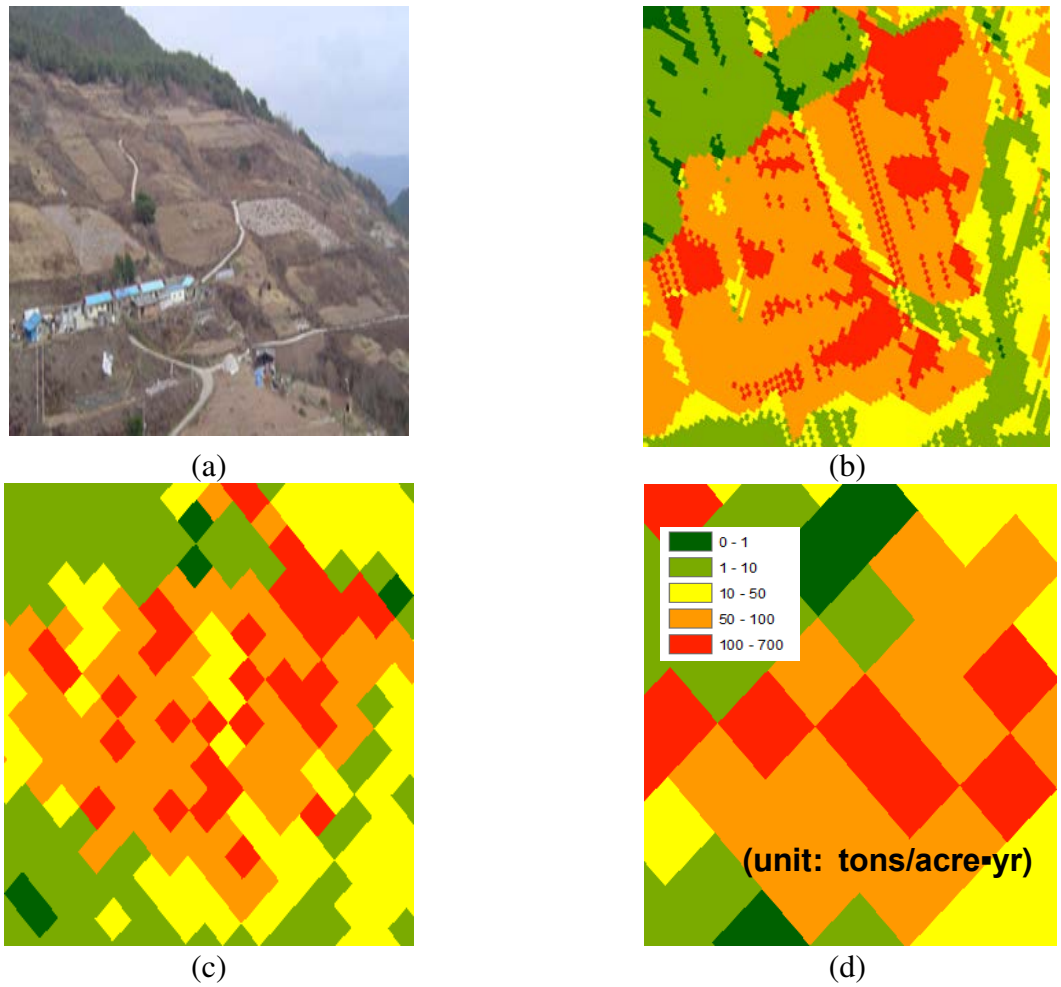

Figure 47. (a) Satellite image for upland high erosion risk site and erosion map at (b) 5m, (c) 30m, and (d) 90m resolution

Since upland includes more rural area and cropland with high slope gradient, so a stream watershed could have very high gross erosion rate compared to than river watersheds. Also, the

erosion map from high resolution shows a far better delineation than one at a low resolution. Second, the wetland is located near the alluvial river in the flat region (*Figure 48*). Considering alluvial rivers on the erosion map at 5m resolution (*Figure 48*b), the gross erosion suggests that the wetland and water is not the main source of sediment yield (0~10 tons/acre▪yr).

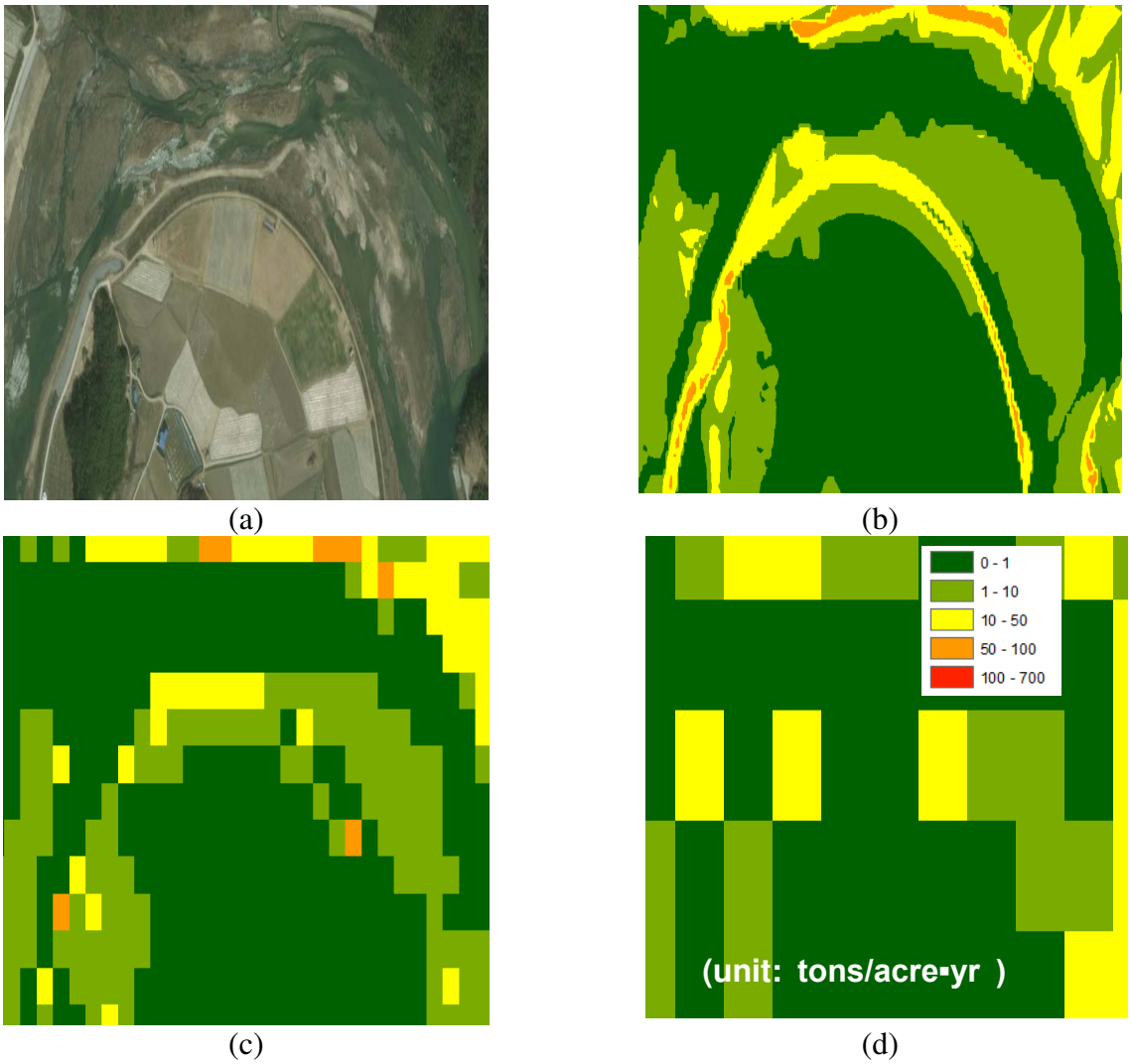

Figure 48. (a) Satellite image for wetland and erosion map at (b) 5m, (c) 30m, and (d) 90m resolution

The wetland was not well represented on erosion maps at 90m resolution (*Figure 48*d). The land cover of water was used with wetland as a meaningful parameter for the developed regression model (M7). As mentioned in chapter 3, there are 17,649 agricultural reservoirs in South Korea.

The land cover of water could well represent them. The scattered small purple dots are agricultural reservoirs (*Figure 43*). In *Figure 45*a, there are two agricultural reservoirs (two orange circles). Since these reservoirs are the main place for sediment deposition in agricultural areas, the annual soil loss for the reservoir is almost 0 tons/acre▪yr (*Figure 49*b). The erosion map at 5m resolution also well display reservoirs, however, the erosion map at 90m suggests that one reservoir has relatively high gross erosion rate (*Figure 49*d).

(a) (b)

(c) (d)

Figure 49. (a) Satellite image for agricultural reservoirs and erosion map at (b) 5m, (c) 30m, and (d) 90m resolution

5.2.4. Geospatial Analysis for Meaningful Parameters: Urbanized Areas

In contrast with the erosion map at 30m and 90m, the erosion map at 5m exactly figures out the roadway (*Figure 50*). The urbanized area (e.g. residential district, parking lot, and roadway) is not a main source of sediment (gross erosion~1 tons/acre▪yr). The results of RUSLE for urbanized areas of N1 are shown in *Figure 50.*

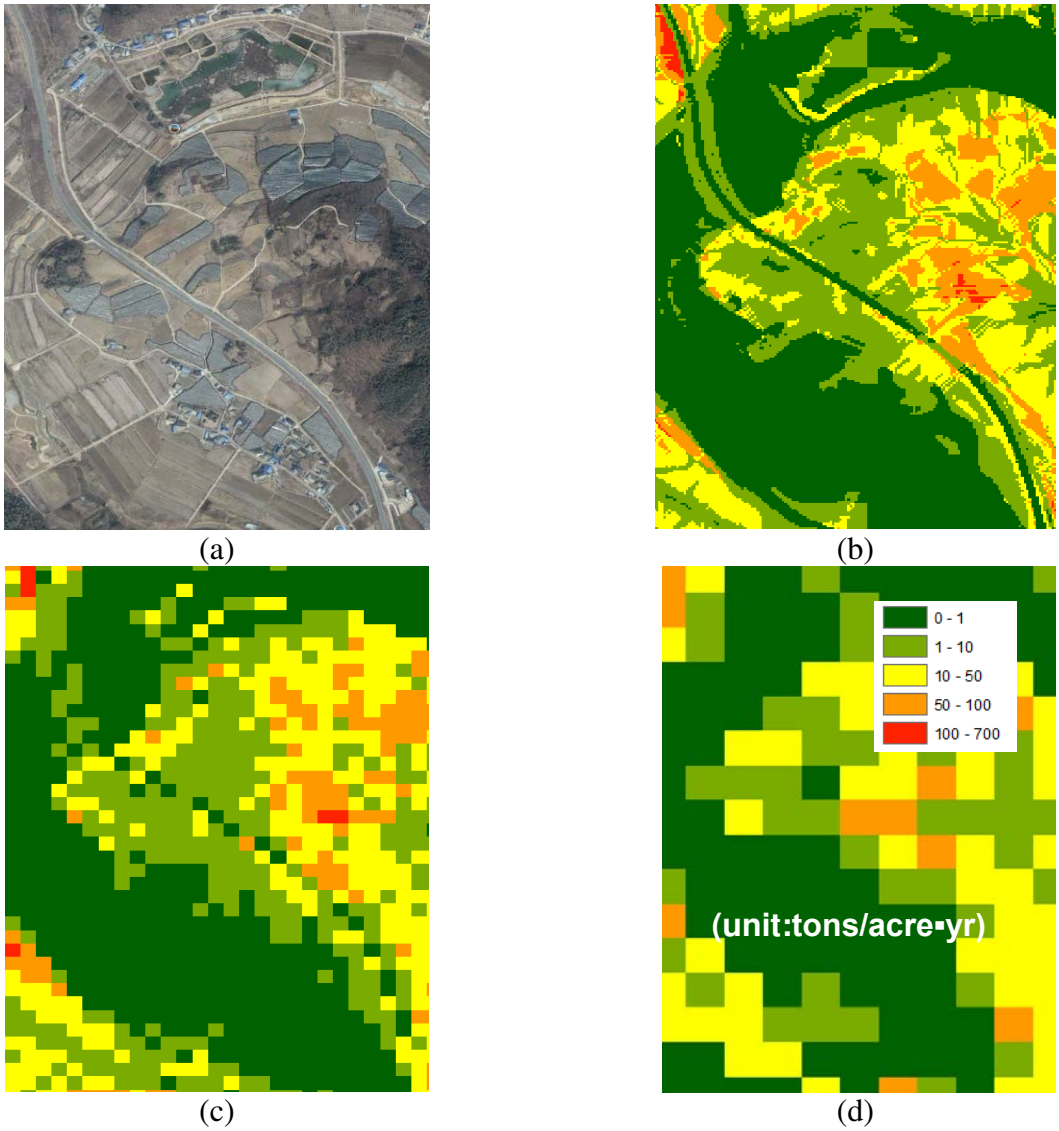

Figure 50. (a) Satellite image for road way and erosion map at (b) 5m, (c) 30m, and (d) 90m resolution

However, there are many pixels which have high annual soil loss value (>50 tons/acre-yr). Most of these areas are a construction site or construction site at hill slope (*Figure 51*). The exposed soils are prone to erosion and can cause large quantities of sediment and they could be easily transported to waterways through surface runoff, especially flood events. Though they change to low erosional risk sites after finishing the construction, urban development is consecutively conducted and spreads throughout watershed.

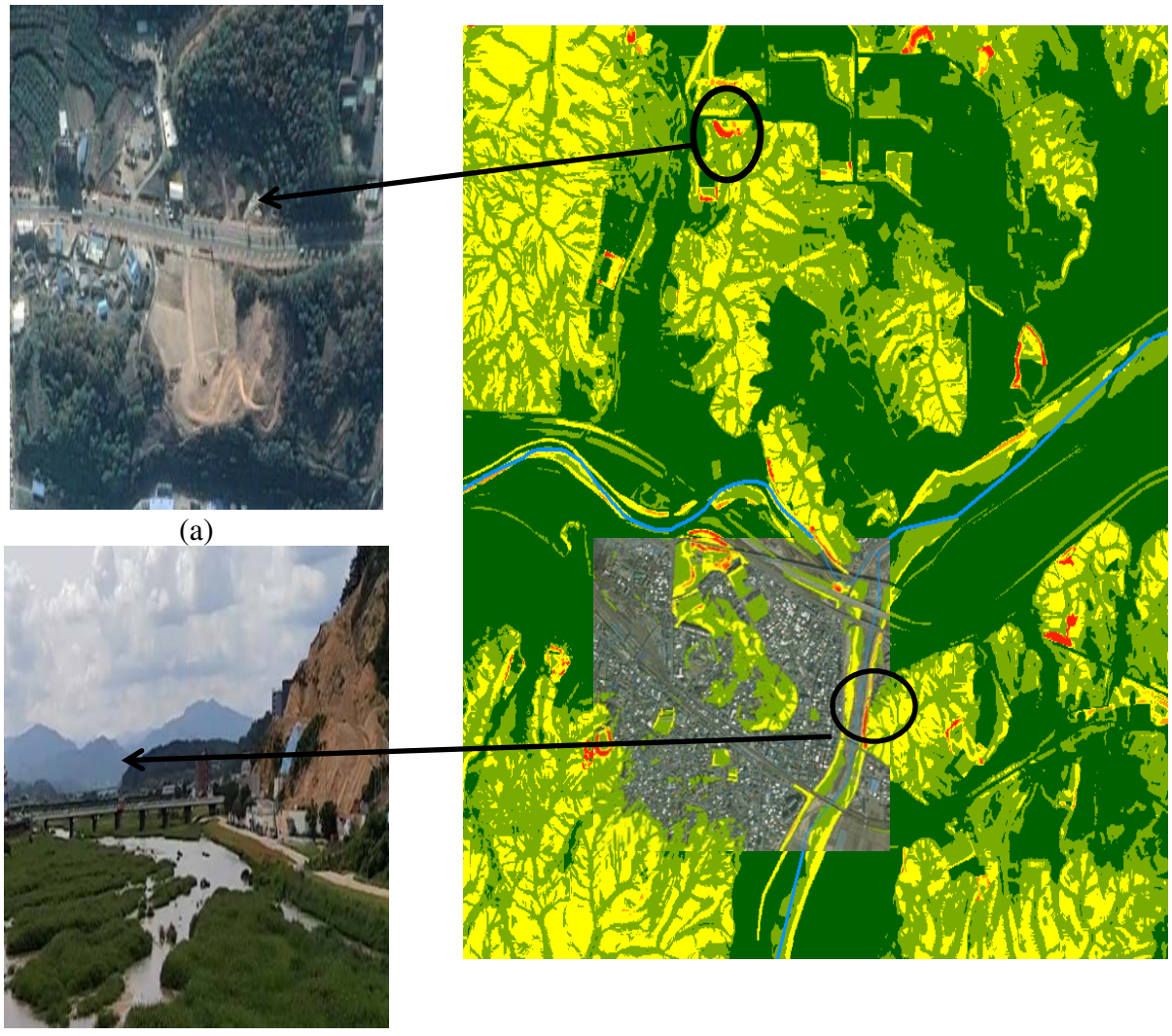

Figure 51. Satellite image and aerial photo of construction sites in urbanized area

The erosion map for construction sites at hill slopes (*Figure 52*a) at three kinds of resolution also generated (*Figure 52*). The results also have similar to the last result for agricultural reservoirs.

The erosion map at 5m and 30m resolution represent construction site at hill slope, however, it is not delineated on the erosion map at 90m resolution. In conclusion, the erosion map at 5m resolution could be helpful for watershed which has localized sediment related problems.

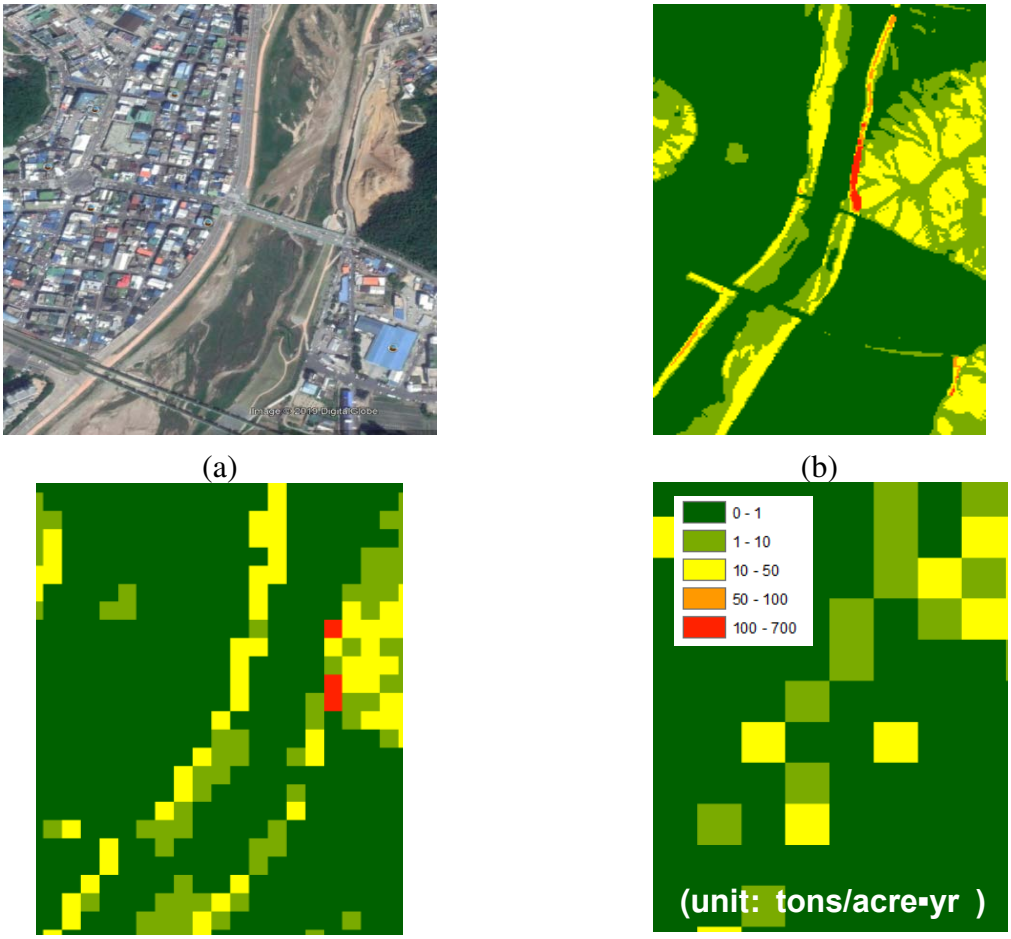

(a) (b)

(c) (d)

Figure 52. (a) Satellite Image, (b) Aerial photo, and erosion map for construction site at hill slope from (a) 5m, (b) 30m, and (c) 90m resolution

5.2.5. Examine Distortion of Erosion Maps at Different Resolutions

Let's now examine whether maps could distort soil loss. The detailed analysis of gross erosion with three resolutions for each land use was conducted. For example, the wetland and water with a low gross erosion rate (0~1 tons/acre▪yr) could be distorted as an erosional feature (10~500 tons/acre▪yr) at erosion map with 90m (*Figure 53*). It also happens in urban area, the

map with 5m resolution well shows the road and small town in the rural area, but the map at 90m resolution could not exactly delineate them.

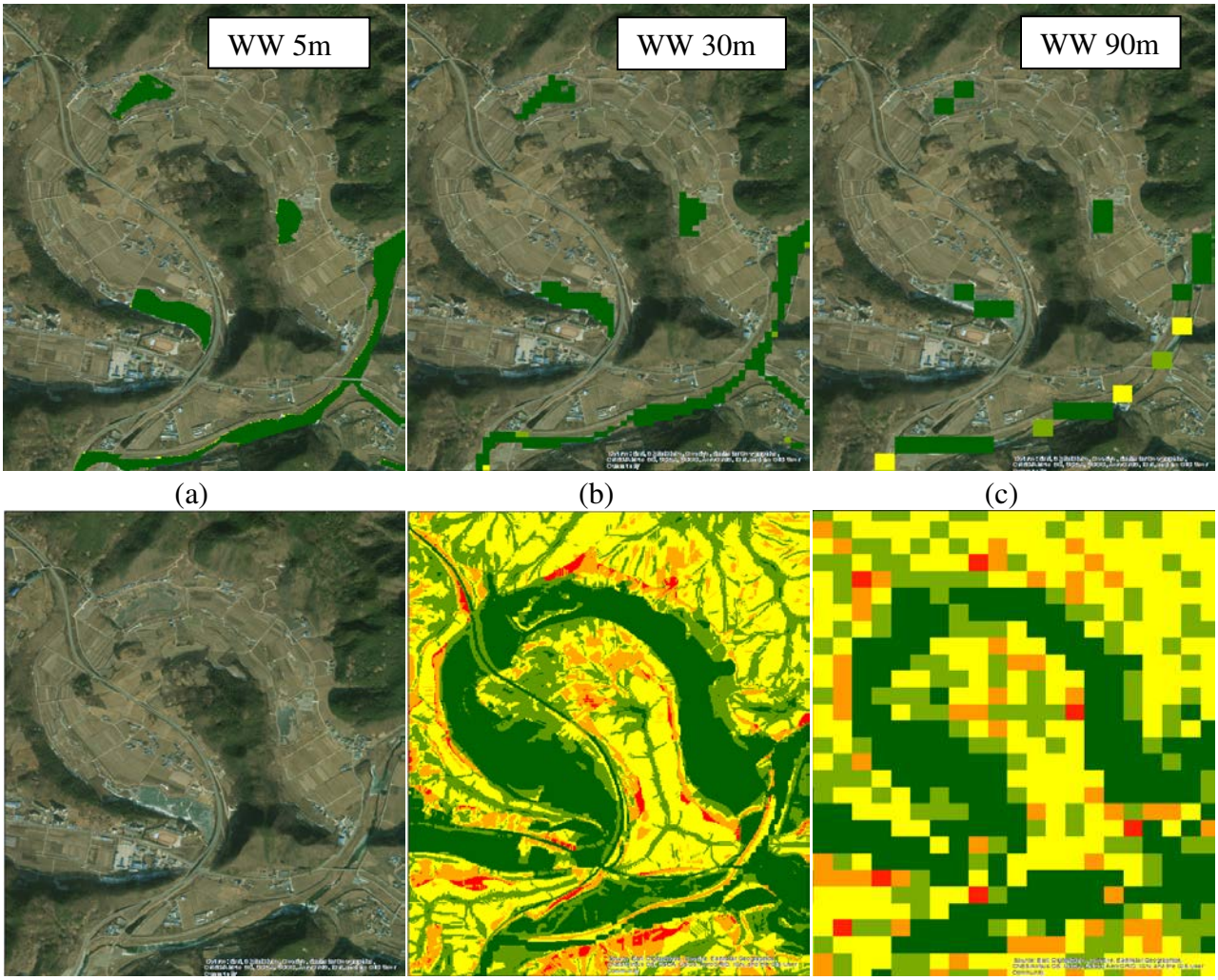

Figure 53. The result of gross erosion at wetland and water with (a) 5m, (b) 30m, and (c) 90m resolution

The gross erosion for wetlands and water are 0.9, 1.7, and 11.9 tons/acre▪yr at 5m, 30m, and 90m resolution, respectively. More specifically, 126,762, 3,360, and 196 pixels were calculated as 0 tons/acre▪yr at 5m, 30m, and 90m resolution, respectively *(Figure 54)*, therefore average gross erosion decreases when the higher resolution is used *(Figure 55)*. In the case of bare land and pasture which could be a main source of sediments, the gross erosion increases at high resolution.

In *Figure 55*, the erosional features (construction site) have high gross erosion and the features related to sedimentation (e.g. wetland and agricultural reservoir) have low gross erosion at low resolution due to the distortion from resolution.

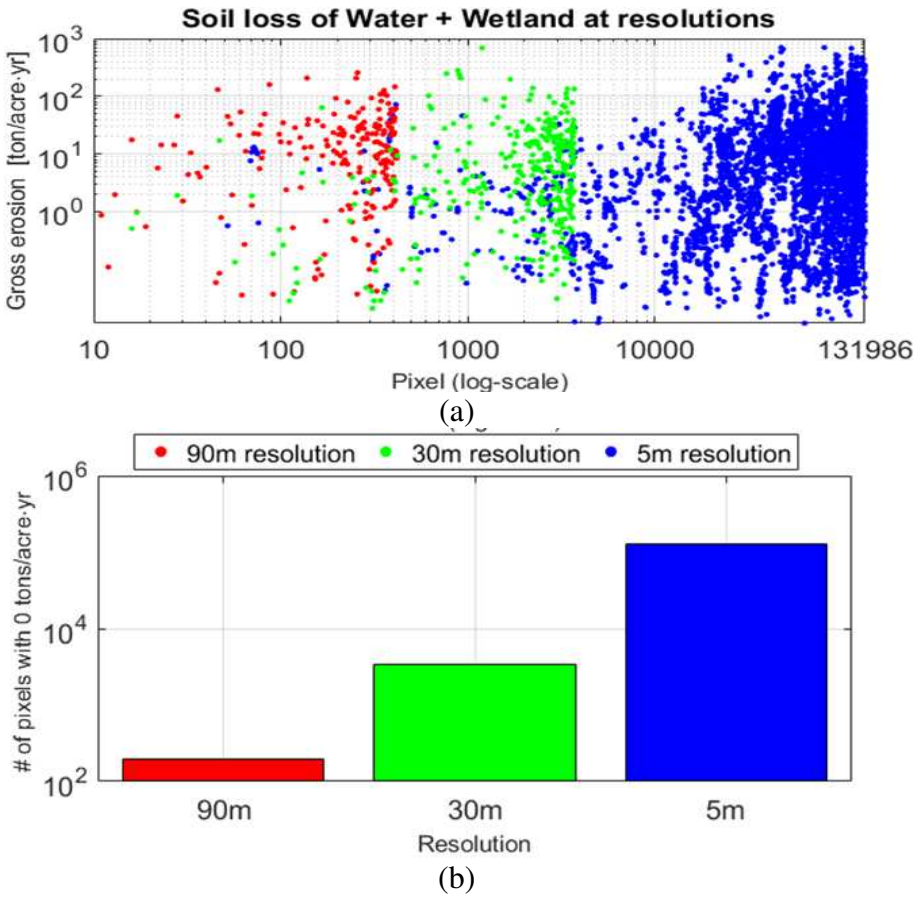

Figure 54. (a) Gross erosion value of wetland and water at each pixel, and (b) Number of pixels with gross erosion is 0 tons/acre▪yr

In this chapter, the erosion maps were generated by RUSLE through GIS at 5m, 30m and 90m resolution and the geospatial analysis was conducted with satellite images and aerial photos. Sediment delivery ratios were estimated and they were within the range which suggested in the literature. The relationship between the sediment delivery ratio and the percentage of wetland/water areas was well correlated. Most wetland areas are located near alluvial rivers and sediment from upland areas deposited here during flood events.

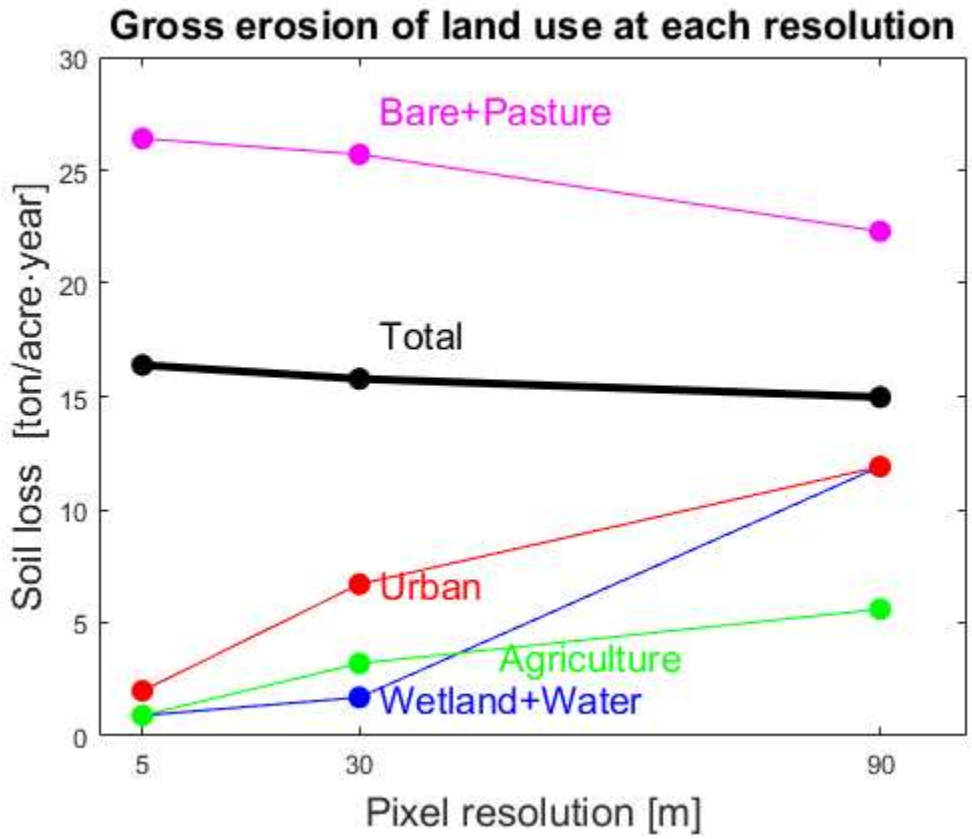

Figure 55. The result of gross erosion at wetland and water with (a) 5m, (b) 30m, and (c) 90m resolution

The erosion map at 5m resolution well represented wetlands and agricultural reservoirs (Water) which are the main place of sediment deposition. In the case of urbanized area, the urbanized area (i.e. residential district and roadway) was not the main source of sediment. However, the construction site for urbanization could provide abundant sediment. In conclusion, the erosion map at 5m resolution could well show risk erosion areas (e.g. upland cropland) and detail features affecting erosion (e.g. construction site at hill slope), and sedimentation (e.g. wetland and agricultural reservoir). However, these features were often not represented in erosion map at 30m and 90m resolutions. When the calculated mean annual soil loss of each land use was compared on erosion map at 5m and 90m resolution, it could be distorted by as much as 60% and 110% for urbanized areas, and wetland and water, respectively.

Chapter 6
Conclusions

6.1 Conclusions

This study investigates the specific degradations of 70 river gauging stations and 13 reservoirs. The Flow Duration and Sediment Rating Curve (FD-SRC) method is used to estimate the specific degradation of rivers with 10-years of daily discharge and 2,993 sediment measurements. The total sediment load of rivers is estimated by using the Modified Einstein Procedure. The specific degradation of the reservoirs is estimated from sediment deposition measurements. Specific degradation ranged from 1,000 tons/km^2▪yr in steep mountain watersheds upstream of reservoirs to 100 tons/km^2▪yr in large rivers and can be as low as 10 tons/km^2▪yr downstream of reservoirs. As expected, the specific degradation decreases from mountain streams to river valleys. It suggests that upland erosion occurs mainly in the upstream part of the watersheds and sedimentation is observed in reservoirs and on flood plains and wetlands as the flood wave propagates downstream. In terms of reservoirs, the specific degradation of reservoirs was the highest. The existing regression models were tested against specific degradation measurements from 35 rivers. The Root Mean Square Error of existing models is in excess of 1,400 tons/km^2▪yr and the Nash-Sutcliffe Efficiency coefficient (NSE) of existing models was highly negative, which is indicative of a very poor predicability.

From my second objective, seven empirical models for specific degradation were developed by multiple regression analysis and validation from other reference was also conducted. Five regression models (M1~M5) based on the USLE architecture were obtained for 28 rivers from 51 explanatory variables. The validation results were best for rivers but underestimated the field measurements for streams. Therefore, another regression model (M6)

was generated for 28 rivers and a last model (M7) was finally developed for 47 rivers and streams to increase the model's predictability. The meaningful parameters were: (1) watershed area; (2) mean annual precipitation at gauging stations; (3) percentage of urbanized area; (4) percentage of wetland; (5) percentage of wetland and water; (6) percentage of sand of the soil surface (upper 50cm); (7) watershed average slope; and (8) two hypsometric curve parameters (e.g. slope of the converted hypsometric curve). Prediction intervals at 95% were developed from the calibrated model. In most cases, the calibration and 15 validation results were within the 95% prediction intervals. The RMSE of the new regression models decreased to 88 tons/km^2▪yr and the Nash-Sutcliffe Efficiency coefficient increased significantly to 0.516. The predictability of the developed models showed better accuracy compared to existing statistical models. The model also avoided multiple collinearity problems. These models can be very helpful to estimate the sediment yield of ungauged watersheds in South Korea and the first five models were independently tested by a Korea research team.

For my third objective, the geospatial analysis of 16 watersheds was conducted with satellite images, aerial photos and erosion maps. For erosion mapping, the gross erosion was calculated with RUSLE using GIS data at 5m, 30m, and 90m resolution. Sediment delivery ratios were estimated from the calculated gross erosion and measured specific degradation. Additionally, the sediment delivery ratio for ungauged watersheds from the developed regression model and erosion map was also calculated. The sediment delivery ratios were within the range suggested in the literature. The relationships between the sediment delivery ratio and land use showed an interesting relationship for wetland and water. Especially, the percentage of wetlands and water was well correlated with the sediment delivery ratio. Most wetland areas are located near alluvial rivers and sediment from upland areas deposited here during flood events. The land

cover of water at 5m resolution well represented approximately 17,000 agricultural reservoirs which are the main place of sediment deposition. Therefore, the land use of wetland and water could become an important indicator for predicting the specific degradation of watersheds. Most of the upland erosion in urbanized areas was located in the lower part of the hypsometric curve. Though the urbanized area (i.e. residential district and roadway) was not the main source of sediment, the urban construction sites could provide abundant sediment on steep roadways. The features related to erosion and sedimentation were clearly delineated on erosion maps at high resolution. More specifically, the erosion maps at 5m resolution could delineate high risk erosion areas (e.g. cropland area on steep slopes) and detail features affecting erosion (e.g. construction site on hill slopes), as well as sedimentation features (wetland and agricultural reservoir). At a 90m resolution, these features were often not visible and mapping of high erosion areas was very difficult to delineate on low resolution maps (> 90m resolution). When comparing average annual soil losses on erosion map at 5m and 90m resolution, the differences were as large as 60% and 110% for urbanized and wetland + water areas, respectively. On high resolution erosion maps, the erosion rates on bare land and pastures showed high gross erosion (50~700 tons/acre▪yr), moreover, the land cover of wetland, water, and urban which are not a main source of sedimentation showed low annual soil loss value (0~50 tons/acre▪yr). The proposed models in the second objective should be useful to find a watershed which has erosion and sediment problems and the erosion map at high resolution (< 10m resolution) should identify the specific location at the watersheds which requires sustainable sediment management.

APPENDIX A. References

Allen, P. (1986). Drainage density versus runoff and sediment yield. In: *Fourth Federal Interagency Sedimentation Conference*, Las Vegas. USGS, pp. 3–38, 33–44.

Bagarello, V., Ferro, V., & Giordano, G. (1991). Contributo alla valutazione del fattore di deflusso di Williams e del coefficiente di resa solida per alcuni bacini idrografici siciliani. *Rivista di Ingegneria Agraria*, 4, 238-251.

Bazzoffi, P., Baldassarre, G., Pellegrini, S., & Bassignana, A. (1997). Models for prediction of water storage decrease in Italian reservoirs. In *Proceedings of the IX World Water Congress IWRA*, 1997. pp 249–252.

Bennett, J. P. (1974). Concepts of mathematical modeling of sediment yield. *Water Resources Research, 10*(3), 485-492. doi:10.1029/WR010i003p00485

Boix-Fayos, C., de Vente, J., Martínez-Mena, M., Barberá, G. G., & Castillo, V. (2008). The impact of land use change and check-dams on catchment sediment yield. *Hydrological Processes: An International Journal*, 22(25), 4922-4935.doi: 10.1002/hyp.7115

Borland, W. M. (1971). Reservoir sedimentation. *River Mechanics*, 2, 29.21-29.38.

Boyce, R. C. (1975). Sediment routing with sediment delivery ratios. *Present and prospective technology for predicting sediment yields and sources*, USDA-ARS-S-40, pp. 61-65.

Brune, G. M. (1953). Trap efficiency of reservoirs. Eos, *Transactions American Geophysical Union*, 34(3), 407-418. doi: 10.1029/TR034i003p00407

Burkham, D. E., & Dawdy, D. R. (1980). General study of the modified Einstein method of computing total sediment discharge (Vol. 2066). US Government Printing Office.

Chow, V. T. (1964). Handbook of applied hydrology: a compendium of water-resources Technology (Vol. 1). McGraw-Hill.

Churchill, M. A. (1948). Discussion of analyses and use of reservoir sedimentation data. by LC

Gottschalk in. In *Proceedings of the federal interagency sedimentation conference*, pp. 139-140.

Colby, B. R., & Hembree, C. H. (1955). Computations of total sediment discharge, Niobrara River near Cody, Nebraska. Water Supply Paper 1357. Washington, D.C., U. S. Geological Survey.

Cowen, J. (1993). A proposed method for calculating the LS factor for use with the USLE in a grid-based environment. In *Proceedings of the Thirteenth Annual ESRI User Conference* (1993), pp. 65-74.

Davies, A. M. (1899). Contributions to the geology of the Thame Valley. In *Proceedings of the Geologists' Association*, 16(1), 15,IN12-58,IN12. doi:10.1016/S0016-7878(99)80037-6

Dendy, F., & Bolton, G. (1976). Sediment yield-runoff-drainage area relationships in the United States. *Journal of Soil and Water Conservation*.

Demmak, A. (1982). Contribution à l'étude de l'érosion et des transports solides en Algérie Septentrionale. Ph.D. Dissertation, Univ. Paris., FR.

Dickinson, W., & Wall, G. (1977). The relationship between source-area erosion and sediment yield. *Hydrological Sciences Journal*, 22(4), 527-530.doi:10.1080/02626667709491755

Desmet, P. J. J., & Govers, G. (1996). A GIS procedure for automatically calculating the USLE LS factor on topographical complex landscape units. *Journal of Soil and Water Conservation*, 51(5), 427-433.

DeVantier, B. A., & Feldman, A. D. (1993). Review of GIS applications in hydrologic modeling. *Journal of Water Resources Planning and Management*, 119(2), 246-261. doi: 10.1061/(ASCE)0733-9496(1993)119:2(246)

Evans, K. G., & Loch, R. J. (1996). Using the RUSLE to identify factors controlling erosion

rates of mine soils. *Land Degradation & Development*, *7*(3), 267-277.

Einstein, H. A. (1950). The bed-load function for sediment transportation in open channel flows. Technical Bulletin no. 1026. Washington, DC: US Department of Agriculture.

ESRI. (2011). What is a GIS? Retrieved from https://www.esri.com/en-us/what-is-gis/overview

Faran Ali, K., & De Boer, D. H. (2008). Factors controlling specific sediment yield in the upper Indus River basin, northern Pakistan. *Hydrological Processes*, 22(16), 3102-3114. doi:10.1002/hyp.6896

Ferro, V., & Minacapilli, M. (1995). Sediment delivery processes at basin scale. *Hydrological Sciences Journal*, 40(6), 703-717. doi:10.1080/02626669509491460

Flaxman, E. (1974). Predicting sediment yield in western United States. *Journal of Hydraulic Division, ASCE*, Vol.100 (HY5), pp. 693-695

Fournier, F. (1960). Climat et érosion": la relation entre l'érosion du sol par l'eau et les précipitations atmosphériques, Presses universitaires de France.

Gravelius, H. (1914). Flusskunde (Vol. 1). Goschenesche Verlagshandlung, Berlin.

Goy, P. N. (2011). GIS-based soil erosion modeling and sediment yield of the N'DJILI River basin, Democratic Republic of Congo, M.S. Thesis, Colorado State University, Colorado, US.

Haan, C. T., Barfield, B. J., & Hayes, J. C. (1994). Design hydrology and sedimentology for small catchments. Elsevier.

Haregeweyn, N., Poesen, J., Nyssen, J., Verstraeten, G., de Vente, J., Govers, G., Deckers, S., and Moeyersons, J. (2005). Specific sediment yield in Tigray-Northern Ethiopia: assessment and semi-quantitative modeling. *Geomorphology*, Vol. 69, Issue 1-4, pp. 315–331, doi: 10.1016/j.geomorph.2005.02.001

Hartley, D. M. (1990). Boundary shear stress induced by raindrop impact. Ph.D. Dissertation, Colorado State University, Colorado, US.

Heinemarm, H. (1981). A new sediment trap efficiency curve for small reservoirs. *JAWRA Journal of the American Water Resources Association*, 17(5), 825-830. doi: 10.1111/j.17521688.1981.tb01304.x

Hickey, R. (2000). Slope angle and slope length solutions for GIS. *Cartography*, 29(1), 1-8. doi: 10.1080/00690805.2000.9714334

Holmquist-Johnson, C. L. (2006). Bureau of Reclamation Automated Modified Einstein Procedure (BORAMEP) program for computing total sediment load. U.S. Department of the Interior, Bureau of Reclamation, Denver, CO.

Horton, R. E. (1932). Drainage-basin characteristics. EOS, *Transactions American Geophysical Union*, 13(1), 350-361.

Horton, R. E. (1945). Erosional development of streams and their drainage basins; Hydrophysical approach to quantitative morphology. *Bulletin of the Geological Society of America*, 56(3), 275-370. doi:10.1130/0016-7606(1945)56[275:EDOSAT]2.0.CO;2

Hovius, N. (1998), Controls on sediment supply by large rivers, *SEPM Spec. Publ. Soc. Sediment Geol.*,**59**, 3– 16.

Ichim, I. (1990). The relationship between sediment delivery ratio and stream order: a Romanian case study. *IAHS Publication*, No. 189, pp. 79-86

Jansen, I. M. L., & Painter, R. B. (1974). Predicting sediment yield from climate and topography. *Journal of Hydrology*, 21(4), 371-380. doi:10.1016/S0022-1694(74)80006-5

Ji, U. (2006). Numerical model for sediment flushing at the Nakdong River Estuary Barrage Ph.D. Dissertation, Colorado State University, Colorado, US.

Ji, U., Julien, P. Y., & Park, S. K. (2011). Sediment flushing at the Nakdong River Estuary Barrage. *Journal of Hydraulic Engineering*, 137(11), 1522-1535.

Jinze, M., & Qingmei, M. (1981). Sediment delivery ratio as used in the computation of watershed sediment yield. *Journal of Hydrology* (New Zealand), 27-38.

Julien, P. Y. (2002). River mechanics. Cambridge University Press.

Julien, P. Y. (2010). Erosion and sedimentation (2nd ed.). Cambridge University Press.

Julien, P. Y. (2018). River mechanics (2nd ed.). Cambridge University Press.

Julien, P. Y., & Frenette, M. (1987). Macroscale analysis of upland erosion. *Hydrological Sciences Journal*, 32(3), 347-358. doi: 10.1080/02626668709491193

Julien, P. Y., Kang, W. C., Yang, C., Lee, J. H., Byeon, S. J. & Lee, J. H. (2017). Multivariate regression analysis and model development for the estimation of sediment yield from ungauged watershed in the Republic of Korea, Fort Collins, CO, US: Colorado State University.

Kane, B. (2003). Specific degradation as function of watershed characteristics and climatic parameters. Ph.D. Dissertation, Colorado State University, Colorado, US.

Kane, B., & Julien, P. (2007). Specific degradation of watersheds. *International Journal of Sediment Research*, 22(2), 114-119.

Keulegan, G. H. (1938). Laws of turbulent flow in open channels (Vol. 21, pp. 707-741). US: National Bureau of Standards.

Kim, H. S. (2006). Soil erosion modeling using RUSLE and GIS on the Imha watershed, South Korea. M.S. Thesis, Colorado State University, Colorado, US.

Kling, G. F. (1975). A computer model of diffuse sources of sediment and phosphorus moving into a lake. Ph.D. Dissertation, Cornell University, Newyork, US.

Knox, J. C. (1977). Human impacts on Wisconsin stream channels. *Annals of the Association of American Geographers,* 67(3), 323-342. doi: 10.1111/j.1467-8306.1977.tb01145.x

Kutner, M. H., Kutner, M. H., Nachtsheim, C., & Neter, J. (2004). Student Solutions Manual for Use with Applied Linear Regression Models. McGraw-Hill/Irwin

K-water. (2002a). 2001 Hapcheon dam sediment survey report. Daejeon, KR: Korea Water Resources Corporation.

K-water. (2002b). Juam(main) dam sediment survey report. Daejeon, KR: Korea Water Resources Corporation.

K-water. (2006a). 2005 Daecheong dam sediment survey report. Daejeon, KR: Korea Water Resources Corporation.

K-water. (2006b). Soyangriver dam sediment survey report. Daejeon, KR: Korea Water Resources Corporation.

K-water. (2008a). 2007 Andong dam sediment survey report. Daejeon, KR: Korea Water Resources Corporation.

K-water. (2008b). 2007 Chungju dam sediment survey report. Daejeon, KR: Korea Water Resources Corporation.

K-water. (2014). 2013 Miryang dam sediment survey report. Daejeon, KR: Korea Water Resources Corporation.

K-water. (2017). Multivariate regression analysis and model development for the estimation of sediment yield and sediment management from ungauged watershed in the Republic of Korea. Daejeon, KR: Korea Water Resources Corporation.

Lane, L., Nichols, M., & Paige, G. (1995). Modeling erosion on hillslopes: Concepts, theory and data. In *Proceedings of the International Congress on Modelling and Simulation* (MODSIM '95), Newcastle, Australia.

Langbein, W. B. (1947). Topographic characteristics of drainage basins. *U.S. Geol. Survey, W.S. Paper* 968-C, p. 125-155.

Langbein, W. B., & Schumm, S. A. (1958). Yield of sediment in relation to mean annual precipitation. Eos, *Transactions American Geophysical Union*, 39(6), 1076-1084. doi: 10.1029/TR039i006p01076

Lara, J. M. (1966). Computation of" Z's" for use in the Modified Einstein Procedure. Department of the Interior, Bureau of Reclamation, Division of Project Investigations, Hydrology Branch, Sedimentation Section.

Lee, J. H., & Heo, J. H. (2011). Evaluation of estimation methods for rainfall erosivity based on annual precipitation in Korea. *Journal of Hydrology*, 409(1), 30-48. doi:10.1016/j.jhydrol.2011.07.031

Lee, Y. K., Go, J. Y., Lee, J. W., & Jung, S. W. (2009). Development of sediment discharge computation system. *Conference of Korea Water Resources Association*, pp. 723-727 (in Korean).

Liu, H., Kiesel, J., Hörmann, G., & Fohrer, N. (2011). Effects of DEM horizontal resolution and methods on calculating the slope length factor in gently rolling landscapes. *Catena*, 87(3), 368-375. doi:10.1016/j.catena.2011.07.003

Ludwig, W., & Probst, J. (1998). River sediment discharge to the oceans: Present-day controls and global budgets. *American Journal of Science*, 298(4), 265-295. doi:10.2475/ajs.298.4.265

Maner, S. B. (1958). Factors affecting sediment delivery rates in the Red Hills physiographic area. Eos, *Transactions American Geophysical Union*, 39(4), 669-675. doi:10.1029/TR039i004p00669.

McCool, D. K., Brown, L. C., Foster, G. R., Mutchler, C. K., & Meyer, L. D. (1987). Revised slope steepness factor for the Universal Soil Loss Equation. *Transactions of the ASAE*, *30*(5), 1387-1396.

Merritt, W. S., Letcher, R. A., & Jakeman, A. J. (2003). A review of erosion and sediment transport models. *Environmental Modelling and Software, 18*(8), 761-799. doi:10.1016/S1364-8152(03)00078-1.

Meyer, L. D., & Wischmeier, W. H. (1969). Mathematical simulation of the process of soil erosion by water. *Transactions of the ASAE*, *12*(6), 754-0758.

ME (Ministry of Environment), (2012). Notification on investigation of soil erosion status. Sejong, KR: ME.

MLTM (Ministry of Land, Transport and Maritime Affairs, Korea), (2008a). Annual hydrological report on Korea. Sejong, KR: MOLIT.

MLTM (Ministry of Land, Transport and Maritime Affairs, Korea), (2008b). Annual hydrological report on Korea. Sejong, KR: MOLIT.

MLTM (Ministry of Land, Transport and Maritime Affairs, Korea), (2010). Annual hydrological report on Korea. Sejong, KR: MOLIT.

MLTM (Ministry of Land, Transport and Maritime Affairs, Korea), (2011). Annual hydrological report on Korea. Sejong, KR: MOLIT.

MLTM (Ministry of Land, Transport and Maritime Affairs, Korea), (2011). Dam design manual and analysis. Sejong, KR: MOLIT.

MLTM (Ministry of Land, Transport and Maritime Affairs, Korea), (2012). Annual hydrological report on Korea. Sejong, KR: MOLIT.

MLTM (Ministry of Land, Transport and Maritime Affairs, Korea), (2013). Annual hydrological report on Korea. Sejong, KR: MOLIT.

MOC (Ministry of Construction), (1992). Research of sediment yield rate for dam design. Sejong, KR: MOLIT.

MOCT (Ministry of Construction and Transportation, Korea), (2006). Annual hydrological report on Korea. Sejong, KR: MOLIT.

MOCT (Ministry of Construction and Transportation, Korea), (2007). Annual hydrological report on Korea. Sejong, KR: MOLIT.

MOLIT (Ministry of Land, Infrastructure, and Transport), (2013). Water vision 2020. Retrieved from KR http://www.codil.or.kr/Codil/cor/viewer/detailView.jsp?org=NHN&type=ORI&code=OTKCRK130113

MOLIT (Ministry of Land, Infrastructure, and Transport), (2014). Annual hydrological report on Korea. Sejong, KR: MOLIT.

MOLIT (Ministry of Land, Infrastructure, and Transport), (2015). Annual hydrological report on Korea. Sejong, KR: MOLIT.

MOLIT (Ministry of Land, Infrastructure, and Transport), (2016). Annual hydrological report on Korea. Sejong, KR: MOLIT.

Molnár, D. K. (1997). Grid size selection for 2-D hydrologic modeling of large watersheds. Ph.D. Dissertation, Colorado State University, Colorado, US.

Moore, I. D., & Burch, G. J. (1986). Physical basis of the length-slope factor in the universal soil

loss equation. *Soil Science Society of America Journal*, 50(5), 1294-1298. doi:10.2136/sssaj1986.03615995005000050042x

Moore, I. D., Grayson, R., & Ladson, A. (1991). Digital terrain modelling: a review of hydrological, geomorphological, and biological applications. *Hydrological processes*, 5(1), 3-30. doi: 10.1002/hyp.3360050103.

Mutchler, C. K., & Bowie, A. J. (1976). Effect of land use on sediment delivery ratios. PB US Natl Tech Inf Serv.

Nash, J. E., & Sutcliffe, J. V. (1970). River flow forecasting through conceptual models part I-A discussion of principles. *Journal of hydrology*, 10(3), 282-290. doi: 10.1016/0022-1694(70)90255-6

Pike, R. J., & Wilson, S. E. (1971). Elevation-relief ratio, hypsometric integral, and geomorphic area-altitude analysis. *Geological Society of America Bulletin*, 82(4), 1079-1083. doi:10.1130/0016-7606(1971)82[1079:ERHIAG]2.0.CO;2

Probst, J. L., & Suchet, P. A. (1992). Fluvial suspended sediment transport and mechanical erosion in the Maghreb (North Africa). *Hydrological Sciences Journal*, 37(6), 621-637. doi:10.1080/02626669209492628

Renard, K. G., Foster, G. R., Weesies, G. A., McCool, D. K., & Yoder, D. C. (1997). Predicting soil erosion by water: a guide to conservation planning with the Revised Universal Soil Loss Equation (RUSLE) (Vol. 703). Washington, DC: United States Department of Agriculture.

Renfro, G. (1975). Use of erosion equations and sediment delivery ratios for predicting sediment yield. Present and prospective technology for predicting sediment yields and sources, 33-45.

Restrepo, J. D., Kjerfve, B., Hermelin, M., & Restrepo, J. C. (2006). Factors controlling sediment yield in a major South American drainage basin: the Magdalena River, Colombia. *Journal of Hydrology*, 316(1), 213-232. doi:10.1016/j.jhydrol.2005.05.002

Roberts P. J. T. (1973) A method of estimating mean annual sediment yields in ungauged catchments. Technical Note No. 44 Department of Water Affairs South Africa, Division of Hydrology

Roehl, J. W. (1962). Sediment source areas, delivery ratios and influencing morphological factors. *International Association of Scientific Hydrology*, 59, 202-213.

Roman, D. C., Vogel, R. M., & Schwarz, G. E. (2012). Regional regression models of watershed suspended-sediment discharge for the eastern United States. *Journal of Hydrology*, 472-473, 53-62. doi:10.1016/j.jhydrol.2012.09.011

Rouse, H. (1937). Modern conceptions of the mechanics of fluid turbulence. *Trans ASCE*, *102*, 463-505.

Sahaar, A. S. (2013). Erosion mapping and sediment yield of the Kabul River Basin, Afghanistan. Colorado State University, Colorado, US.

Schumm, S. A. (1977). The fluvial system (Vol. 338). New York: Wiley.

Shah-Fairbank, S. C. (2009). Series Expansion of the Modified Einstein Procedure. Ph.D. Dissertation, Colorado State University, Colorado, US.

Shen, H. W., & Hung, C. S. (1983). Remodified Einstein procedure for sediment load. *Journal of Hydraulic Engineering*, 109(4), 565-578. doi:10.1061/(ASCE)07339429(1984)110:4(559)

Shreve, R. L. (1967). Infinite topologically random channel networks. *The Journal of Geology*, 75(2), 178-186. doi:10.1086/627245

Simons, D. B., & Sentürk, F. (1976). Sediment transport technology (No. 04; TC175. 2, S5.). Fort Collins, Colorado: Water Resources Publications.

Strahler, A. N. (1952). Hypsometric (area-altitude curve) analysis of erosional topography. *Bulletin of the Geological Society of America*, 63(11), 1117-1141. doi:10.1130/0016-7606(1952)63[1117:HAAOET]2.0.CO;2

Syvitski, J. P. M., Peckham, S. D., Hilberman, R., & Mulder, T. (2003). Predicting the terrestrial flux of sediment to the global ocean: a planetary perspective. *Sedimentary Geology*, 162(1), 5-24. doi:10.1016/S0037-0738(03)00232-X

Syvitski, James P. M., & Milliman, John D. (2007). Geology, geography, and humans battle for dominance over the delivery of fluvial sediment to the coastal ocean. *The Journal of Geology*, 115(1), 1-19. doi:10.1086/509246

Tamene, L., Park, S. J., Dikau, R., & Vlek, P. L. G. (2006). Analysis of factors determining sediment yield variability in the highlands of northern Ethiopia. *Geomorphology*, 76(1), 76-91. doi:10.1016/j.geomorph.2005.10.007

Tarboton, D. G., Bras, R. L., & Rodriguez-Iturbe, I. (1991). On the extraction of channel networks from digital elevation data. *Hydrological Processes*, 5(1), 81-100. doi:10.1002/hyp.3360050107

Teh, S. H. (2011). Soil erosion modeling using RUSLE and GIS on Cameron highlands, Malaysia for hydropower development. M.S. Thesis, The School for Renewable Energy Science RES in affiliation with University of Iceland & University of Akureyri, Akureyri, Iceland.

Thompson, J. A., Bell, J. C., & Butler, C. A. (2001). Digital elevation model resolution: effects on terrain attribute calculation and quantitative soil-landscape modeling. *Geoderma*,

100(1), 67-89. doi:10.1016/S0016-7061(00)00081-1

Vanmaercke, M., Poesen, J., Broeckx, J., & Nyssen, J. (2013). Sediment yield in Africa. *Earth-Science Reviews*, 136, 350-368. doi:10.1016/j.earscirev.2014.06.004

Vanoni, V. A. (1975). Sedimentation engineering, ASCE manuals and reports on engineering Practice-No. 54. *American Society of Civil Engineers*.

Vente, J., Verduyn, R., Verstraeten, G., Vanmaercke, M., & Poesen, J. (2011). Factors controlling sediment yield at the catchment scale in NW Mediterranean geoecosystems. *Journal of Soils and Sediments*, 11(4), 690-707. doi:10.1007/s11368-011-0346-3

Verstraeten, G., & Poesen, J. (2001). Factors controlling sediment yield from small intensively cultivated catchments in a temperate humid climate. *Geomorphology*, 40(1), 123-144. doi:10.1016/S0169-555X(01)00040-X

Verstraeten, G., Poesen, J., de Vente, J., & Koninckx, X. (2003). Sediment yield variability in Spain: a quantitative and semi-qualitative analysis using reservoir sedimentation rates. *Geomorphology*, 50(4), 327-348. doi:10.1016/S0169-555X(02)00220-9

Walling, D. E. (1983). The sediment delivery problem. *Journal of hydrology*, 65(1-3), 209-237. doi:10.1016/0022-1694(83)90217-2

Walling, D. E. (1999). Linking land use, erosion and sediment yields in river basins. *Man and River Systems*, 223-240. doi:10.1007/978-94-017-2163-9_24

Wheater, H., Jakeman, A., & Beven, K. (1993). Progress and directions in rainfall-runoff modeling. *Modeling Change in Environmental Systems*, 101–132. Wiley.

Williams, J. R., & Berndt, H. D. (1972). Sediment yield computed with universal equation. *Journal of the Hydraulics Division*, *98*(Hy 12).

Williams, J. R. (1975). Sediment-yield prediction with universal equation using runoff energy

factor. ARS-S-40. *Brooksville*, FL: US Department of Agriculture, Agricultural Research Service, 244–252

Williams, J. R. (1977). Sediment delivery ratios determined with sediment and runoff models. *IAHS Publ*, 122, 168-179.

Wischmeier, W., & Smith, D. D. (1965). Rainfall-erosion losses from cropland east of the Rocky Mountains, guide for selection of practices for soil and water conservation. Agriculture Handbook, 282. Washington DC: Agricultural Research Service, US Department of Agriculture

Wischmeier, W. H., Johnson, C., & Cross, B. (1971). Soil erodibility nomograph for farmland and construction sites. *Journal of soil and water conservation.*

Wischmeier, W. H., & Smith, D. D. (1978). Predicting rainfall erosion losses-a guide to conservation planning. Predicting rainfall erosion losses-a guide to conservation planning.

Wood, W. F., & Snell, J. B. (1960). A quantitative system for classifying landforms. Quartermaster Research and Engineering Center, Technical Report EP-124, Natick, Massachusetts, 20pp

Woo, H., Lee, B. K., & Yu, K. (1991). Sedimentation aspects of floodplain management. In *Hydraulic Engineering* (pp. 1102-1107). *ASCE.*

Woo, H. S., Kim, W., & Ji, U. (2015). River hydraulics. Paju-Si, Korea: CheongMoonGak publishing.

Wu, S., Li, J., & Huang, G. (2005). An evaluation of grid size uncertainty in empirical soil loss modeling with digital elevation models. *Environmental Modeling and Assessment*. 10(1), 33-42. doi:10.1007/s10666-004-6595-4

Wuttichaikitcharoen, P., & Babel, M. S. (2014). Principal component and multiple regression analyses for the estimation of suspended sediment yield in ungauged basins of Northern Thailand. *Water*, 6(8), 2412-2435. doi:10.3390/w6082412

Yang, C. T. (2006). Erosion and sedimentation manual. US Department of the Interior Bureau of Reclamation Technical Service Center Sedimentation and River Hydraulics Group Denver, Colorado.

Yoon, B., and Woo, H. (2000). Sediment problems in Korea. *Journal of Hydraulic Engineering,* Vol. 126, No. 7, pp. 486–491, DOI: 10.1061/(asce)0733-9429(2000)126:7(486)

Yoon, Y. N. (1981). Estimation of silting load and capacity loss rate of irrigation reservoir. *Journal of the Korean Society of Civil Engineers*, Vol. 1, No. 1, pp. 69-76

You, S. C., and Min, B. H. (1975). A study for sedimentation in reservoir on district of Chin young. *Journal of the Korean Society of Agricultural Engineers*, Vol. 17, No. 3, pp. 46-53

APPENDIX B. Watershed Characteristics from GIS analysis

Name	Id	SD	Area	P_point	P_area	R_point	R_area	c010	SI010	SA010	R010
Yeoju	HD1	117.19	11,114.2	1361.11	1410.25	5461.1	4714.55	14.14	32.06	37.15	16.65
Heungcheon	HD2	403.57	294.8	1383.43	1368.74	5650.22	5470.36	12.75	31.93	43.89	11.43
Munmak	HD3	1146.71	1,348.0	1349.44	1397.79	5366.12	5460.34	11.13	27.79	48.23	12.85
Yulgeuk	HD4	202.52	177.3	1380.21	1350.99	5364.05	5264.21	12.64	32.36	46.04	8.96
Cheongmi	HD5	411.74	519.5	1327.40	1309.37	5409.91	4979.17	13.07	31.70	43.89	11.34
Namhanriver	HD6	16.51	8,840.3	1328.55	1420.37	5144.41	4556.88	14.82	32.90	34.51	17.77
Heukcheon	HD7	75.29	307.4	1414.26	1401.42	6211.4	6013.14	11.38	31.55	34.58	22.48
Yeongchun	HU1	124.00	4,690.0	1410.93	1513.09	4177.34	4657.5	14.72	33.61	31.01	20.67
Samok Bridge	HU2	1056.55	2,447.9	1459.60	1560.04	4562.77	4534.81	13.89	35.09	30.45	20.57
Yeongwol1	HU3	218.03	1,615.8	1450.48	1496.65	4389.89	5041.25	16.10	32.55	34.89	16.46
Dalcheon	HU4	-	1,375.1	1251.59	1269.09	4702.38	4310.64	16.06	35.93	41.28	6.73
Maeil	HU5	1307.54	174.5	1434.71	1454.76	3798.29	5223.66	13.56	30.31	43.07	13.07
Bukcheon	HU6	278.45	304.1	1247.20	-	3979.93	-				
Naerincheon	HU7	106.81	1,039.1	1273.96	-	3782.12	-				
Wontong	HU8	325.97	531.0	1229.24	-	5367.38	-				
Seonsan	ND1	70.69	987.5	1104.41	1161.00	2870.07	3085.47	13.81	27.46	46.25	12.48
Dongchon	ND2	43.30	1,537.7	1072.46	1080.85	2889.04	2896.6	17.41	35.23	31.03	16.34
Gumi	ND3	20.99	10,915.4	1074.27	1170.01	2845.72	3230.5	13.01	28.80	42.39	15.79
Nakdong	ND4	43.90	9,400.0	1140.89	1175.54	3059.41	3265.94	12.96	28.66	41.74	16.64
Waegwan	ND5	56.08	11,103.9	1089.16	1168.56	2930.45	3224.59	13.01	28.87	42.36	15.75
Ilseon bridge	ND6	4.06	9,532.8	1105.65	1174.86	2907.2	3261.98	12.94	28.67	41.80	16.58
Jindong	ND7	102.38	20,354.8	1339.41	1221.15	5082.15	3725.78	14.31	30.15	40.28	15.26
Jeongam	ND8	33.45	2,990.7	1406.74	1467.10	5535.75	5614.35	15.04	31.01	37.92	16.03
Hyangseok	ND9	84.28	1,514.3	1228.30	1277.18	3423.72	3737.14	11.24	28.04	46.60	14.12
Dongmun	ND10	74.81	177.2	1193.88	1179.91	3241.22	3119.42	11.89	32.22	42.20	13.69
Jeomchon	ND11	31.34	609.4	1259.69	1284.21	3486.95	3850.07	12.14	30.90	38.63	18.34
Yonggok	ND12	46.33	1,312.2	1126.68	1049.33	3402.98	2841.9	15.29	29.81	41.15	13.75

Name	Id	SD	Area	P_point	P_area	R_point	R_area	c010	SI010	SA010	R010
Jukgo	ND13	37.22	1,240.7	1265.52	1305.10	4387.03	4267.64	13.81	27.46	46.25	12.48
Gaejin2	ND14	51.76	749.8	1205.14	1209.23	3837.38	3652.73	14.50	27.76	43.71	14.02
Socheon	NU1	200.53	696.8	1218.08	1274.04	3229.05	3329.93	13.79	27.26	38.11	20.84
Yangsam	NU2	202.51	1,148.0	1198.66	1262.67	3318.94	3356.54	13.67	27.52	39.26	19.56
Yeongyang	NU3	193.33	334.0	1120.85	1131.52	2898.18	2898.23	12.07	26.10	29.12	32.70
Dongcheon	NU4	317.56	142.7	1114.97	1146.62	2974.36	3042.27	15.57	27.43	34.84	22.16
Cheongsong	NU5	23.66	305.0	1074.43	1077.24	2949.83	2859.69	13.99	33.02	35.43	17.56
Geochang1	NU6	172.49	227.0	1309.47	1298.51	2747.96	4063.6	12.23	25.75	48.19	13.83
Geochang2	NU7	98.63	180.7	1290.96	1262.15	2755.24	3789.28	12.46	26.78	49.94	10.83
Jisan	NU8	1093.11	159.9	1296.63	1255.64	4095.36	3837.5	13.09	27.77	45.40	13.75
Donggok2	NU9	61.60	78.5	1037.91	1040.60	3992.24	2754.93	13.40	36.93	33.16	16.51
Gohyeon	NU10	400.11	14.8	1051.58	1048.53	4171.53	2754.63	13.25	37.95	29.82	18.98
Daeri	NU11	1433.50	59.4	1268.86	1246.93	4528.7	4278.62	15.35	46.16	19.97	18.52
Changchon	NU12	122.01	335.5	1535.60	1526.40	6100.32	6074.31	12.78	30.78	31.58	24.86
Sancheong	NU13	145.29	1,134.1	1546.38	1416.85	5658.66	5174.77	11.83	28.69	44.06	15.41
Taesu	NU14	214.52	143.0	1528.83	1523.73	6008.32	6056.78	11.15	27.51	32.52	28.82
Imcheon	NU15	1131.63	431.7	1483.24	1442.27	6154.32	5492.04	11.44	28.58	40.02	19.96
Oesong	NU16	103.55	1,233.0	1523.14	1426.13	6058.21	5246.32	11.84	28.70	43.25	16.21
Hoedeok	GD1	119.12	609.4	1350.63	1337.10	5242.01	5064.34	12.10	29.75	37.06	21.09
Gongju	GD2	108.76	7,213.3	1322.79	1277.62	5485.53	4484.62	13.45	30.80	41.14	14.60
Hapgang	GD3	133.54	131.0	1306.29	1263.87	5125.2	4792.95	14.02	31.54	42.84	11.60
Useong	GD4	61.23	257.4	1318.79	1306.96	5511.55	5474.6	12.73	21.06	45.93	20.29
Guryong	GD5	60.08	209.0	1332.94	1311.02	5714.95	5646.55	17.36	39.46	29.36	13.83
Okcheon	GU1	225.64	2,017.8	1275.13	1247.90	4173.91	3785.68	11.93	27.99	41.38	18.70
Cheongseong	GU2	114.53	481.9	1272.51	1281.15	4036.39	4346.74	13.91	34.69	40.61	10.79
Hotan	GU3	17.96	991.9	1266.86	1268.62	4185.04	4006.64	11.35	24.76	43.05	20.84
CheonCheon	GU4	230.25	290.9	1317.08	1335.27	4404.81	4510.55	10.85	28.68	45.76	14.72
Donghyang	GU5	148.31	164.4	1304.87	1292.67	4314.46	4115.39	10.50	24.69	41.86	22.94

Name	Id	SD	Area	P_point	P_area	R_point	R_area	c010	SI010	SA010	R010
Hakgyo	YD1	97.44	193.4	1265.54	1288.87	4812.96	4896.48	14.83	41.65	30.20	13.33
Naju	YD2	114.35	2,055.8	1330.60	1365.92	5297.06	5478.95	15.40	39.14	29.97	15.49
Mareuk	YD3	165.99	683.5	1366.46	1372.75	5548.46	5468.12	17.54	42.29	31.40	8.76
Nampyeong	YD4	46.72	585.1	1373.58	1399.03	5611.64	5865.3	12.31	35.12	25.29	27.28
Seonam	YD5	40.34	555.1	1347.97	1328.96	5419.75	5104.41	14.36	36.92	33.93	14.78
Bongdeok	YU1	77.27	46.6	1415.54	1392.47	6033.02	5835.58	8.56	26.16	23.12	42.16
Jukgok	SD1	32.15	1,273.6	1410.61	1420.26	5691.34	6004.54	15.27	34.14	32.39	18.19
Gokseong	SD2	44.85	1,795.7	1371.17	1347.08	5291.94	4097.75	13.94	30.78	35.16	20.12
Gurye2	SD3	45.15	3,827.8	1437.32	1377.21	5807.02	5327.43	14.13	32.41	34.60	18.86
Yongseo	SD4	28.43	128.7	1442.95	1443.44	5850.94	5912.65	11.51	24.43	34.31	29.74
Gwanchon	SU1	120.43	364.4	1334.92	1348.58	4672.26	4626.6	14.83	30.18	37.41	17.58
Ssangchi2	SU2	134.64	134.0	1339.68	1342.81	4936.41	5010.4	10.25	29.07	24.82	35.86
Gyeombaek	SU3	56.00	298.1	1434.22	1444.41	6294.17	6359.75	17.97	37.00	31.66	13.36
Jangjeon2	SU4	207.35	267.3	1410.60	1402.41	5940.74	5758.2	14.17	38.42	23.25	24.17
Songjeon	SU5	330.87	60.1	1445.34	1437.88	6072.68	5997.99	14.10	24.81	43.71	17.39

Name	Id	C1030	SI1030	SA1030	R1030	C3050	SI3050	SA3050	R3050	C030	SI030
Yeoju	HD1	14.17	29.52	36.17	20.13	14.25	28.43	38.39	18.92	14.17	30.38
Heungcheon	HD2	12.35	29.49	45.37	12.80	11.41	28.12	47.72	12.75	12.48	30.30
Munmak	HD3	9.79	25.73	49.66	14.82	9.36	23.20	52.06	15.38	10.24	26.42
Yulgeuk	HD4	11.91	30.01	48.95	9.13	10.82	27.99	50.94	10.25	12.15	30.79
Cheongmi	HD5	12.58	28.70	44.35	14.37	11.93	27.61	46.14	14.32	12.74	29.70
Namhanriver	HD6	15.16	30.32	32.92	21.60	15.44	29.57	35.02	19.97	15.05	31.19
Heukcheon	HD7	9.97	23.85	31.80	34.38	10.19	23.11	35.11	31.59	10.44	26.42
Yeongchun	HU1	14.82	30.03	29.08	26.08	15.00	28.87	31.39	24.74	14.80	31.24
Samok Bridge	HU2	13.49	29.49	27.79	29.22	12.54	27.50	29.73	30.23	13.65	31.40
Yeongwol1	HU3	16.40	31.16	33.78	18.66	16.60	29.85	36.01	17.54	16.30	31.63
Dalcheon	HU4	17.07	35.62	39.04	8.26	16.88	35.07	39.56	8.49	16.73	35.73
Maeil	HU5	11.79	28.97	43.46	15.79	10.81	26.88	45.11	17.19	12.38	29.41
Bukcheon	HU6										
Naerincheon	HU7										
Wontong	HU8										
Seonsan	ND1	13.13	25.43	45.12	16.32	14.17	26.48	49.00	10.35	13.39	26.18
Dongchon	ND2	16.58	30.26	25.00	28.17	21.33	34.31	27.12	17.25	16.99	32.19
Gumi	ND3	13.01	28.80	42.39	15.79	13.33	26.86	43.39	16.42	12.71	26.95
Nakdong	ND4	12.33	25.43	38.18	24.06	13.24	26.58	42.63	17.55	12.62	26.68
Waegwan	ND5	12.48	25.91	39.31	22.30	13.35	26.95	43.34	16.36	12.73	27.04
Ilseon bridge	ND6	12.33	25.47	38.26	23.93	13.24	26.61	42.65	17.51	12.62	26.71
Jindong	ND7	13.61	26.95	37.12	22.32	15.17	28.80	41.64	14.39	13.92	28.17
Jeongam	ND8	14.48	28.41	35.73	21.38	17.64	31.44	39.47	11.46	14.74	29.40
Hyangseok	ND9	10.76	25.88	48.40	14.96	11.02	24.79	49.96	14.23	10.93	26.63
Dongmun	ND10	11.50	29.96	44.05	14.49	12.30	28.51	43.22	15.98	11.73	30.86
Jeomchon	ND11	13.52	27.17	36.83	22.48	13.73	24.34	40.07	21.87	13.05	28.42
Yonggok	ND12	14.55	26.00	33.70	25.76	17.35	31.11	39.43	12.11	14.95	27.54

Name	Id	C1030	SI1030	SA1030	R1030	C3050	SI3050	SA3050	R3050	C030	SI030
Jukgo	ND13	13.13	25.43	45.12	16.32	14.17	26.48	49.00	10.35	13.39	26.18
Gaejin2	ND14	13.44	25.42	41.59	19.55	15.30	28.38	47.05	9.28	13.86	26.31
Socheon	NU1	13.13	24.53	35.75	26.59	16.47	27.70	44.21	11.61	13.46	25.87
Yangsam	NU2	13.07	25.28	36.64	25.00	15.05	27.12	42.72	15.11	13.35	26.30
Yeongyang	NU3	10.87	22.81	22.41	43.91	15.42	28.74	23.69	32.15	11.40	24.14
Dongcheon	NU4	12.40	20.51	26.35	40.74	17.42	33.05	32.27	17.26	13.73	23.28
Cheongsong	NU5	14.18	29.38	28.88	27.55	14.40	27.42	33.03	25.14	14.14	30.68
Geochang1	NU6	11.63	24.41	48.43	15.53	12.33	24.41	50.95	12.32	11.83	24.85
Geochang2	NU7	12.17	25.48	49.89	12.46	12.65	25.13	50.04	12.17	12.27	25.91
Jisan	NU8	13.25	27.01	44.66	15.08	14.26	27.20	47.80	10.74	13.19	27.27
Donggok2	NU9	14.71	33.95	30.04	21.30	12.16	25.46	35.03	27.36	14.23	34.96
Gohyeon	NU10	15.17	34.70	24.70	25.43	13.81	28.65	26.49	31.05	14.49	35.80
Daeri	NU11	18.57	44.45	17.52	19.46	19.01	41.58	17.00	22.40	17.43	45.04
Changchon	NU12	14.39	30.38	31.90	23.33	22.77	34.24	34.51	8.48	13.85	30.51
Sancheong	NU13	11.48	27.29	43.93	17.30	12.77	27.15	45.52	14.56	11.60	27.76
Taesu	NU14	12.76	27.40	32.50	27.34	22.22	31.65	37.13	9.00	12.23	27.43
Imcheon	NU15	11.14	27.37	39.12	22.36	12.73	28.55	42.60	16.12	11.24	27.77
Oesong	NU16	11.61	27.37	43.07	17.94	13.17	27.49	44.86	14.48	11.69	27.81
Hoedeok	GD1	11.72	26.26	34.81	27.22	12.40	27.75	38.46	21.39	11.85	27.42
Gongju	GD2	14.03	30.02	39.94	16.01	13.59	30.75	42.63	13.04	13.84	30.31
Hapgang	GD3	14.27	30.43	42.48	12.82	13.27	30.30	44.48	11.95	14.19	30.80
Useong	GD4	16.31	26.26	43.72	13.70	13.15	29.66	48.07	9.12	15.12	24.52
Guryong	GD5	15.87	28.47	27.15	28.52	15.75	27.79	27.96	28.51	16.36	32.13
Okcheon	GU1	12.54	27.49	39.85	20.12	12.79	28.93	43.46	14.82	12.36	27.77
Cheongseong	GU2	14.47	33.26	40.39	11.88	13.27	31.09	42.07	13.57	14.27	33.74
Hotan	GU3	11.95	24.92	41.42	21.71	12.28	27.28	46.69	13.75	11.75	24.87
CheonCheon	GU4	10.33	28.66	45.09	15.92	10.02	27.58	44.35	18.04	10.50	28.67
Donghyang	GU5	10.32	24.40	41.25	24.02	12.34	25.99	49.27	12.40	10.38	24.50

Name	Id	C1030	SI1030	SA1030	R1030	C3050	SI3050	SA3050	R3050	C030	SI030
Hakgyo	YD1	16.76	39.07	26.55	17.61	19.14	39.57	26.41	14.89	16.11	39.93
Naju	YD2	17.51	37.25	27.26	17.97	19.63	34.74	28.86	16.77	16.79	37.89
Mareuk	YD3	20.56	40.36	29.50	9.59	23.36	35.32	32.26	9.07	19.52	41.02
Nampyeong	YD4	12.88	33.07	20.35	33.70	15.21	34.29	19.75	30.74	12.69	33.75
Seonam	YD5	16.06	35.68	32.15	16.12	15.19	32.13	35.95	16.72	15.46	36.10
Bongdeok	YU1	10.62	26.89	19.00	43.49	15.45	28.74	19.72	36.09	9.94	26.64
Jukgok	SD1	15.34	29.18	29.87	25.61	16.30	30.21	32.76	20.74	15.32	30.85
Gokseong	SD2	13.62	27.84	32.57	25.96	15.18	29.92	37.05	17.85	13.77	28.90
Gurye2	SD3	13.79	28.54	32.36	25.30	14.71	29.62	35.61	20.06	13.93	29.87
Yongseo	SD4	13.42	27.00	32.15	27.42	16.48	31.35	41.31	10.87	12.79	26.14
Gwanchon	SU1	13.19	25.51	32.56	28.74	15.62	31.44	34.45	18.49	13.86	27.27
Ssangchi2	SU2	12.09	29.45	19.59	38.87	16.04	30.69	20.18	33.08	11.47	29.32
Gyeombaek	SU3	18.41	31.74	30.32	19.53	18.81	32.00	31.63	17.56	18.26	33.49
Jangjeon2	SU4	14.54	32.36	19.01	34.10	16.75	33.59	18.78	30.88	14.43	34.46
Songjeon	SU5	15.08	26.38	42.00	16.54	15.01	29.30	47.62	8.06	14.75	25.86

Name	Id	SA030	R030	C050	SI050	SA050	R050	Urban	Agriculture	Forest	pasture
Yeoju	HD1	36.51	18.95	13.95	29.46	36.69	19.90	2.64	14.61	75.08	3.45
Heungcheon	HD2	44.88	12.34	12.01	29.38	45.89	12.72	10.27	32.41	37.91	11.73
Munmak	HD3	49.19	14.16	9.81	25.21	49.47	15.51	3.98	15.18	74.47	2.53
Yulgeuk	HD4	47.98	9.07	11.62	29.67	49.16	9.55	8.97	48.01	22.99	13.84
Cheongmi	HD5	44.20	13.36	12.38	28.83	44.85	13.94	7.04	36.56	40.61	10.04
Namhanriver	HD6	33.46	20.30	14.89	30.34	33.59	21.19	2.10	13.00	77.90	2.97
Heukcheon	HD7	32.73	30.41	9.92	24.87	32.90	32.31	3.39	10.29	75.34	7.74
Yeongchun	HU1	29.74	24.23	14.51	30.08	29.96	25.45	1.26	9.98	83.48	2.38
Samok Bridge	HU2	28.71	26.24	13.21	29.81	28.96	28.03	0.97	9.10	84.05	2.98
Yeongwol1	HU3	34.15	17.92	16.09	30.73	34.45	18.73	1.66	12.76	80.62	1.98
Dalcheon	HU4	39.79	7.75	16.76	35.49	39.52	8.22	2.52	18.41	72.00	4.03
Maeil	HU5	43.33	14.88	11.65	28.37	43.47	16.52	0.54	12.12	85.15	0.87
Bukcheon	HU6										
Naerincheon	HU7										
Wontong	HU8										
Seonsan	ND1	45.55	14.88	13.55	25.95	45.69	14.81	3.70	20.47	64.63	6.76
Dongchon	ND2	27.24	23.58	17.64	31.97	26.44	23.95	6.24	19.08	63.17	6.36
Gumi	ND3	40.37	19.97	12.88	26.47	40.12	20.53	2.88	17.23	70.65	4.79
Nakdong	ND4	39.43	21.27	12.80	26.15	39.12	21.93	2.59	16.67	71.99	4.51
Waegwan	ND5	40.38	19.86	12.90	26.57	40.12	20.42	3.10	17.20	70.35	4.85
Ilseon bridge	ND6	39.50	21.17	12.79	26.19	39.19	21.83	2.59	16.72	71.88	4.52
Jindong	ND7	38.27	19.64	14.21	27.78	37.99	20.01	4.19	16.72	68.56	5.57
Jeongam	ND8	36.57	19.29	15.24	29.10	36.27	19.38	3.93	15.01	69.78	6.38
Hyangseok	ND9	47.74	14.70	10.84	25.83	48.15	15.18	3.57	24.14	63.17	5.33
Dongmun	ND10	42.99	14.42	12.01	30.04	42.82	15.13	3.64	31.58	54.41	6.27
Jeomchon	ND11	37.43	21.10	13.22	27.32	37.46	22.00	2.51	11.01	79.79	3.58
Yonggok	ND12	36.42	21.10	15.43	27.34	35.54	21.70	2.66	17.34	71.52	4.67

Name	Id	SA030	R030	C050	SI050	SA050	R050	Urban	Agriculture	Forest	pasture
Jukgo	ND13	45.55	14.88	13.55	25.95	45.69	14.81	2.94	13.87	73.02	4.93
Gaejin2	ND14	42.39	17.44	14.03	26.29	42.48	17.20	2.53	11.85	75.98	5.47
Socheon	NU1	36.40	24.27	13.59	25.68	36.89	23.83	1.80	3.13	90.46	2.17
Yangsam	NU2	37.41	22.94	13.38	26.02	37.76	22.85	1.68	6.29	87.18	2.56
Yeongyang	NU3	24.85	39.61	11.55	23.67	24.04	40.74	1.29	6.25	86.55	3.76
Dongcheon	NU4	29.59	33.40	14.03	23.18	28.88	33.91	0.92	8.07	85.85	3.49
Cheongsong	NU5	31.13	24.04	14.49	30.45	30.51	24.56	1.40	9.25	83.68	3.04
Geochang1	NU6	48.35	14.96	11.82	24.57	48.75	14.85	1.94	11.10	81.49	3.48
Geochang2	NU7	49.91	11.92	12.39	25.58	49.86	12.17	2.51	16.50	72.37	5.94
Jisan	NU8	44.91	14.63	13.38	27.29	45.00	14.33	2.31	13.80	76.93	4.28
Donggok2	NU9	31.09	19.72	14.38	34.22	30.59	20.81	0.91	8.18	87.32	2.68
Gohyeon	NU10	26.41	23.29	14.92	35.40	25.57	24.10	1.62	12.47	75.74	8.56
Daeri	NU11	18.36	19.17	18.17	45.21	18.37	18.26	1.14	1.18	92.62	3.47
Changchon	NU12	31.80	23.84	15.26	30.37	31.44	22.92	1.96	8.04	83.51	3.73
Sancheong	NU13	43.97	16.67	11.76	27.29	43.83	17.12	2.78	14.26	73.46	6.32
Taesu	NU14	32.51	27.83	13.57	27.41	32.19	26.83	1.59	4.66	88.39	3.21
Imcheon	NU15	39.42	21.56	11.24	27.55	39.37	21.84	2.09	14.00	76.70	4.65
Oesong	NU16	43.13	17.37	11.91	27.40	42.95	17.74	2.84	13.84	73.69	6.36
Hoedeok	GD1	35.56	25.17	11.53	27.10	35.75	25.62	14.57	13.45	59.99	6.73
Gongju	GD2	40.29	15.56	13.54	30.30	40.67	15.50	5.71	22.14	60.46	6.06
Hapgang	GD3	42.60	12.41	13.82	30.58	43.33	12.27	8.16	33.13	46.70	6.25
Useong	GD4	44.46	15.90	14.28	26.53	45.78	13.41	2.22	17.52	73.55	4.34
Guryong	GD5	27.89	23.62	16.14	30.53	27.86	25.47	2.86	21.14	67.99	4.58
Okcheon	GU1	40.20	19.66	12.17	27.91	40.53	19.39	2.28	15.61	73.36	5.26
Cheongseong	GU2	40.47	11.52	14.08	33.25	40.37	12.31	2.61	25.60	62.44	5.42
Hotan	GU3	41.97	21.42	11.35	25.15	42.61	20.89	2.21	13.95	74.72	5.54
CheonCheon	GU4	45.31	15.52	10.26	28.17	44.74	16.83	3.43	25.55	63.03	6.01
Donghyang	GU5	41.45	23.66	10.16	24.37	41.71	23.76	2.88	26.64	67.15	1.92

Name	Id	SA030	R030	C050	SI050	SA050	R050	Urban	Agriculture	Forest	pasture
Hakgyo	YD1	27.77	16.18	17.19	39.74	27.02	16.06	4.48	40.89	45.64	4.92
Naju	YD2	28.17	17.15	17.56	37.04	27.62	17.78	8.81	26.41	52.64	6.45
Mareuk	YD3	30.14	9.32	20.68	40.01	29.74	9.57	15.04	27.73	43.80	7.89
Nampyeong	YD4	22.00	31.56	12.94	32.93	20.91	33.22	8.38	50.78	18.54	9.82
Seonam	YD5	32.75	15.68	15.64	35.76	32.57	16.04	4.63	22.02	60.61	7.05
Bongdeok	YU1	20.37	43.05	10.23	26.08	19.65	44.04	0.93	8.81	86.36	2.83
Jukgok	SD1	30.73	23.10	15.26	30.41	30.80	23.53	2.10	18.60	71.19	3.24
Gokseong	SD2	33.50	23.83	13.67	28.33	33.48	24.52	2.58	23.11	63.57	5.79
Gurye2	SD3	33.14	23.06	13.79	29.24	33.16	23.80	2.58	20.82	66.95	4.81
Yongseo	SD4	32.87	28.20	12.77	26.82	32.95	27.46	1.95	20.33	67.89	7.08
Gwanchon	SU1	34.36	24.51	13.88	26.69	34.10	25.33	2.54	19.50	66.66	7.43
Ssangchi2	SU2	21.33	37.87	11.68	28.51	20.43	39.38	1.95	19.59	71.61	2.86
Gyeombaek	SU3	30.77	17.48	18.24	32.84	30.74	18.17	3.04	28.51	61.75	2.36
Jangjeon2	SU4	20.49	30.62	14.65	33.74	20.32	31.29	1.58	12.62	75.33	5.76
Songjeon	SU5	42.57	16.82	14.37	26.83	43.54	15.25	2.66	19.83	72.71	3.59

Name	Id	wetland	bare	water	WW	Total	Main	Tri	SO1	SO2	SO3
Yeoju	HD1	0.80	1.59	1.83	2.63	2,802.24	339.71	2,462.52	7	5	236
Heungcheon	HD2	1.70	5.07	0.91	2.61	100.91	31.09	69.83	6	2	7
Munmak	HD3	0.78	1.65	1.42	2.20	352.26	81.88	270.37	6	3	28
Yulgeuk	HD4	2.26	3.06	0.87	3.13	57.57	26.25	31.32	6	2	3
Cheongmi	HD5	1.55	2.58	1.63	3.18	153.65	44.24	109.40	6	3	11
Namhanriver	HD6	0.72	1.45	1.87	2.59	2,160.92	321.21	1,839.71	6	5	190
Heukcheon	HD7	1.13	1.48	0.63	1.77	105.01	36.99	68.02	7	3	8
Yeongchun	HU1	0.67	1.40	0.83	1.50	1,084.09	187.75	896.34	7	5	102
Samok Bridge	HU2	0.60	1.52	0.79	1.38	478.22	165.42	312.80	7	4	49
Yeongwol1	HU3	0.87	1.15	0.97	1.83	425.20	107.32	317.88	6	4	38
Dalcheon	HU4	1.00	0.87	1.17	2.17	385.52	116.73	268.79	6	3	29
Maeil	HU5	0.45	0.23	0.64	1.10	32.06	10.66	21.40	5	3	4
Bukcheon	HU6										
Naerincheon	HU7										
Wontong	HU8										
Seonsan	ND1	1.04	2.69	0.70	1.74	199.14	64.20	134.94	7	3	25
Dongchon	ND2	1.30	1.84	2.01	3.31	419.92	74.09	345.83	7	4	38
Gumi	ND3	1.23	1.92	1.29	2.52	2,700.48	300.41	2,400.07	8	5	251
Nakdong	ND4	1.23	1.71	1.31	2.53	2,376.89	265.41	2,111.48	8	5	211
Waegwan	ND5	1.22	1.97	1.31	2.53	2,760.55	314.19	2,446.36	8	5	257
Ilseon bridge	ND6	1.23	1.74	1.32	2.55	2,394.51	278.22	2,116.29	8	5	214
Jindong	ND7	1.27	2.03	1.66	2.93	6,032.14	425.98	5,606.16	8	5	493
Jeongam	ND8	1.11	1.73	2.06	3.17	1,229.18	154.56	1,074.62	7	4	73
Hyangseok	ND9	1.05	1.97	0.78	1.82	342.45	101.68	240.77	7	4	31
Dongmun	ND10	1.59	2.09	0.41	2.01	35.60	19.91	15.69	7	3	9
Jeomchon	ND11	0.96	1.56	0.58	1.54	113.60	51.03	62.57	7	3	14
Yonggok	ND12	1.29	1.19	1.35	2.63	331.28	103.47	227.81	7	4	31

Name	Id	wetland	bare	water	WW	Total	Main	Tri	SO1	SO2	SO3
Jukgo	ND13	1.27	1.61	2.36	3.63	500.77	103.35	397.42	7	3	31
Gaejin2	ND14	1.36	1.86	0.95	2.31	206.01	62.91	143.10	7	3	21
Socheon	NU1	0.50	1.47	0.48	0.97	180.86	85.93	94.93	8	3	15
Yangsam	NU2	0.51	1.30	0.48	0.99	295.66	109.22	186.44	8	4	24
Yeongyang	NU3	1.15	0.65	0.35	1.50	80.43	30.26	50.17	6	3	10
Dongcheon	NU4	0.86	0.32	0.49	1.35	32.40	27.54	4.86	6	2	4
Cheongsong	NU5	1.32	0.81	0.51	1.83	98.66	37.28	61.38	7	2	6
Geochang1	NU6	0.50	1.02	0.48	0.98	71.17	24.70	46.47	6	2	7
Geochang2	NU7	0.84	1.27	0.58	1.41	58.84	23.23	35.61	5	3	5
Jisan	NU8	1.04	1.21	0.42	1.46	52.12	22.22	29.90	6	2	5
Donggok2	NU9	0.32	0.38	0.21	0.53	4.76	4.76	0.00	6	2	2
Gohyeon	NU10	0.67	0.47	0.47	1.15					1	1
Daeri	NU11	0.29	1.06	0.24	0.53	10.73	10.73	0.00	6	2	2
Changchon	NU12	0.80	1.15	0.80	1.60	114.50	32.39	82.11	6	3	7
Sancheong	NU13	0.86	1.55	0.77	1.63	374.50	59.44	315.06	7	4	27
Taesu	NU14	0.46	1.15	0.53	1.00	74.92	21.16	53.76	6	3	5
Imcheon	NU15	0.67	1.19	0.71	1.38	117.43	47.62	69.81	6	3	12
Oesong	NU16	0.85	1.61	0.81	1.66	401.13	72.79	328.34	7	4	29
Hoedeok	GD1	1.23	3.06	0.98	2.20	223.07	47.80	175.27	7	4	361
Gongju	GD2	1.60	2.15	1.88	3.48	2,046.01	265.52	1,780.49	8	5	392
Hapgang	GD3	1.65	2.71	1.39	3.04	519.94	80.66	439.28	7	4	104
Useong	GD4	1.28	0.62	0.47	1.75	101.33	31.43	69.90	7	3	14
Guryong	GD5	1.56	0.81	1.06	2.62	115.38	43.38	72.00	7	3	14
Okcheon	GU1	1.43	1.10	0.97	2.39	672.20	126.40	545.80	8	5	150
Cheongseong	GU2	1.88	1.08	0.97	2.85	133.56	52.01	81.55	7	4	27
Hotan	GU3	1.35	1.26	0.97	2.31	394.23	95.77	298.46	8	5	95
CheonCheon	GU4	0.34	0.57	1.07	1.41	113.42	29.45	83.97	8	3	15
Donghyang	GU5	0.26	0.17	0.98	1.24	67.51	22.23	45.28	7	3	9

Name	Id	wetland	bare	water	WW	Total	Main	Tri	SO1	SO2	SO3
Hakgyo	YD1	1.56	0.80	1.71	3.26	74.28	30.17	44.11	4	3	24
Naju	YD2	1.47	1.75	2.47	3.94	793.67	69.43	724.24	5	5	246
Mareuk	YD3	1.81	1.80	1.93	3.74	198.53	40.07	158.46	5	1	1
Nampyeong	YD4	2.20	3.00	7.29	9.49	263.20	45.41	217.79	4	1	1
Seonam	YD5	1.43	1.51	2.73	4.17	226.55	54.59	171.96	4	4	56
Bongdeok	YU1	0.08	0.44	0.55	0.63					3	29
Jukgok	SD1	0.97	0.96	2.94	3.91	511.14	113.13	398.01	5	5	220
Gokseong	SD2	1.48	1.15	2.31	3.79	767.40	138.28	629.12	6	5	292
Gurye2	SD3	1.35	1.16	2.32	3.68	1,587.25	164.84	1,422.41	6	6	634
Yongseo	SD4	0.95	1.43	0.37	1.32	43.16	16.38	26.78	5	3	23
Gwanchon	SU1	1.23	1.52	1.11	2.34	162.30	42.63	119.67	6	4	59
Ssangchi2	SU2	1.02	1.68	1.29	2.31	57.24	24.26	32.98	5	3	21
Gyeombaek	SU3	0.53	1.82	1.97	2.50	117.63	42.68	74.95	5	4	53
Jangjeon2	SU4	1.19	0.78	2.74	3.93	113.98	36.28	77.70	4	4	47
Songjeon	SU5	0.50	0.41	0.31	0.80	29.01	9.84	19.17	3	4	55

Name	Id	DD	SF	AXL	LF	(A*)	(A**)	Avgslp	hyp1	hyp2	hyp3
Yeoju	HD1	0.25	10.38	166.42	0.40	0.40	0.60	44.42	0.28	464.49	0.58
Heungcheon	HD2	0.34	3.28	25.24	0.46	0.00	1.00	16.60	0.17	133.75	0.28
Munmak	HD3	0.26	4.97	57.91	0.40	0.16	0.84	42.96	0.22	329.16	0.40
Yulgeuk	HD4	0.32	3.89	24.81	0.29	0.00	1.00	10.00	0.17	105.16	0.17
Cheongmi	HD5	0.30	3.77	42.71	0.28	0.03	0.97	19.95	0.21	183.00	0.37
Namhanriver	HD6	0.24	11.67	166.42	0.32	0.48	0.52	46.77	0.33	545.78	0.58
Heukcheon	HD7	0.34	4.45	30.18	0.34	0.00	1.00	42.85	0.22	278.60	0.34
Yeongchun	HU1	0.23	7.52	90.45	0.57	0.18	0.82	25.71	0.42	804.83	0.72
Samok Bridge	HU2	0.20	11.18	72.29	0.47	0.35	0.65	26.23	0.47	471.99	0.84
Yeongwol1	HU3	0.26	7.13	65.95	0.37	0.00	1.00	23.91	0.48	684.22	1.00
Dalcheon	HU4	0.28	9.91	51.95	0.51	0.49	0.51	21.17	0.28	497.38	0.60
Maeil	HU5	0.18	0.65	17.19	0.59	0.00	1.00	27.61	0.24	541.26	0.40
Bukcheon	HU6										
Naerincheon	HU7										
Wontong	HU8										
Seonsan	ND1	0.20	4.17	56.83	0.31	0.08	0.92	34.86	0.19	276.37	0.44
Dongchon	ND2	0.27	3.57	72.09	0.30	0.17	0.83	33.46	0.18	233.39	0.40
Gumi	ND3	0.25	8.27	178.45	0.34	0.34	0.66	38.05	0.19	318.50	0.38
Nakdong	ND4	0.25	7.49	137.54	0.50	0.39	0.61	38.98	0.20	330.98	0.38
Waegwan	ND5	0.25	8.89	178.45	0.35	0.33	0.67	37.87	0.19	316.19	0.38
Ilseon bridge	ND6	0.25	8.12	137.54	0.50	0.38	0.62	38.84	0.20	329.14	0.38
Jindong	ND7	0.30	8.91	255.09	0.31	0.37	0.63	36.92	0.15	291.77	0.32
Jeongam	ND8	0.41	7.99	101.38	0.29	0.76	0.24	38.41	0.15	301.64	0.42
Hyangseok	ND9	0.23	6.83	65.26	0.36	0.33	0.67	32.97	0.19	308.86	0.36
Dongmun	ND10	0.20	2.24	23.19	0.33	0.00	1.00	27.20	0.22	211.46	0.50
Jeomchon	ND11	0.19	4.27	43.95	0.32	0.00	1.00	45.37	0.34	416.03	0.56
Yonggok	ND12	0.25	8.16	53.87	0.45	0.07	0.93	35.08	0.17	234.25	0.26

Name	Id	DD	SF	AXL	LF	(A*)	(A**)	Avgslp	hyp1	hyp2	hyp3
Jukgo	ND13	0.40	8.61	59.78	0.35	0.75	0.25	39.45	0.28	427.55	0.50
Gaejin2	ND14	0.27	5.28	41.57	0.43	0.20	0.80	41.09	0.24	352.37	0.53
Socheon	NU1	0.26	10.60	47.39	0.31	0.00	1.00	55.49	0.42	804.83	0.43
Yangsam	NU2	0.26	10.39	52.90	0.41	0.00	1.00	52.41	0.38	705.83	0.50
Yeongyang	NU3	0.24	2.74	30.68	0.35	0.00	1.00	51.69	0.31	525.24	0.43
Dongcheon	NU4	0.23	5.32	22.93	0.27	0.00	1.00	50.29	0.28	474.63	0.32
Cheongsong	NU5	0.32	4.56	28.47	0.38	0.00	1.00	47.24	0.37	455.36	0.54
Geochang1	NU6	0.31	2.69	23.02	0.43	0.00	1.00	45.39	0.34	639.34	0.62
Geochang2	NU7	0.33	2.99	22.10	0.37	0.00	1.00	40.06	0.34	558.14	0.52
Jisan	NU8	0.33	3.09	22.97	0.30	0.00	1.00	42.08	0.37	634.52	0.69
Donggok2	NU9	0.06	0.29	9.51	0.87	0.00	1.00	52.53	0.47	483.54	0.65
Gohyeon	NU10			5.86	0.43	0.00	1.00	45.43	0.47	471.99	0.67
Daeri	NU11	0.18	1.94	12.57	0.38	0.00	1.00	54.10	0.48	684.22	0.68
Changchon	NU12	0.34	3.13	27.31	0.45	0.00	1.00	48.47	0.28	497.38	0.62
Sancheong	NU13	0.33	3.12	54.69	0.38	0.03	0.97	40.49	0.24	541.26	0.46
Taesu	NU14	0.52	3.13	20.17	0.35	0.12	0.88	52.86	0.29	616.18	0.54
Imcheon	NU15	0.27	5.25	32.36	0.41	0.00	1.00	42.36	0.29	648.97	0.48
Oesong	NU16	0.33	4.30	54.69	0.41	0.00	1.00	40.87	0.25	529.85	0.45
Hoedeok	GD1	0.37	3.75	37.76	0.43	0.00	1.00	32.48	0.22	215.20	0.40
Gongju	GD2	0.28	9.77	137.45	0.38	0.70	0.30	33.26	0.15	240.05	0.28
Hapgang	GD3	3.97	49.65	63.03	0.03	0.12	0.88	23.71	0.23	162.37	0.48
Useong	GD4	0.39	3.84	25.35	0.40	0.00	1.00	39.08	0.36	239.65	0.51
Guryong	GD5	0.55	9.00	20.98	0.47	0.00	1.00	33.04	0.34	214.47	0.40
Okcheon	GU1	0.33	7.92	73.35	0.38	0.00	1.00	41.61	0.19	374.58	0.35
Cheongseong	GU2	0.28	5.61	32.33	0.46	0.00	1.00	35.45	0.21	295.10	0.36
Hotan	GU3	0.40	9.25	48.89	0.41	0.04	0.96	44.42	0.20	416.91	0.42
CheonCheon	GU4	0.39	2.98	27.74	0.38	0.00	1.00	38.70	0.25	577.96	0.35
Donghyang	GU5	0.41	3.01	19.12	0.45	0.00	1.00	42.20	0.24	608.45	0.57

Name	Id	DD	SF	AXL	LF	(A*)	(A**)	Avgslp	hyp1	hyp2	hyp3
Hakgyo	YD1	0.38	4.71	26.28	0.28	0.00	1.00	21.16	0.18	105.04	0.42
Naju	YD2	0.39	2.34	74.71	0.37	0.16	0.84	27.73	0.14	161.81	0.32
Mareuk	YD3	0.29	2.35	44.46	0.35	0.14	0.86	23.98	0.12	140.51	0.31
Nampyeong	YD4	0.45	3.52	33.59	0.52	0.15	0.85	36.05	0.21	205.62	0.39
Seonam	YD5	0.41	5.37	41.79	0.32	0.26	0.74	30.85	0.22	191.13	0.50
Bongdeok	YU1			12.84	0.28	0.00	1.00	44.39	0.47	339.57	0.47
Jukgok	SD1	0.40	10.05	66.96	0.28	0.81	0.19	37.58	0.22	295.09	0.55
Gokseong	SD2	0.43	10.65	72.76	0.34	0.42	0.58	34.08	0.24	314.95	0.59
Gurye2	SD3	0.41	7.10	131.46	0.22	0.48	0.52	35.87	0.21	306.83	0.53
Yongseo	SD4	0.34	2.08	18.41	0.38	0.00	1.00	43.28	0.30	276.82	0.79
Gwanchon	SU1	0.45	4.99	31.31	0.37	0.00	1.00	38.01	0.22	413.35	0.60
Ssangchi2	SU2	0.43	4.39	18.32	0.40	0.00	1.00	36.05	0.34	400.56	0.86
Gyeombaek	SU3	0.39	6.11	29.19	0.35	0.92	0.08	28.83	0.23	264.98	0.57
Jangjeon2	SU4	0.43	4.92	26.37	0.38	0.00	1.00	41.68	0.22	341.09	0.53
Songjeon	SU5	0.48	1.61	12.43	0.39	0.00	1.00	38.30	0.29	327.39	0.74

Name	Id	hypc1	LE	ME	HI	Name	Id	hypc1	LE	ME	HI
Yeoju	HD1	0.61	35	469.91	0.282	Jukgo	ND13	0.69	9.44	416.65	0.273
Heungcheon	HD2	1.10	35	112.47	0.130	Gaejin2	ND14	0.68	11.27	360.34	0.247
Munmak	HD3	0.77	55	319.99	0.216	Socheon	NU1	0.63	251.53	757.63	0.384
Yulgeuk	HD4	1.26	35	84.18	0.121	Yangsam	NU2	0.59	173.52	663.13	0.351
Cheongmi	HD5	1.02	55	144.86	0.145	Yeongyang	NU3	0.57	210.71	492.4	0.280
Namhanriver	HD6	0.57	45	525.68	0.314	Dongcheon	NU4	0.49	191.67	438.26	0.241
Heukcheon	HD7	0.90	35	255.98	0.197	Cheongsong	NU5	0.60	174.13	421.19	0.329
Yeongchun	HU1	0.63	160	683.49	0.370	Geochang1	NU6	0.63	193.82	623.36	0.329
Samok Bridge	HU2	0.55	190	758.28	0.412	Geochang2	NU7	0.53	195.79	518.41	0.307
Yeongwol1	HU3	0.62	195	612.62	0.303	Jisan	NU8	0.83	227.11	605.19	0.344
Dalcheon	HU4	0.87	70	318.24	0.251	Donggok2	NU9	0.72	204.61	437.35	0.393
Maeil	HU5	0.73	188	481.82	0.275	Gohyeon	NU10	0.55	223.64	426.08	0.386
Bukcheon	HU6					Daeri	NU11	0.62	223.29	638.6	0.431
Naerincheon	HU7					Changchon	NU12	0.87	52.29	523.46	0.254
Wontong	HU8					Sancheong	NU13	0.73	87.13	547.21	0.252
Seonsan	ND1	0.79	31.67	276.37	0.192	Taesu	NU14	0.56	80.02	620.38	0.295
Dongchon	ND2	0.88	23.23	231.83	0.176	Imcheon	NU15	0.58	123.68	673.9	0.308
Gumi	ND3	0.81	18.92	319.94	0.195	Oesong	NU16	0.41	52.51	531.95	0.258
Nakdong	ND4	0.79	29.94	333.98	0.198	Hoedeok	GD1	0.99	31.03	181.43	0.179
Waegwan	ND5	0.82	15.49	317.32	0.195	Gongju	GD2	0.97	6.86	234.09	0.142
Ilseon bridge	ND6	0.80	24.62	331.77	0.199	Hapgang	GD3	1.00	13.44	136.56	0.192
Jindong	ND7	0.88	0.02	301.7	0.158	Useong	GD4	0.81	15.28	209.92	0.310
Jeongam	ND8	0.77	0.2	349.09	0.183	Guryong	GD5	1.03	6.19	172.45	0.271
Hyangseok	ND9	0.76	52.48	314.54	0.189	Okcheon	GU1	0.67	88.25	380.37	0.192
Dongmun	ND10	0.81	48.1	194.09	0.194	Cheongseong	GU2	0.78	92.35	266.99	0.183
Jeomchon	ND11	0.57	64.52	389.86	0.312	Hotan	GU3	0.77	113.87	426.72	0.209
Yonggok	ND12	0.95	39.09	216.48	0.151	CheonCheon	GU4	0.73	275.8	554.69	0.231

Name	Id	hypc1	LE	ME	HI
Hakgyo	YD1	1.18	1.32	82.86	0.140
Naju	YD2	1.04	0.2	146.67	0.124
Mareuk	YD3	1.02	4.42	141.23	0.116
Nampyeong	YD4	1.02	12.66	173.36	0.177
Seonam	YD5	0.91	9.82	170.84	0.199
Bongdeok	YU1	0.88	105.82	293.86	0.378
Jukgok	SD1	0.90	38.02	265.48	0.199
Gokseong	SD2	1.02	47.95	283.92	0.215
Gurye2	SD3	0.79	23.05	284.33	0.195
Yongseo	SD4	0.69	28.32	250.71	0.267
Gwanchon	SU1	0.59	202.2	402.7	0.213
Ssangchi2	SU2	0.43	218.8	361.46	0.267
Gyeombaek	SU3	0.54	113.67	231.55	0.177
Jangjeon2	SU4	0.53	107.84	316.51	0.194
Songjeon	SU5	0.60	108.15	295.29	0.250

*Watershed for HU6, HU7, HU9 include the North Korea region (No data)

- Parameters

Area: Watershed area (km^2)
P_point: Mean annual precipitation at gauging station (mm)
P_area: Area averaged mean annual precipitation (mm)
R_point: Point R-value at gauging station (10^7J/ha▪mm▪hr)
R_area: Area averaged R-value (10^7J/ha▪mm▪hr),
C010: Percentage of clay at effective soil depth 0~10cm (%)
SI010: Percentage of silt at effective soil depth 0~10cm (%)
SA010: Percentage of sand at effective soil depth 0~10cm (%)
R010: Percentage of rock at effective soil depth 0~10cm (%)
C1030: Percentage of clay at effective soil depth 10~30cm (%)
SI1030: Percentage of silt at effective soil depth 10~30cm (%)
SA1030: Percentage of sand at effective soil depth 10~30cm (%)
R1030: Percentage of rock at effective soil depth 10~30cm (%)
C3050: Percentage of clay at effective soil depth 30~50cm (%)
SI3050: Percentage of silt at effective soil depth 30~50cm (%)
SA3050: Percentage of sand at effective soil depth 30~50cm (%)
R3050: Percentage of rock at effective soil depth 30~50cm (%)
C050: Percentage of clay at effective soil depth 0~50cm (%)
SI050: Percentage of silt at effective soil depth 0~50cm (%)
SA050: Percentage of sand at effective soil depth 0~50cm (%)
R050: Percentage of rock at effective soil depth 0~50cm (%)
Urban: Percentage of urbanized area (%)
Agriculture: Percentage of agricultural land (%)
Forest: Percentage of forest (%)
Pasture: Percentage of pasture (%)
Wetland: Percentage of wetland (%)
Bare: Percentage of bare land (%)
Water: Percentage of Water (%)
WW: Percentage of wetland+water (%)
Total: Total stream length (km)
Main: Main stream length (km)
Tri: Tributary length (km)
SO1: Strahler's stream order from KRF
SO2: Shreve's stream order from KRF
SO3: Strahler's stream order from delineated stream
DD: Drainage density (km/km^2)
SF: Shape factor,
AXL: Axial length
LF: Length factor
A* and A*: Ratio considering reservoirs area versus specific degradation (details in APPENDIX C)
Avgslp: watershed average slope
hyp1: Relative height at the mid relative area
hyp2: elevation at the mid relative area

hyp3: Slope between 0.2 and 0.8 of the relative area
hypc1:Slope of the logarithmic hypsometric curve
LE: Low elevation
ME: Mean elevation
HI Hypsometric index (details in APPENDIX C)

APPENDIX C.

Process for Watershed Characteristics from GIS Analysis

C1.Linear Aspects of Watershed Morphometry

In a watershed, the water is the main agent for sediment delivery from upland to a single outlet. Concentrated of water creates the stream network and watershed delineation with GIS analysis express stream network as a line. From the 5m by 5m resolution DEM, the watershed delineation process was conducted to define the watershed for all gauging stations and reservoirs and then stream network in each watershed was delineated. However, it is difficult to figure out the stream network exactly by GIS, because drawing the stream networks depends on the subjective judgment (Tarboton et al., 1991). Natural streams could change from the condition of precipitation and other related characteristics. This dissertation used the Korean Reach File (KRF) version 3 provided by the Ministry of Environments (ME) for the stream network. Additional stream network was generated from 5m by 5m resolution DEM which has a similar shape to KRF, but it had more tributaries in the same watershed (*Figure C-1*). Assigning a numeric order to streams is beginning of the analysis. The classic stream order system is based on Gravelius stream order (Gravelius, 1914). And then Horton (1945) suggested Horton's law as downstream ordering system and it was subsequently modified and developed by various researchers (Shreve, 1967; Strahler, 1952). The most popular Strahler's stream order system fixed the ambiguity of Hortons by removing upstream extensions of the highest ordering system. Shreve's ordering system assigns 1 to every source stream and a sum of tributary's magnitude is order of downstream at bifurcation. The results from 3 methods of Socheon station (NU1) are demonstrated in *Figure C-1*. Horton's stream order is not used in this dissertation since it is difficult to separate upstream and downstream.

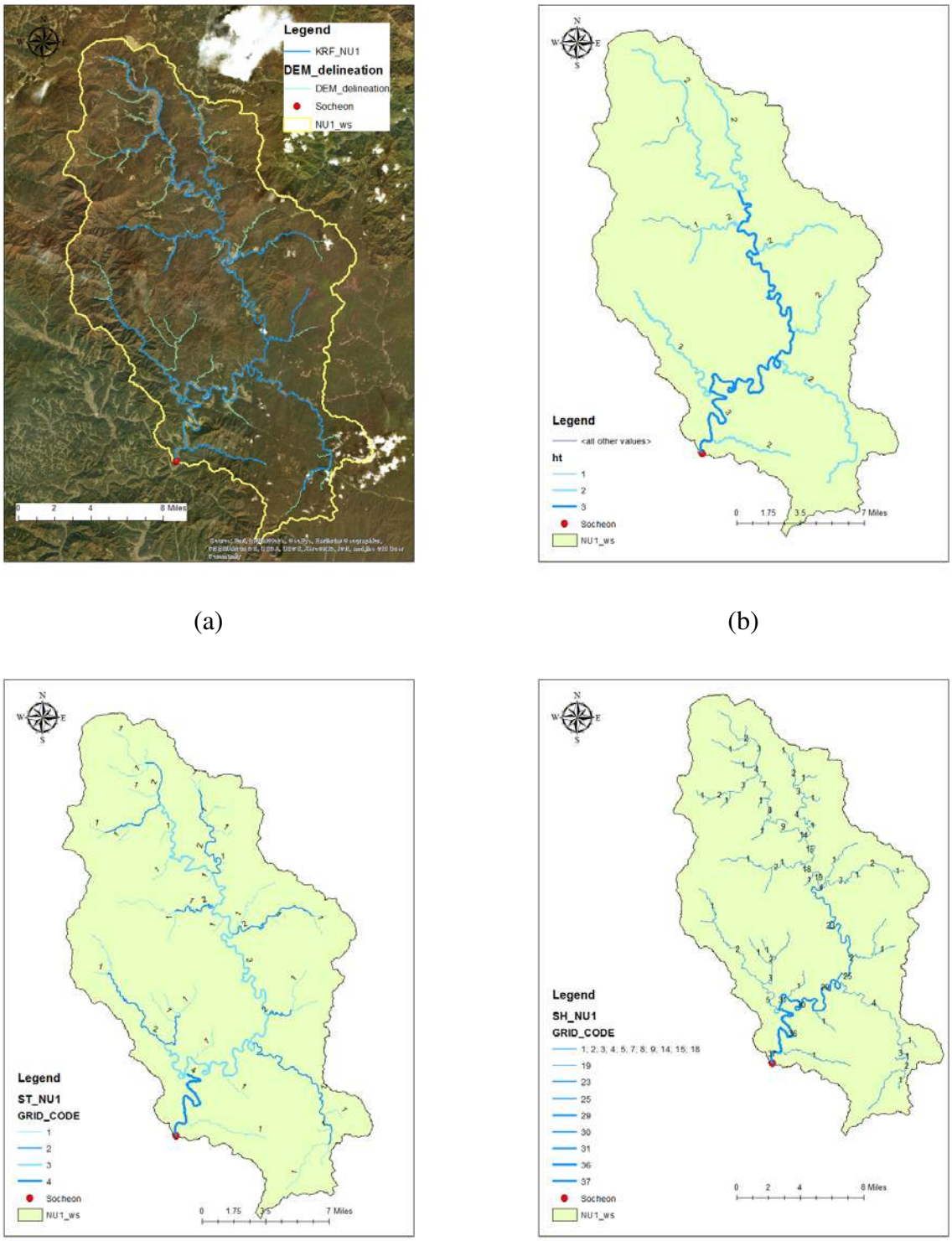

Figure C-1. Stream order of Socheon station (NU1); (a) difference between KRF and delineated stream from DEM, (b) KRF's stream order from Strahler's method, (c) Delineated stream order from Strahler's method, and (d) Delineated stream order from Shreve's method

C2. Areal Aspects of Watershed Morphometry

The areal aspect includes common 2-dimensional characteristics, such as watershed area (A, Area), drainage density (DD), and length factor. The watershed area is directly related to a size of storm events, so that it has an inverse relationship with characteristics related to run off and discharge per unit area. The area for each watershed is estimated with common watershed delineation process with 5m by 5m resolution DEM. Drainage density is the ratio of the total stream length within a basin to basin area with an inverse of length dimension (Horton, 1945). In this paper, the drainage density is calculated with KRF stream and the delineated watershed area from DEM [km /km^2]. High drainage density means the runoff discharge could be high at outlet, so it could have the possibility to have much sedimentation but it does not consider other factors impacting runoff (e.g. vegetation and geology). Additionally, the shape of the basin is considered, because it is another parameter representing the discharge from runoff in the outlet. Length factor (LF) and shape factor (SF) are considered as watershed shape characteristics, and they are calculated with A/ L_b^2 and L_b^2/A respectively. The length of watershed (L_b) could be estimated with various methods. (Horton, 1932). In this dissertation, two methods are used to estimate the basin length. In *Figure C-2,* the mainstream length (blue), and axial length (red) are used, because the mainstream length can well represent travel time and sinuosity of channel and the boundary axial length more focuses on the watershed shape (AXL). The mainstream length is used for shape factor and boundary length is applied to length factor. In case of NU1, mainstream length is 85.93Km, boundary length is 47.39km and the delineated watershed area is 697.1km^2, so that the calculated shape factor is 10.59 and length factor is 0.31.

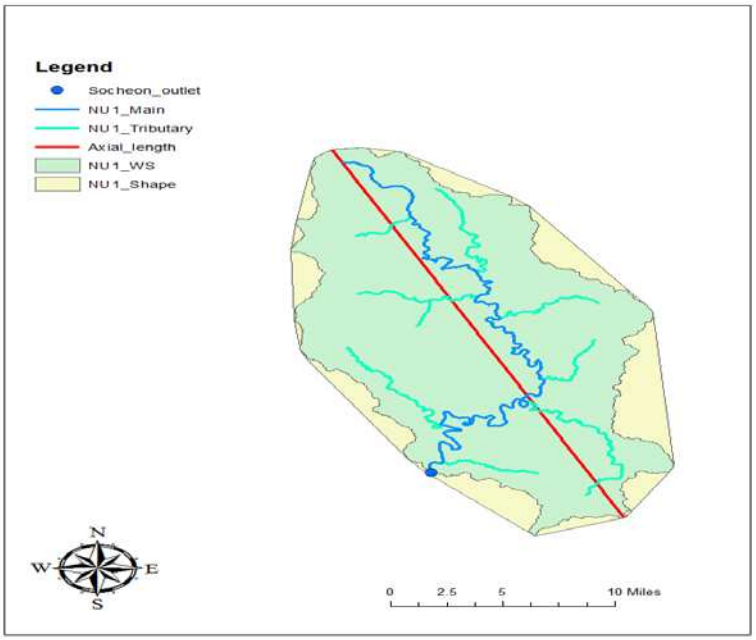

Figure C-2. Two basin lengths of Socheon (NU1) watershed

Additionally, two ratios considering reservoir area were applied because sedimentation deposition occurs in the reservoir, and they are represented as A* and A**, respectively

$$A^{*} = \frac{Reservoir\ catchment\ area\ [Km^2]}{watershed\ area\ [Km^2]} \qquad \text{Eqn C-0-1}$$

$$A^{**} = \frac{(Watershed\ area - Reservoir\ catchment\ area)\ [Km^2]}{watershed\ area\ [Km^2]} \qquad \text{Eqn C-0-2}$$

Unfortunately, there is no information about all reservoirs (i.e. agricultural reservoirs) in South Korea. In this paper, reservoirs from main dams except agricultural reservoirs are considered. Therefore, ratios of some watersheds are 0 or 1 for each parameter. The simple equations are used to represent reservoir effects on sedimentation.

C3. Relief Aspects of Watershed Morphometry

The 3-dimensional variables introduced as relief aspects to consider elevation differences. It is expected that relief factor is most important variables to explain the different SD due to different location. Commonly, mean elevation (ME) and watershed average slope (Sl, Avg_slope) have been used to express the difference between mountain-valley and alluvial plain. In this dissertation, the hypsometric curve is used for relief aspect. The hypsometric analysis is the distribution of surface area with respect to elevation. It has been generally used for calculation of hydrologic information because the basin hypsometry is related to flood response and soil erosion and sedimentation process (Langbein, 1947; Strahler, 1952). The hypsometric curve can figure out the hypsometric analysis, and commonly it expressed with the normalized cumulative area and normalized height from the outlet of the watershed outlet. Common index for the hypsometric curve is the integral value of hypsometric curve (Strahler, 1952), and simple mathematical equation often used to express hypsometric analysis expressed as below (Wood & Snell, 1960; Pike & Wilson, 1971).

$$HI = \frac{E_{mean} - E_{min}}{E_{max} - E_{min}} \qquad \text{Eqn C-3}$$

where E is the elevation.

In this paper, the 5m resolution of DEM is reclassified with every 100m in each watershed, and the result is normalized to make the hypsometric curve. The created hypsometric curves for every watershed are in *Figure C-3*.

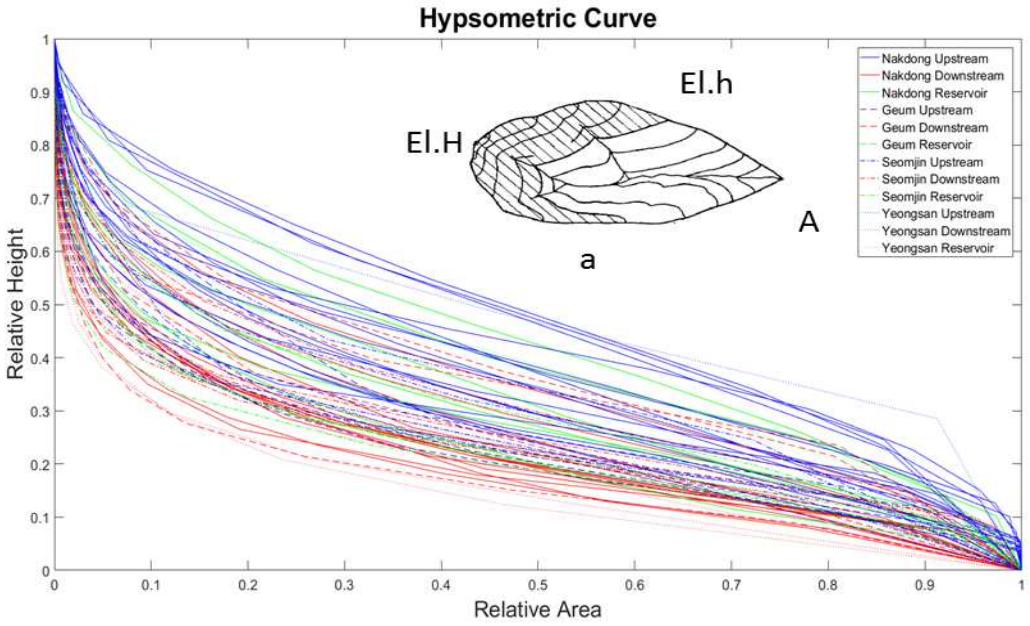

Figure C-3. The hypsometric curve for all watersheds

Based on Davies concept "the cycle of erosion" (1899), geographical features of South Korea is in old and mature age. The results also indicated the most watersheds have the same characteristics. From the hypsometric curve, the dominant geomorphic processes in a watershed could be approximately determined. In old stage with a convex curve, most of the watershed area in low elevation, and channelized, fluvial and alluvial processes occur, whereas the hillslope process is dominant in youth stage with a concave curve. The hypsometric curve is created for all watersheds and obvious different curves are created between upstream and downstream. Three values are exported from hypsometric curve: (1) Relative height at the mid relative area (hyp1); (2) Elevation at the mid relative area (hyp2); and (3) Slope between 0.2 and 0.8 of the relative area (hyp3). In *Figure C-3*, the generated hypsometric curve is expressed as below equation (Strahler, 1952)

$$\frac{h}{H} = \left[\left(\frac{d-x}{x}\right)\left(\frac{a}{d-a}\right)\right]^{z} \qquad \text{Eqn C-2}$$

where, a is the fitted to measurements, while d=1, and a < d

z is the exponent (z > 0).

The horizontal x-axis is the relative area ranging from 0 to d, and z is estimated after the fitting curve to equation *C-2*. This equation is similar to the equation of relative concentration with reference elevation as derived by Rouse (1937). Therefore, a similar conversion of suspended sediment concentration profile was conducted for hypsometric curve and slope of generated results is exported as an additional relief aspect (hypc). The relationships between the specific degradation and existing parameters related to relief aspect are shown in *Figure C-4*

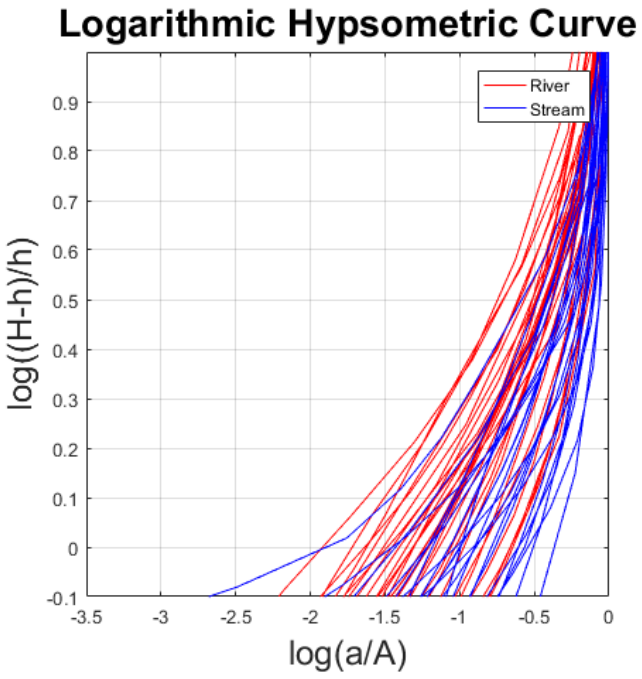

Figure C-4. Logarithmic Hypsometric Curve

.

C4. Mean Annual Precipitation and R factor in RUSLE

Precipitation is the main agent of erosion and sedimentation process. It directly impacts on soil detachment with raindrop hit and delivers the sediment to downstream after changing as runoff. From the 60 points of daily precipitation data from the Korea Meteorological Administration (KMA), the mean annual precipitation (mm) is calculated. To estimate the precipitation in the watershed, the Kriging method applied with 60-point mean annual precipitation value by 30m resolution (*Figure C-5*). Kriging is the geostatistical procedure to predict a value for the unmeasured region from the measured value. It assumes that the distance between sample points has a spatial correlation and it can use to explain variation. Original kriging which is the most general kriging method with the assumption of unknown constant mean value and spherical model is applied to predict mean annual precipitation in watershed (ArcGIS, 2016). From the raster result of kriging, two values of mean annual precipitation are exported. One is the point value of mean annual precipitation at gauging station (P, P_point); another is averaged mean annual precipitation value from watershed area (P_area). The rainfall erosivity (R-factor) for the same 60 points are calculated with Eqn 5-1 and original kriging is also applied for estimation of gross erosion. The point value of R-factor at gauging station (P, R_point); another is averaged R-factor from watershed area (R_area) are exported for regression parameters.

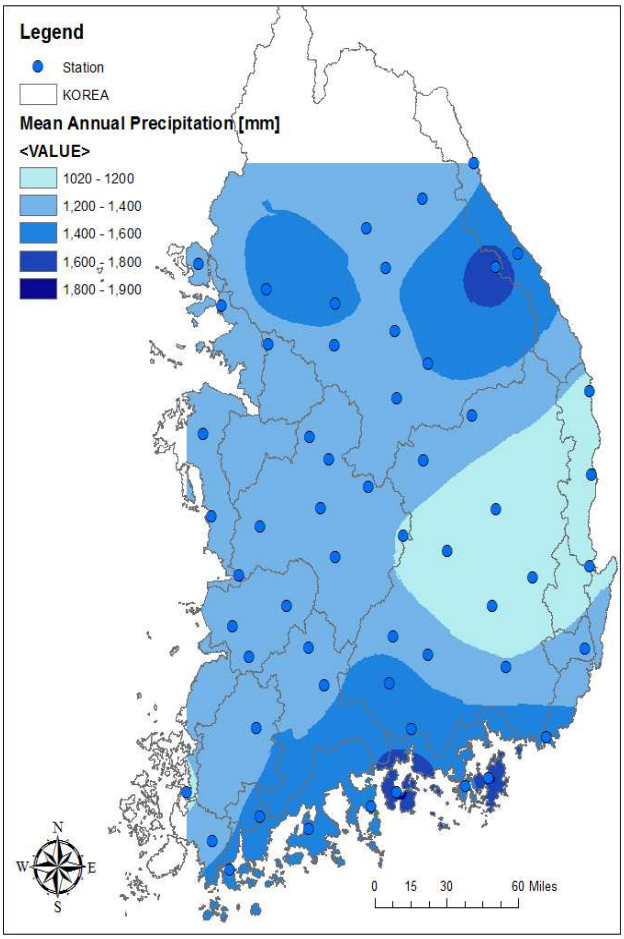

Figure C-5. Kriging result from 60-point mean annual precipitation value

C5. Soil Type and K, L and S-factor

Soil type has influenced on soil erosion and sedimentation process. To estimate the percentage of soil type and K factor, the detailed soil map from National Institute of Agriculture Sciences is used. The detailed soil map has information about 390 soil series. The specific information of the percentage of soil and rock is exported from soil database from SWAT-K developed from the Korea Institute of Construction Technology. The example of NU1, it has 133 soil series in the watershed (*Figure C-6*). The SWAT-K includes the percentage of soil and rock

and soil is classified into clay, silt, sand and rock by a radius of particles from sieve analysis: (1) clay ($d_{clay} \leq 0.002mm$); (2) silt ($0.002 < d_{silt} \leq 0.05mm$); (3) sand ($0.05 < d_{sand} \leq 2mm$); and (4) rock ($2mm < d_{rock}$). Each soil series has a different percentage of soil and rock in different effective depth. With the assumption of homogeneous soil in each layer, the percentage of soil is calculated in 5 classified effective soil depths: (1) 0~10cm; (2) 10~30cm; (3) 30~50cm; (4) 0~30cm; and (5) 0~50cm. The calculation of the percentage of soil for "Gacheon" in Socheon station is detailed below. The first layer has the same effective soil depth with classified depth so that the percentage of soil is directly exported from the SWAT-K.

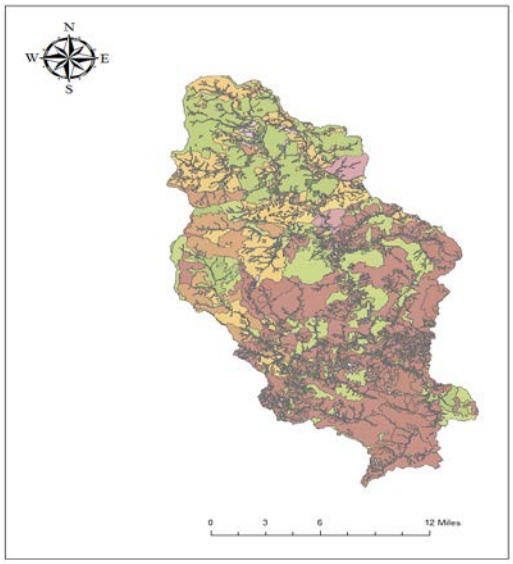

(a)

Gacheon properties					
Layer	Depth [cm]	Clay [%]	Silt [%]	Sand [%]	Rock [%]
1	10	5.5	24.5	70	3.8
2	25	11.2	34.6	54.2	12.5
3	50	18.7	45.3	36	15
4	90	21.5	314	47.1	15.8

(b)

Figure C-6. (a) Detailed soil map for Socheon station (NU1), and (b) percentage of soil and rock for Gacheon in Socheon station

In case of soil depth from 10~30cm, the percentage of clay is calculated as

$$\%\ clay\ (10\sim30cm) = \left(11.2\% \times \frac{15cm}{20cm} + 18.7\% \times \frac{5cm}{20cm}\right) = 13.08\% \qquad \text{Eqn C-3}$$

The summation of the percentage of clay, silt, and sand is 100% and rock has an independent percentage, therefore the result is recalculated with consideration of the percentage of rock. To

be specific, the total percentage of soil change as 96.2% in the first layer. The final result is estimated by area weighted average method. In case of Gacheon, it is only 1.47% of total watershed area. The result of percentage of clay (dark blue), silt (blue), sand (green), and rock (yellow) in 5 classified effective soil depths for 70 watersheds are in *Figure C-7*. The percentage of rock in stream watershed is higher than one of in downstream, but it is hard to find other distinct differences between upstream and downstream.

C6. Land USE and C & P factor

Land use and soil type have influenced on soil erosion and sedimentation process. The land cover raster (10m resolution) from the ME and detailed soil map (vector) from the National Institute of Agriculture Sciences are used for analysis. In terms of land use, the land cover raster classified 23 types of land cover and they are simplified as 7 types: (1) Urban; (2) Agriculture; (3) forest; (4) wetland; (5) pasture; (6) bare land; and (7) water. After conversion from raster to vector, the area and percentage of each land use is estimated. The most watershed area is mountain region, on the other hand, the watersheds for downstream have a large portion of urbanized and agricultural land (*Figure* C-8) than watersheds in upstream.

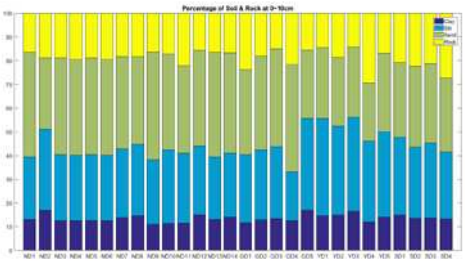

(a) 0~10cm

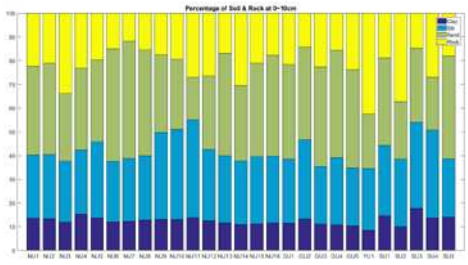

(f) 0~10cm

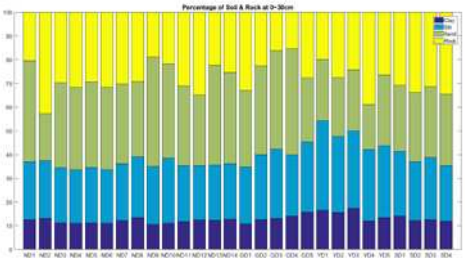

(b) 10~30cm

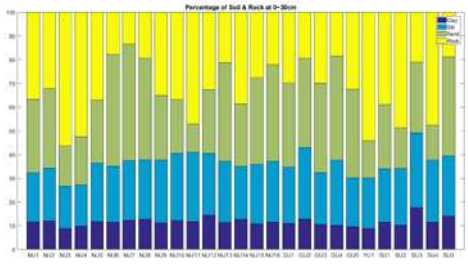

(g) 10~30cm

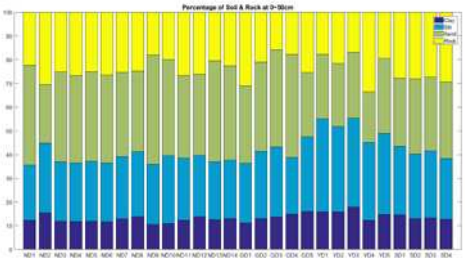

(c) 30 ~50cm

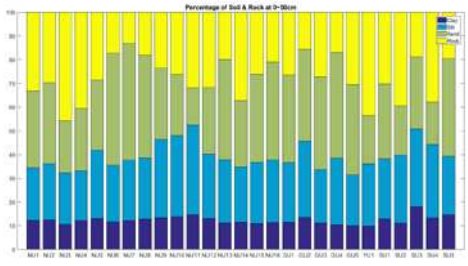

(h) 30 ~50cm

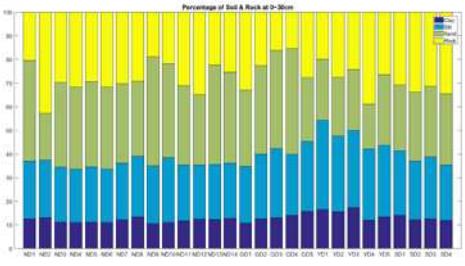

(d) 0~30cm

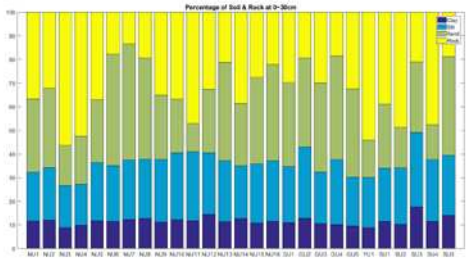

(i) 0~30cm

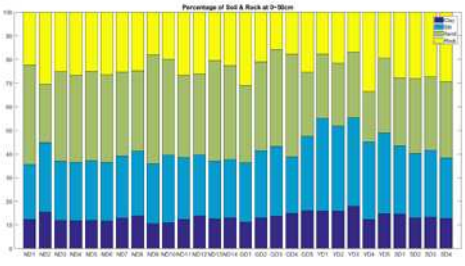

(e) 0~50cm

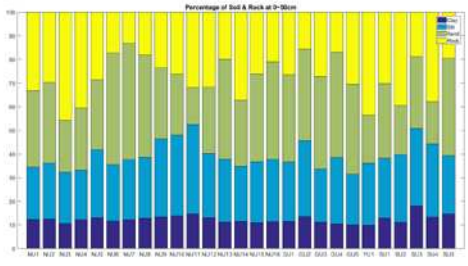

(j) 0~50cm

Figure C-7. Percentage of soil and rock for a watershed in downstream (a ~ e) and upstream (f ~ j) in each effective soil depth.

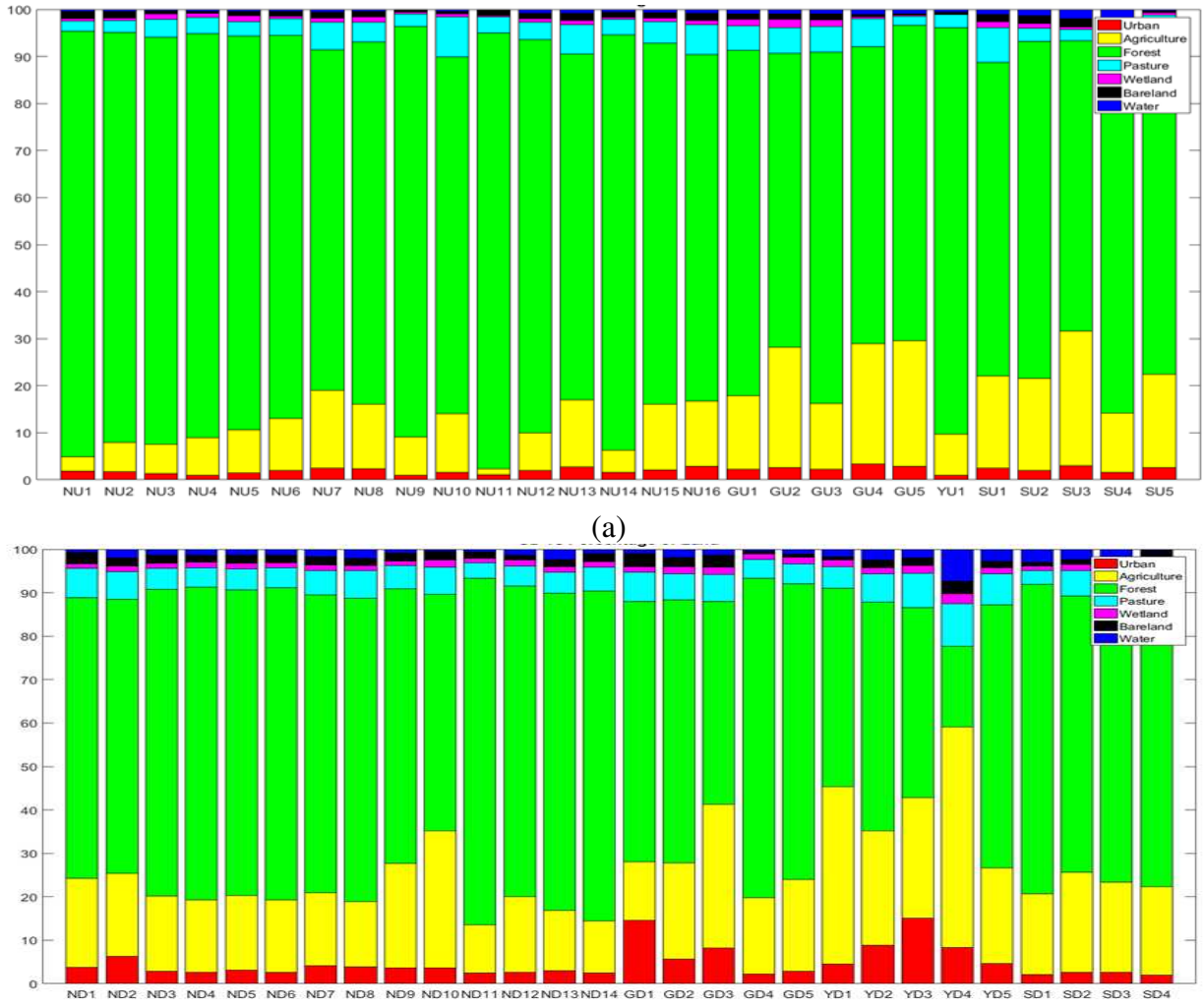

Figure C-8. Land use percentage of a watershed for gauging stations (a) upstream and (b) downstream

APPENDIX D. Flow Duration and Sediment Rating Curve Results

H1 Yeoju

Daily Stage and Discharge

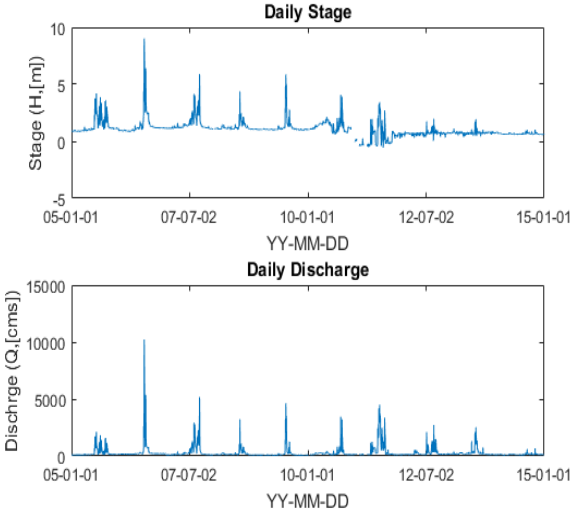

Sediment Rating Curve

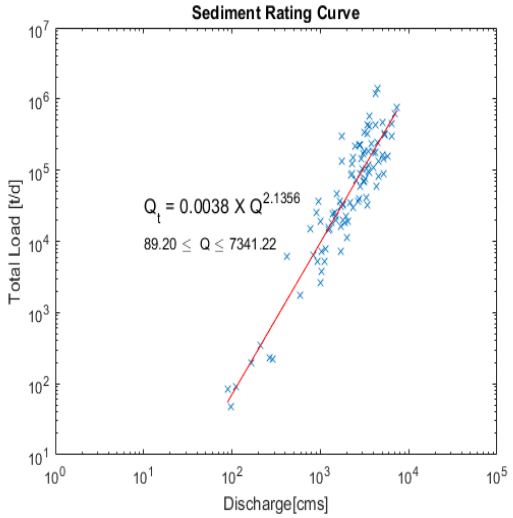

Flow Duration Curve

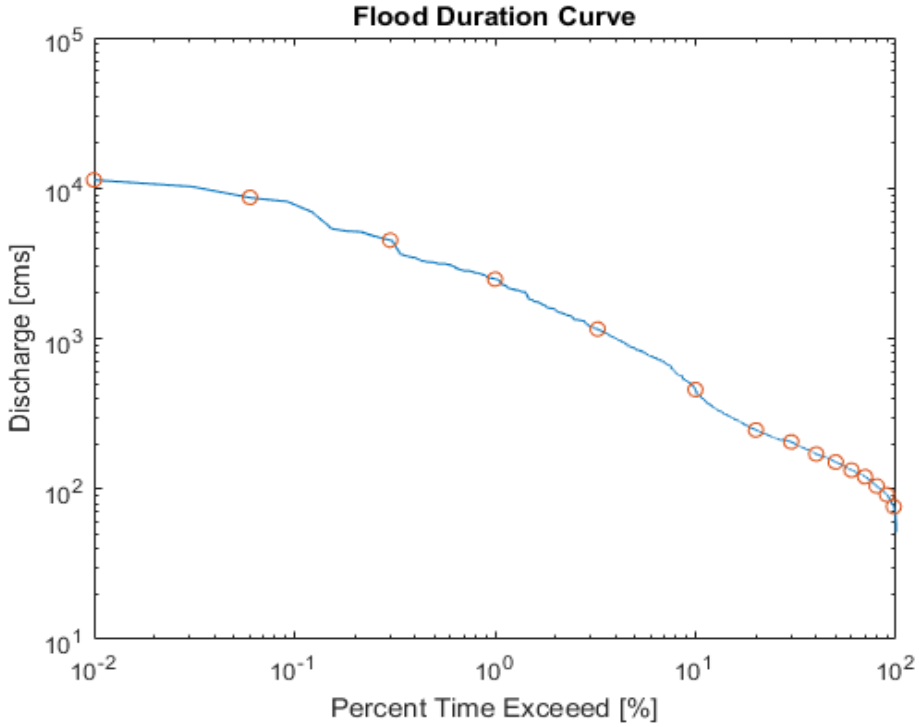

Specific Degradation

$$SD = 365 \times Q_s \left[\frac{tons}{day}\right] \div Area[km^2] = \frac{3546.85 \times 365}{11074} = 117.02 \frac{tons}{km^2 \cdot year}$$

Opinion

H2 Heungcheon

Daily Stage and Discharge

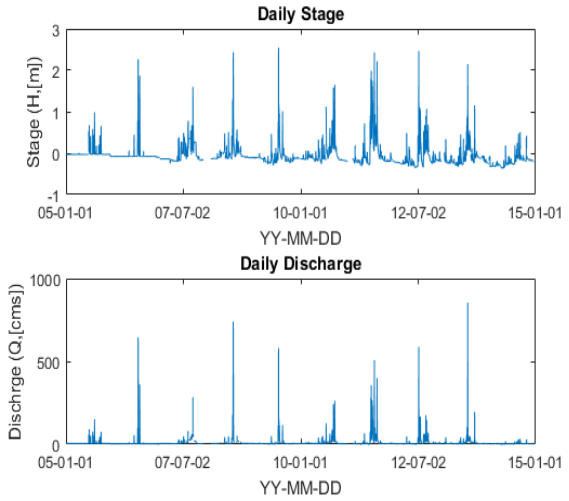

Sediment Rating Curve

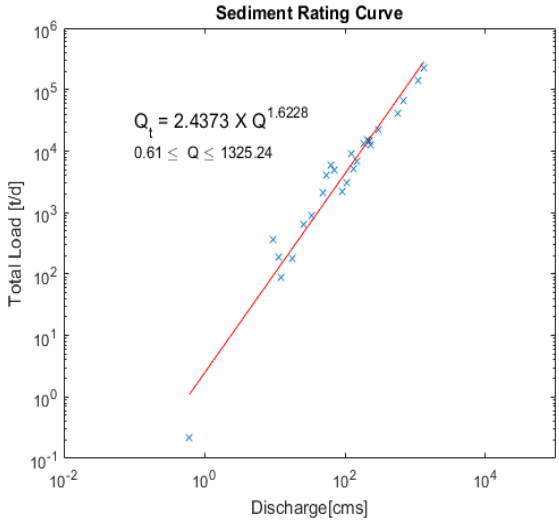

Flow Duration Curve

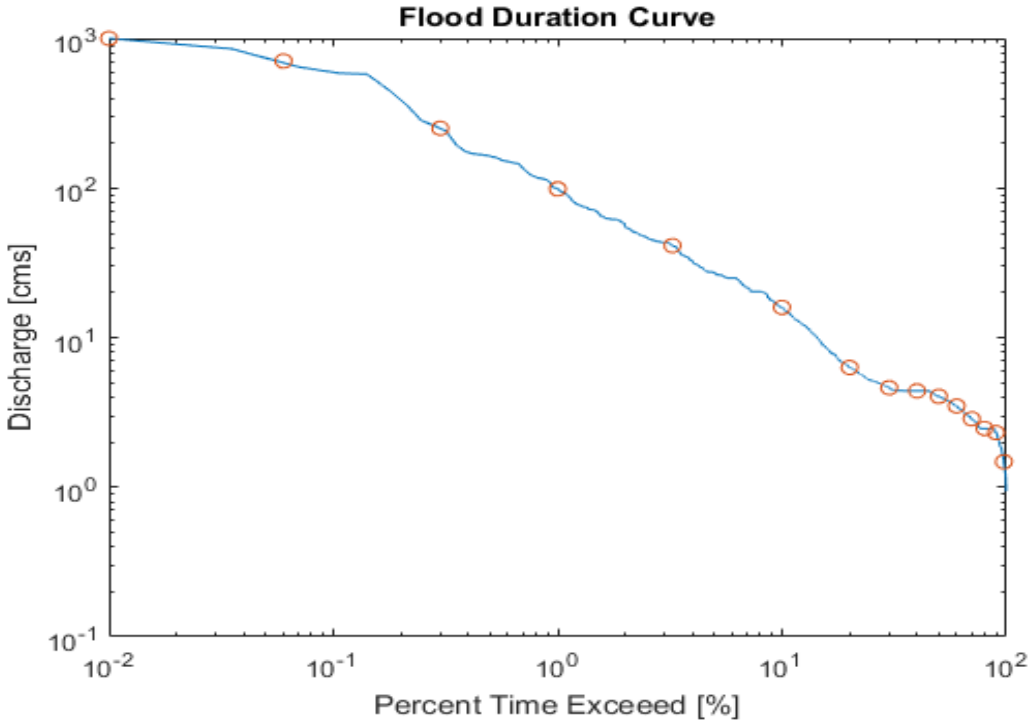

Specific Degradation

$$SD = 365 \times Q_s \left[\frac{tons}{day}\right] \div Area[km^2] = \frac{313.41 \times 365}{283.5} = 403.57 \frac{tons}{km^2 \cdot year}$$

Opinion

Relatively high SD from high discharge in small watershed area

H3 Munmak

Daily Stage and Discharge

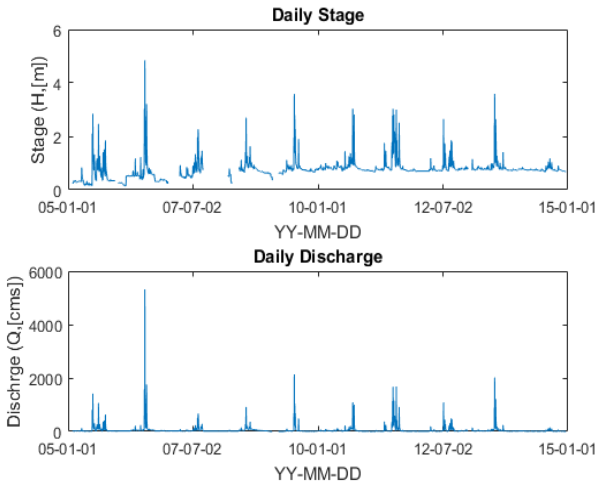

Sediment Rating Curve

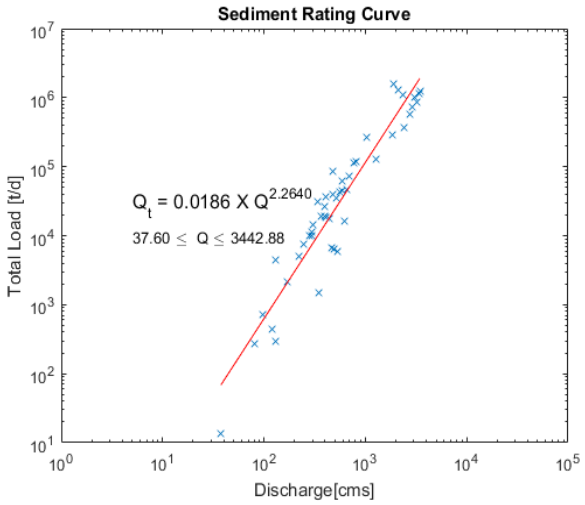

Flow Duration Curve

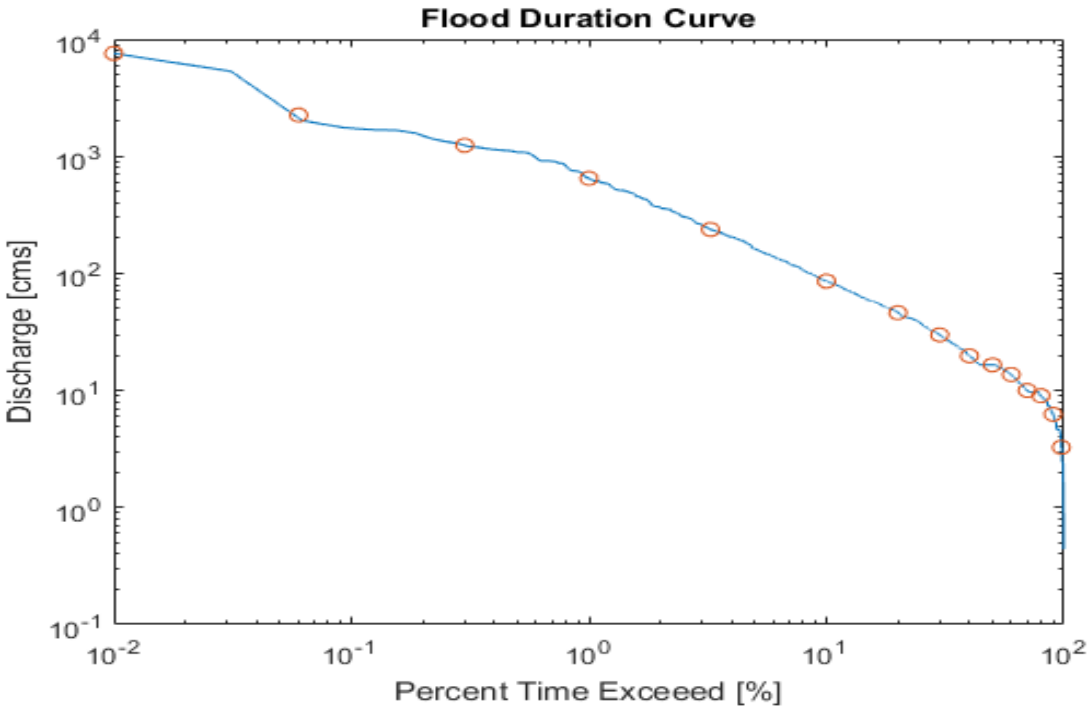

Specific Degradation

$$SD = 365 \times Q_s \left[\frac{tons}{day}\right] \div Area[km^2] = \frac{4228.72 \times 365}{1346} = 1147.8 \frac{tons}{km^2 \cdot year}$$

Opinion

Sediment measurement could not cover big flood event in 2007 (distortion could happen)

H4 Yulgeuk

Daily Stage and Discharge

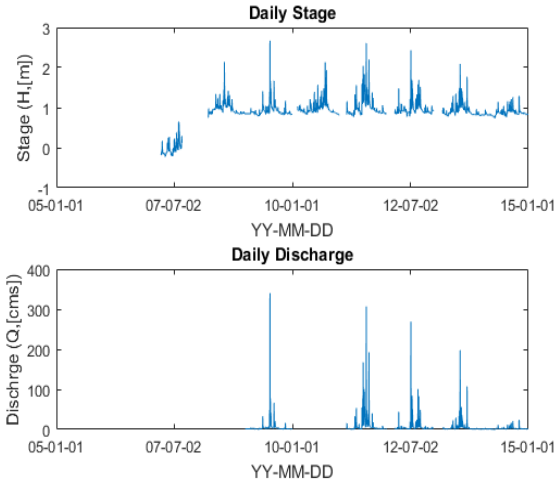

Sediment Rating Curve

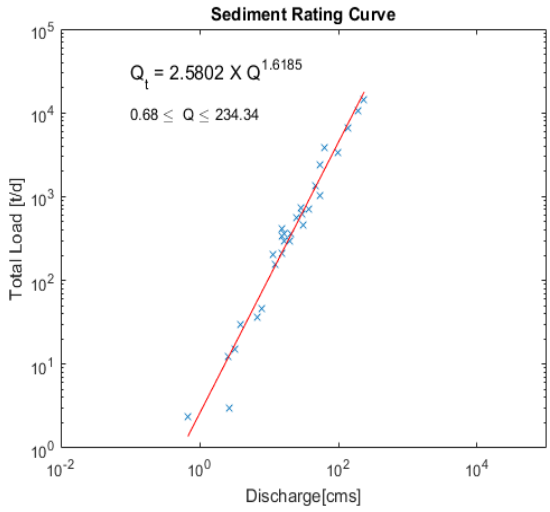

Flow Duration Curve

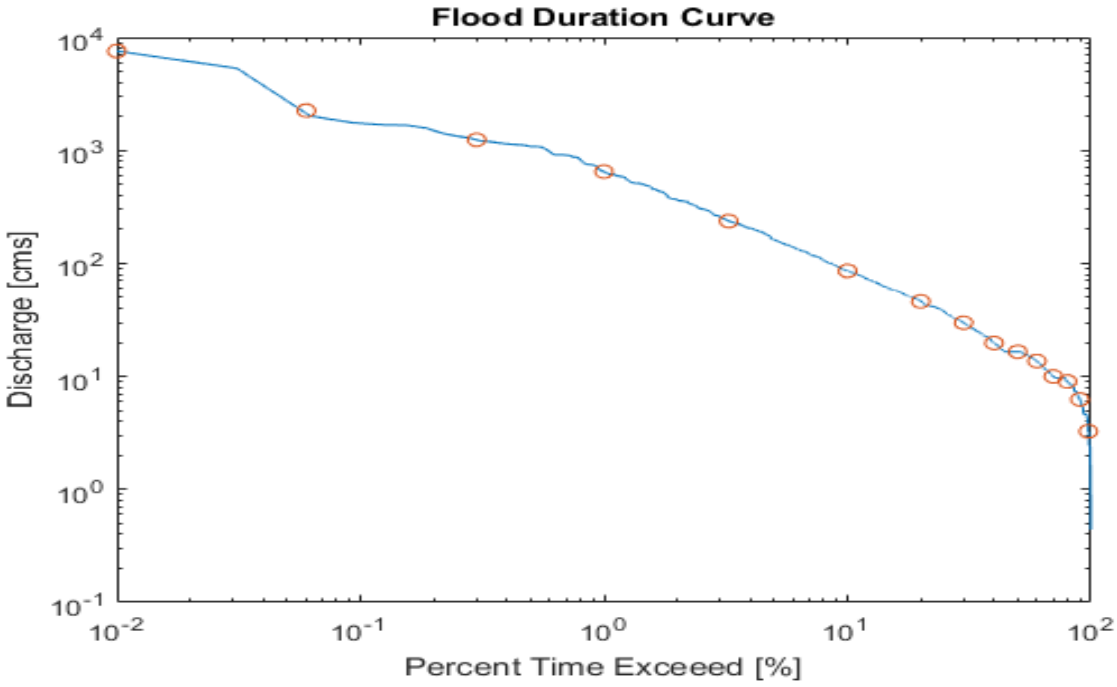

Specific Degradation

$$SD = 365 \times Q_s \left[\frac{tons}{day}\right] \div Area[km^2] = \frac{95.89 \times 365}{173} = 202.7 \frac{tons}{km^2 \cdot year}$$

Opinion

H5 Cheongmi

Daily Stage and Discharge

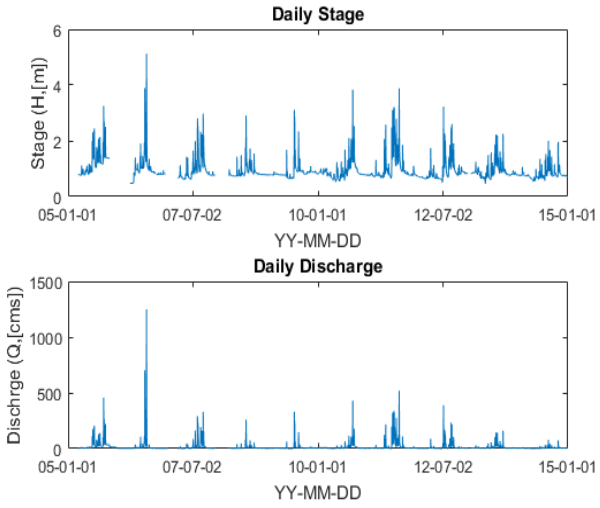

Sediment Rating Curve

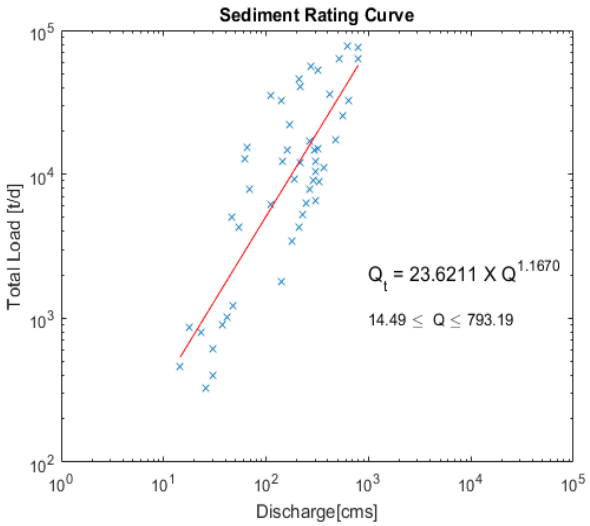

Flow Duration Curve

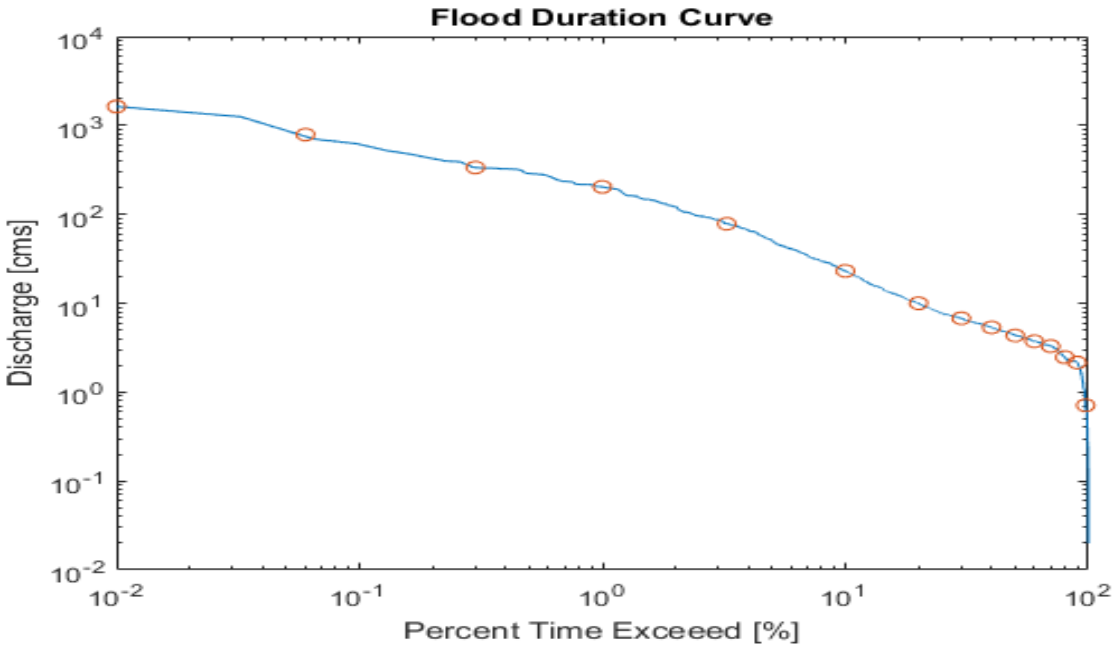

Specific Degradation

$$SD = 365 \times Q_s \left[\frac{tons}{day}\right] \div Area[km^2] = \frac{584.97 \times 365}{518.6} = 412.1 \frac{tons}{km^2 \cdot year}$$

Opinion

H6 Cheongmi

Daily Stage and Discharge

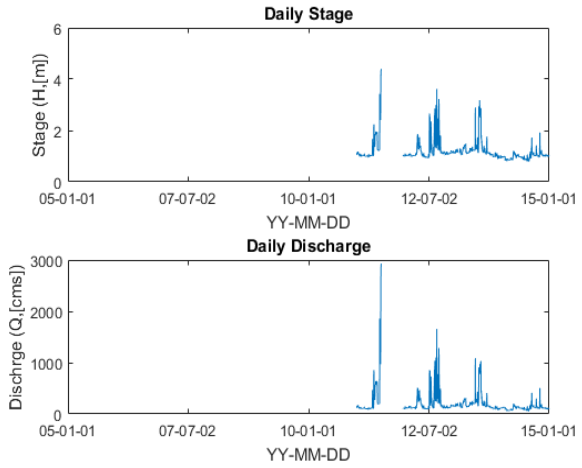

Sediment Rating Curve

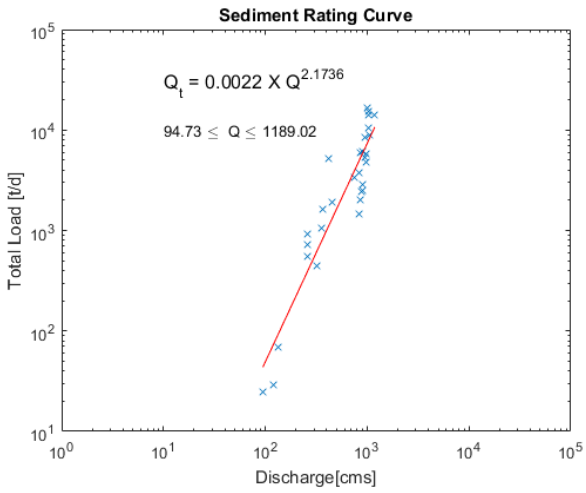

Flow Duration Curve

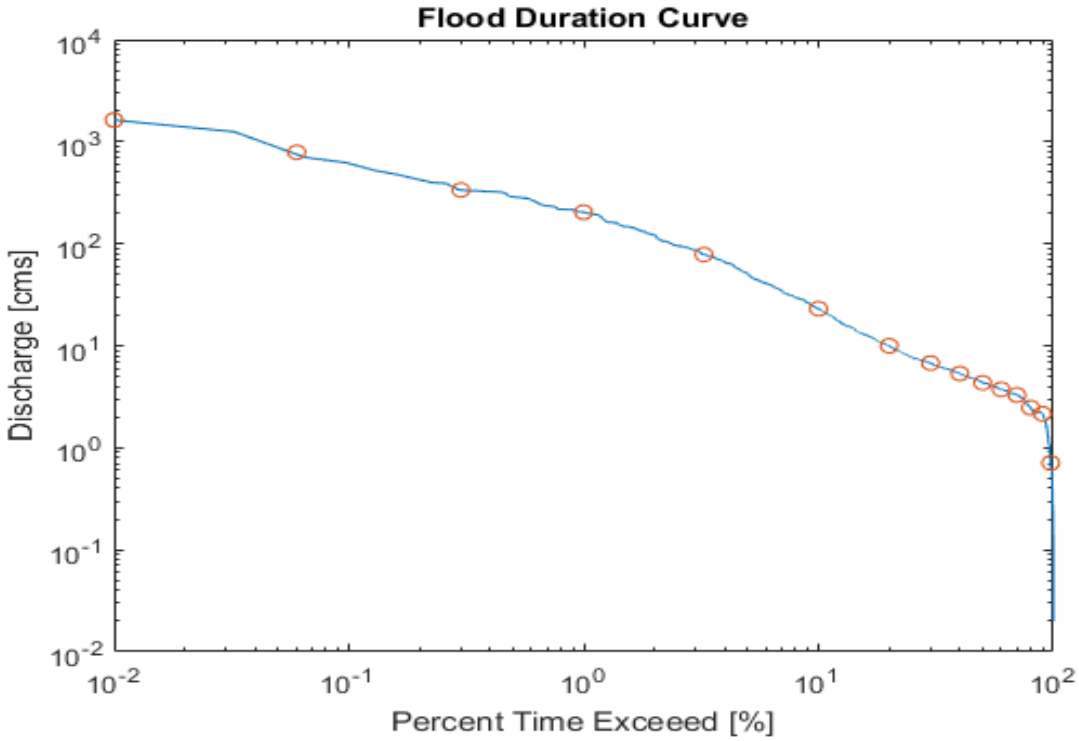

Specific Degradation

$$SD = 365 \times Q_s \left[\frac{tons}{day}\right] \div Area[km^2] = \frac{584.97 \times 365}{518.6} = 412.1 \frac{tons}{km^2 \cdot year}$$

Opinion

H7 Heukcheon bridge

Daily Stage and Discharge

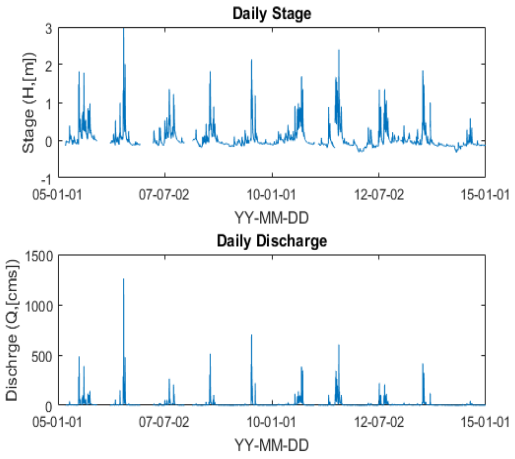

Sediment Rating Curve

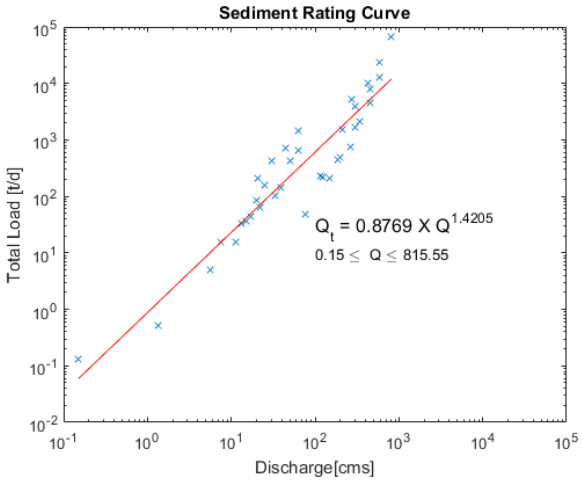

Flow Duration Curve

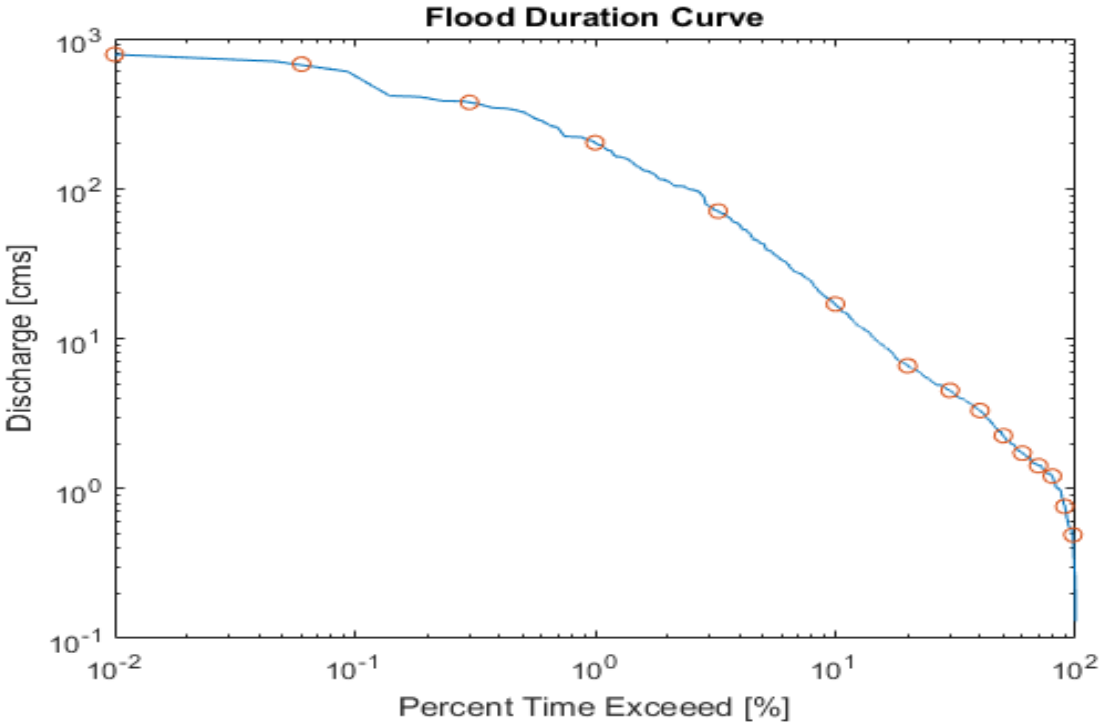

Specific Degradation

$$SD = 365 \times Q_s \left[\frac{tons}{day}\right] \div Area[km^2] = \frac{63.25 \times 365}{306.7} = 75.29 \frac{tons}{km^2 \cdot year}$$

Opinion

HU1 Yeongchun

Daily Stage and Discharge

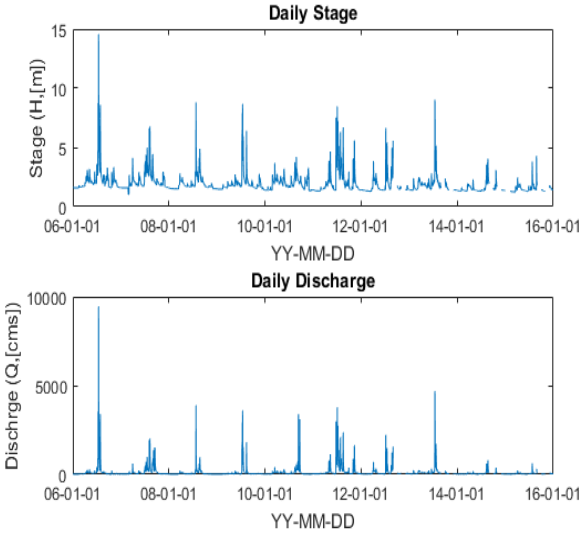

Sediment Rating Curve

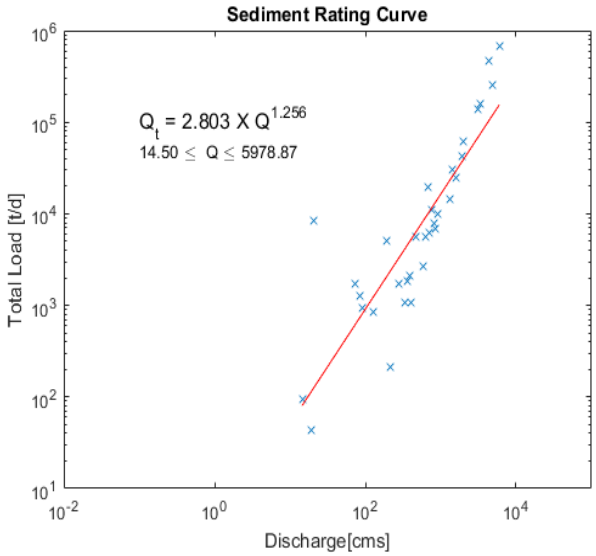

Flow Duration Curve

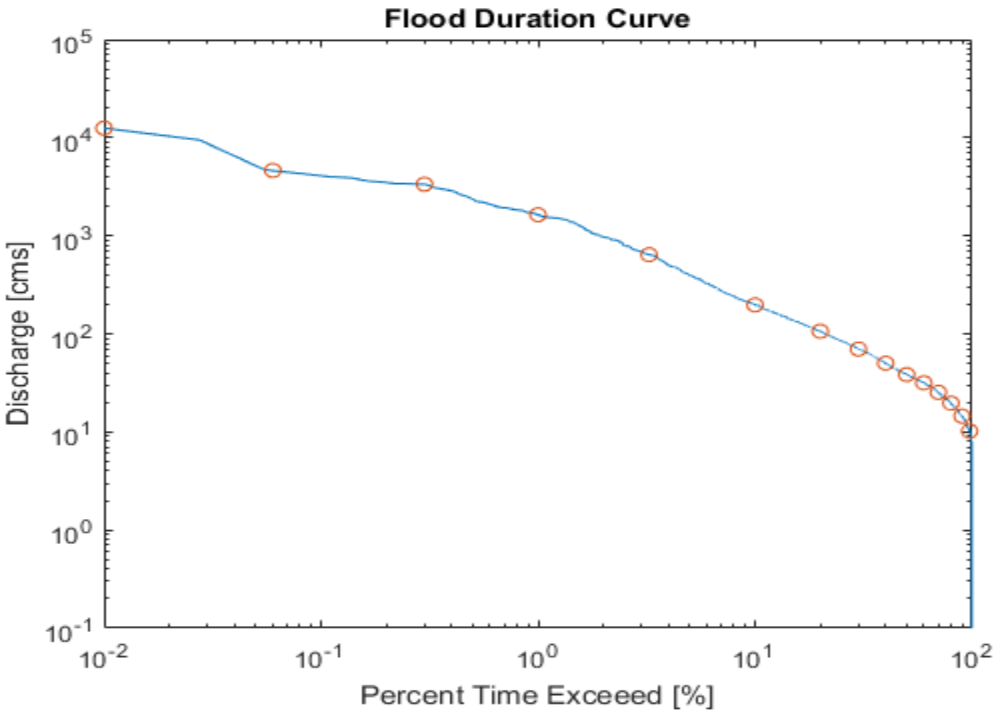

Specific Degradation

$$SD = 365 \times Q_s \left[\frac{tons}{day}\right] \div Area[km^2] = \frac{1626.01 \times 365}{4782} = 124.11 \frac{tons}{km^2 \cdot year}$$

Opinion

HU2 Samok Bridge

Daily Stage and Discharge

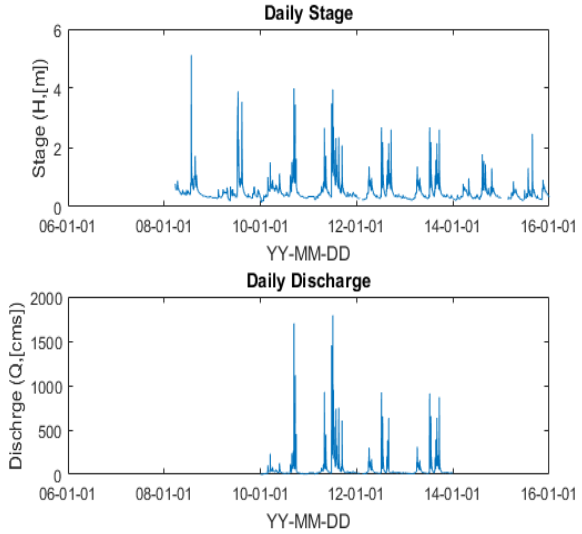

Sediment Rating Curve

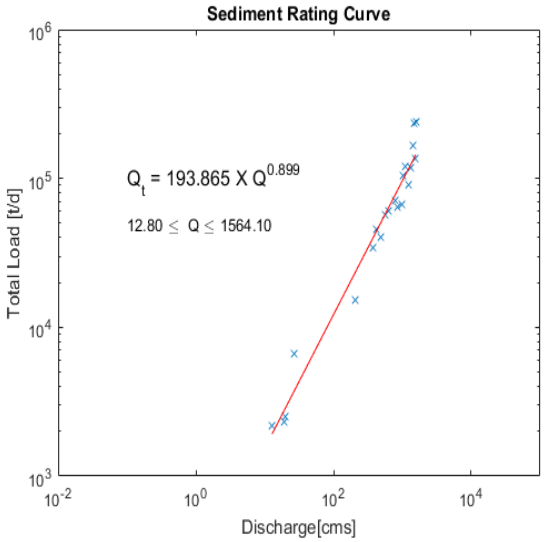

Flow Duration Curve

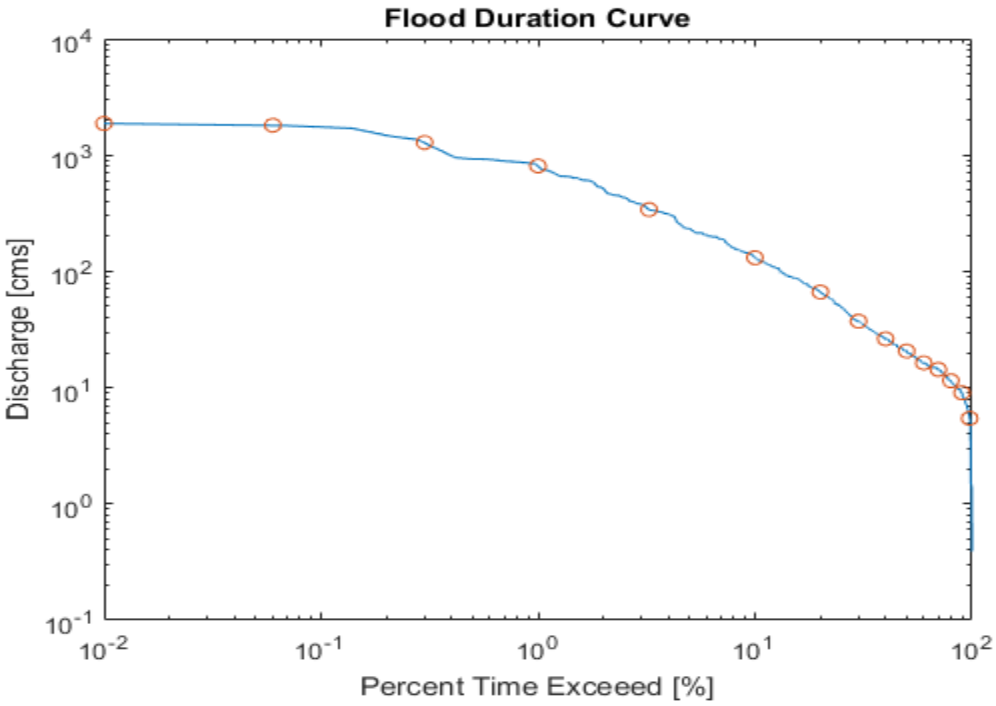

Specific Degradation

$$SD = 365 \times Q_s \left[\frac{tons}{day}\right] \div Area[km^2] = \frac{6654.76 \times 365}{2298} = 1057 \frac{tons}{km^2 \cdot year}$$

Opinion

SRC could be distorted due to small measurements

HU3 Yeongwol1

Daily Stage and Discharge

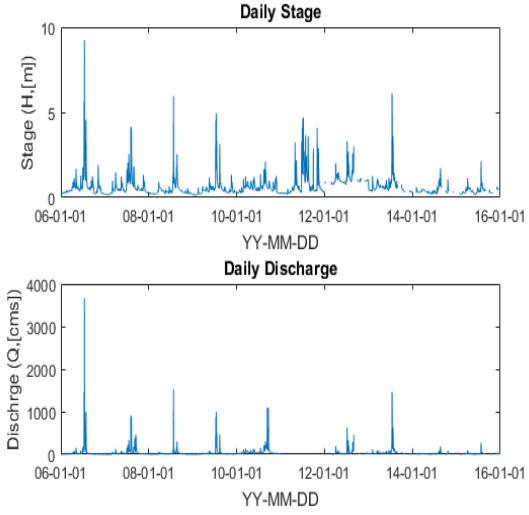

Sediment Rating Curve

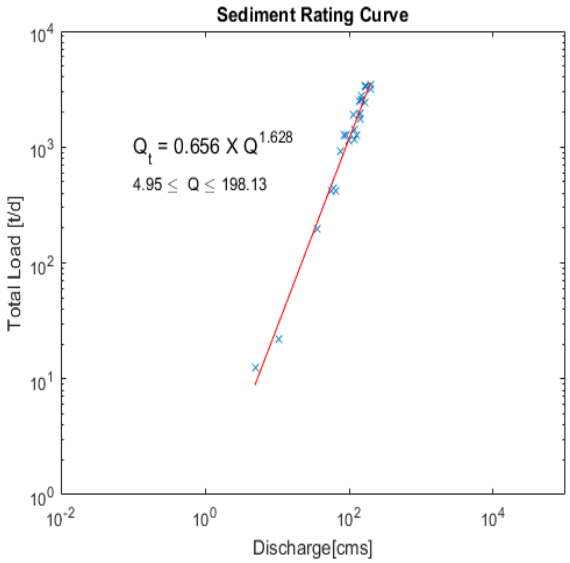

Flow Duration Curve

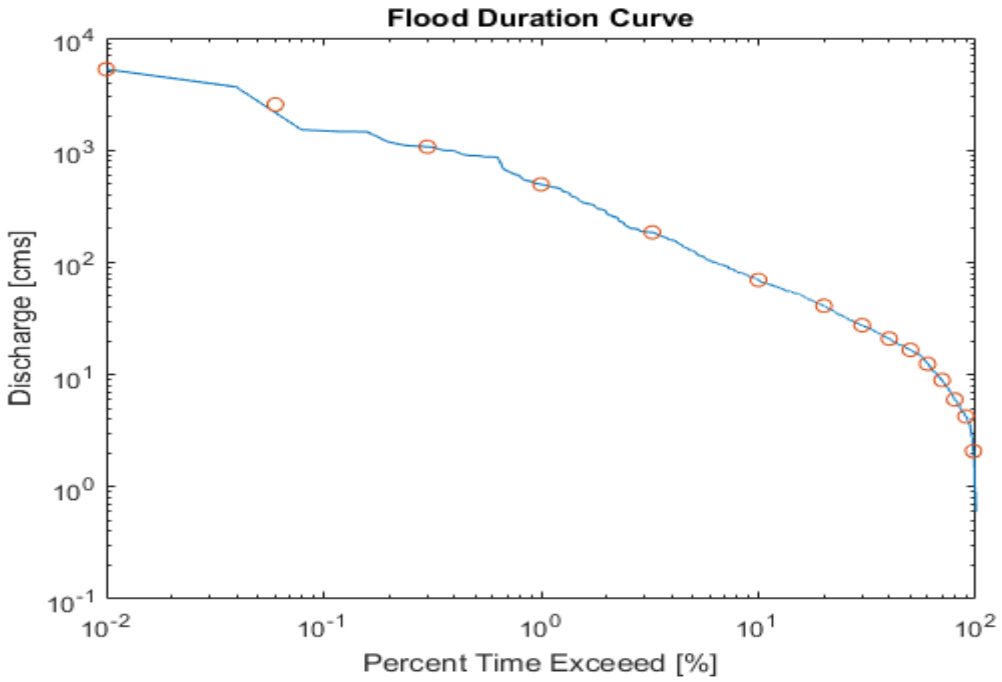

Specific Degradation

$$SD = 365 \times Q_s \left[\frac{tons}{day}\right] \div Area[km^2] = \frac{965.19 \times 365}{1615.8} = 213 \frac{tons}{km^2 \cdot year}$$

Opinion

HU4 Dalceon

Daily Stage and Discharge

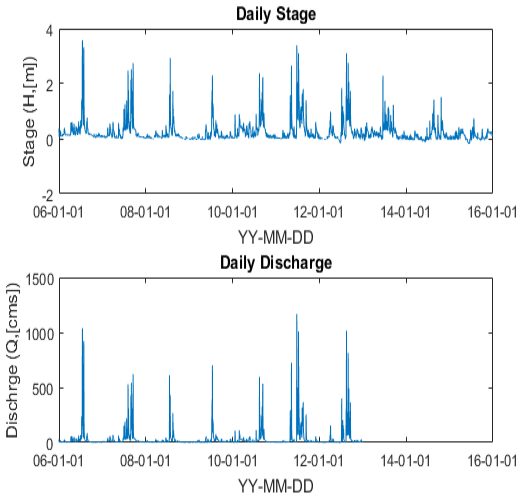

Sediment Rating Curve

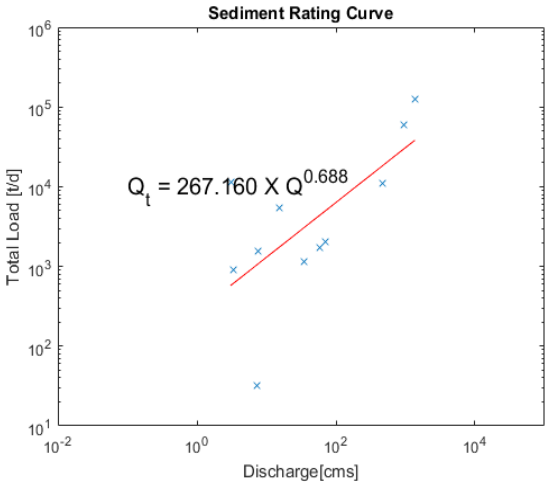

Flow Duration Curve

Specific Degradation

$$Q_t = 1.3646 \times Q^{1.3123} \quad (2011)$$

Opinion

Provided data is not matched with the K-water report

HU5 Maeil

Daily Stage and Discharge

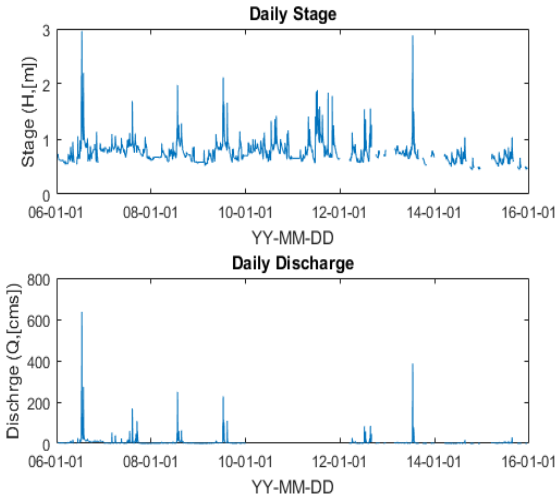

Sediment Rating Curve

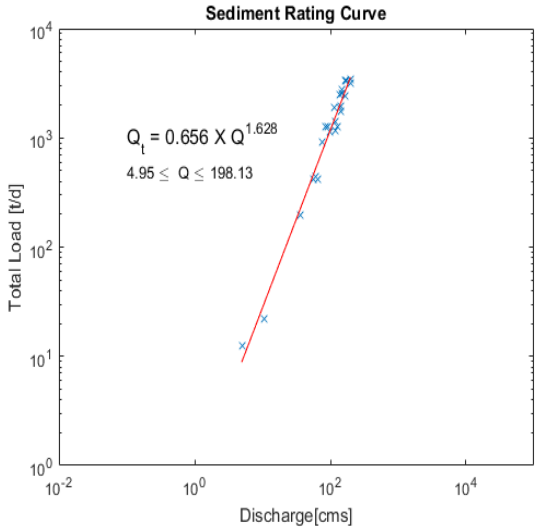

Flow Duration Curve

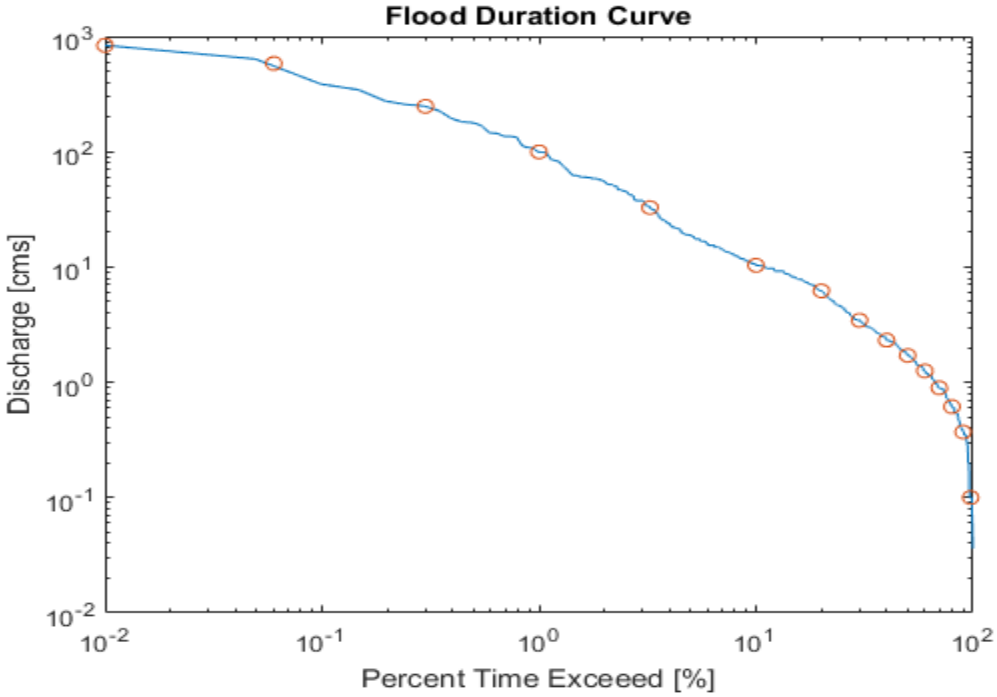

Specific Degradation

$$SD = 365 \times Q_s \left[\frac{tons}{day}\right] \div Area[km^2] = \frac{587.48 \times 365}{164} = 1307.54 \frac{tons}{km^2 \cdot year}$$

Opinion

Sediment measurement could not cover big flood event in 2007 (distortion could happen)

HU6 Bukcheon

Daily Stage and Discharge

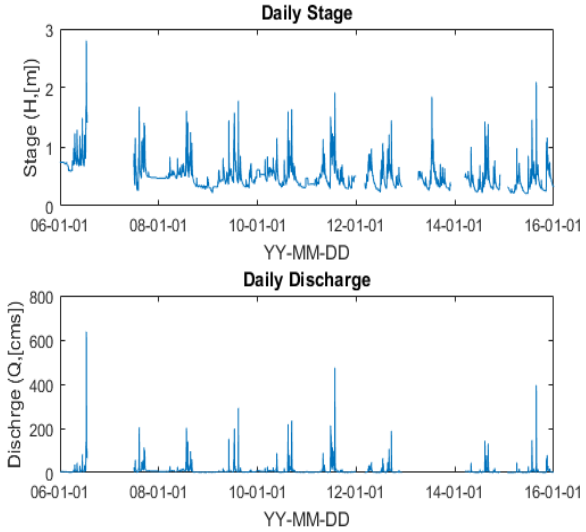

Sediment Rating Curve

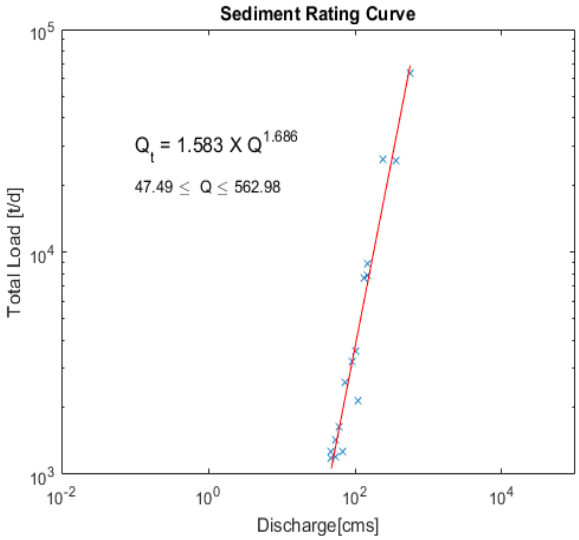

Flow Duration Curve

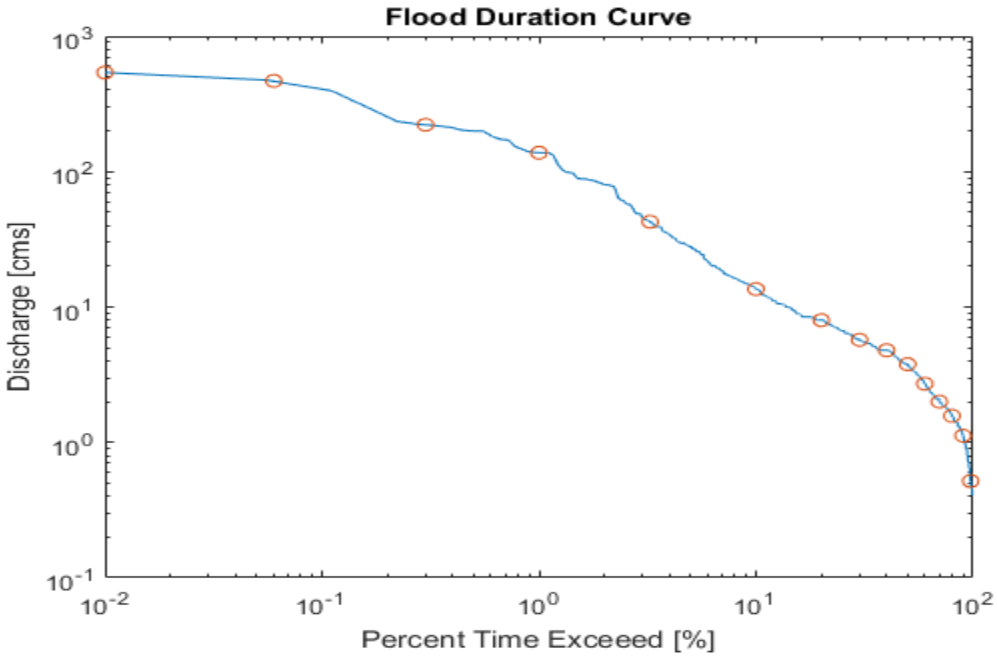

Specific Degradation

$$SD = 365 \times Q_s \left[\frac{tons}{day}\right] \div Area[km^2] = \frac{231.99 \times 365}{304.1} = 278.72 \frac{tons}{km^2 \cdot year}$$

Opinion

HU7 Naerincehon

Daily Stage and Discharge

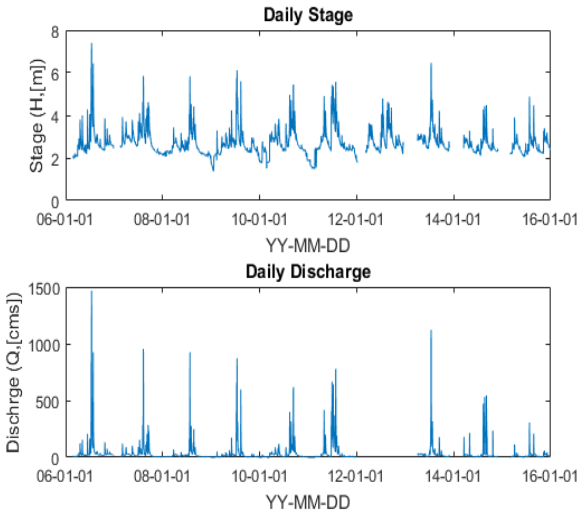

Sediment Rating Curve

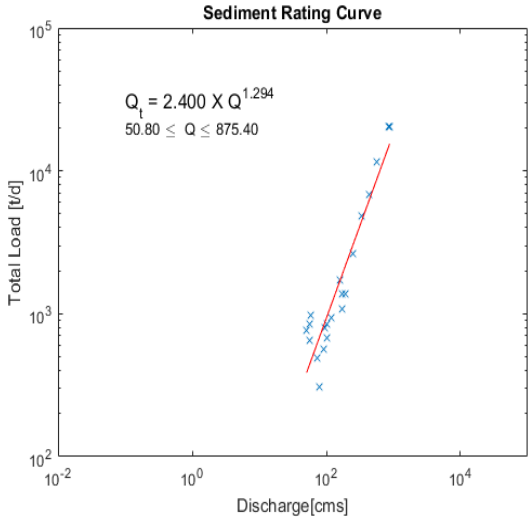

Flow Duration Curve

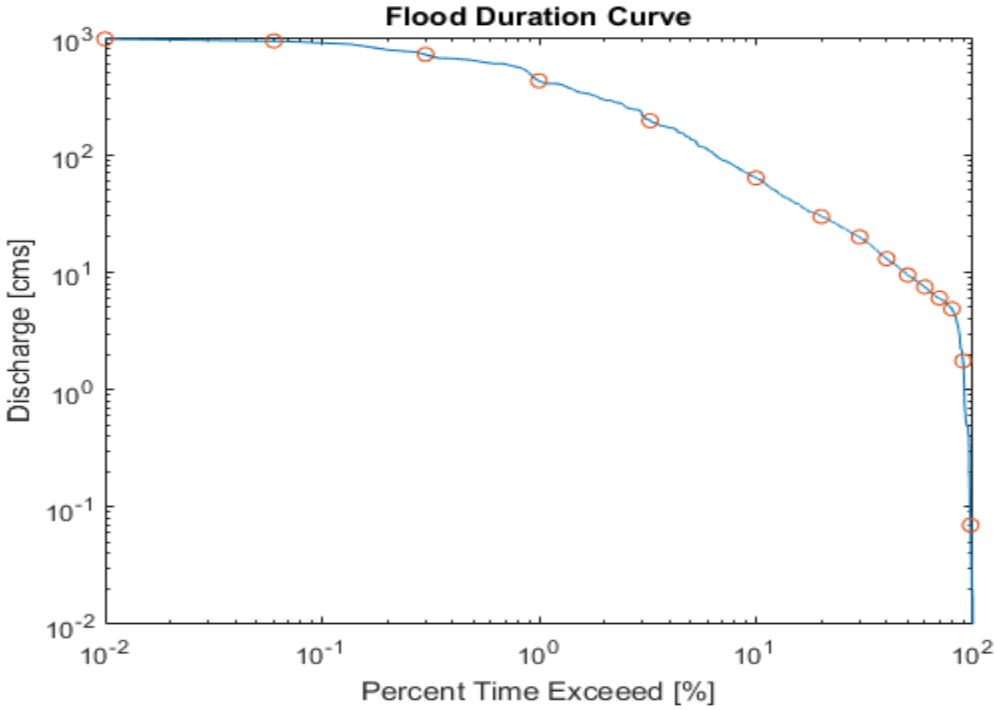

Specific Degradation

$$SD = 365 \times Q_s \left[\frac{tons}{day}\right] \div Area[km^2] = \frac{304.06 \times 365}{1039.1} = 106.9 \frac{tons}{km^2 \cdot year}$$

Opinion

HU8 Wontong

Daily Stage and Discharge

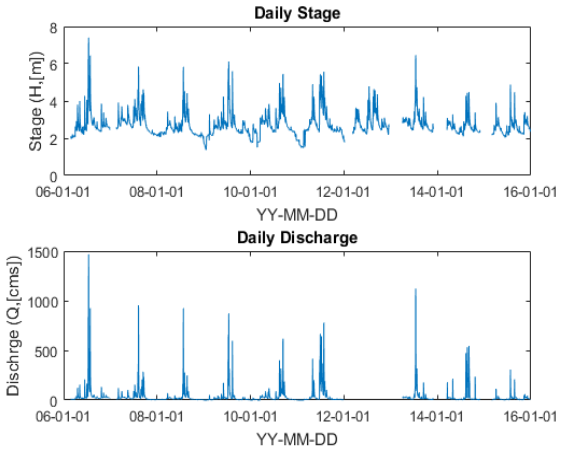

Sediment Rating Curve

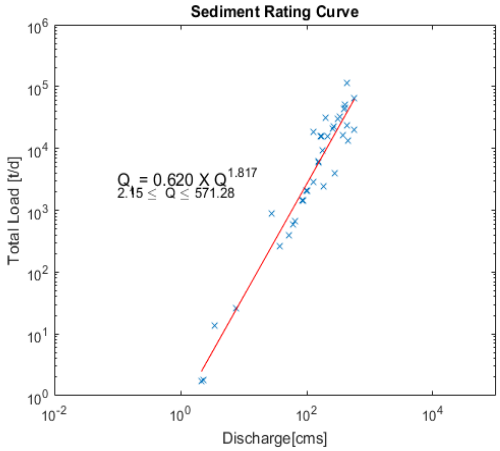

Flow Duration Curve

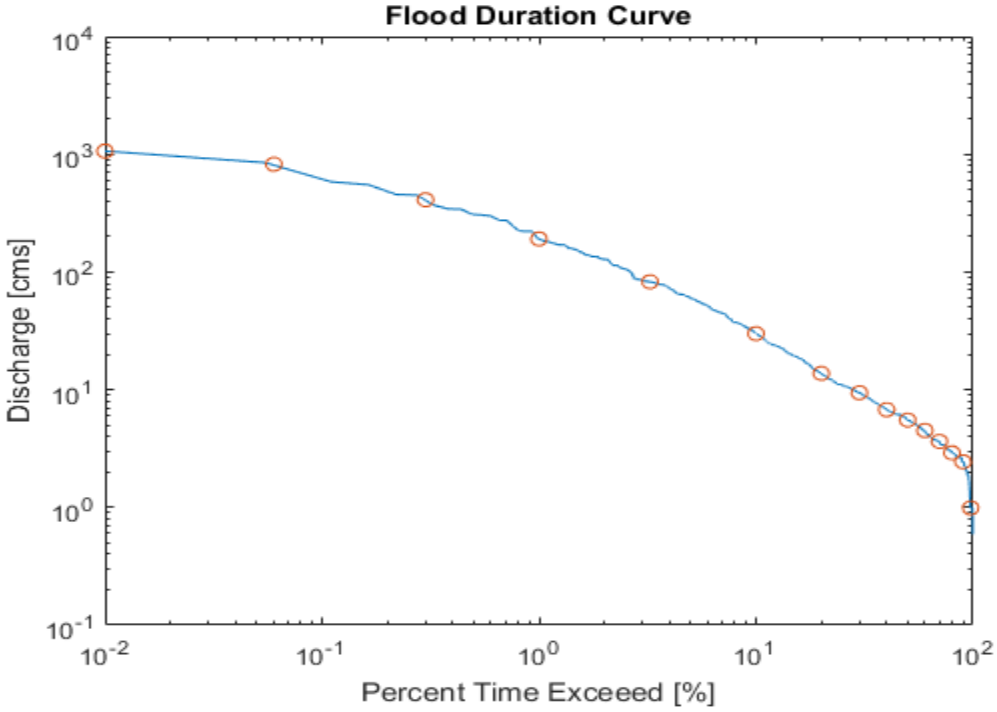

Specific Degradation

$$SD = 365 \times Q_s \left[\frac{tons}{day}\right] \div Area[km^2] = \frac{473.23 \times 365}{531} = 326.44 \frac{tons}{km^2 \cdot year}$$

Opinion

N1 Seonsan

Daily Stage and Discharge

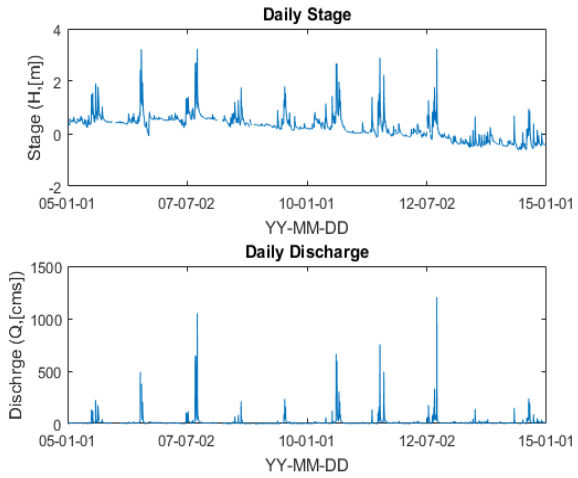

Sediment Rating Curve

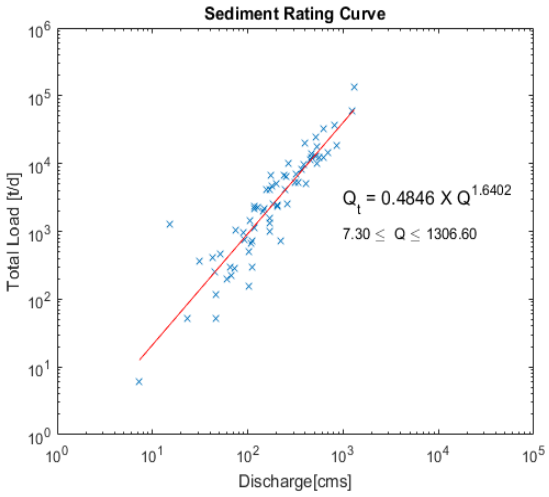

Flow Duration Curve

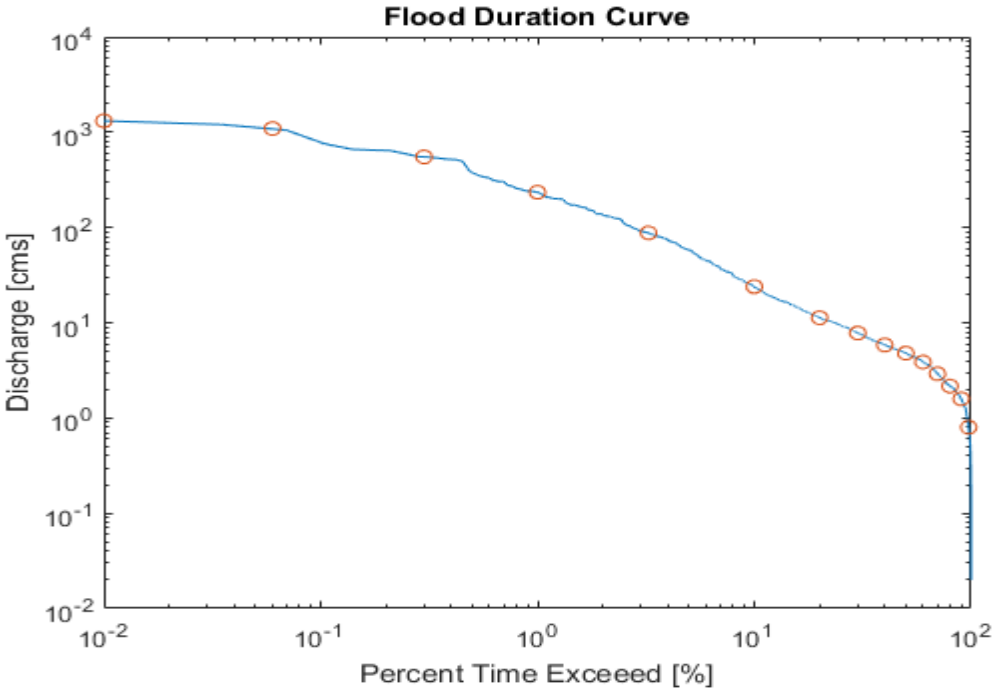

Specific Degradation

$$SD = 365 \times Q_s \left[\frac{tons}{day}\right] \div Area[km^2] = \frac{189.56 \times 365}{978.8} = 70.69 \frac{tons}{km^2 \cdot year}$$

Opinion

N2 Dongcheon

Daily Stage and Discharge

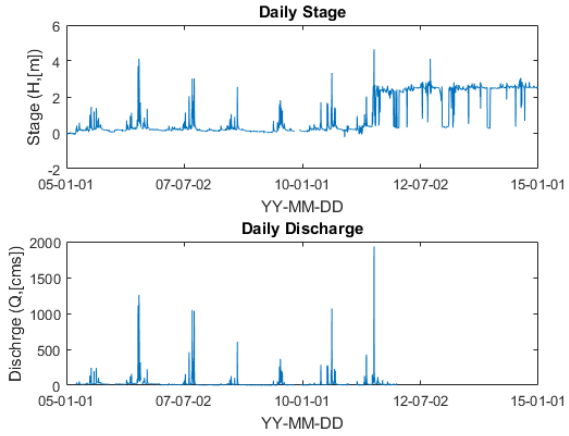

Sediment Rating Curve

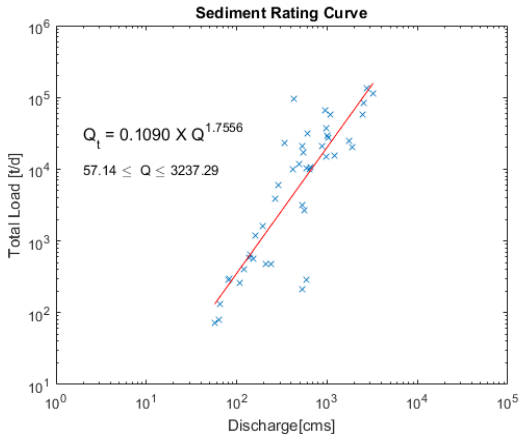

Flow Duration Curve

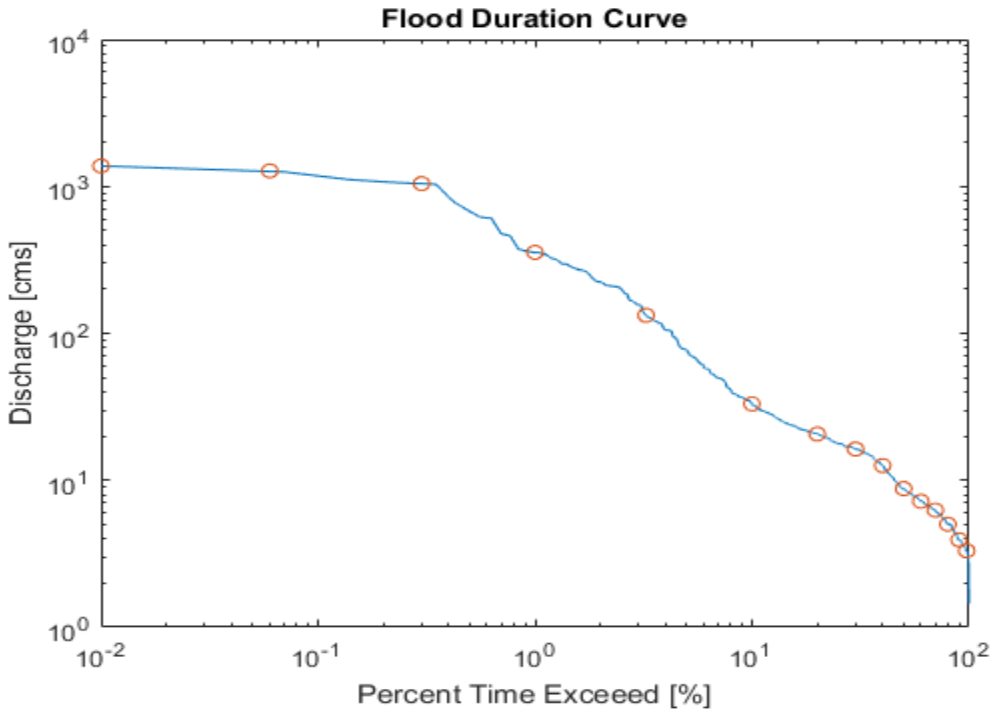

Specific Degradation

$$SD = 365 \times Q_s \left[\frac{tons}{day}\right] \div Area[km^2] = \frac{182.86 \times 365}{1039.1} = 43.3 \frac{tons}{km^2 \cdot year}$$

Opinion

N3 Gumi

Daily Stage and Discharge

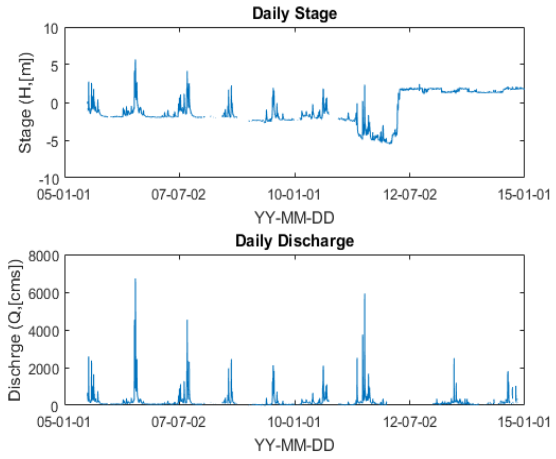

Sediment Rating Curve

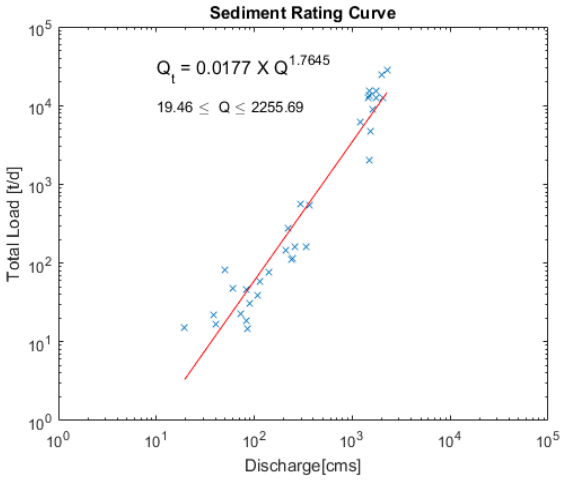

Flow Duration Curve

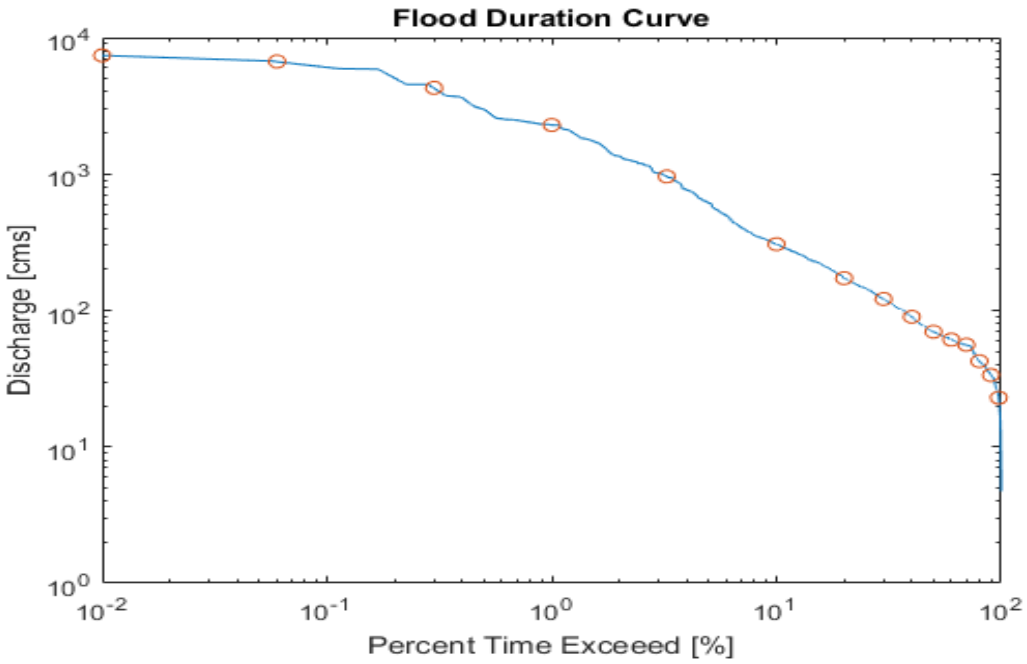

Specific Degradation

$$SD = 365 \times Q_s \left[\frac{tons}{day}\right] \div Area[km^2] = \frac{627.58 \times 365}{10912.8} = 21.01 \frac{tons}{km^2 \cdot year}$$

Opinion

N4 Nakdong

Daily Stage and Discharge

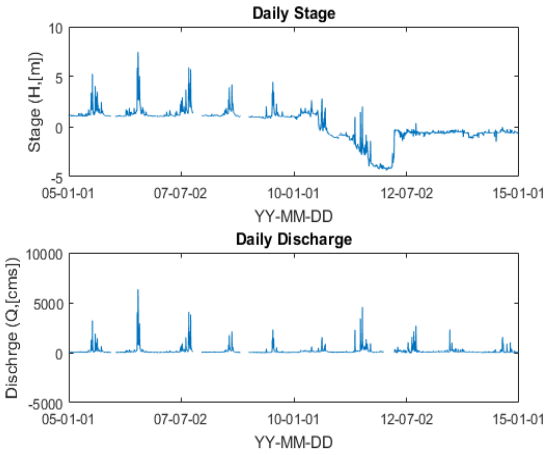

Sediment Rating Curve

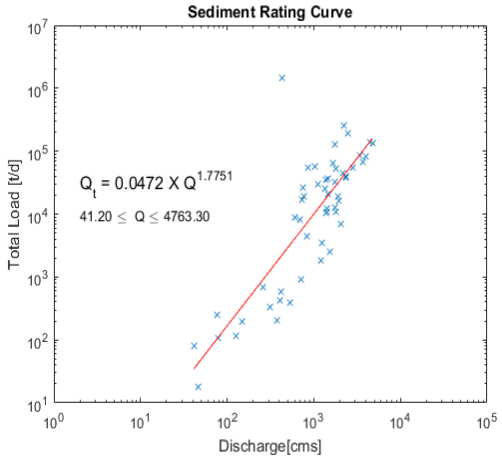

Flow Duration Curve

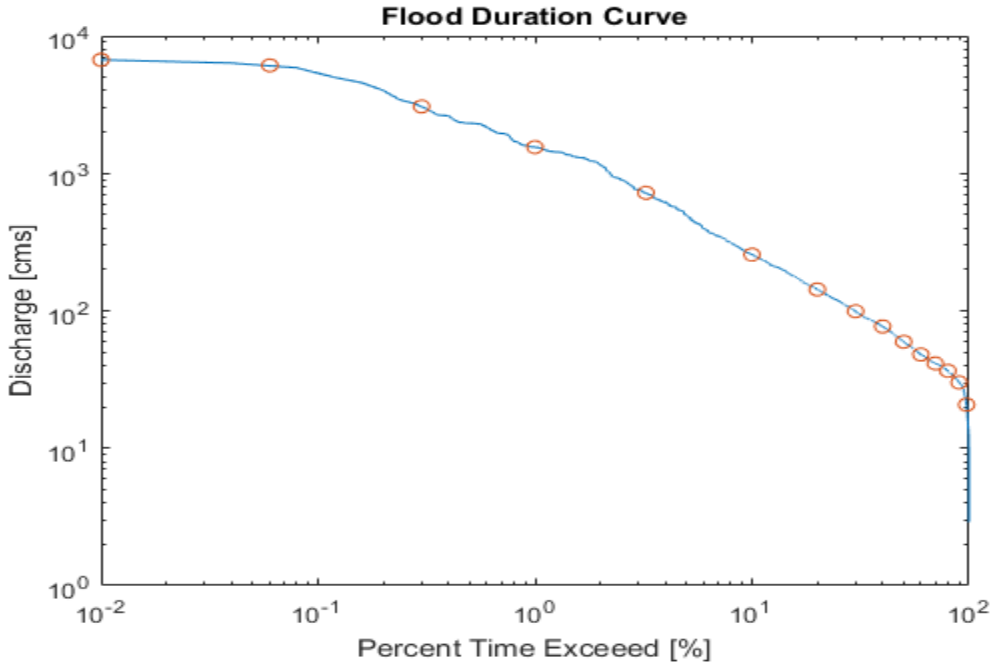

Specific Degradation

$$SD = 365 \times Q_s \left[\frac{tons}{day}\right] \div Area[km^2] = \frac{1134.41 \times 365}{9406.8} = 43.9 \frac{tons}{km^2 \cdot year}$$

Opinion

N5 Waegwan

Daily Stage and Discharge

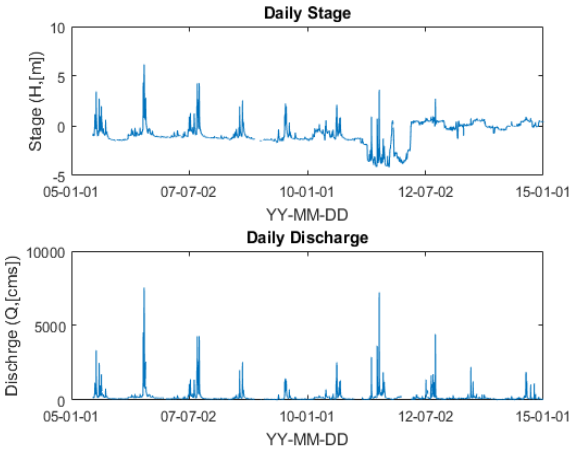

Sediment Rating Curve

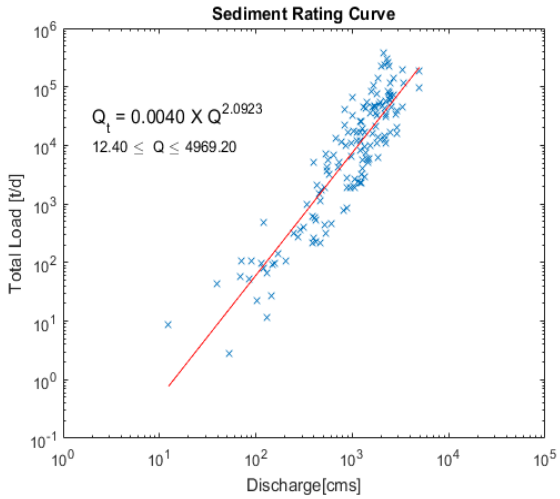

Flow Duration Curve

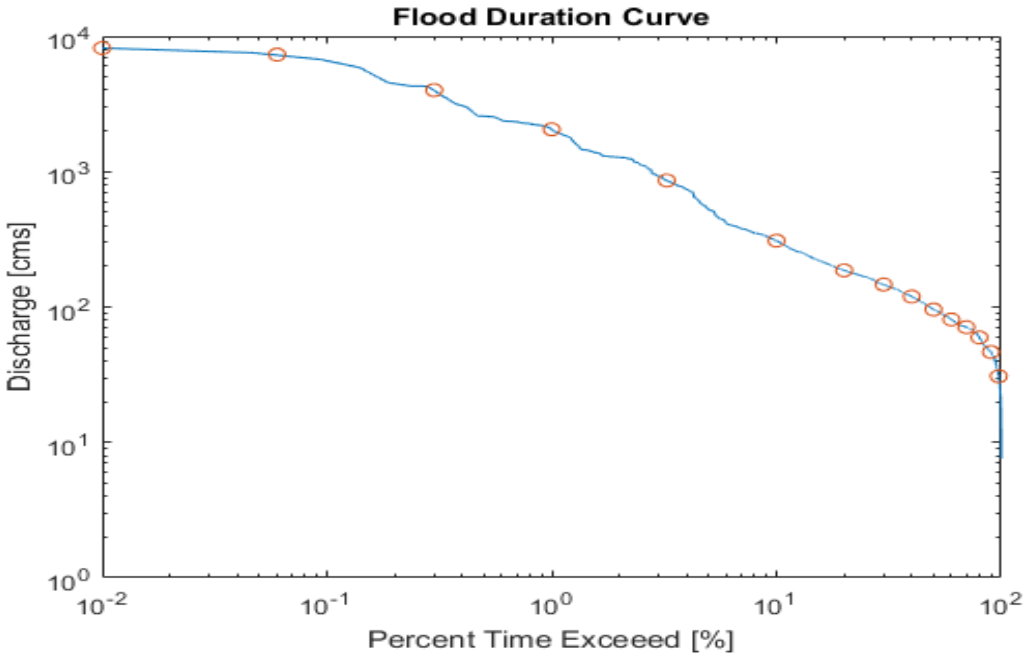

Specific Degradation

$$SD = 365 \times Q_s \left[\frac{tons}{day}\right] \div Area[km^2] = \frac{1705.39 \times 365}{11100.6} = 56.08 \frac{tons}{km^2 \cdot year}$$

Opinion

N6 Ilseon Bridge

Daily Stage and Discharge

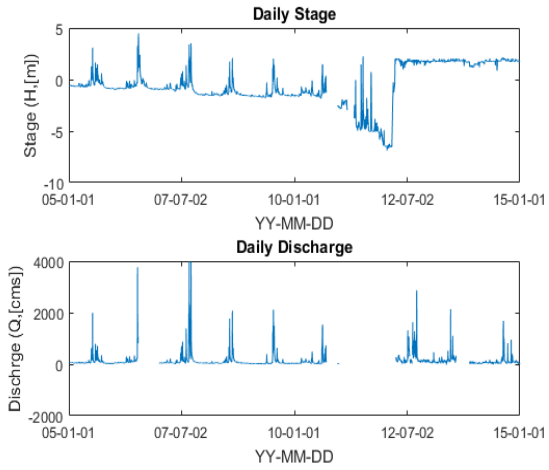

Sediment Rating Curve

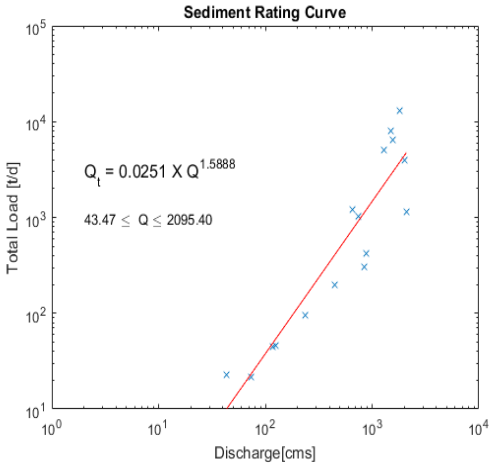

Flow Duration Curve

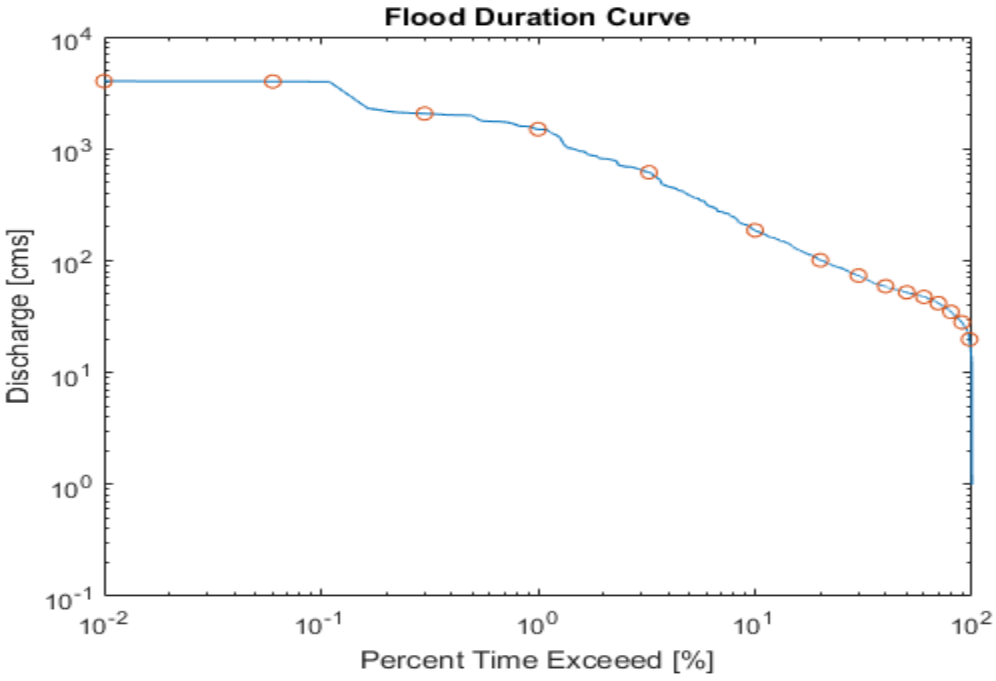

Specific Degradation

$$SD = 365 \times Q_s \left[\frac{tons}{day}\right] \div Area[km^2] = \frac{105.95 \times 365}{978.8} = 4.06 \frac{tons}{km^2 \cdot year}$$

Opinion

SD could be distorted due to small measurements

N7 Jindong

Daily Stage and Discharge

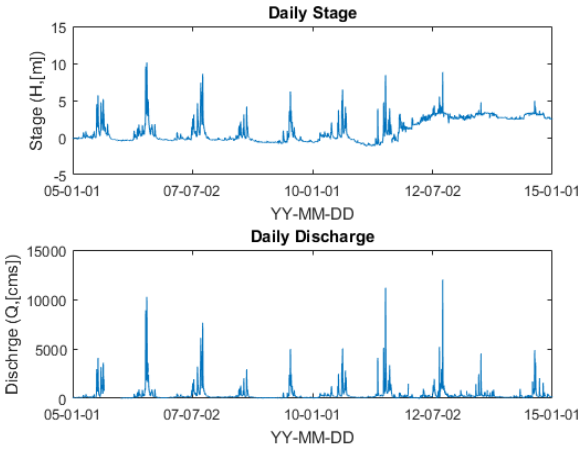

Sediment Rating Curve

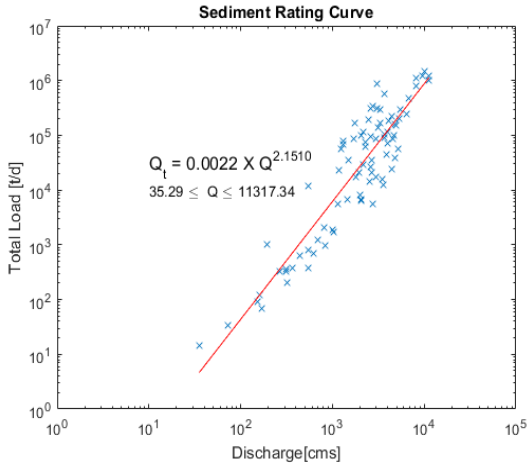

Flow Duration Curve

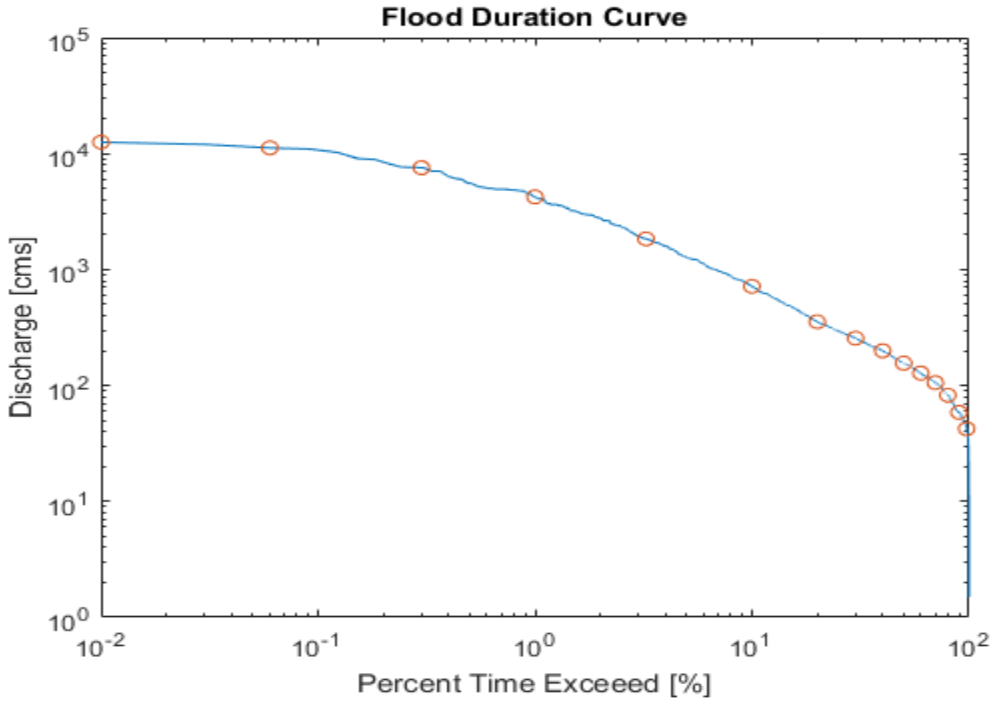

Specific Degradation

$$SD = 365 \times Q_s \left[\frac{tons}{day}\right] \div Area[km^2] = \frac{5716.93 \times 365}{20381} = 102.4 \frac{tons}{km^2 \cdot year}$$

Opinion

N8 Jeongam

Daily Stage and Discharge

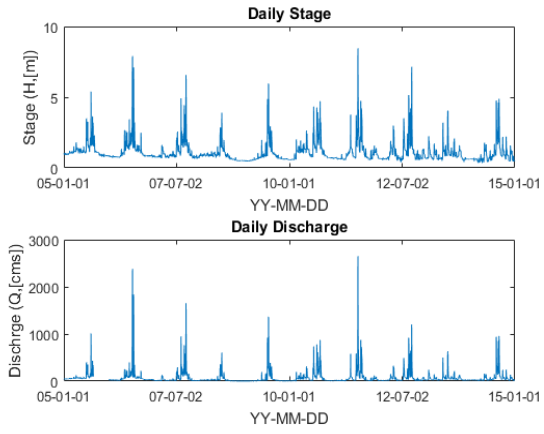

Sediment Rating Curve

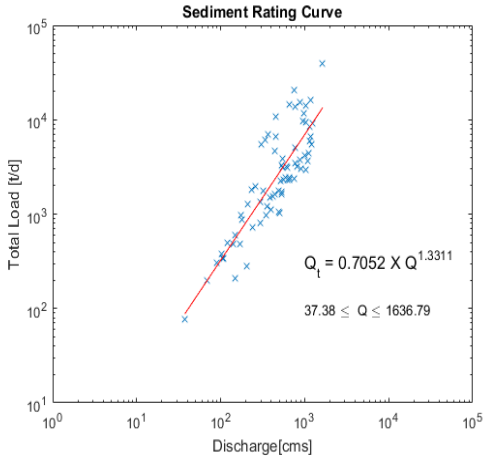

Flow Duration Curve

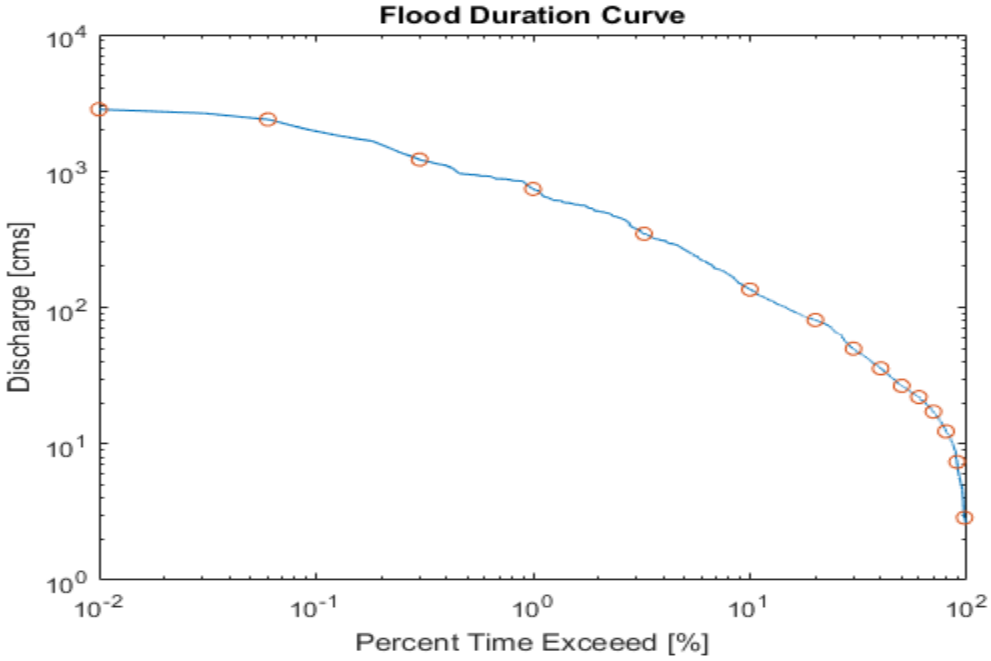

Specific Degradation

$$SD = 365 \times Q_s \left[\frac{tons}{day}\right] \div Area[km^2] = \frac{274.79 \times 365}{2998.6} = 33.48 \frac{tons}{km^2 \cdot year}$$

Opinion

N9 Hyangseok

Daily Stage and Discharge

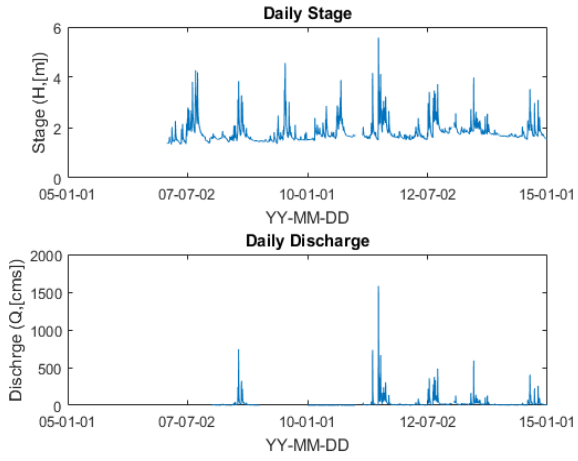

Sediment Rating Curve

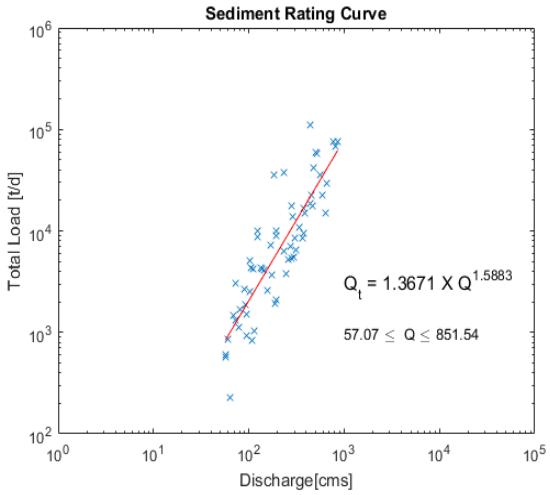

Flow Duration Curve

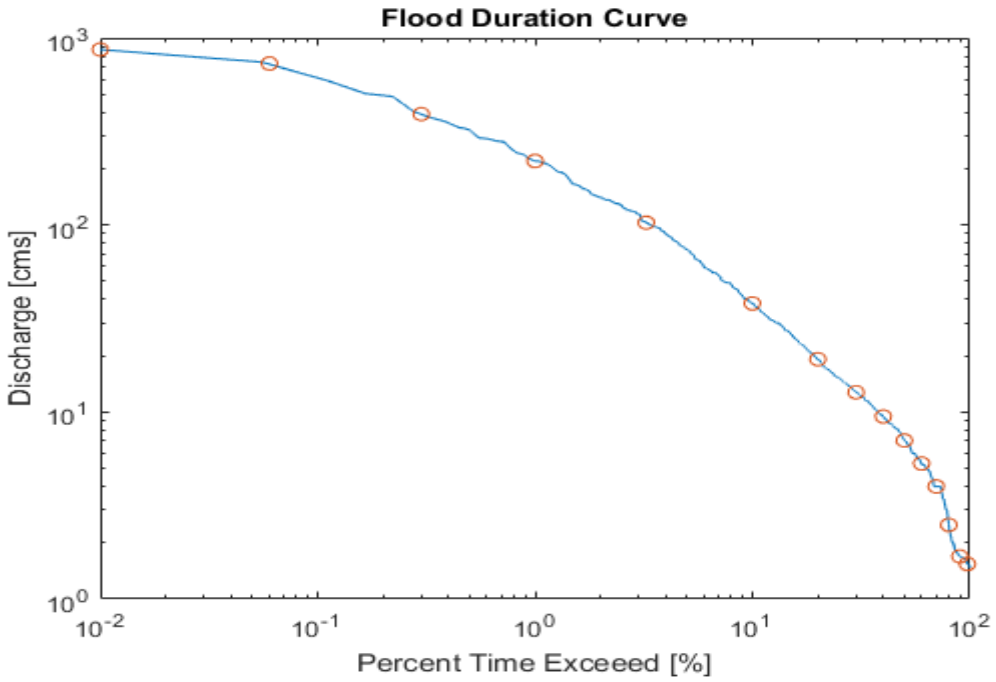

Specific Degradation

$$SD = 365 \times Q_s \left[\frac{tons}{day}\right] \div Area[km^2] = \frac{349.15 \times 365}{1512} = 84.28 \frac{tons}{km^2 \cdot year}$$

Opinion

N10 Dongmun

Daily Stage and Discharge

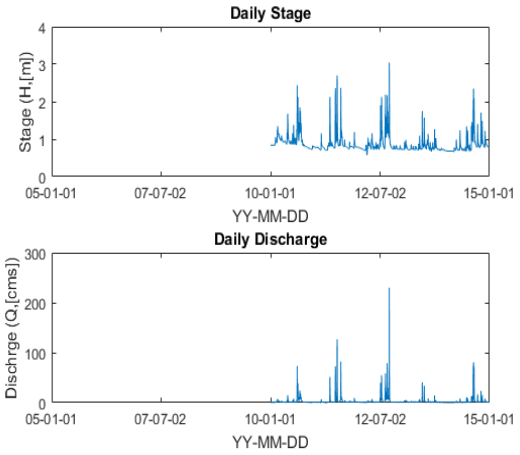

Sediment Rating Curve

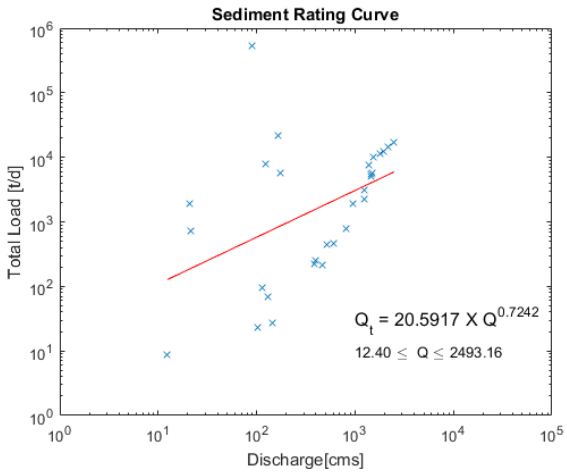

Flow Duration Curve

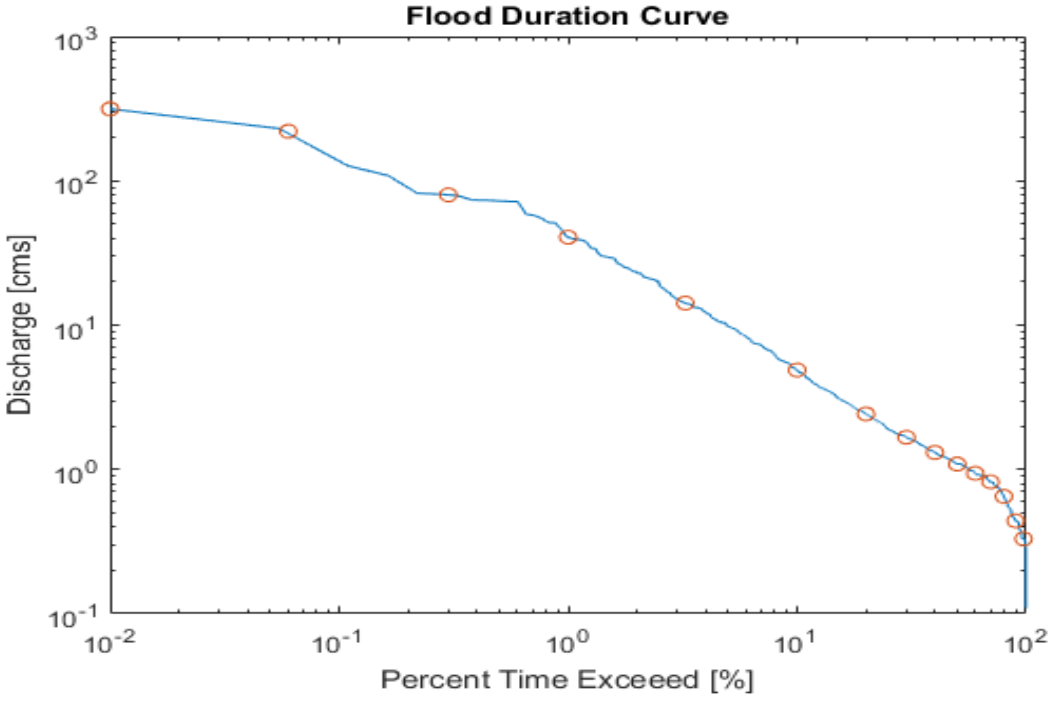

Specific Degradation

$$SD = 365 \times Q_s \left[\frac{tons}{day}\right] \div Area[km^2] = \frac{35.92 \times 365}{175.3} = 74.81 \frac{tons}{km^2 \cdot year}$$

Opinion

N11 Jeomchon

Daily Stage and Discharge

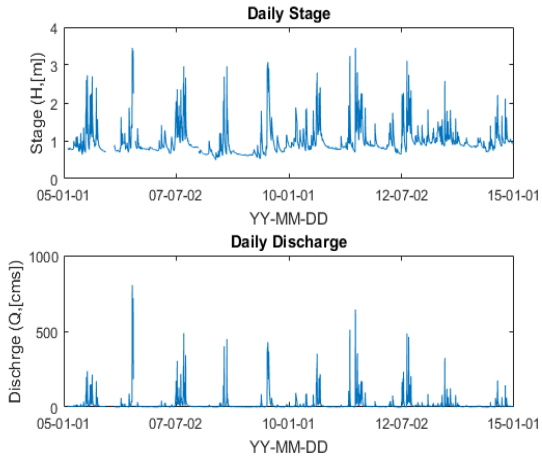

Sediment Rating Curve

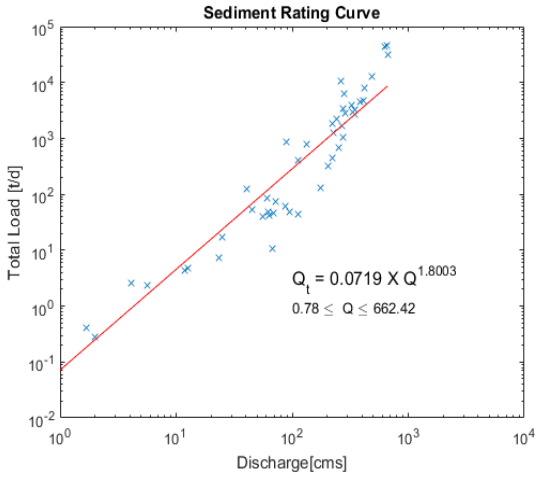

Flow Duration Curve

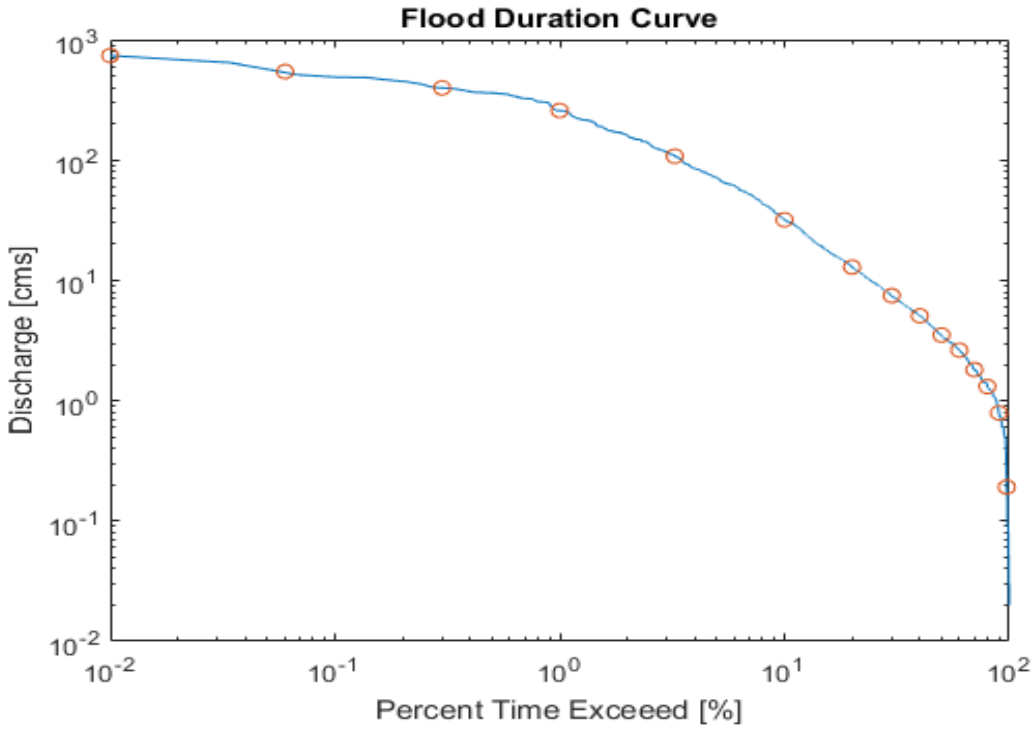

Specific Degradation

$$SD = 365 \times Q_s \left[\frac{tons}{day}\right] \div Area[km^2] = \frac{64.54 \times 365}{614.5} = 38.34 \frac{tons}{km^2 \cdot year}$$

Opinion

N12 Yonggok

Daily Stage and Discharge

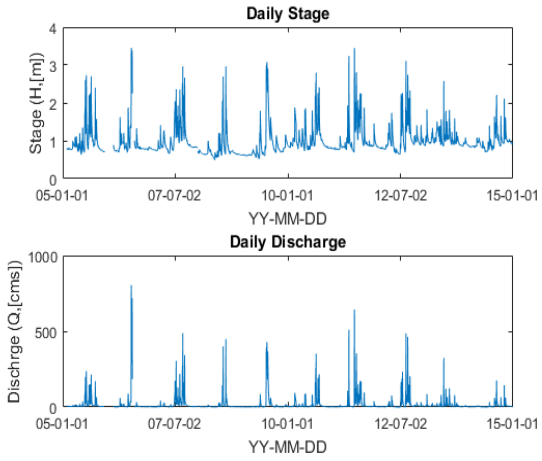

Sediment Rating Curve

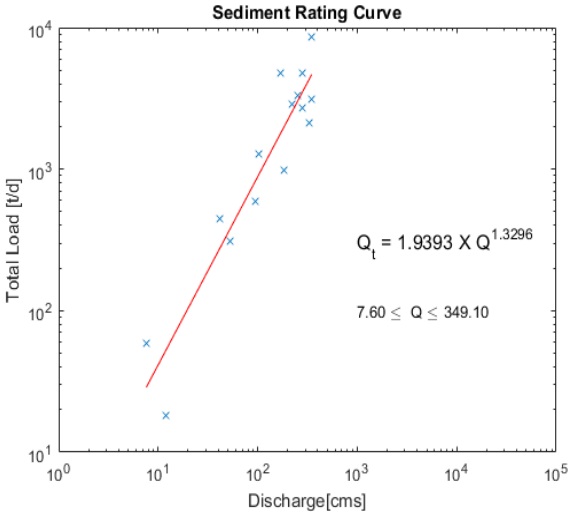

Flow Duration Curve

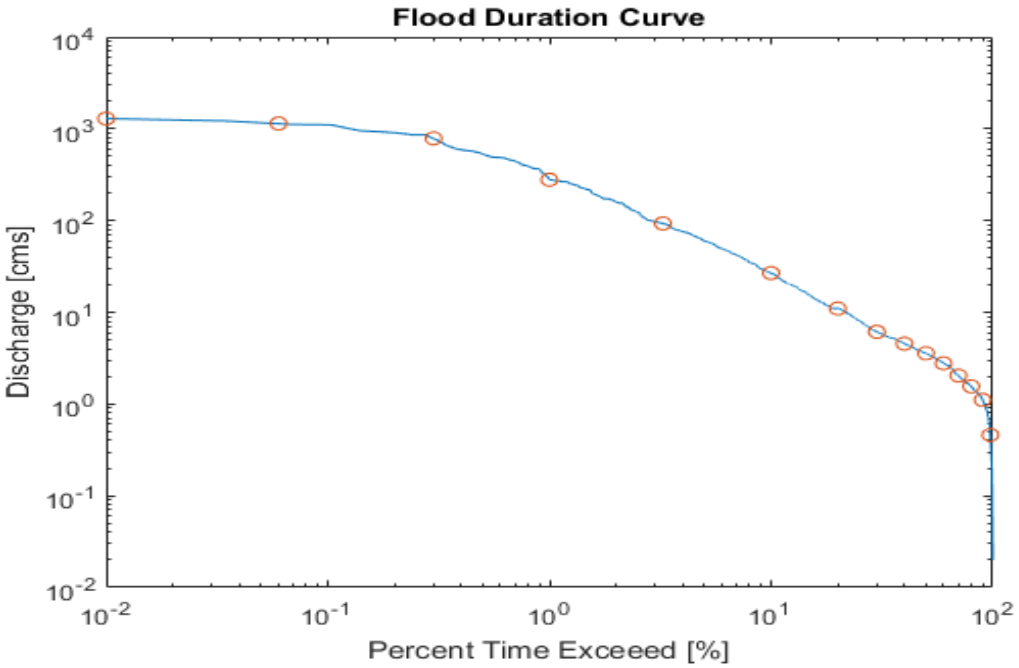

Specific Degradation

$$SD = 365 \times Q_s \left[\frac{tons}{day}\right] \div Area[km^2] = \frac{189.56 \times 365}{1318} = 46.33 \frac{tons}{km^2 \cdot year}$$

Opinion

SD could be distorted due to small measurements

N13 Jukgo

Daily Stage and Discharge

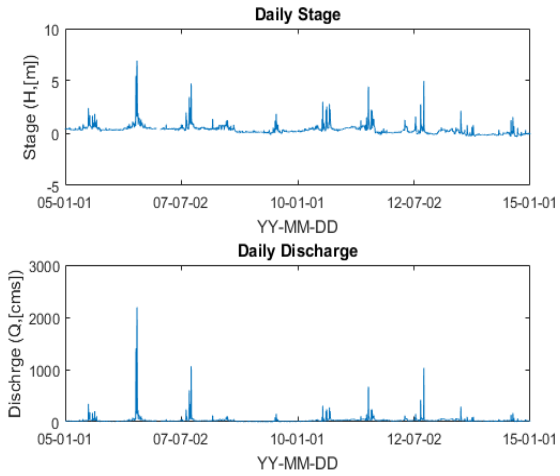

Sediment Rating Curve

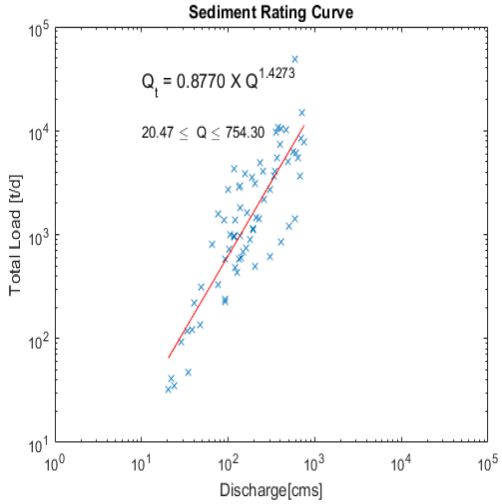

Flow Duration Curve

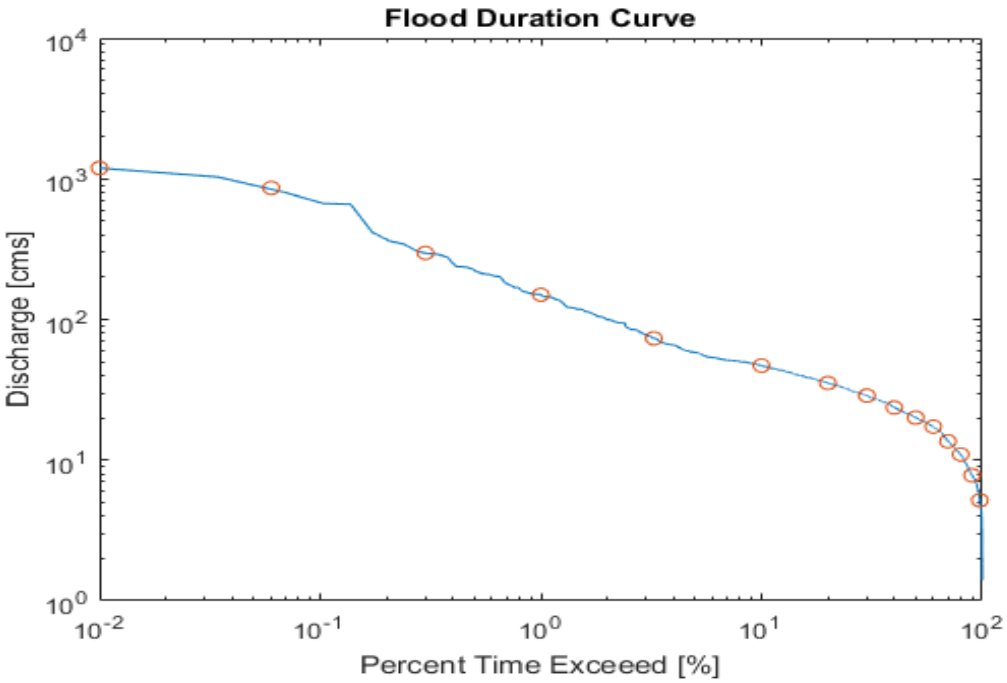

Specific Degradation

$$SD = 365 \times Q_s \left[\frac{tons}{day}\right] \div Area[km^2] = \frac{126.36 \times 365}{1239.1} = 37.22 \frac{tons}{km^2 \cdot year}$$

Opinion

N14 Gaejin2

Daily Stage and Discharge

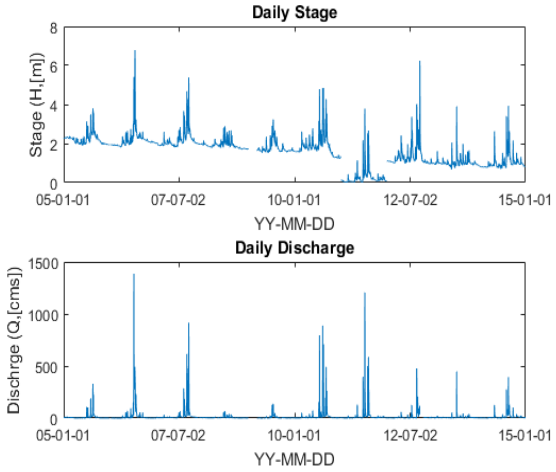

Sediment Rating Curve

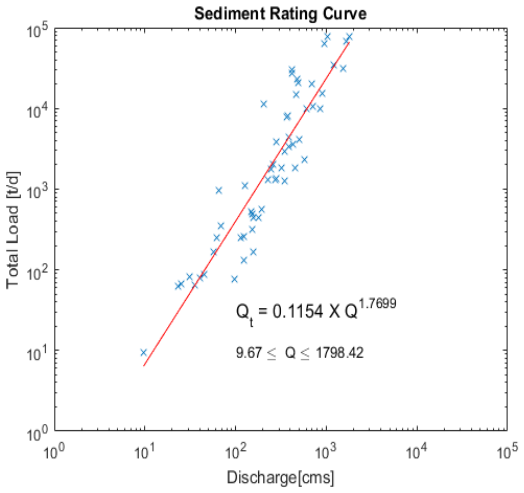

Flow Duration Curve

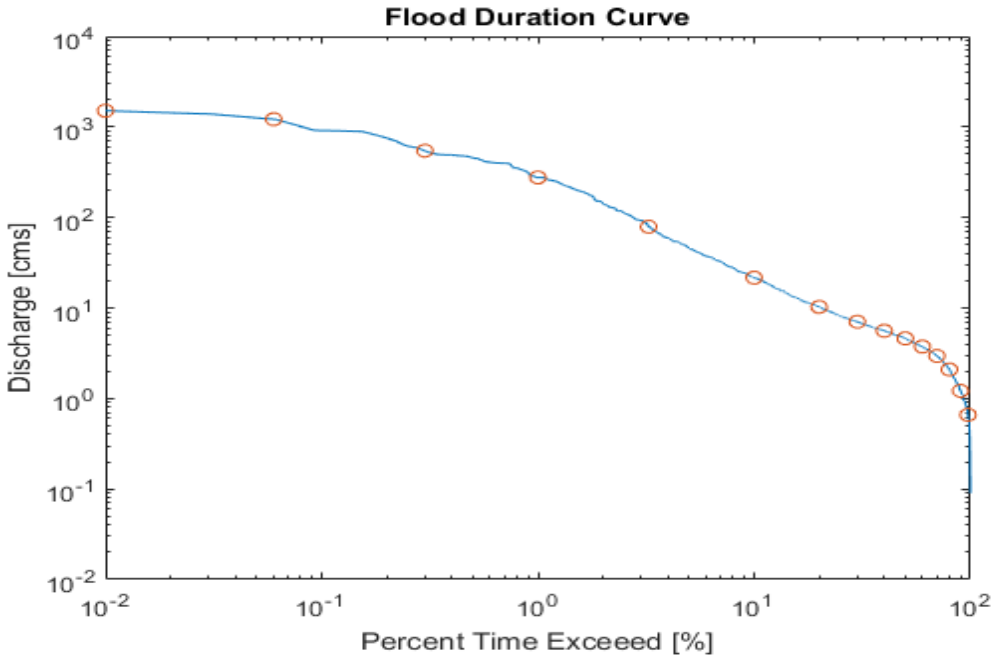

Specific Degradation

$$SD = 365 \times Q_s \left[\frac{tons}{day}\right] \div Area[km^2] = \frac{106.34 \times 365}{749.9} = 51.8 \frac{tons}{km^2 \cdot year}$$

Opinion

NU1 Socheon

Daily Stage and Discharge

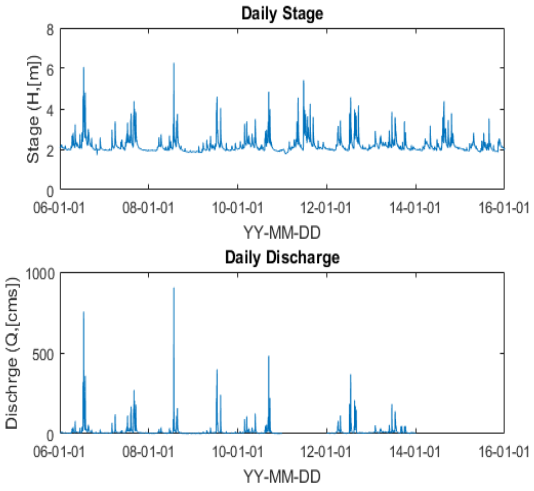

Sediment Rating Curve

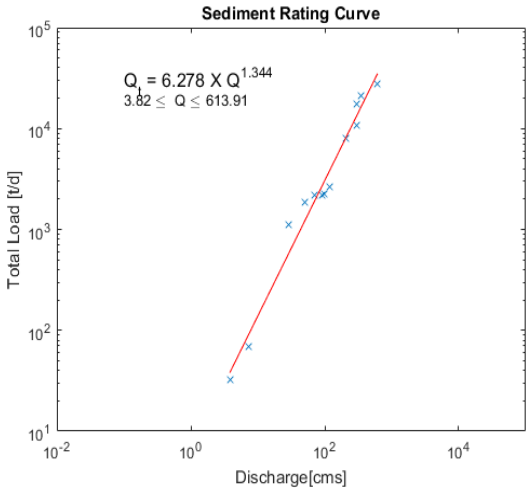

Flow Duration Curve

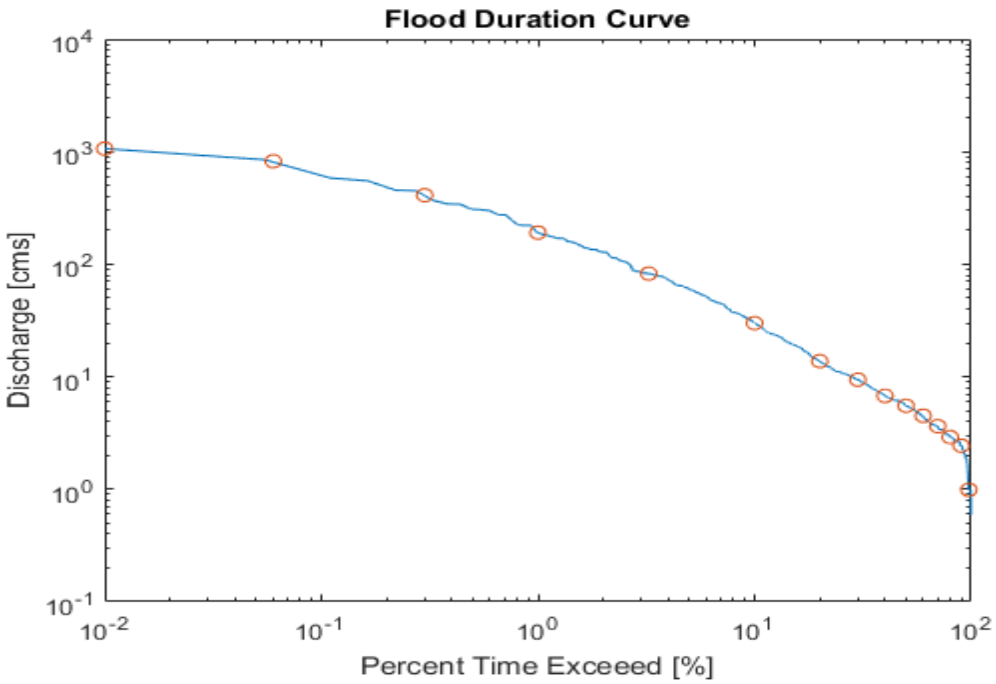

Specific Degradation

$$SD = 365 \times Q_s \left[\frac{tons}{day}\right] \div Area[km^2] = \frac{382.99 \times 365}{697.1} = 200.53 \frac{tons}{km^2 \cdot year}$$

Opinion

SRC could be distorted due to small measurements

NU2 Yangsam

Daily Stage and Discharge

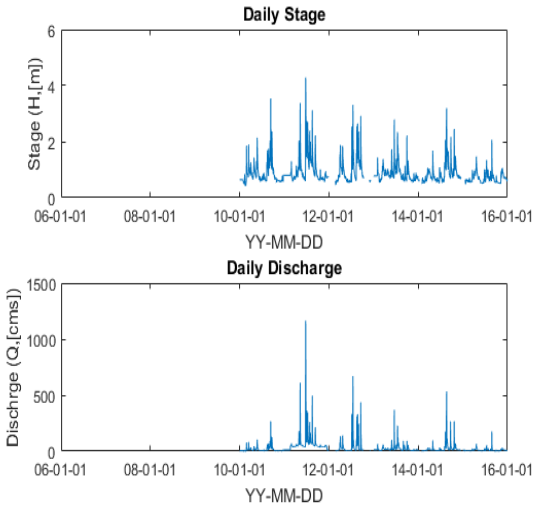

Sediment Rating Curve

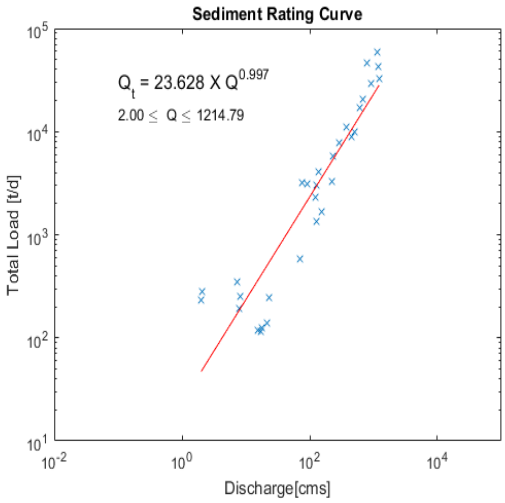

Flow Duration Curve

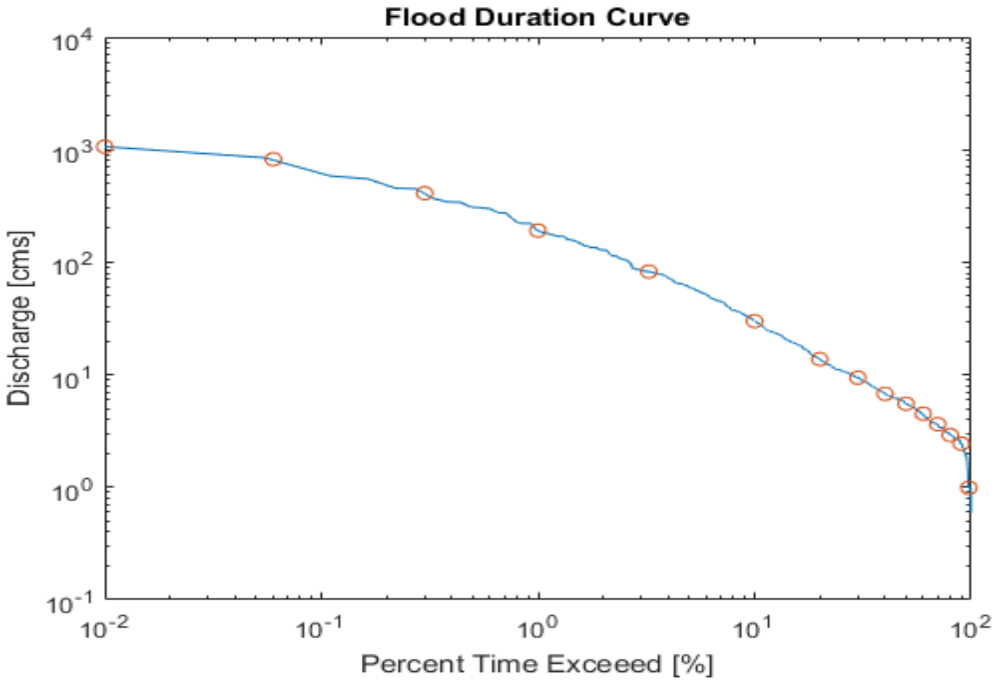

Specific Degradation

$$SD = 365 \times Q_s \left[\frac{tons}{day}\right] \div Area[km^2] = \frac{636.61 \times 365}{1147.4} = 202.51 \frac{tons}{km^2 \cdot year}$$

Opinion

NU3 Yeongyang

Daily Stage and Discharge

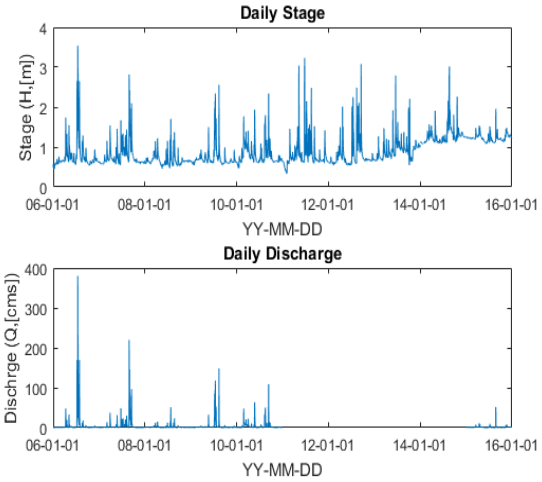

Sediment Rating Curve

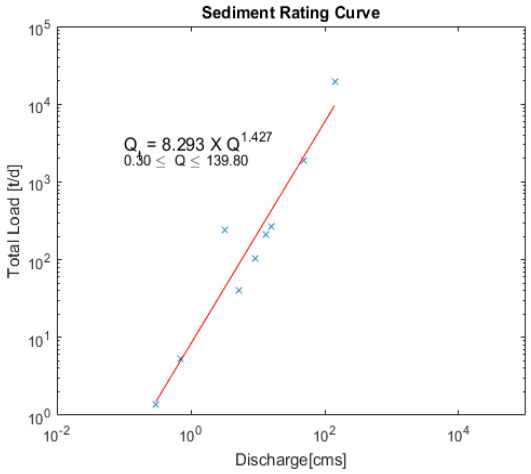

Flow Duration Curve

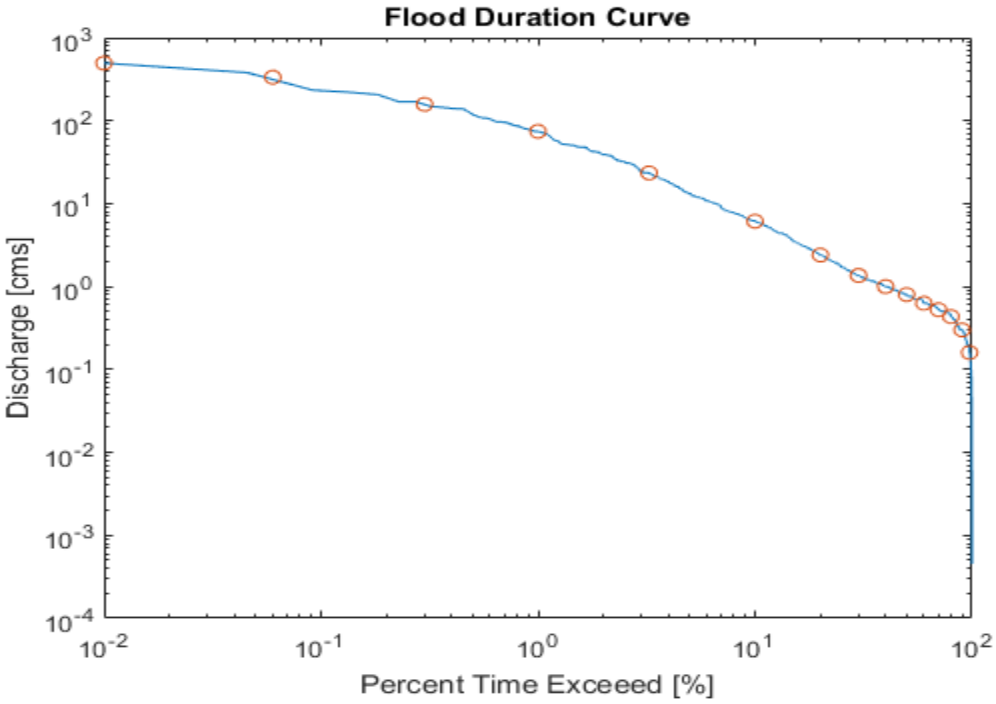

Specific Degradation

$$SD = 365 \times Q_s \left[\frac{tons}{day}\right] \div Area[km^2] = \frac{166.48 \times 365}{314} = 193.41 \frac{tons}{km^2 \cdot year}$$

Opinion

NU4 Dongcheon

Daily Stage and Discharge

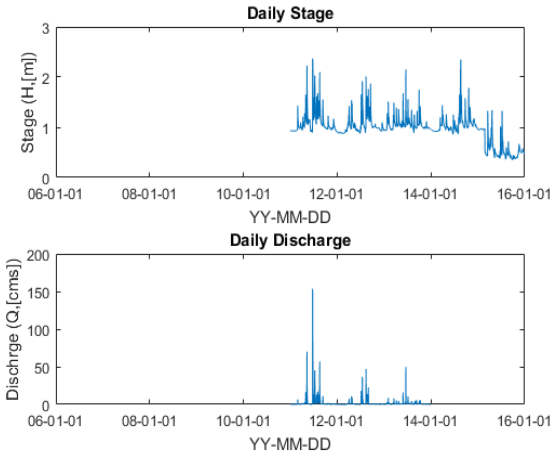

Sediment Rating Curve

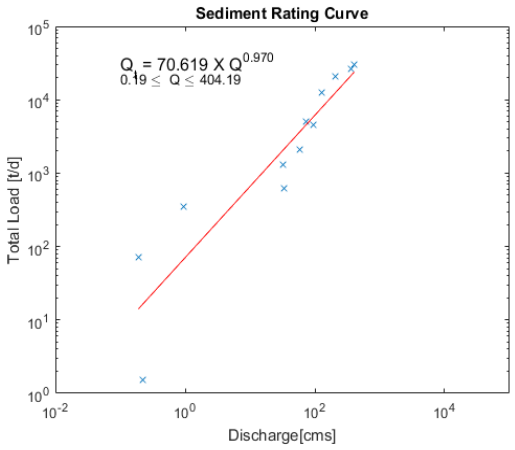

Flow Duration Curve

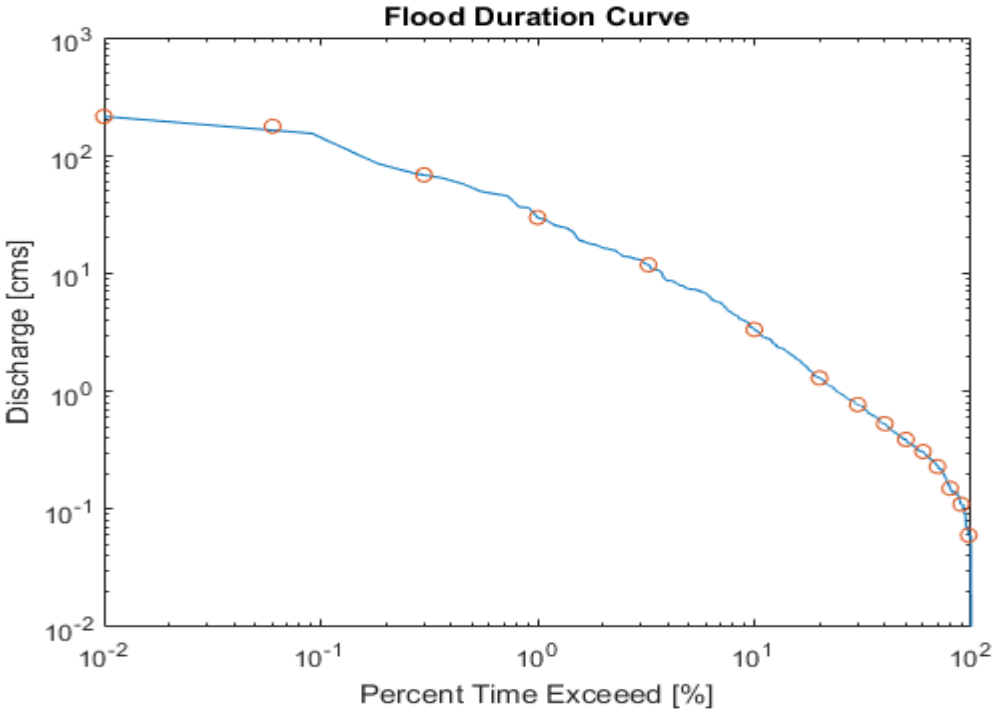

Specific Degradation

$$SD = 365 \times Q_s \left[\frac{tons}{day}\right] \div Area[km^2] = \frac{124.33 \times 365}{142.9} = 317.56 \frac{tons}{km^2 \cdot year}$$

Opinion

SRC could be distorted due to small measurements

NU5 Cheongsong

Daily Stage and Discharge

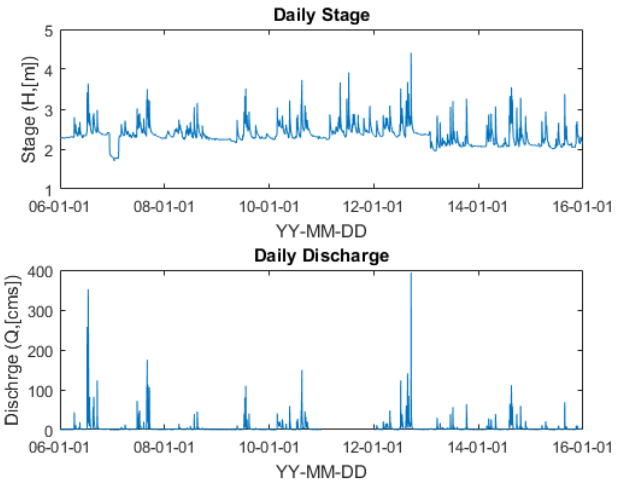

Sediment Rating Curve

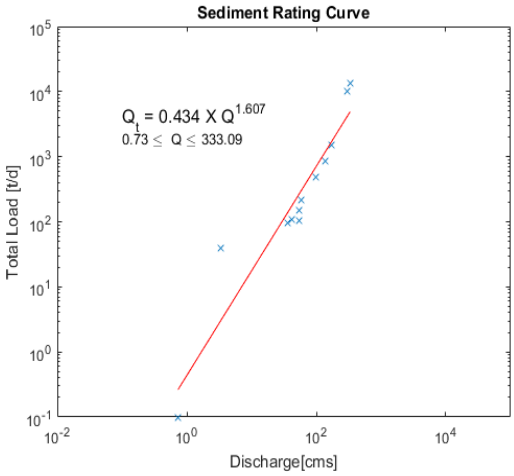

Flow Duration Curve

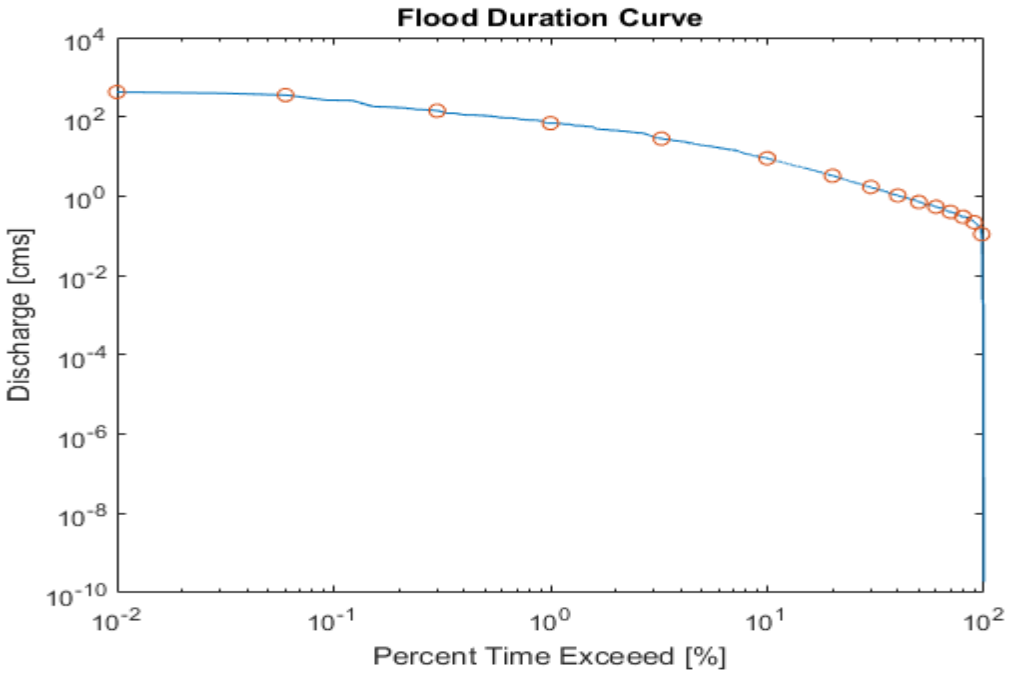

Specific Degradation

$$SD = 365 \times Q_s \left[\frac{tons}{day}\right] \div Area[km^2] = \frac{19.96 \times 365}{305} = 23.91 \frac{tons}{km^2 \cdot year}$$

Opinion

SD could be distorted due to small measurements

NU6 Geochang1

Daily Stage and Discharge

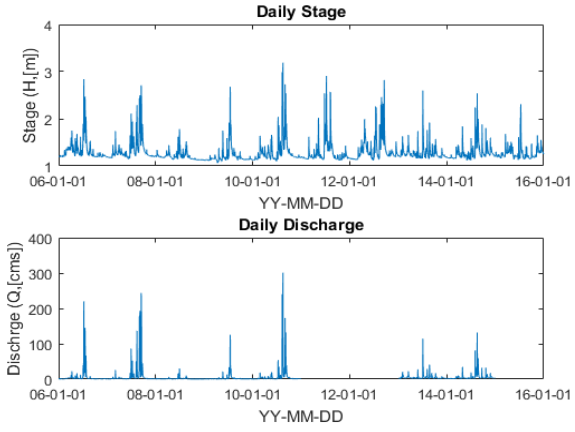

Sediment Rating Curve

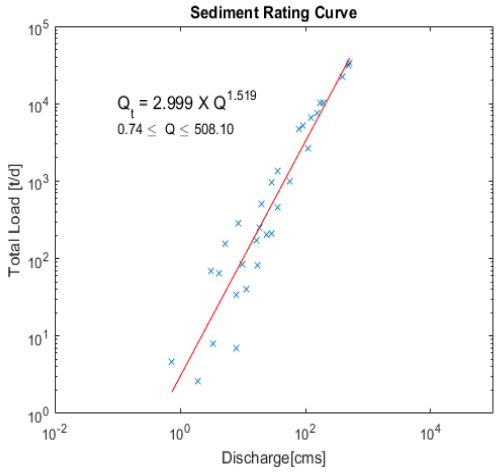

Flow Duration Curve

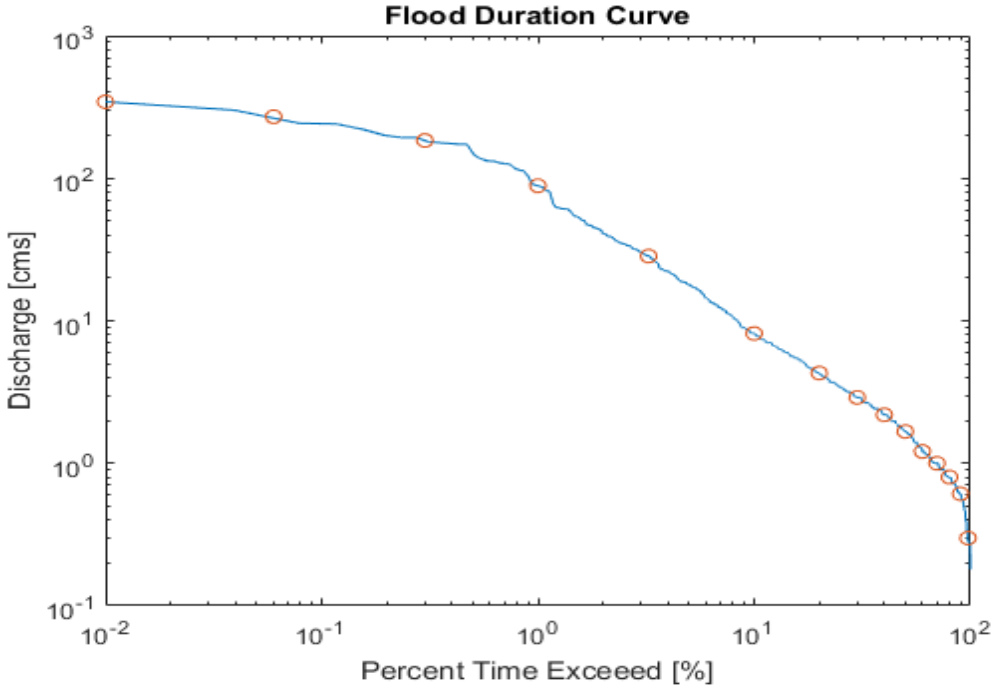

Specific Degradation

$$SD = 365 \times Q_s \left[\frac{tons}{day}\right] \div Area[km^2] = \frac{107.60 \times 365}{227} = 173.18 \frac{tons}{km^2 \cdot year}$$

Opinion

NU7 Geochang2

Daily Stage and Discharge

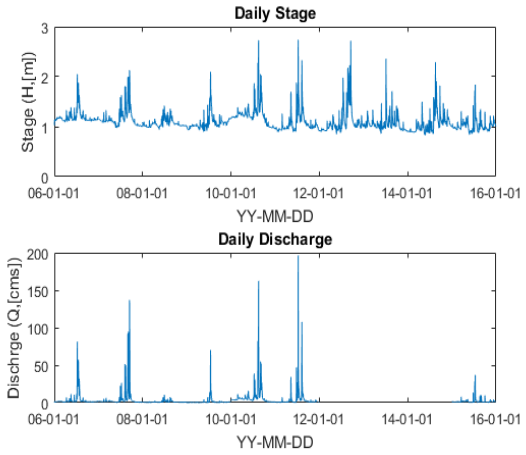

Sediment Rating Curve

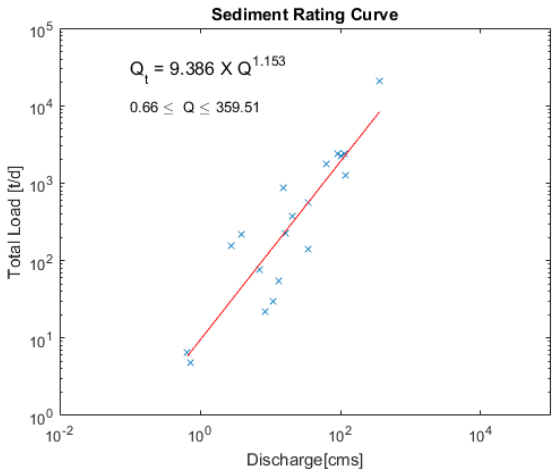

Flow Duration Curve

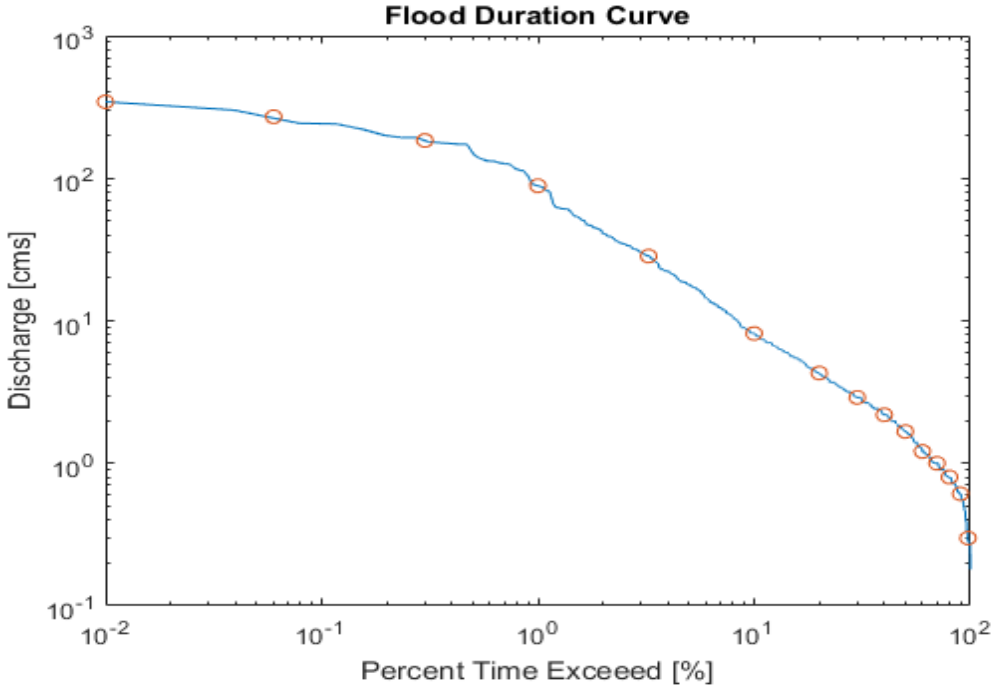

Specific Degradation

$$SD = 365 \times Q_s \left[\frac{tons}{day}\right] \div Area[km^2] = \frac{48.37 \times 365}{180.7} = 97.79 \frac{tons}{km^2 \cdot year}$$

Opinion

NU8 Jisan

Daily Stage and Discharge

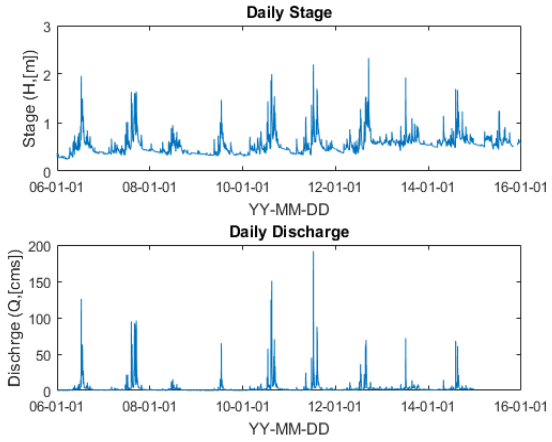

Sediment Rating Curve

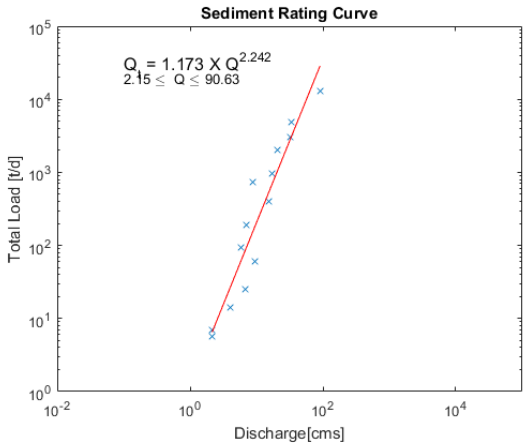

Flow Duration Curve

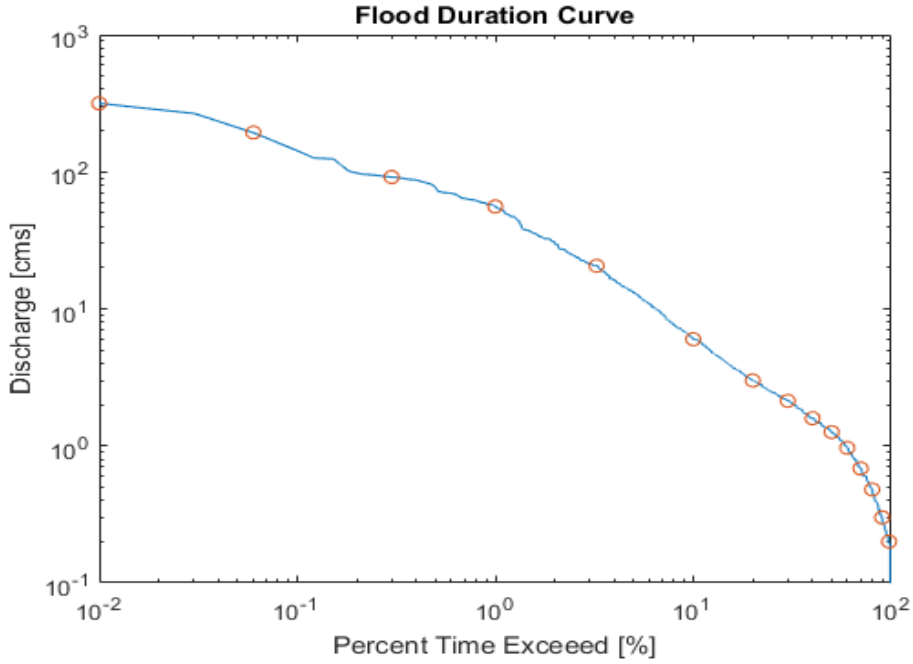

Specific Degradation

$$SD = 365 \times Q_s \left[\frac{tons}{day}\right] \div Area[km^2] = \frac{480.97 \times 365}{143} = 1092.9 \frac{tons}{km^2 \cdot year}$$

Opinion

SD could be distorted due to small measurements

NU9 Donggok2

Daily Stage and Discharge

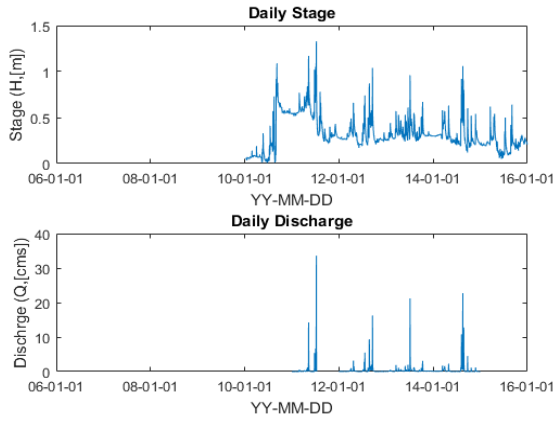

Sediment Rating Curve

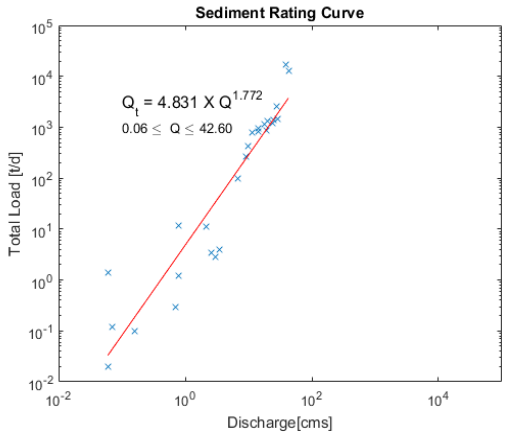

Flow Duration Curve

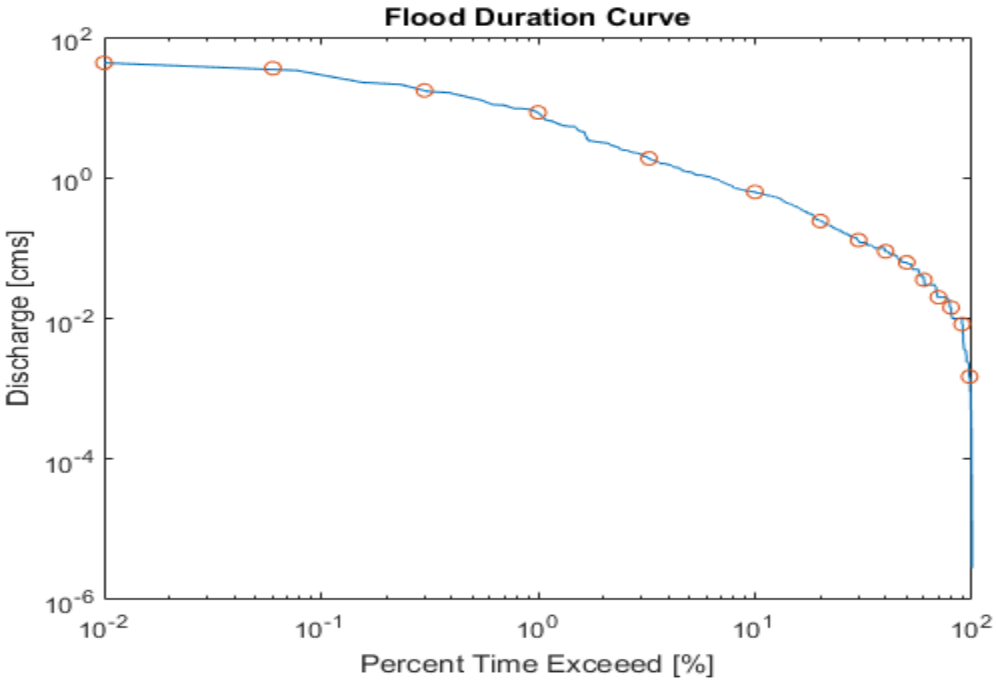

Specific Degradation

$$SD = 365 \times Q_s \left[\frac{tons}{day}\right] \div Area[km^2] = \frac{5.74 \times 365}{34} = 61.6 \frac{tons}{km^2 \cdot year}$$

Opinion

SD could be distorted due to small measurements

NU10 Gohyeon

Daily Stage and Discharge

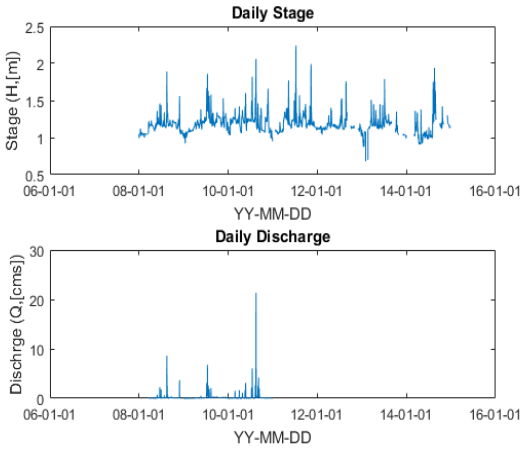

Sediment Rating Curve

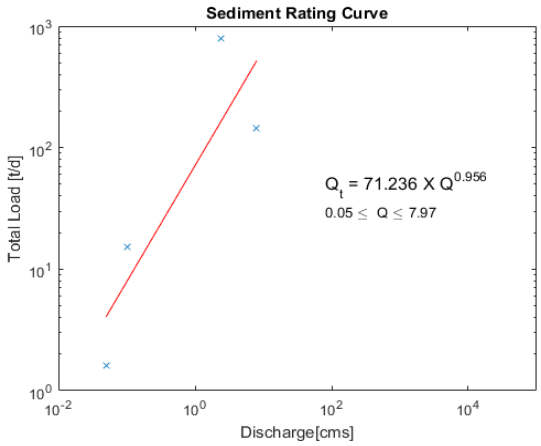

Flow Duration Curve

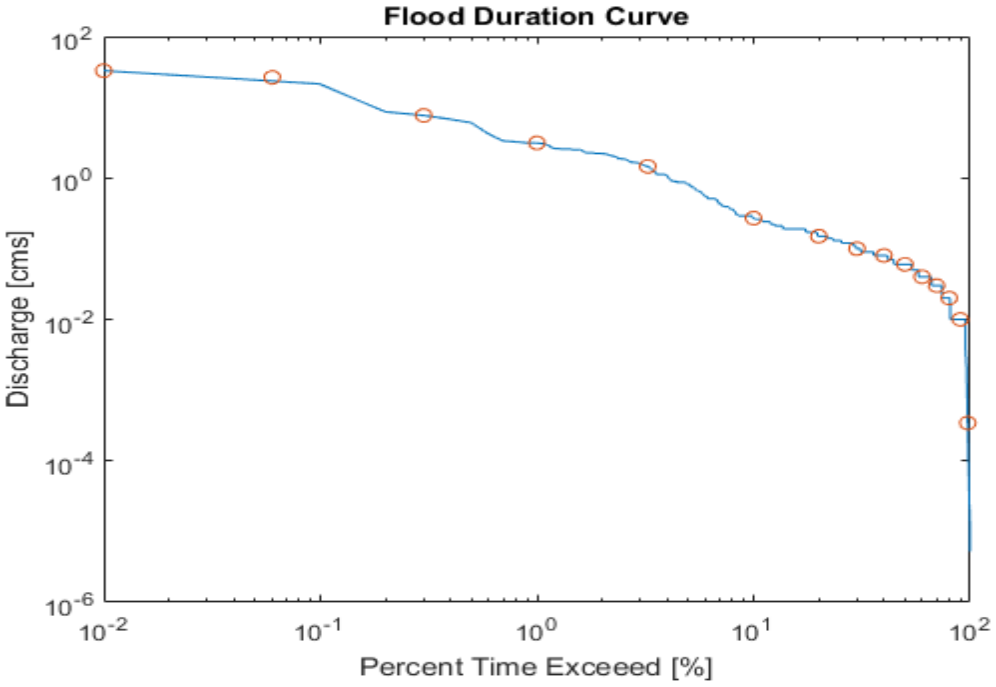

Specific Degradation

$$SD = 365 \times Q_s \left[\frac{tons}{day}\right] \div Area[km^2] = \frac{16.33 \times 365}{14.8} = 400.11 \frac{tons}{km^2 \cdot year}$$

Opinion

SD could be distorted due to small measurements

NU11 Daeri

Daily Stage and Discharge

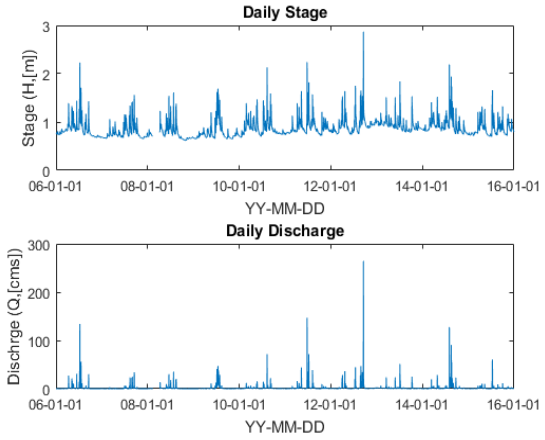

Sediment Rating Curve

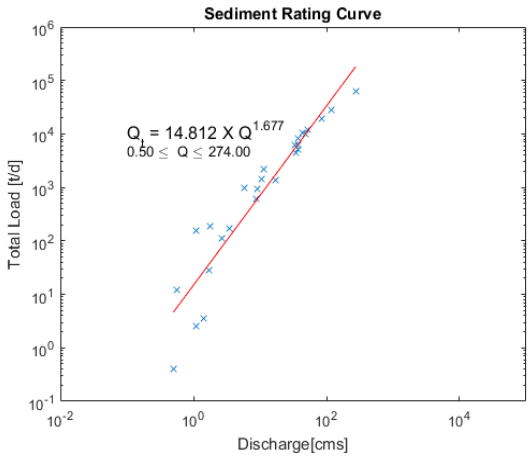

Flow Duration Curve

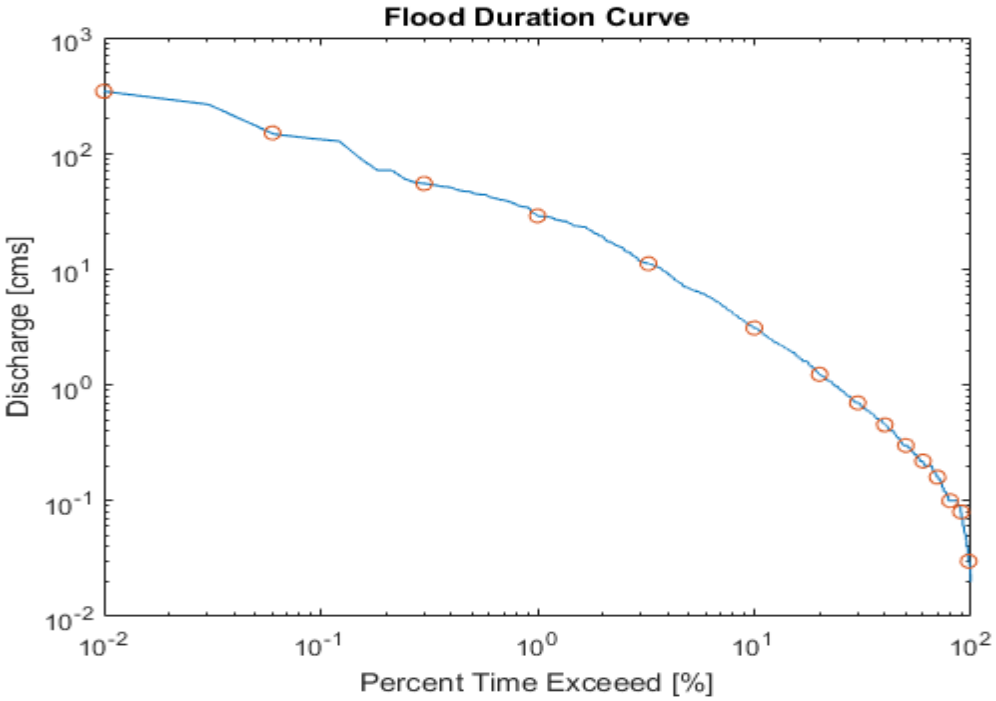

Specific Degradation

$$SD = 365 \times Q_s \left[\frac{tons}{day}\right] \div Area[km^2] = \frac{239.53 \times 365}{61} = 1433.5 \frac{tons}{km^2 \cdot year}$$

Opinion
High SD

NU12 Changcheon

Daily Stage and Discharge

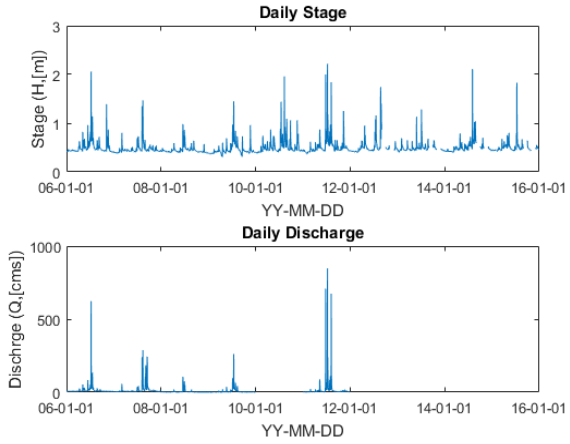

Sediment Rating Curve

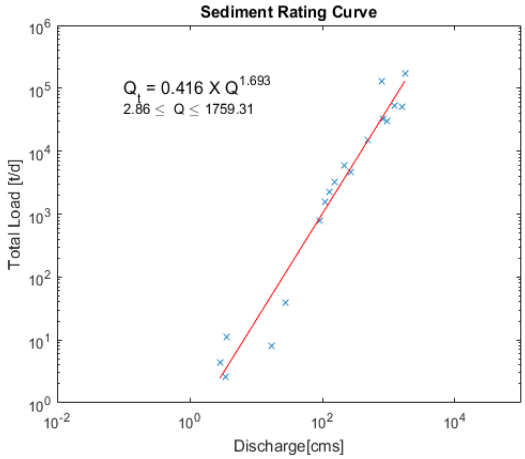

Flow Duration Curve

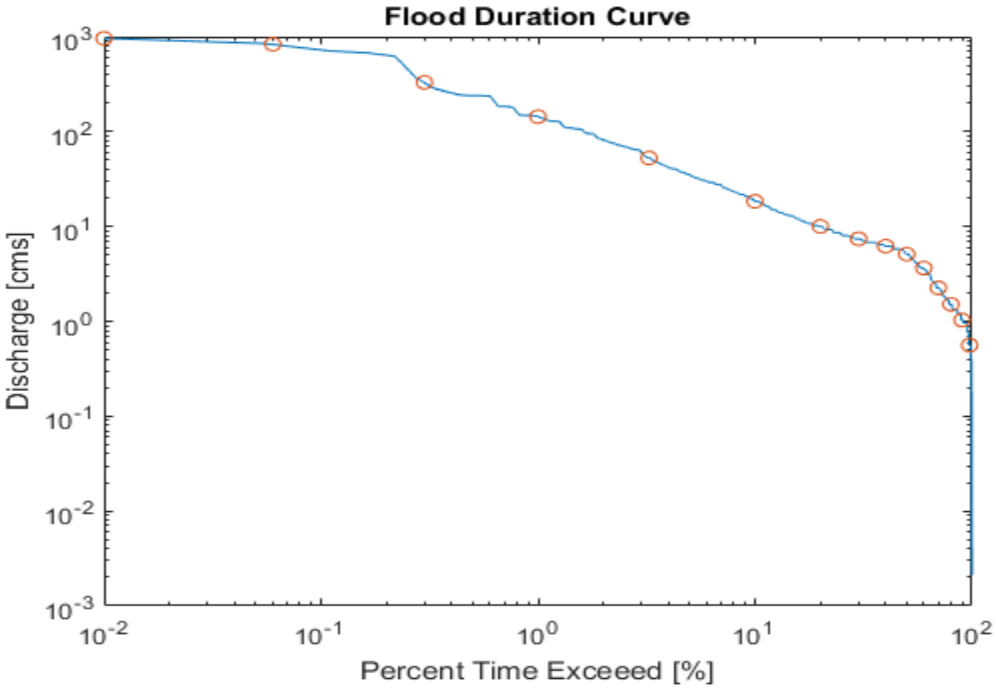

Specific Degradation

$$SD = 365 \times Q_s \left[\frac{tons}{day}\right] \div Area[km^2] = \frac{111.71 \times 365}{334.2} = 122.01 \frac{tons}{km^2 \cdot year}$$

Opinion

NU13 Sancheong

Daily Stage and Discharge

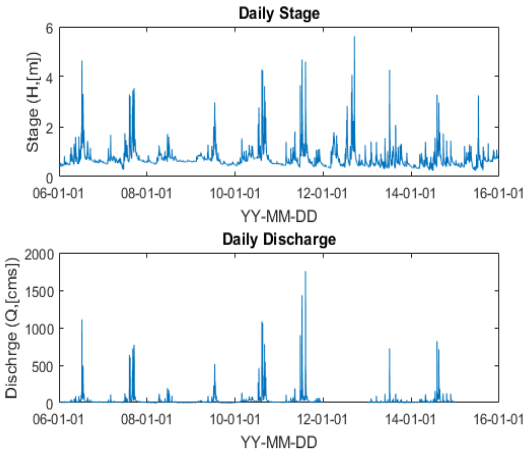

Sediment Rating Curve

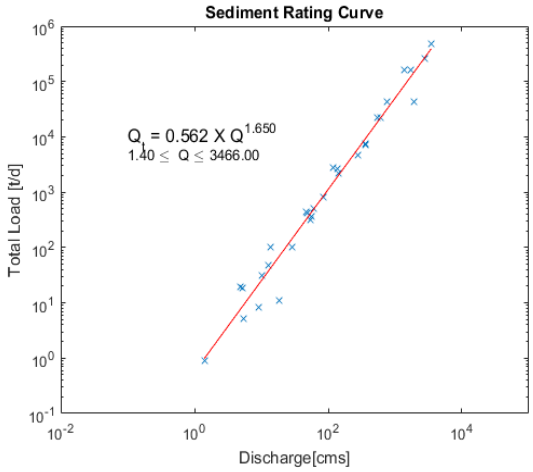

Flow Duration Curve

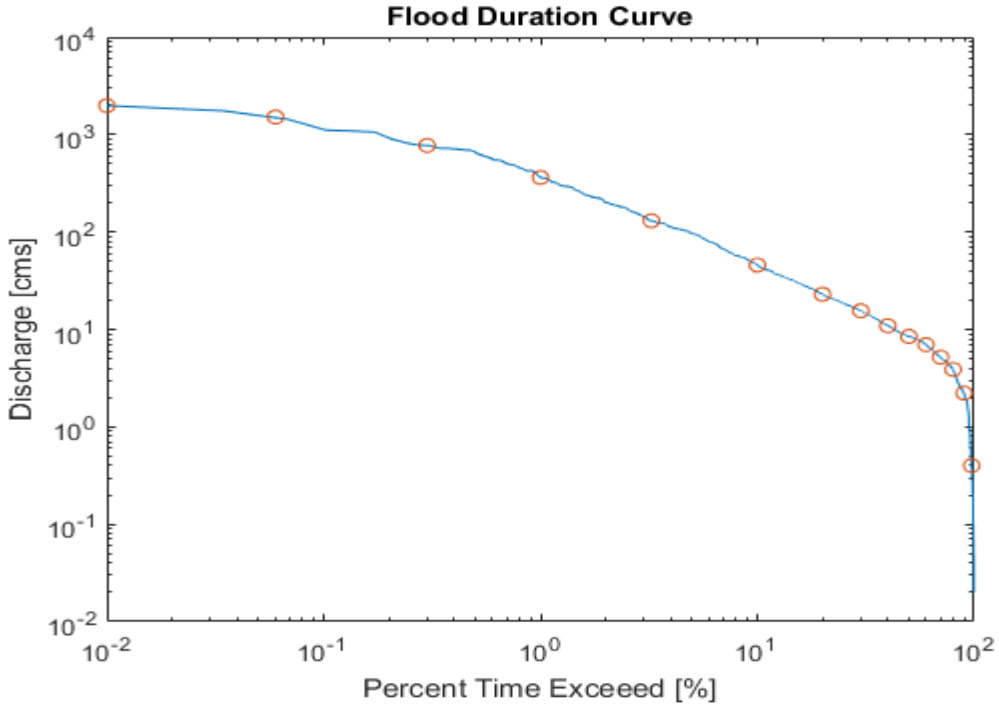

Specific Degradation

$$SD = 365 \times Q_s \left[\frac{tons}{day}\right] \div Area[km^2] = \frac{450.60 \times 365}{1134.1} = 145.16 \frac{tons}{km^2 \cdot year}$$

Opinion

NU14 Taesu

Daily Stage and Discharge

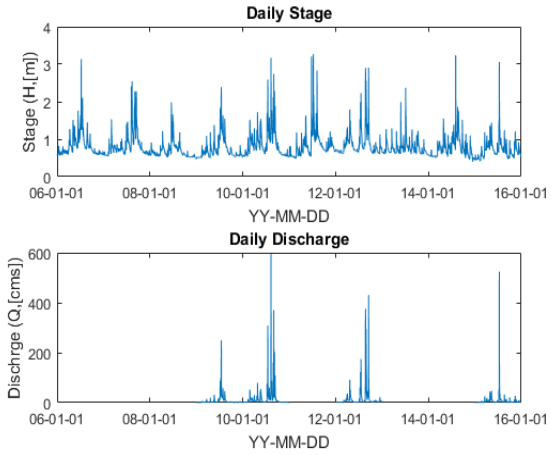

Sediment Rating Curve

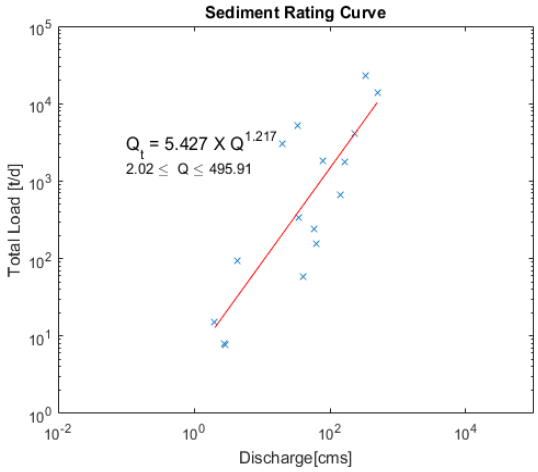

Flow Duration Curve

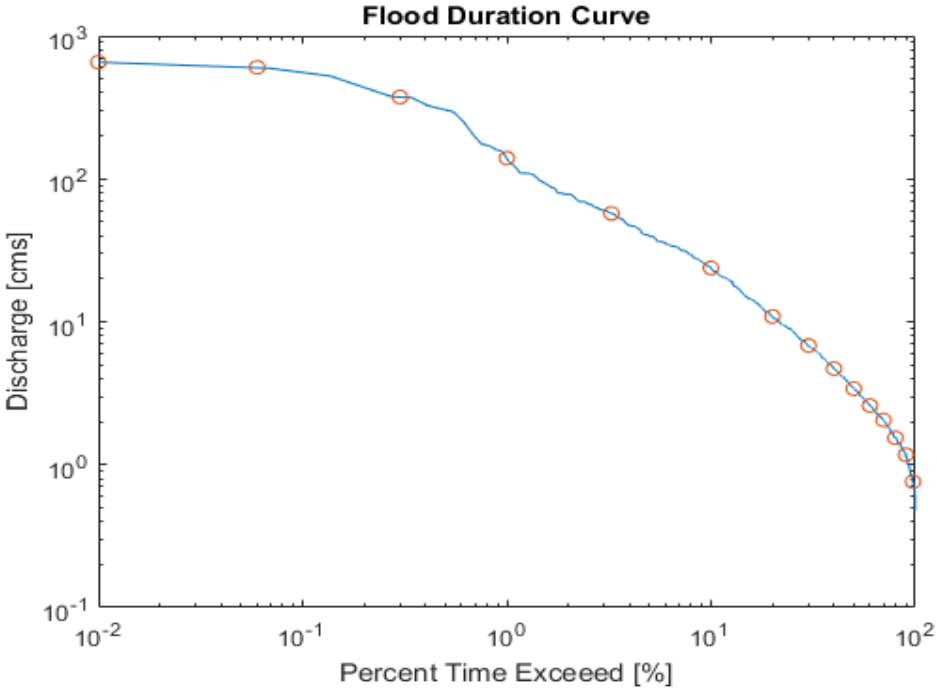

Specific Degradation

$$SD = 365 \times Q_s \left[\frac{tons}{day}\right] \div Area[km^2] = \frac{142.82 \times 365}{243} = 214.5 \frac{tons}{km^2 \cdot year}$$

Opinion

NU15 Imcheon

Daily Stage and Discharge

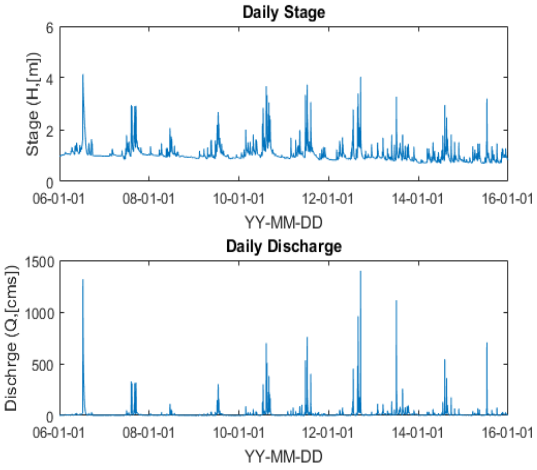

Sediment Rating Curve

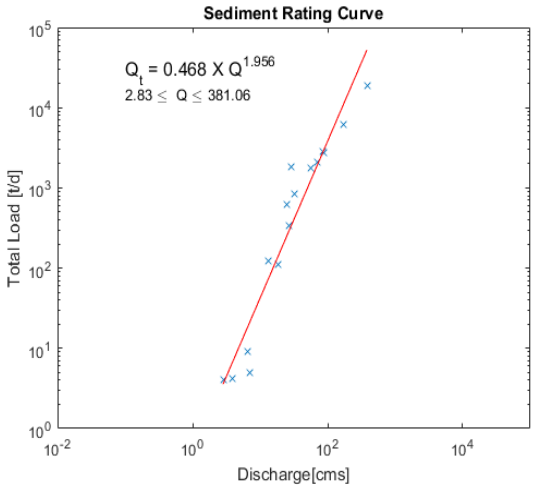

Flow Duration Curve

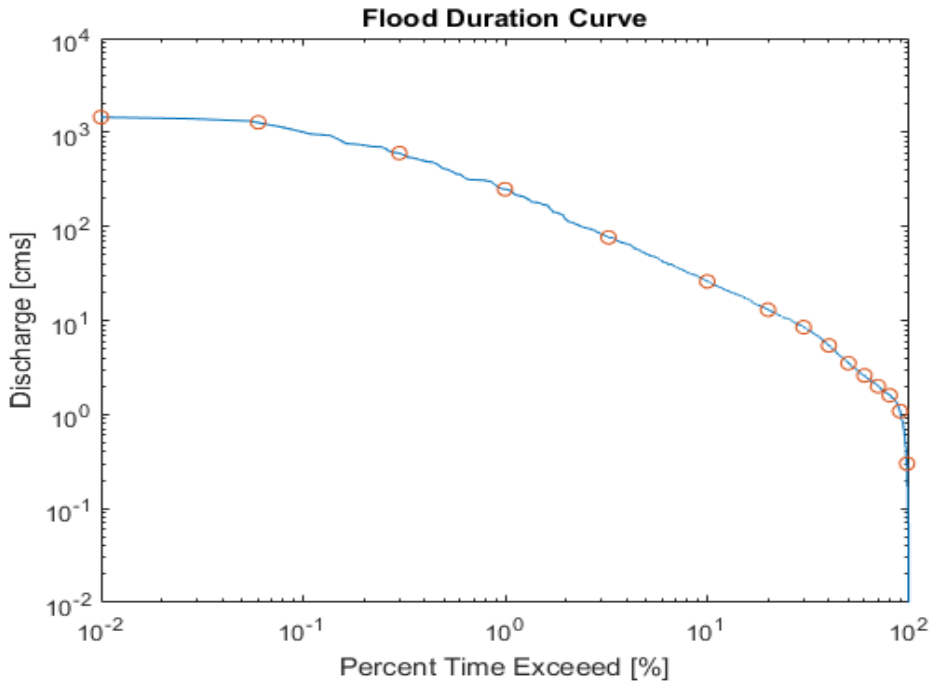

Specific Degradation

$$SD = 365 \times Q_s \left[\frac{tons}{day}\right] \div Area[km^2] = \frac{142.82 \times 365}{243} = 214.5 \frac{tons}{km^2 \cdot year}$$

Opinion

SD could be distorted due to small measurements

NU16 Oesong

Daily Stage and Discharge

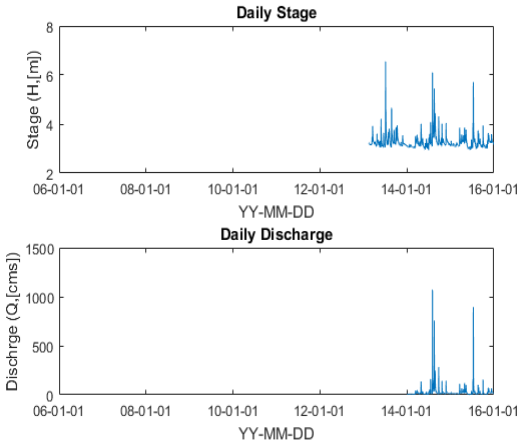

Sediment Rating Curve

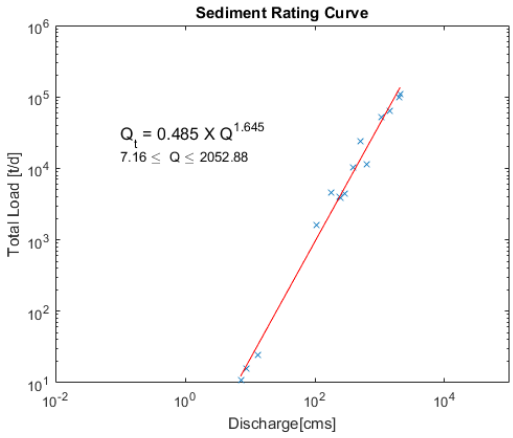

Flow Duration Curve

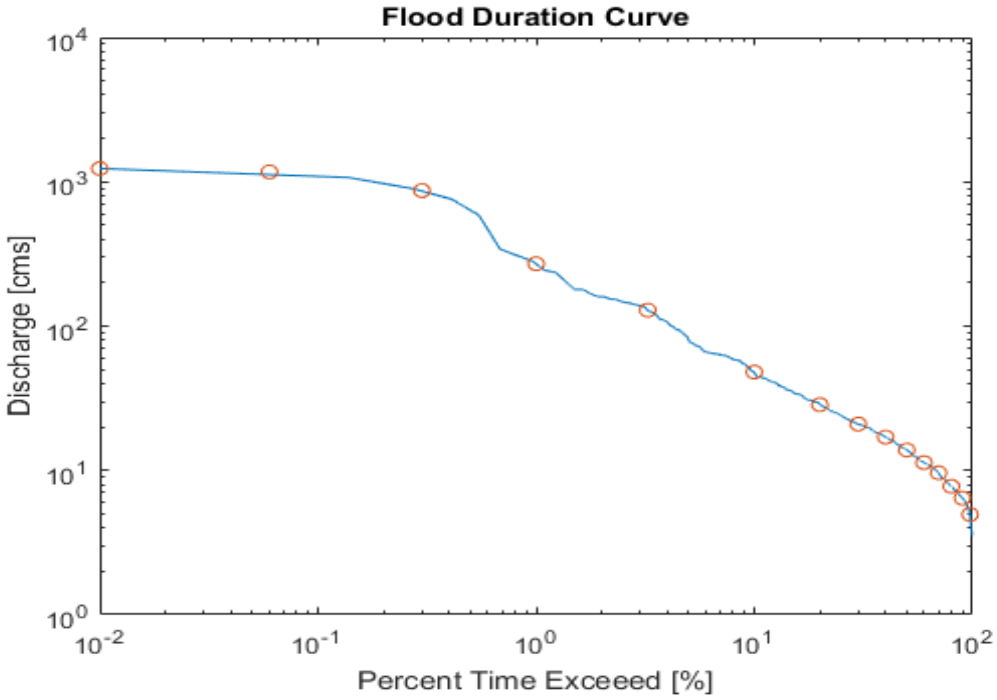

Specific Degradation

$$SD = 365 \times Q_s \left[\frac{tons}{day}\right] \div Area[km^2] = \frac{349.39 \times 365}{1231.5} = 103.65 \frac{tons}{km^2 \cdot year}$$

Opinion

G1 Hoedeok

Daily Stage and Discharge

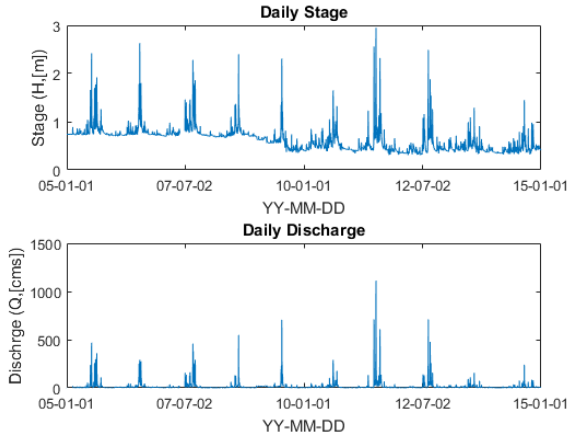

Sediment Rating Curve

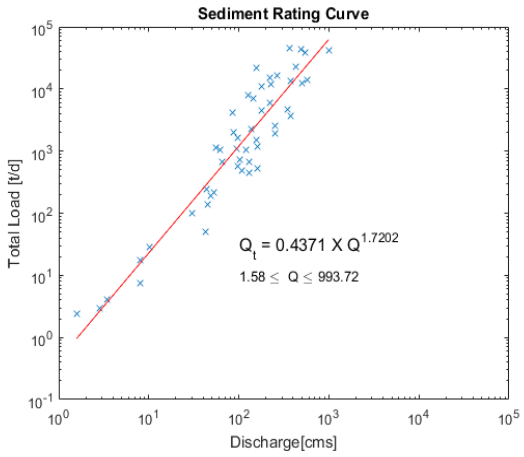

Flow Duration Curve

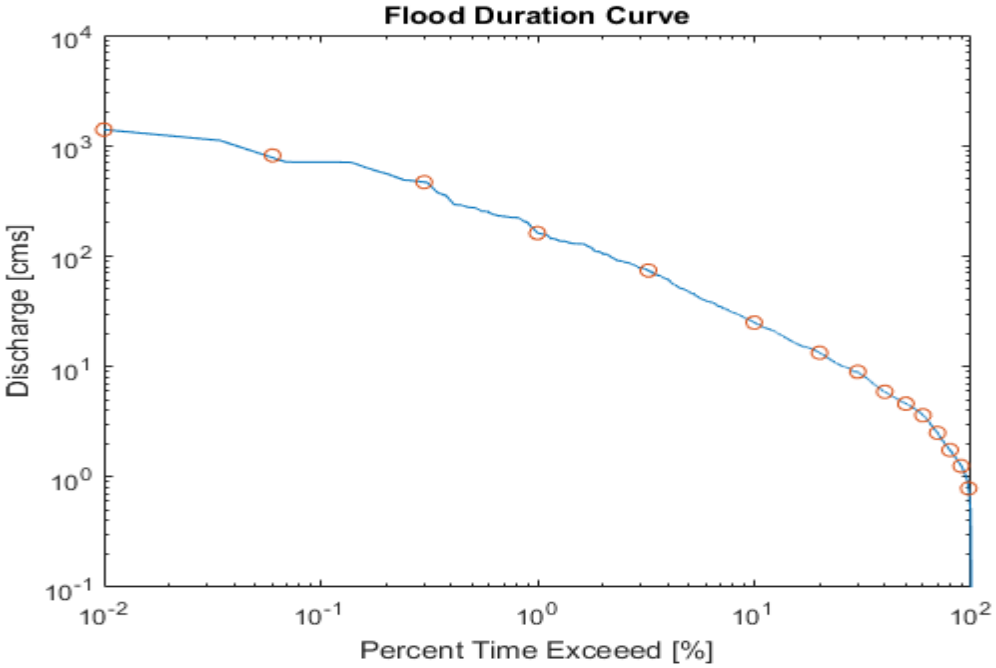

Specific Degradation

$$SD = 365 \times Q_s \left[\frac{tons}{day}\right] \div Area[km^2] = \frac{197.91 \times 365}{606.4} = 119.24 \frac{tons}{km^2 \cdot year}$$

Opinion

G2 Gongju

Daily Stage and Discharge

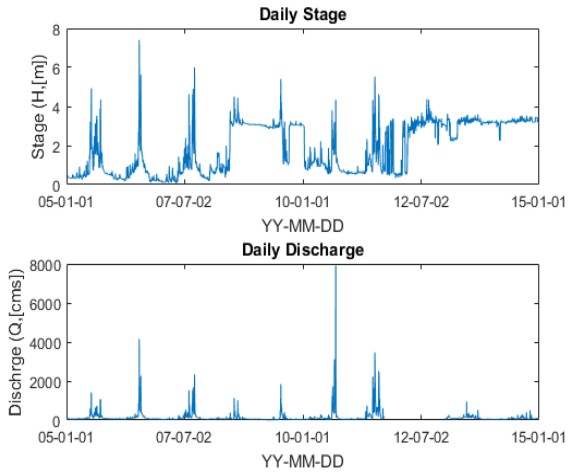

Sediment Rating Curve

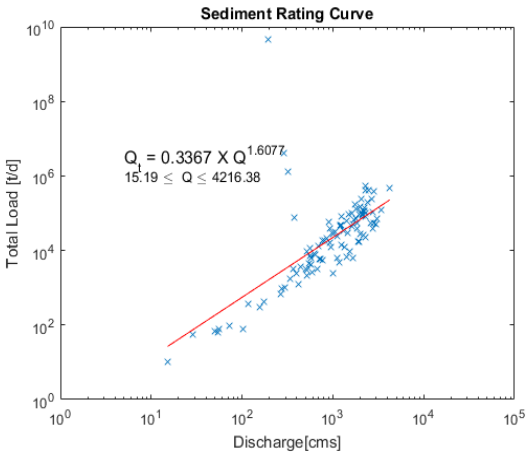

Flow Duration Curve

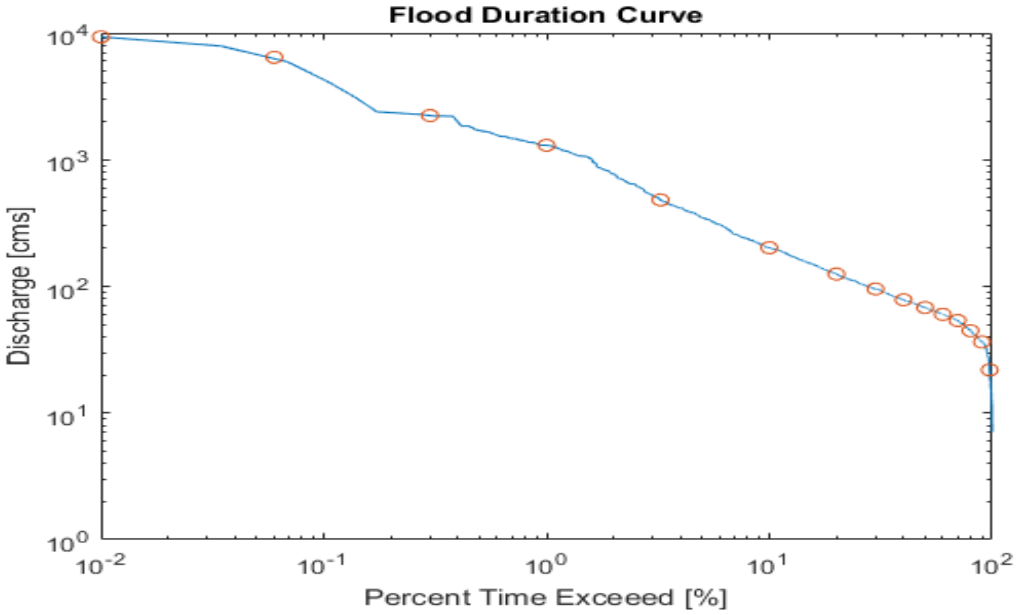

Specific Degradation

$$SD = 365 \times Q_s \left[\frac{tons}{day}\right] \div Area[km^2] = \frac{1869.76 \times 365}{6275.1} = 108.76 \frac{tons}{km^2 \cdot year}$$

Opinion

G3 Hapgang

Daily Stage and Discharge

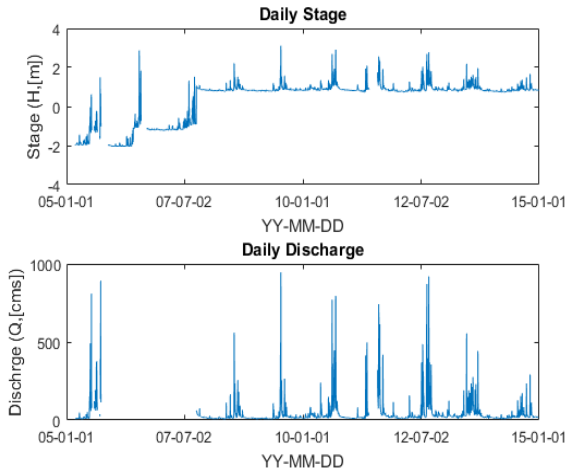

Sediment Rating Curve

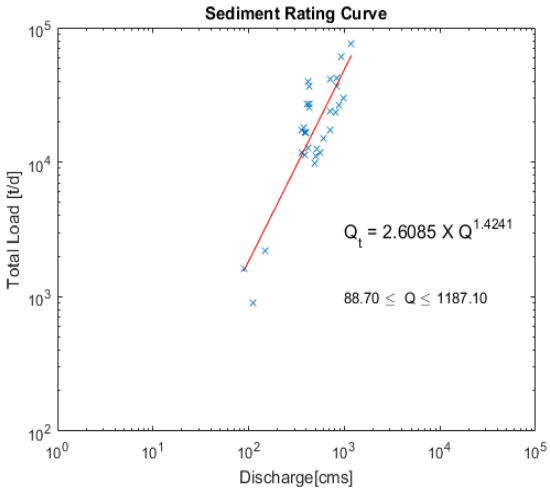

Flow Duration Curve

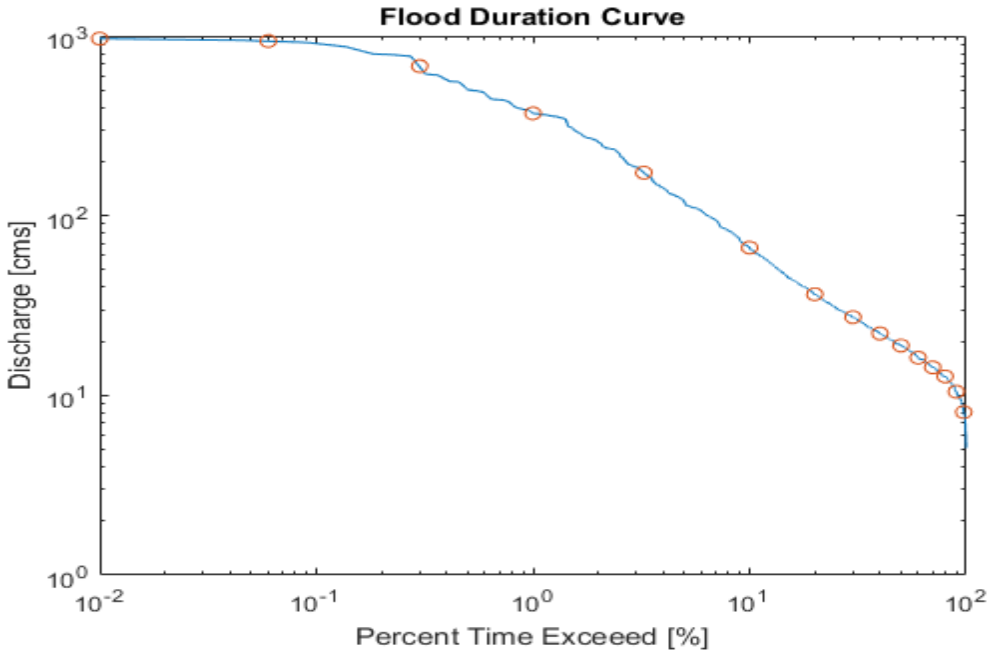

Specific Degradation

$$SD = 365 \times Q_s \left[\frac{tons}{day}\right] \div Area[km^2] = \frac{676.88 \times 365}{1850} = 133.54 \frac{tons}{km^2 \cdot year}$$

Opinion

G4 Useong

Daily Stage and Discharge

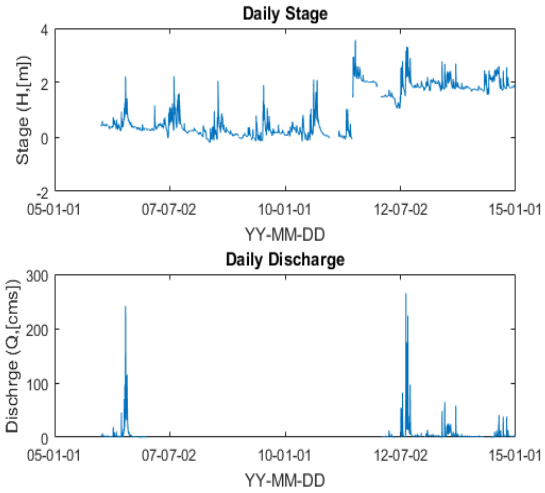

Sediment Rating Curve

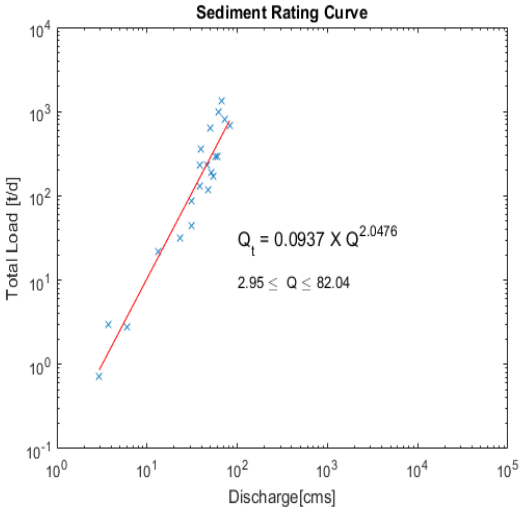

Flow Duration Curve

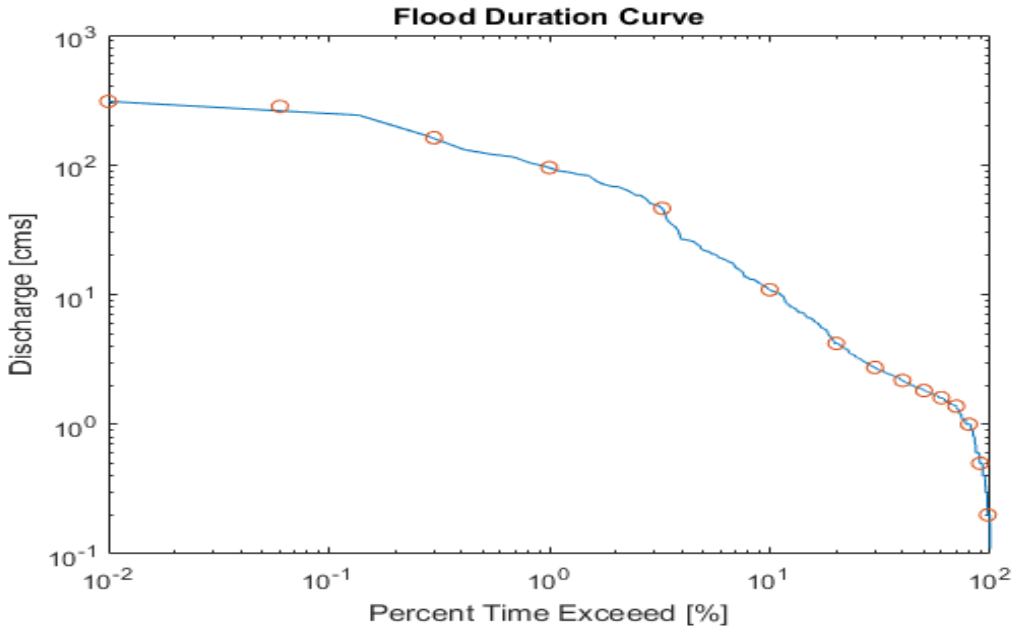

Specific Degradation

$$SD = 365 \times Q_s \left[\frac{tons}{day}\right] \div Area[km^2] = \frac{43.2 \times 365}{257.5} = 61.23 \frac{tons}{km^2 \cdot year}$$

Opinion

G5 Guryong

Daily Stage and Discharge

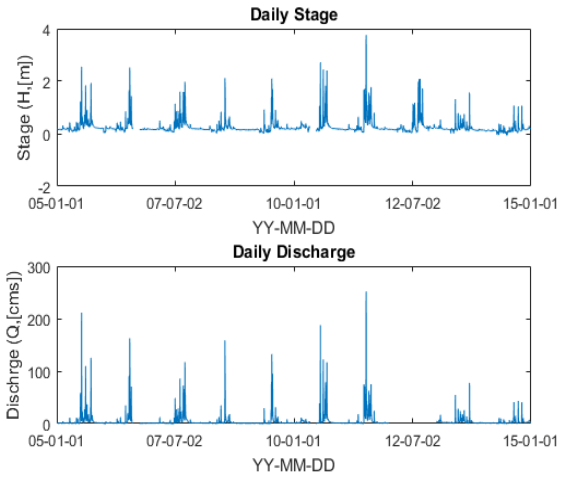

Sediment Rating Curve

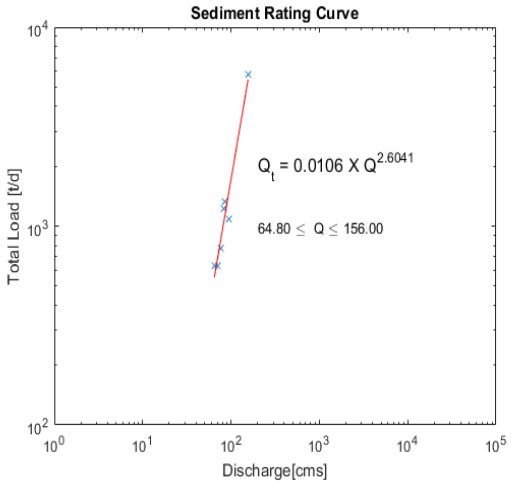

Flow Duration Curve

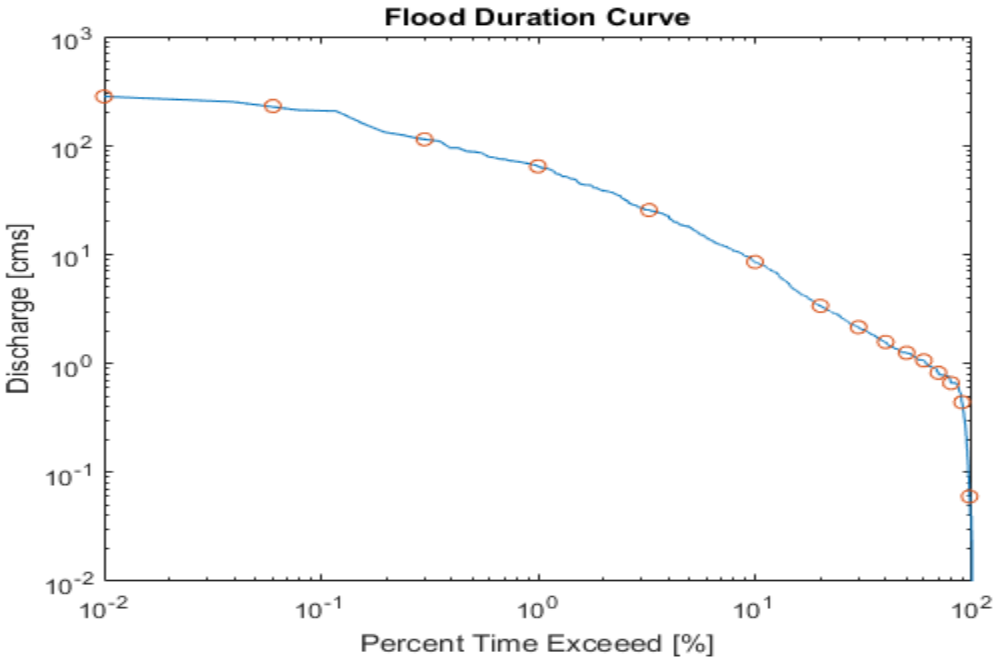

Specific Degradation

$$SD = 365 \times Q_s \left[\frac{tons}{day}\right] \div Area[km^2] = \frac{34.16 \times 365}{207.5} = 60.08 \frac{tons}{km^2 \cdot year}$$

Opinion

GU1 Okcheon

Daily Stage and Discharge

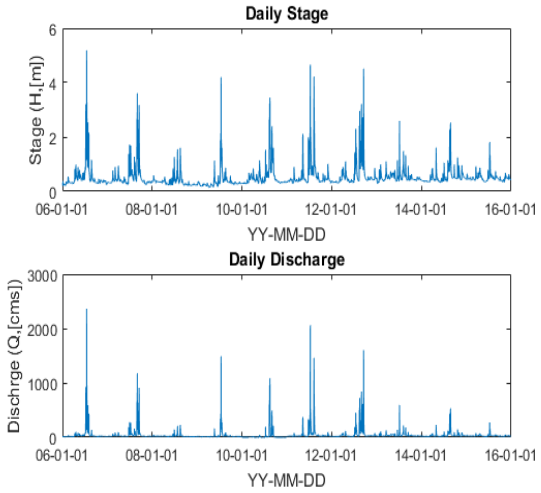

Sediment Rating Curve

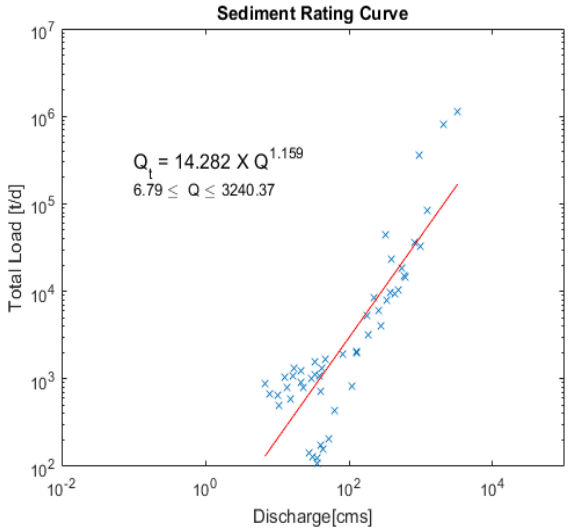

Flow Duration Curve

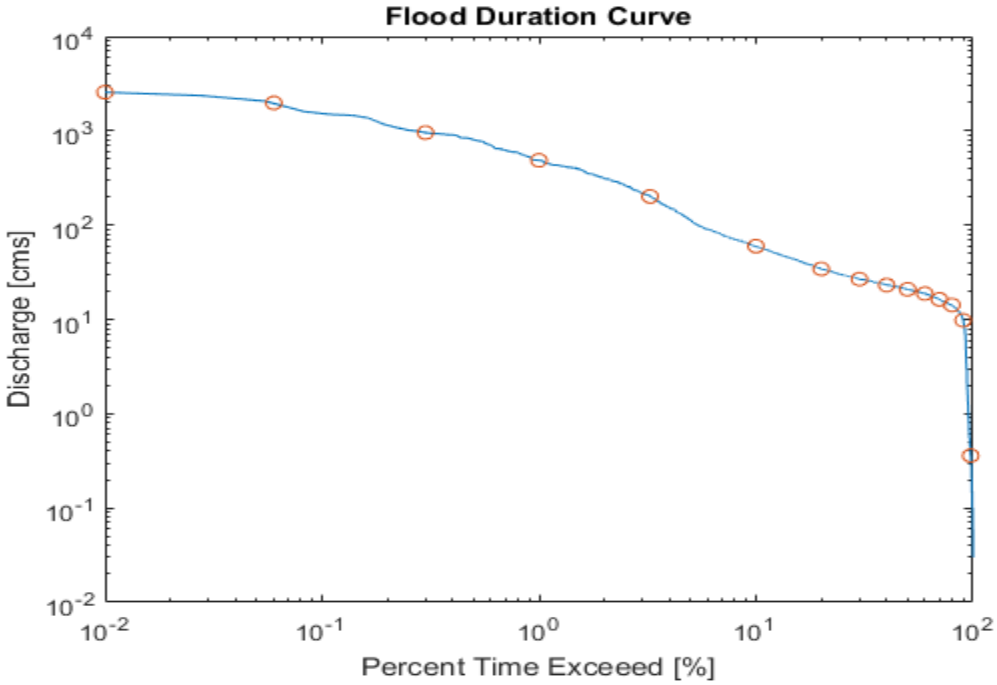

Specific Degradation

$$SD = 365 \times Q_s \left[\frac{tons}{day}\right] \div Area[km^2] = \frac{1226.92 \times 365}{1984.7} = 225.85 \frac{tons}{km^2 \cdot year}$$

Opinion

Different SRC result in each year 2009, 2010, 2015

GU2 Cheongseong

Daily Stage and Discharge

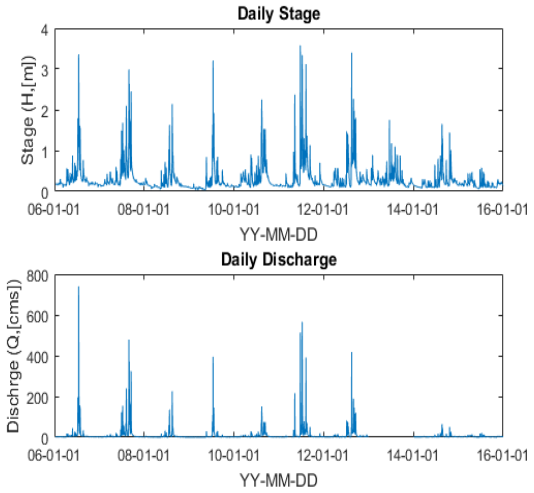

Sediment Rating Curve

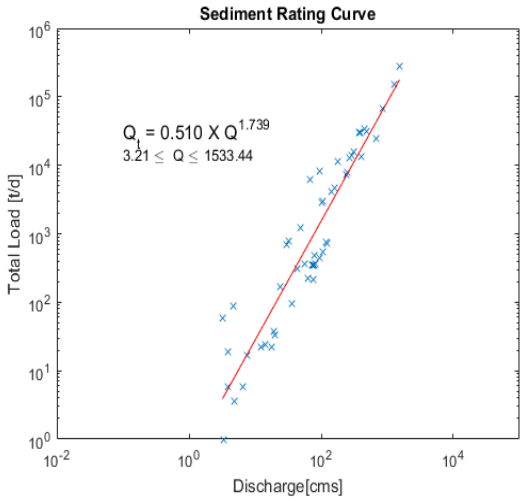

Flow Duration Curve

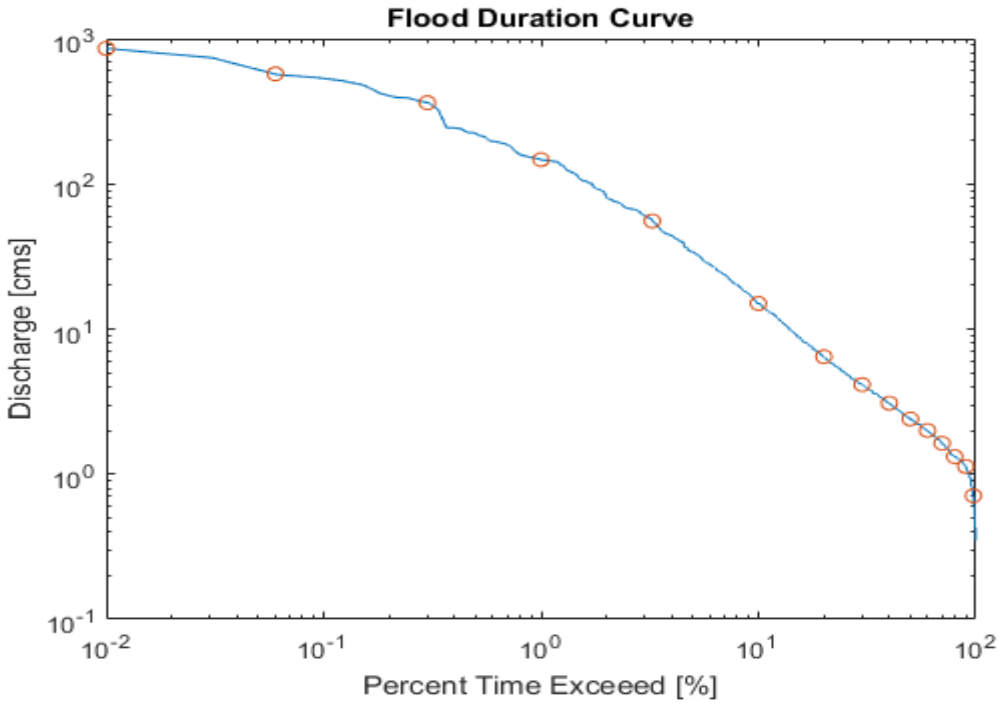

Specific Degradation

$$SD = 365 \times Q_s \left[\frac{tons}{day}\right] \div Area[km^2] = \frac{154.01 \times 365}{481.9} = 114.76 \frac{tons}{km^2 \cdot year}$$

Opinion

GU3 Hotan

Daily Stage and Discharge

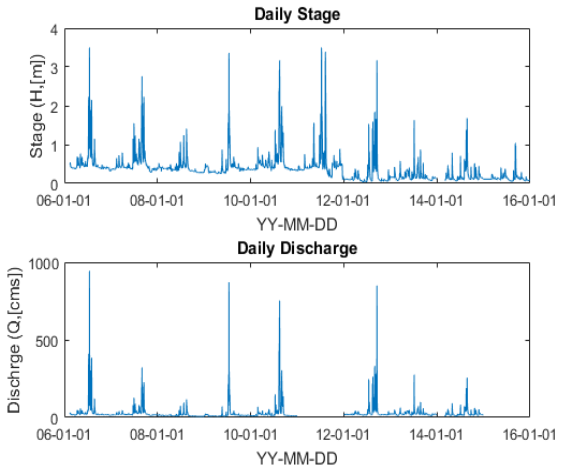

Sediment Rating Curve

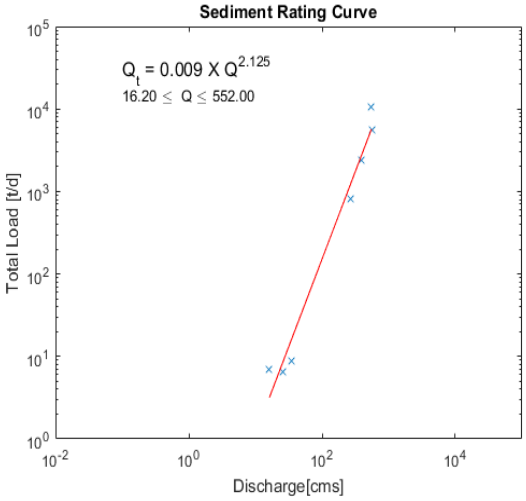

Flow Duration Curve

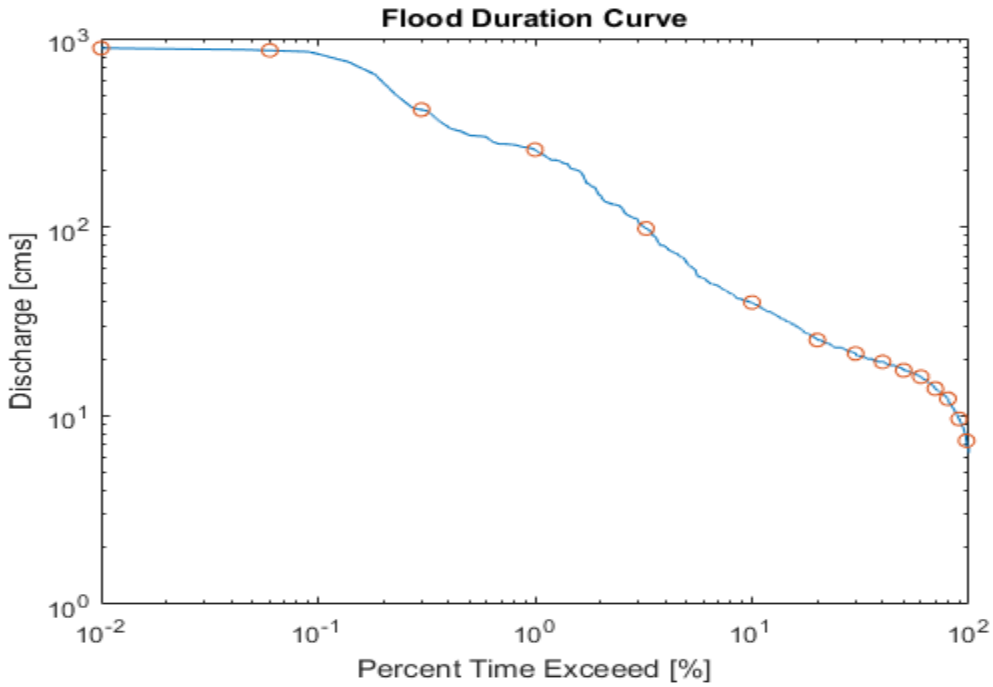

Specific Degradation

$$SD = 365 \times Q_s \left[\frac{tons}{day}\right] \div Area[km^2] = \frac{49.35 \times 365}{991.90} = 18.18 \frac{tons}{km^2 \cdot year}$$

Opinion

SD could be distorted due to small measurements

GU4 Cheoncheon

Daily Stage and Discharge

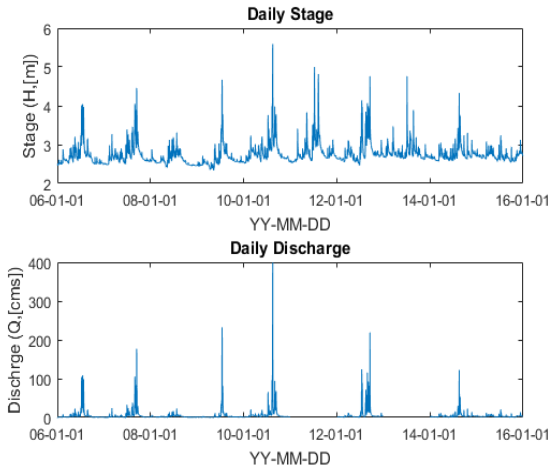

Sediment Rating Curve

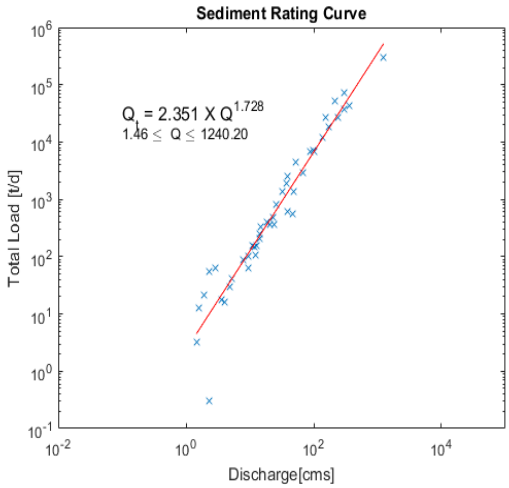

Flow Duration Curve

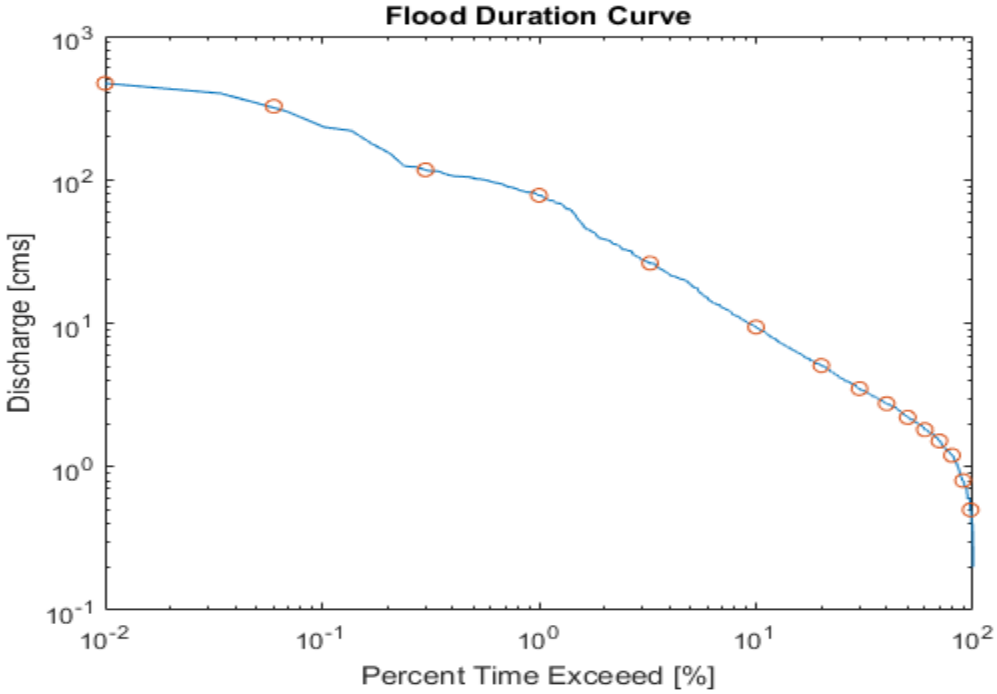

Specific Degradation

$$SD = 365 \times Q_s \left[\frac{tons}{day}\right] \div Area[km^2] = \frac{183.57 \times 365}{291.0} = 230.47 \frac{tons}{km^2 \cdot year}$$

Opinion

GU5 Donghyang

Daily Stage and Discharge

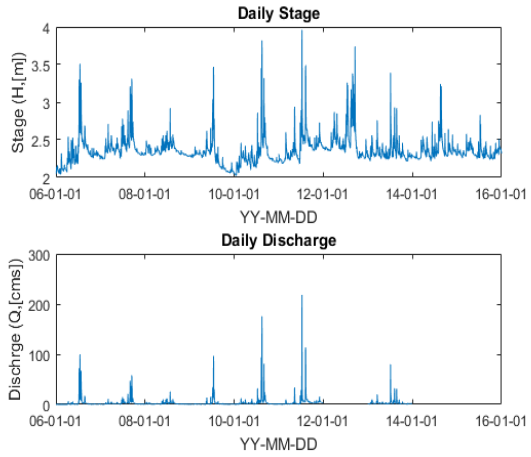

Sediment Rating Curve

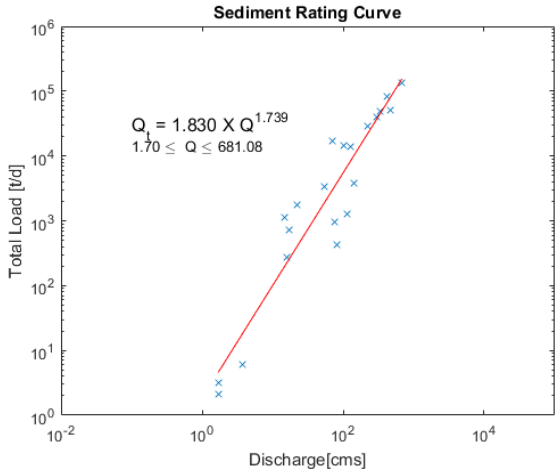

Flow Duration Curve

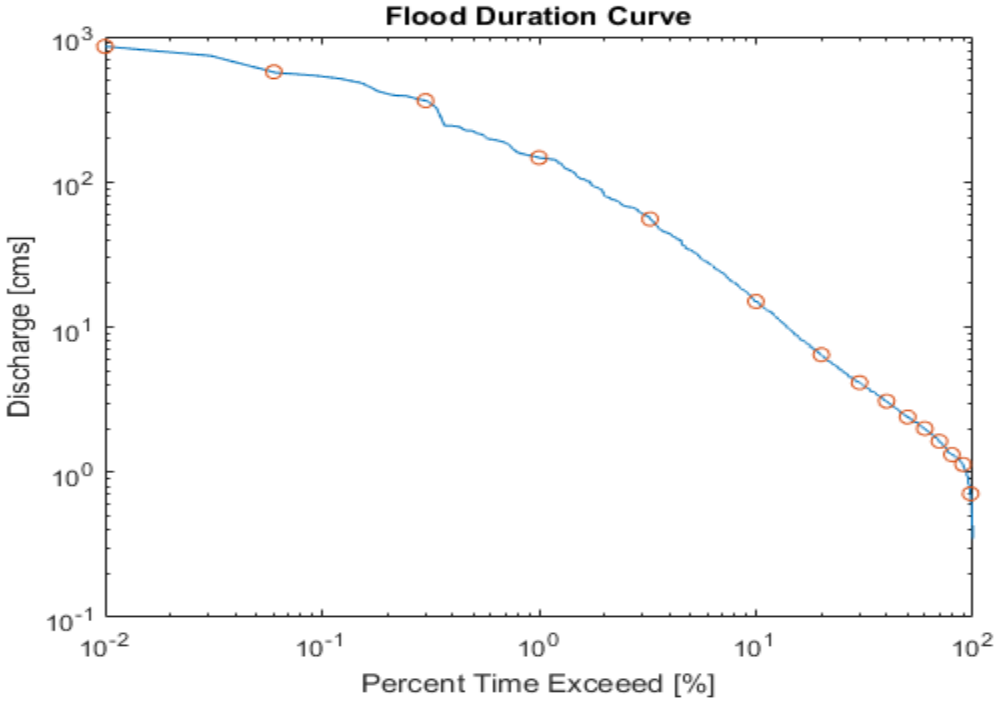

Specific Degradation

$$SD = 365 \times Q_s \left[\frac{tons}{day}\right] \div Area[km^2] = \frac{67.04 \times 365}{166.2} = 147.38 \frac{tons}{km^2 \cdot year}$$

Opinion

Y1 Hakgyo

Daily Stage and Discharge

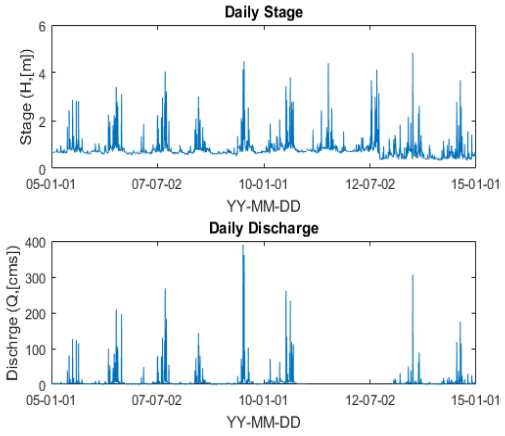

Sediment Rating Curve

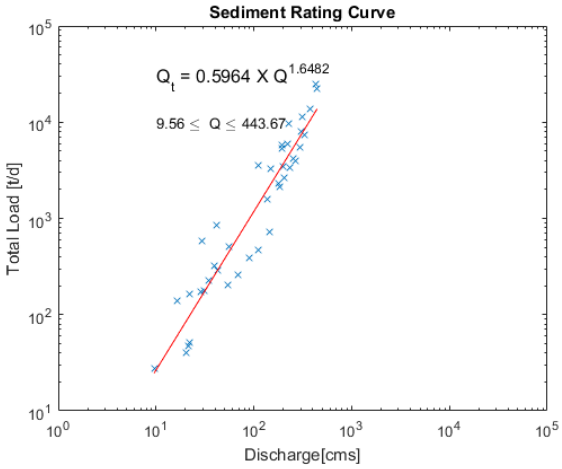

Flow Duration Curve

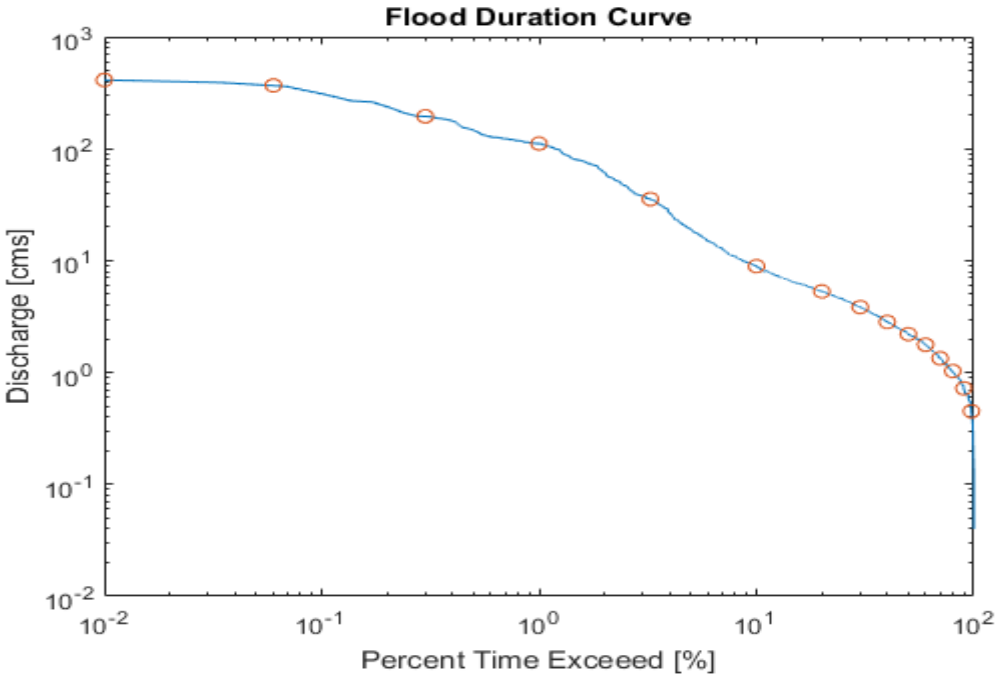

Specific Degradation

$$SD = 365 \times Q_s \left[\frac{tons}{day}\right] \div Area[km^2] = \frac{50.76 \times 365}{190.1} = 97.45 \frac{tons}{km^2 \cdot year}$$

Opinion

Y2 Naju

Daily Stage and Discharge

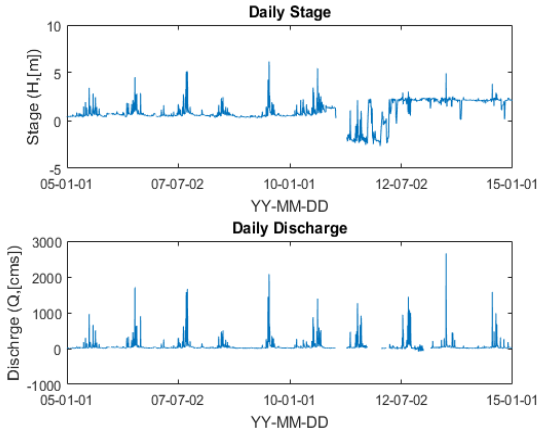

Sediment Rating Curve

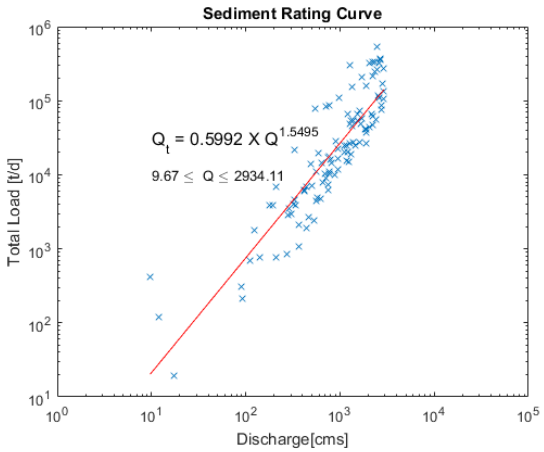

Flow Duration Curve

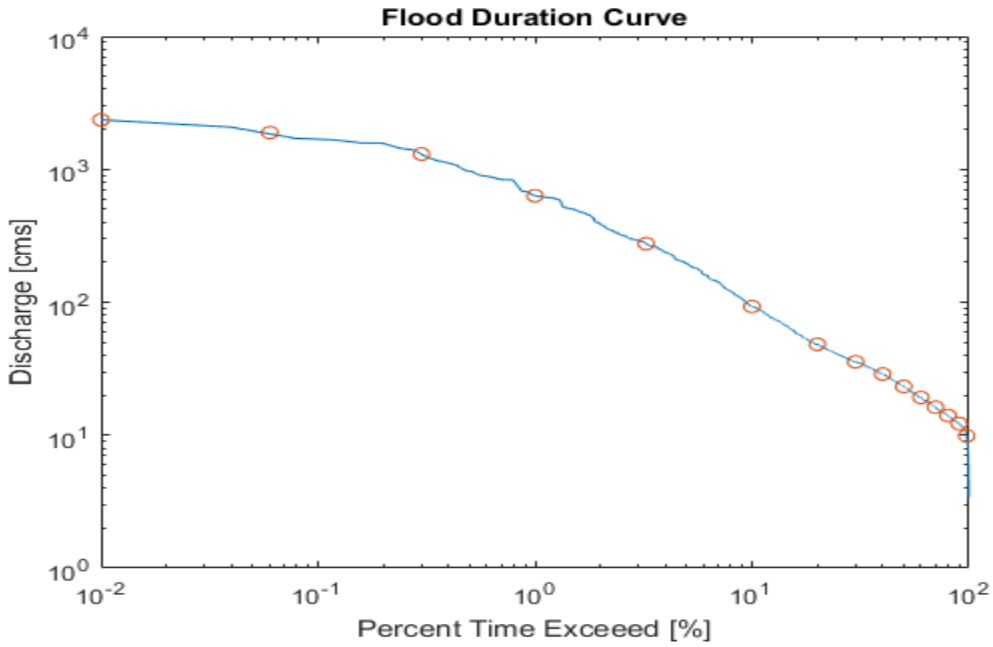

Specific Degradation

$$SD = 365 \times Q_s \left[\frac{tons}{day}\right] \div Area[km^2] = \frac{638.8 \times 365}{2039} = 114.35 \frac{tons}{km^2 \cdot year}$$

Opinion

Y3 Mareuk

Daily Stage and Discharge

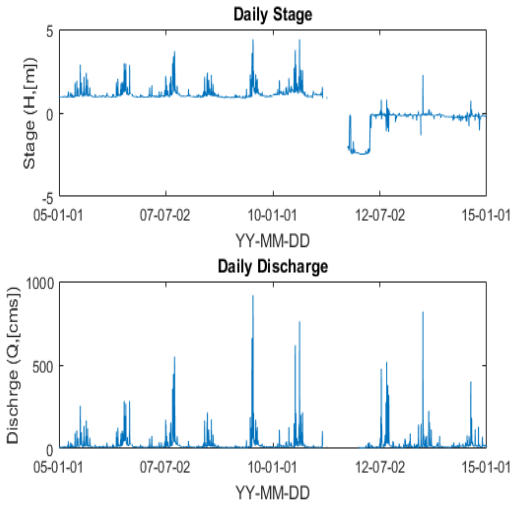

Sediment Rating Curve

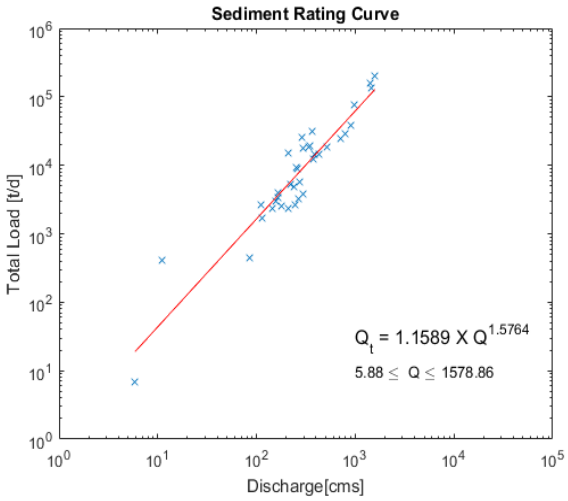

Flow Duration Curve

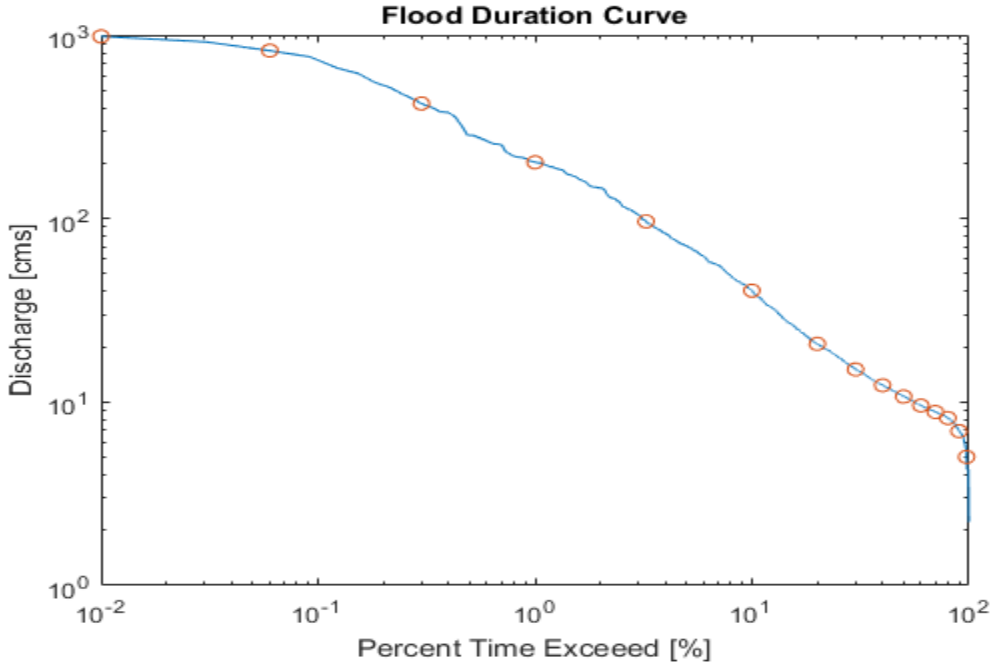

Specific Degradation

$$SD = 365 \times Q_s \left[\frac{tons}{day}\right] \div Area[km^2] = \frac{189.56 \times 365}{668.2} = 165.99 \frac{tons}{km^2 \cdot year}$$

Opinion

Y4 Nampyeong

Daily Stage and Discharge

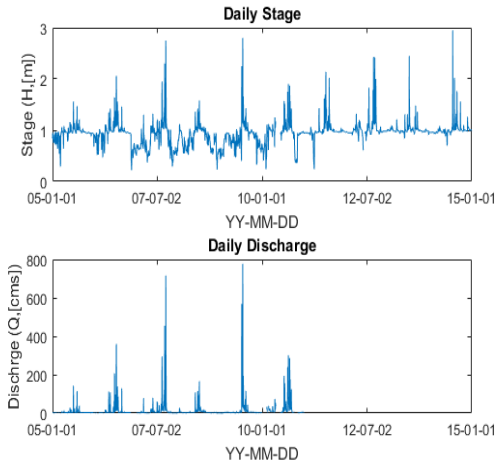

Sediment Rating Curve

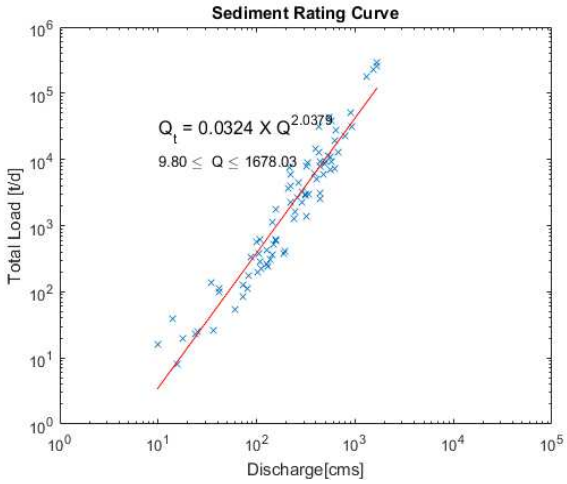

Flow Duration Curve

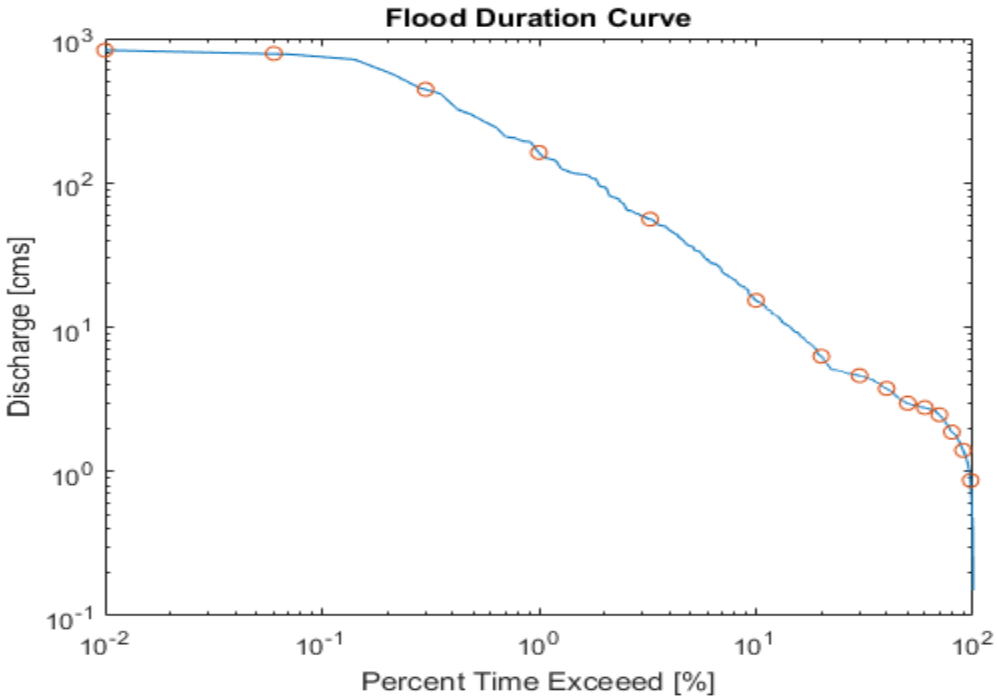

Specific Degradation

$$SD = 365 \times Q_s \left[\frac{tons}{day}\right] \div Area[km^2] = \frac{74.27 \times 365}{580.7} = 46.75 \frac{tons}{km^2 \cdot year}$$

Opinion

Y5 Seonam

Daily Stage and Discharge

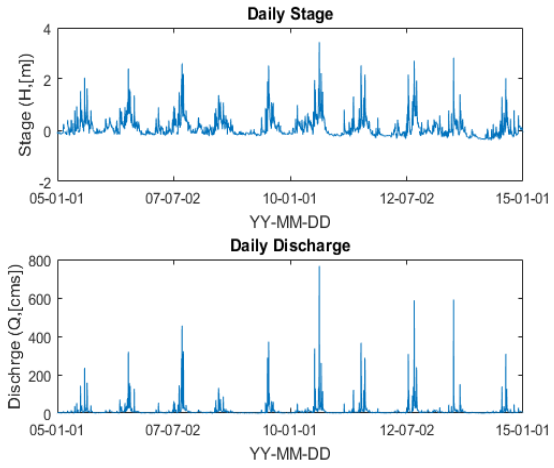

Sediment Rating Curve

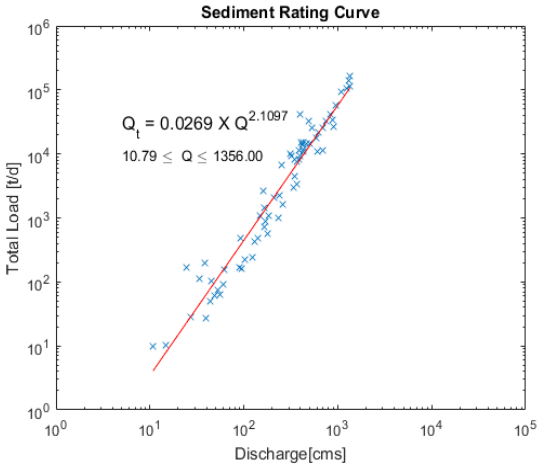

Flow Duration Curve

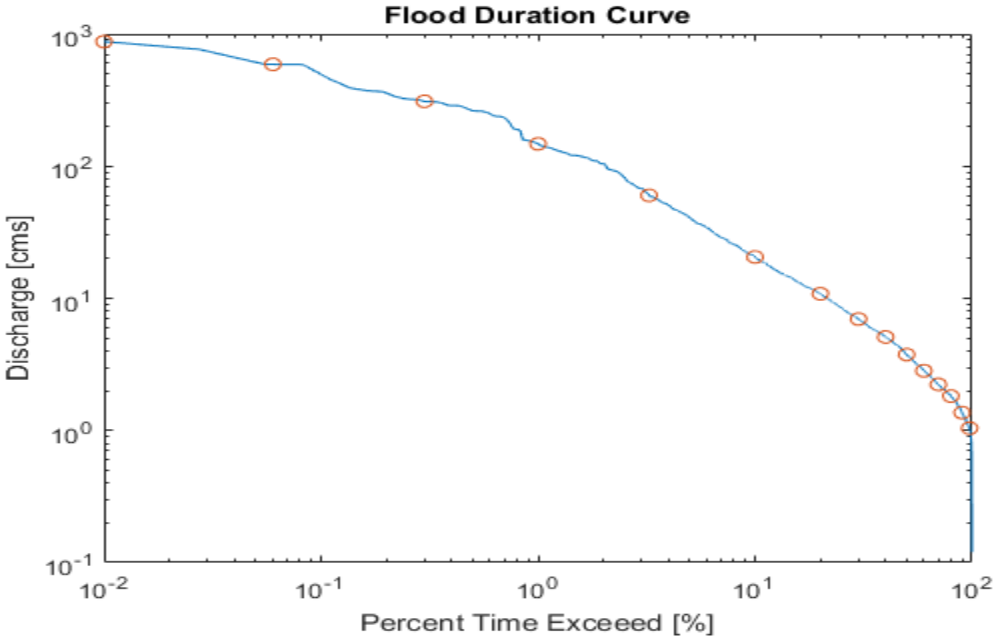

Specific Degradation

$$SD = 365 \times Q_s \left[\frac{tons}{day}\right] \div Area[km^2] = \frac{61.00 \times 365}{551.9} = 40.37 \frac{tons}{km^2 \cdot year}$$

Opinion

YU1 Bongdeok

Daily Stage and Discharge

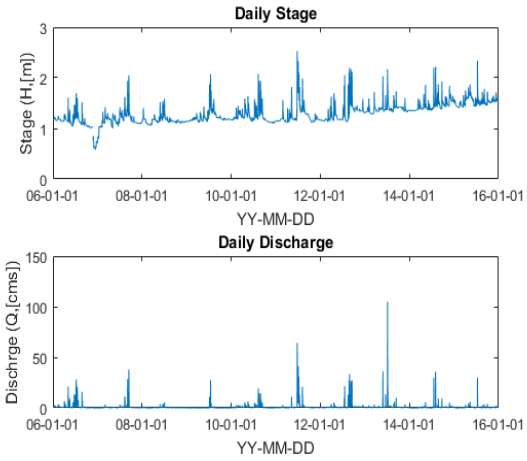

Sediment Rating Curve

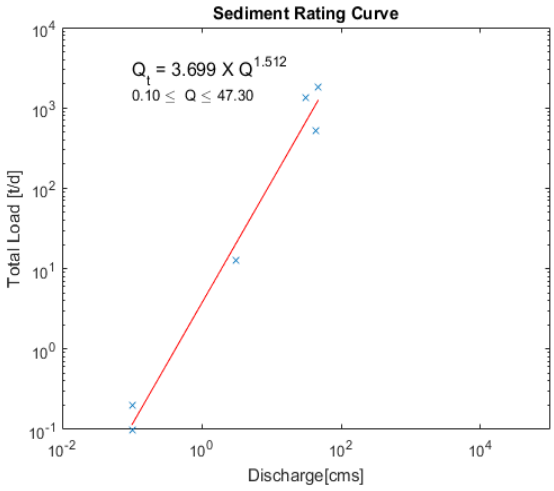

Flow Duration Curve

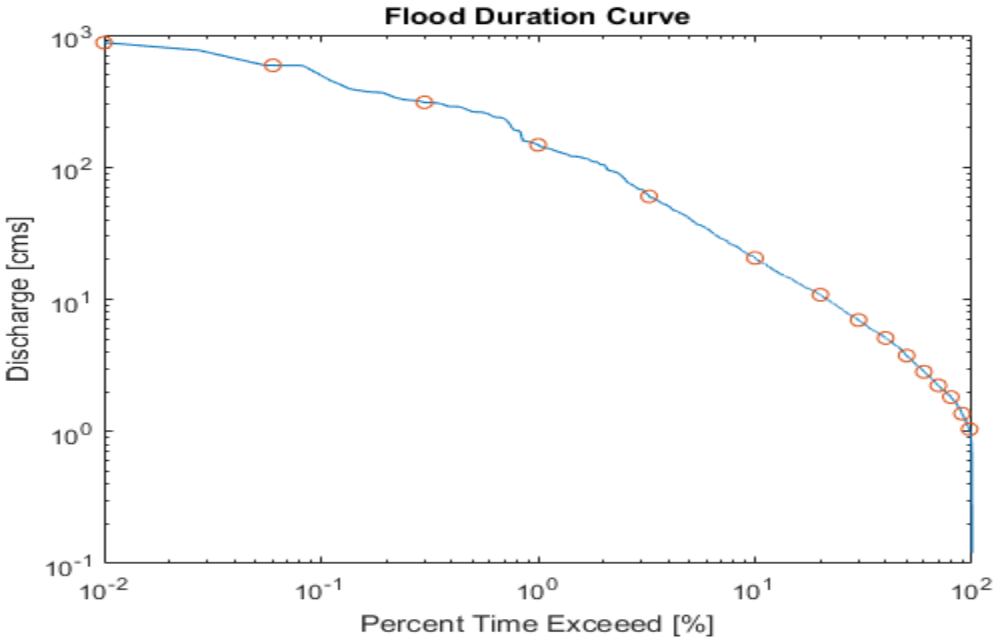

Specific Degradation

$$SD = 365 \times Q_s \left[\frac{tons}{day}\right] \div Area[km^2] = \frac{9.83 \times 365}{46.6} = 77.36 \frac{tons}{km^2 \cdot year}$$

Opinion

SD could be distorted due to small measurements

S1 Jukgok

Daily Stage and Discharge

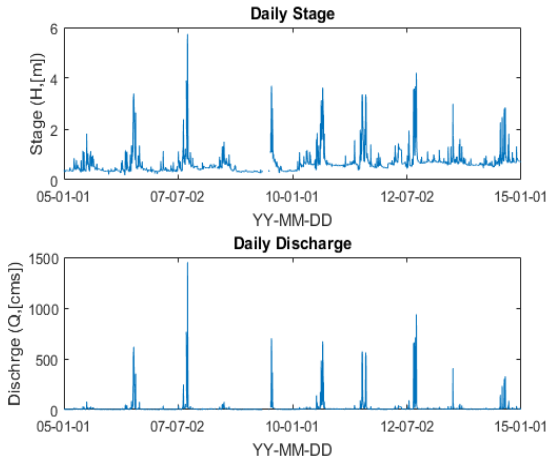

Sediment Rating Curve

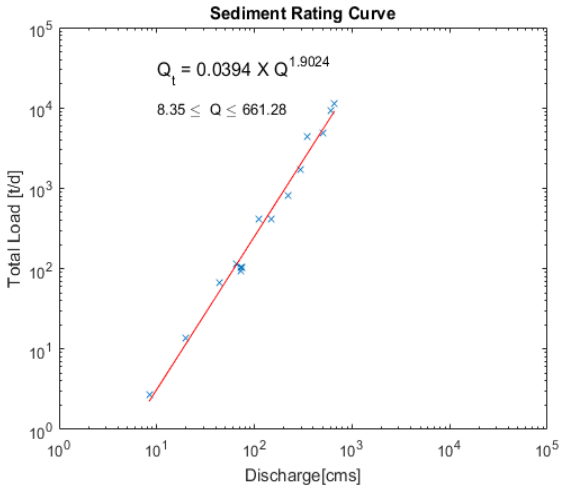

Flow Duration Curve

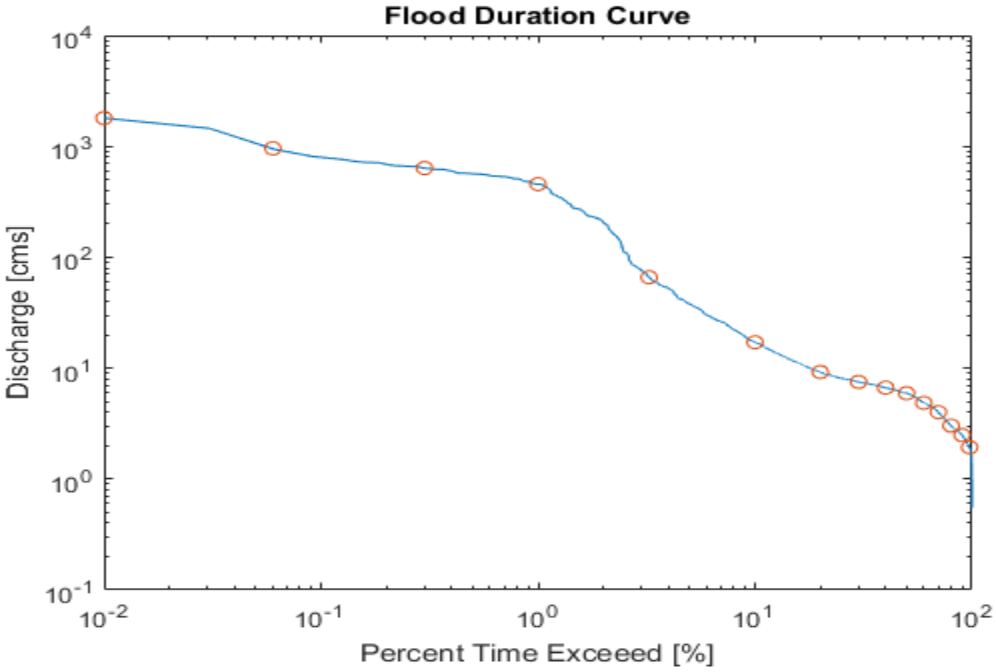

Specific Degradation

$$SD = 365 \times Q_s \left[\frac{tons}{day}\right] \div Area[km^2] = \frac{111.72 \times 365}{1268.5} = 32.15 \frac{tons}{km^2 \cdot year}$$

Opinion

SD could be distorted due to small measurements

S2 Gokseong

Daily Stage and Discharge

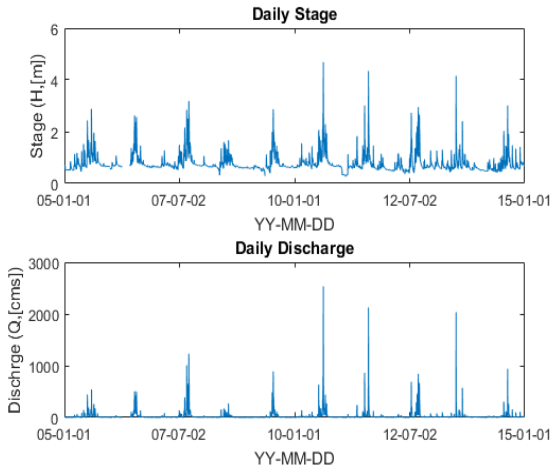

Sediment Rating Curve

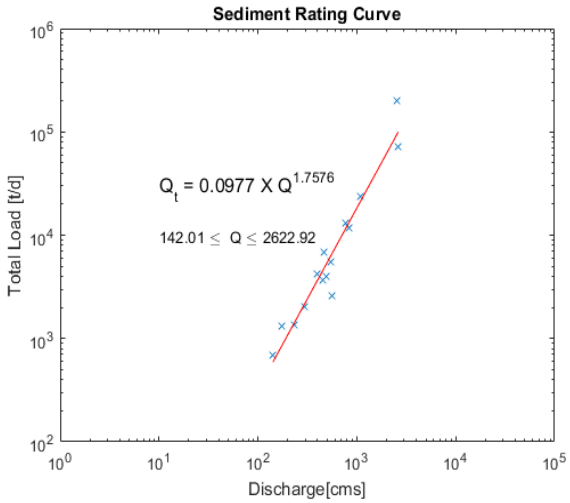

Flow Duration Curve

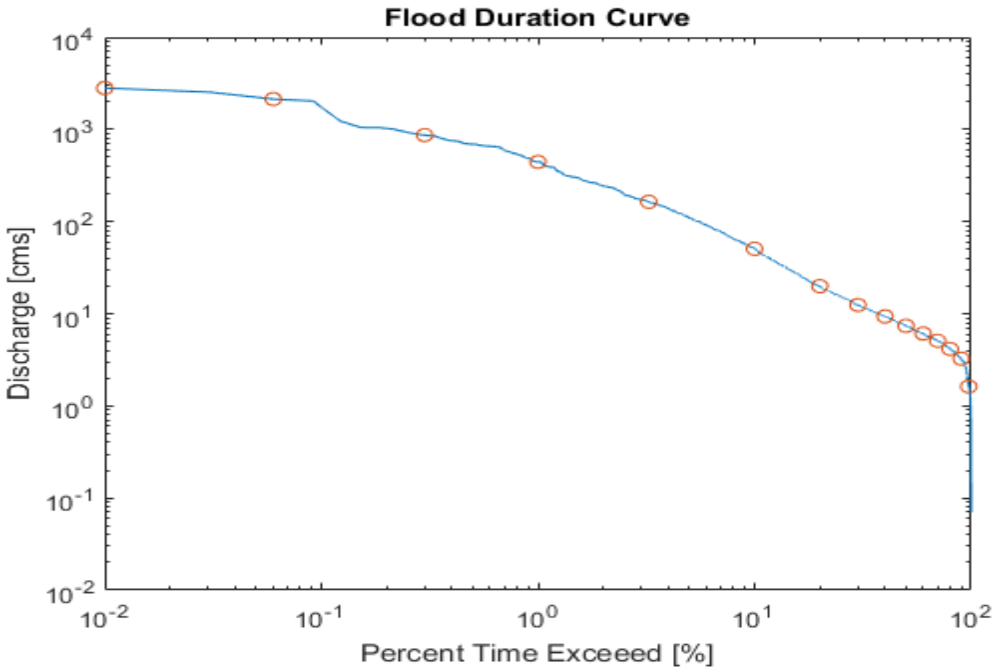

Specific Degradation

$$SD = 365 \times Q_s \left[\frac{tons}{day}\right] \div Area[km^2] = \frac{189.56 \times 365}{1787.7} = 44.85 \frac{tons}{km^2 \cdot year}$$

Opinion

SD could be distorted due to small measurements

S3 Gurye2

Daily Stage and Discharge

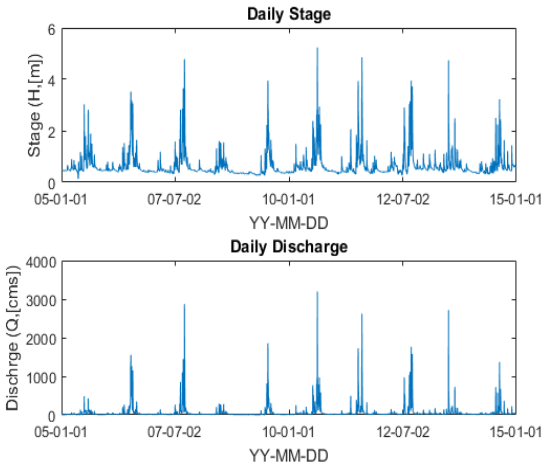

Sediment Rating Curve

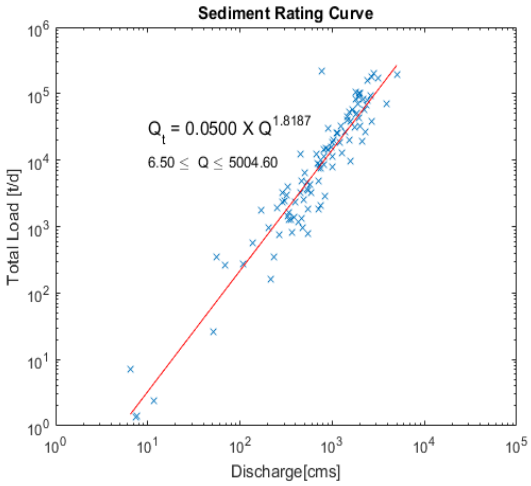

Flow Duration Curve

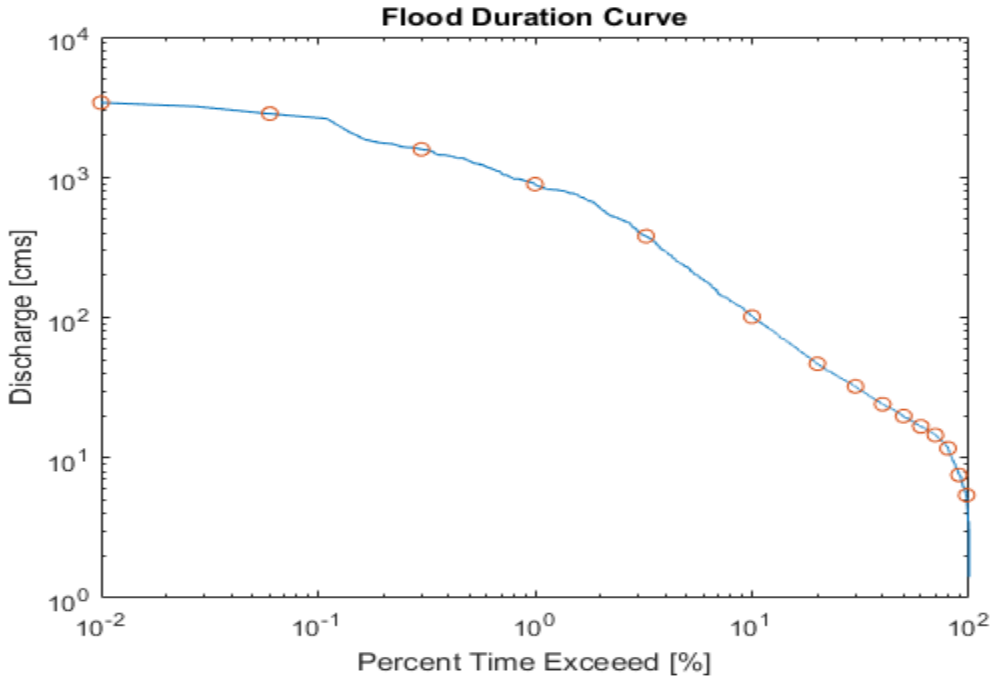

Specific Degradation

$$SD = 365 \times Q_s \left[\frac{tons}{day}\right] \div Area[km^2] = \frac{472.23 \times 365}{3817.7} = 70.69 \frac{tons}{km^2 \cdot year}$$

Opinion

S4 Yongseo

Daily Stage and Discharge

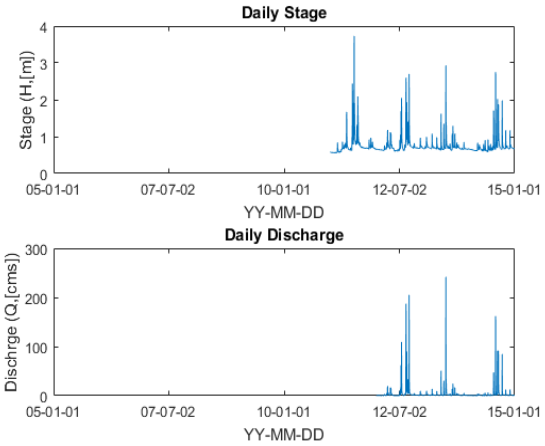

Sediment Rating Curve

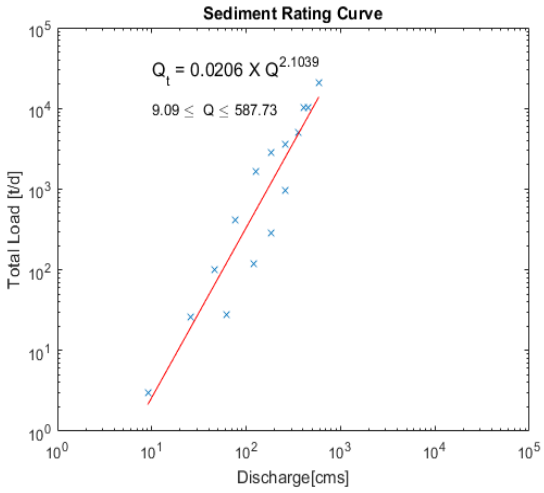

Flow Duration Curve

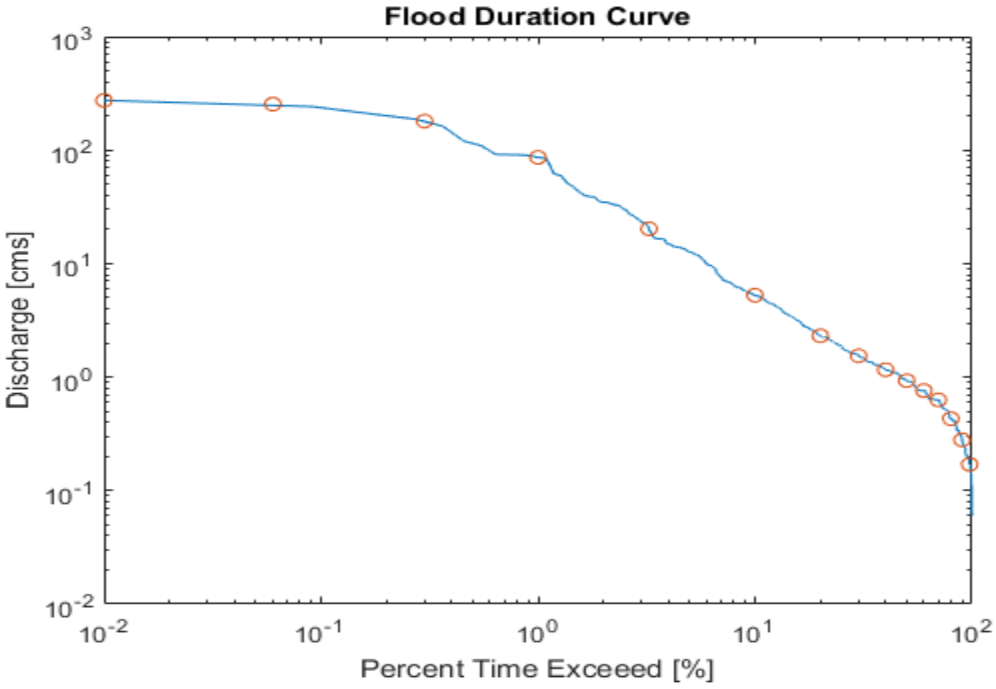

Specific Degradation

$$SD = 365 \times Q_s \left[\frac{tons}{day}\right] \div Area[km^2] = \frac{9.95 \times 365}{127.8} = 28.44 \frac{tons}{km^2 \cdot year}$$

Opinion

SD could be distorted due to small measurements

SU1 Gwanchon

Daily Stage and Discharge

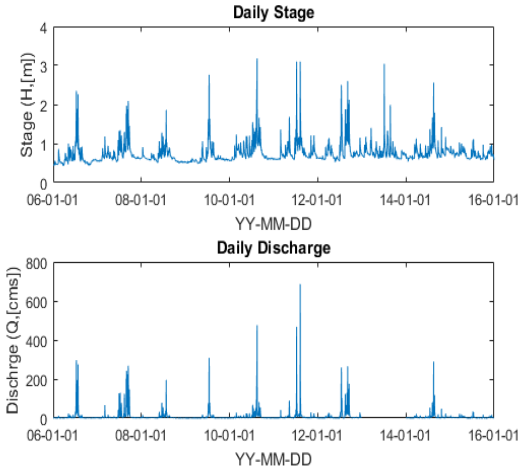

Sediment Rating Curve

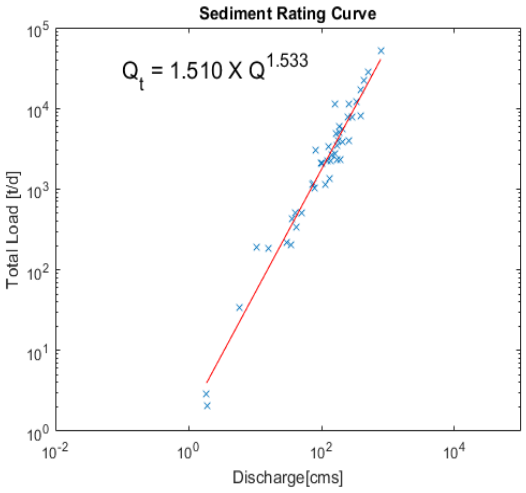

Flow Duration Curve

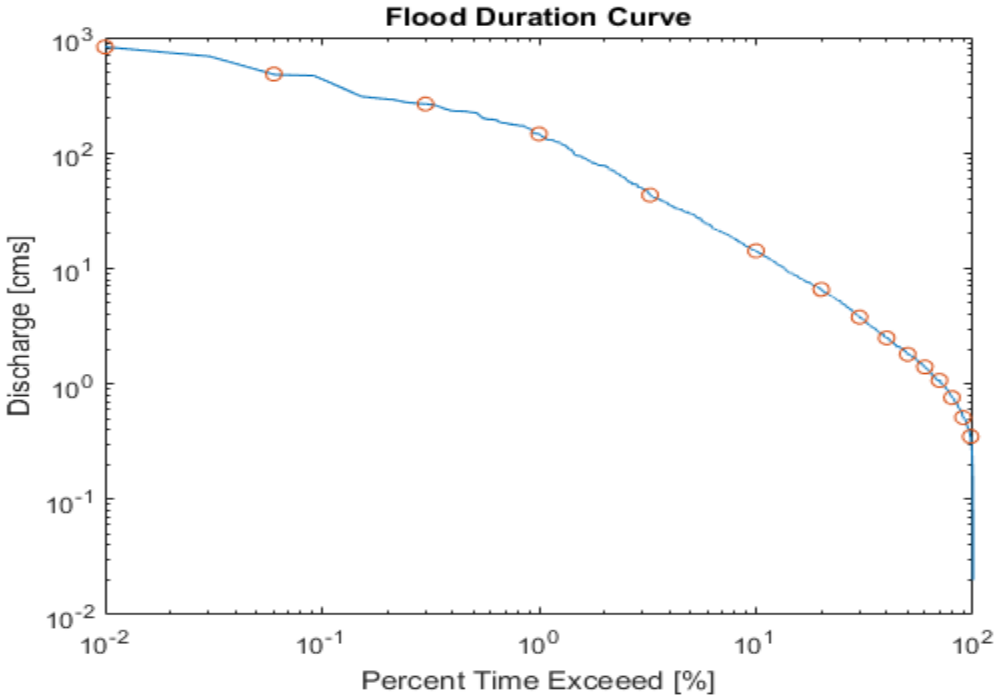

Specific Degradation

$$SD = 365 \times Q_s \left[\frac{tons}{day}\right] \div Area[km^2] = \frac{118.49 \times 365}{359.1} = 120.45 \frac{tons}{km^2 \cdot year}$$

Opinion

SU2 Ssangchi2

Daily Stage and Discharge

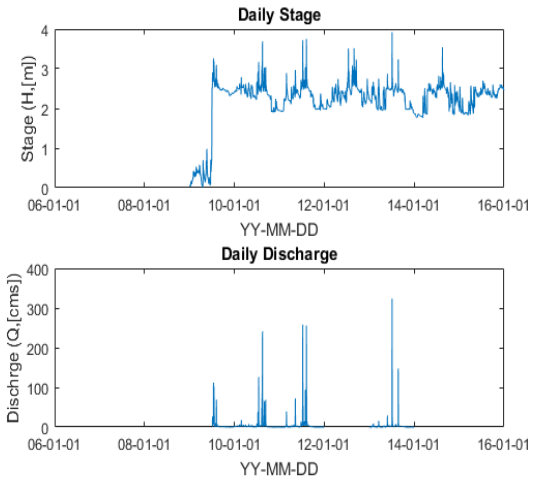

Sediment Rating Curve

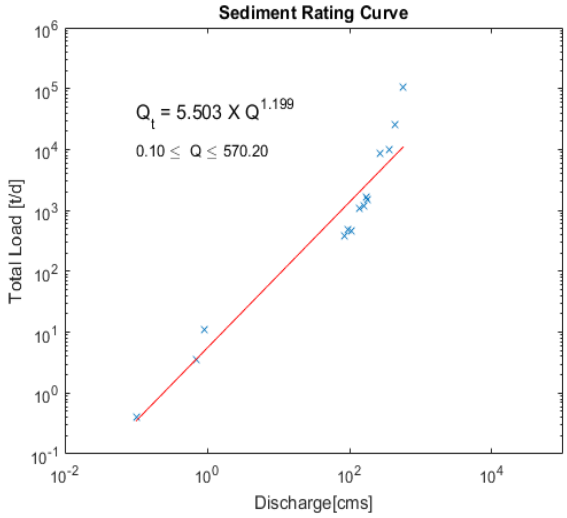

Flow Duration Curve

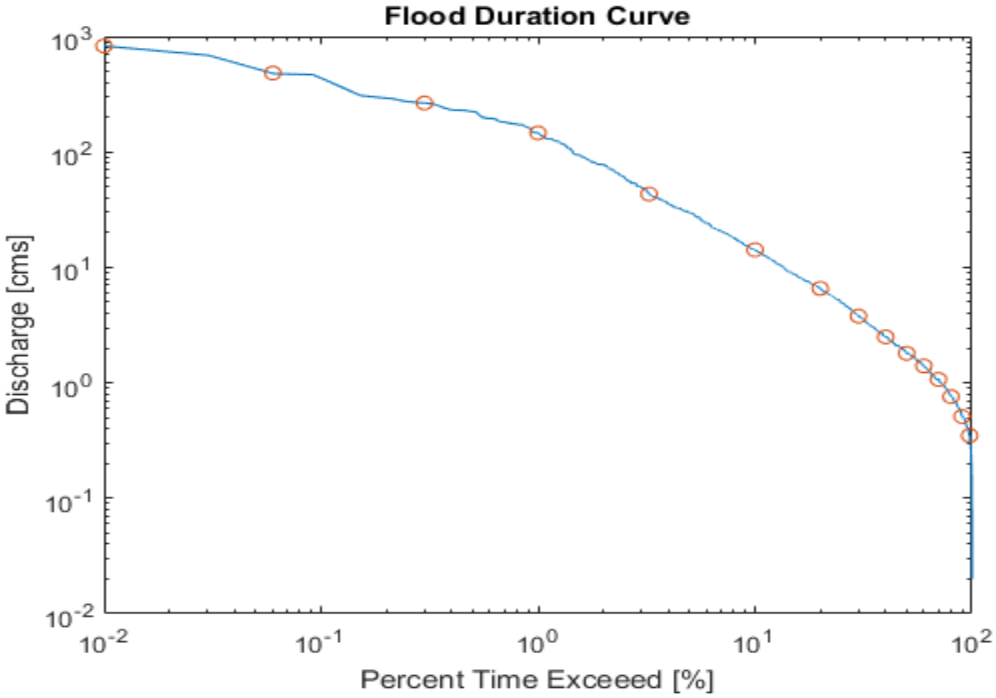

Specific Degradation

$$SD = 365 \times Q_s \left[\frac{tons}{day}\right] \div Area[km^2] = \frac{49.10 \times 365}{134} = 134.86 \frac{tons}{km^2 \cdot year}$$

Opinion

SD could be distorted due to small measurements

SU3 Gyeombaek

Daily Stage and Discharge

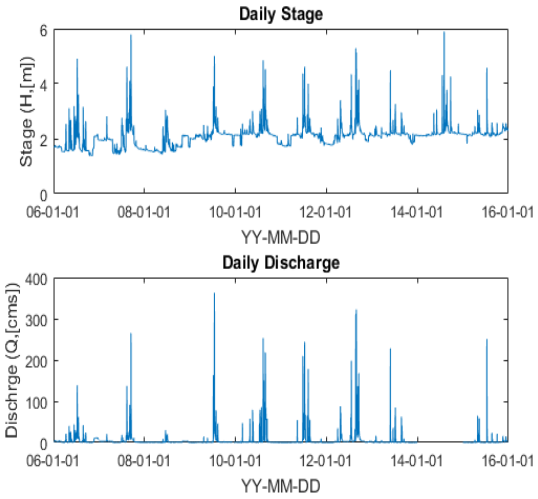

Sediment Rating Curve

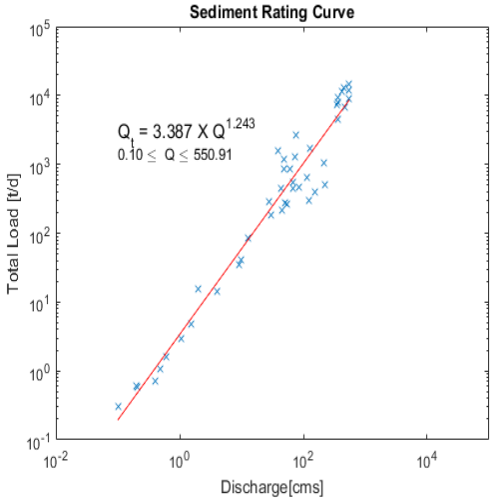

Flow Duration Curve

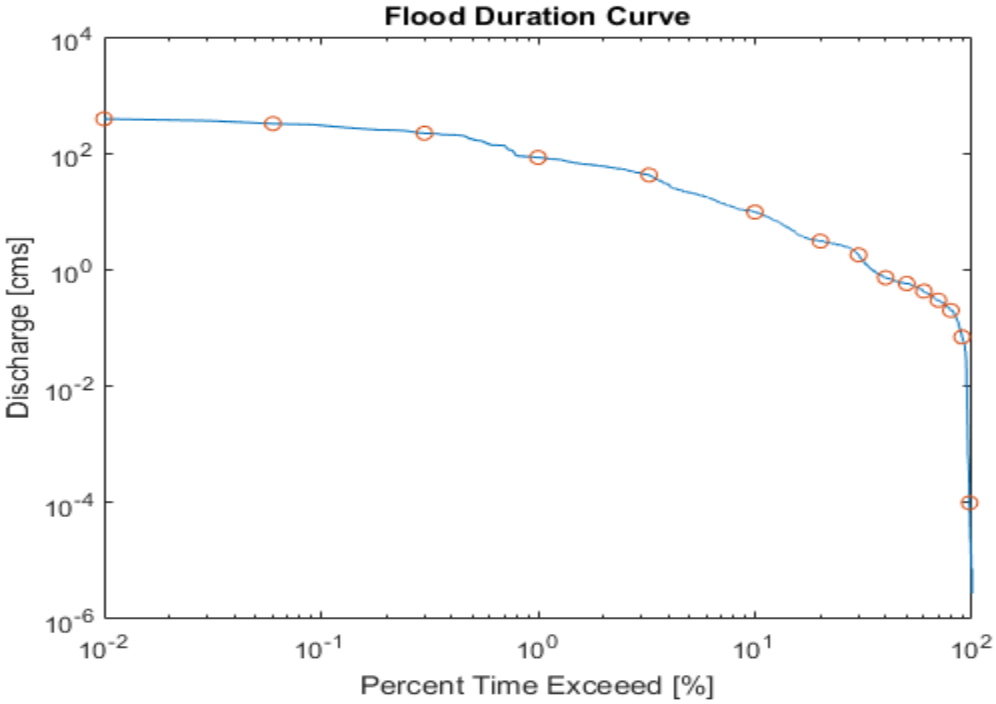

Specific Degradation

$$SD = 365 \times Q_s \left[\frac{tons}{day}\right] \div Area[km^2] = \frac{45.27 \times 365}{298.1} = 55.58 \frac{tons}{km^2 \cdot year}$$

Opinion

SU4 Jangjeon2

Daily Stage and Discharge

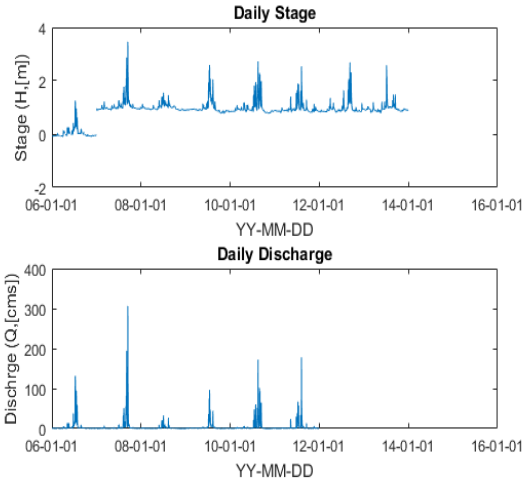

Sediment Rating Curve

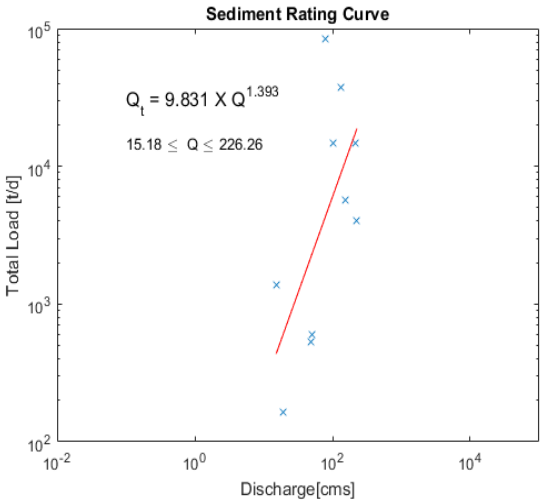

Flow Duration Curve

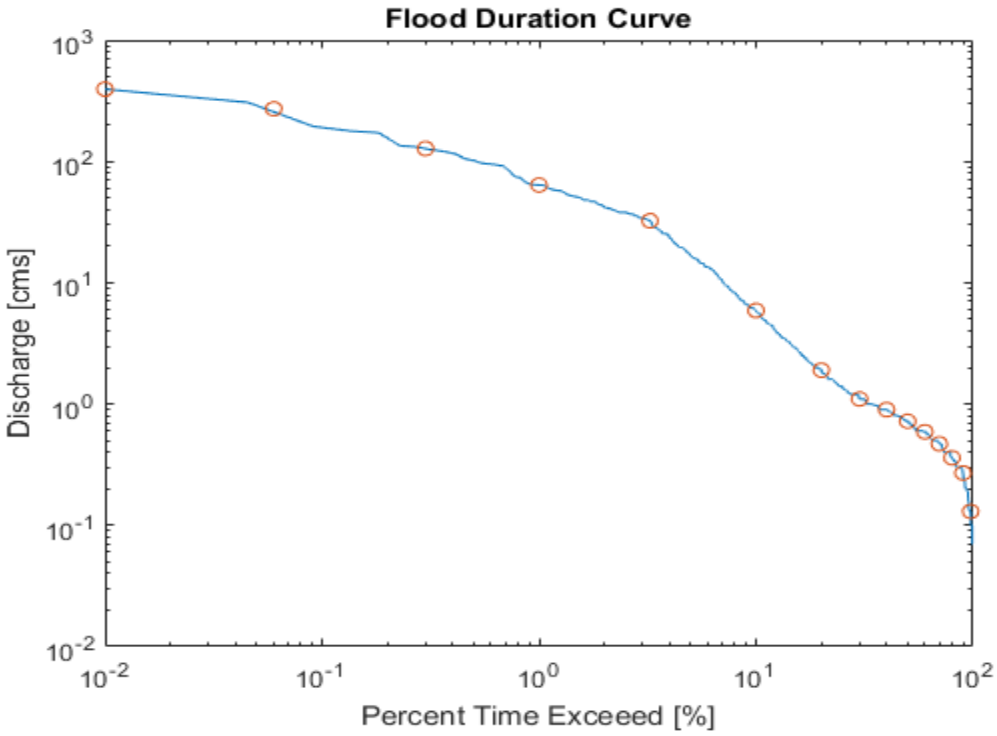

Specific Degradation

$$SD = 365 \times Q_s \left[\frac{tons}{day}\right] \div Area[km^2] = \frac{155.2 \times 365}{273.2} = 207.44 \frac{tons}{km^2 \cdot year}$$

Opinion

SD could be distorted due to small measurements

SU5 Songjeon

Daily Stage and Discharge

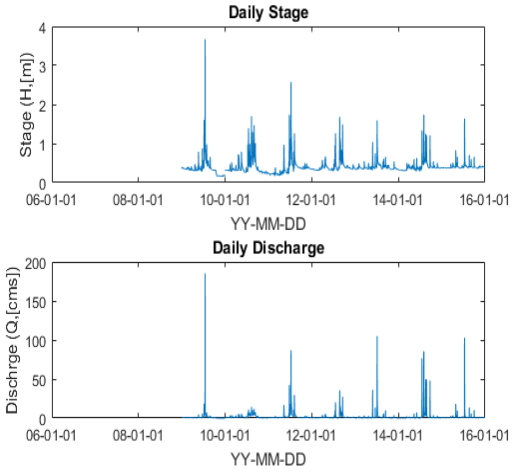

Sediment Rating Curve

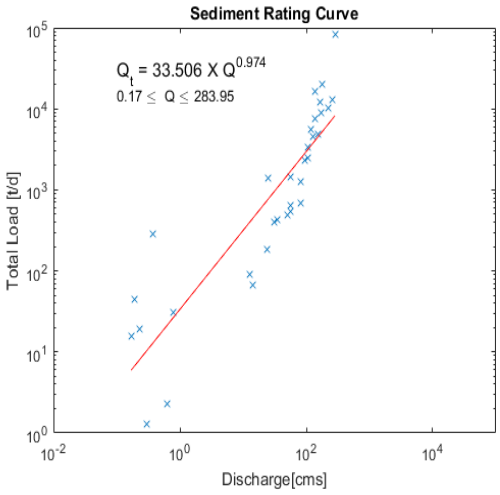

Flow Duration Curve

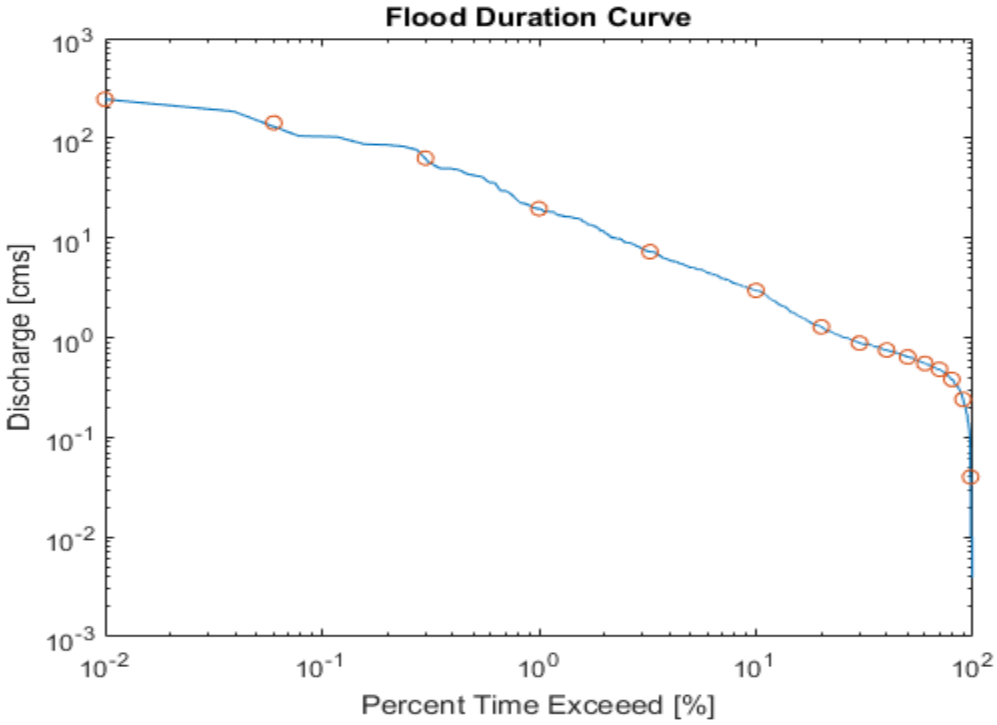

Specific Degradation

$$SD = 365 \times Q_s \left[\frac{tons}{day}\right] \div Area[km^2] = \frac{54.5 \times 365}{60.1} = 331.33 \frac{tons}{km^2 \cdot year}$$

Opinion

SD could be distorted due to small measurements